



**The Investigation of Tree-Retardant Ethylene
Propylene Rubber Insulated Medium Voltage
Cable as an Alternative Underground Cable for
Victorian Power Distribution Network**

**A Thesis
Submitted to the Faculty of
Health, Engineering and Science**

By

Fernando Esma Agustin

for

Doctor of Philosophy

Principal Supervisor

Professor Akhtar Kalam

Associate Supervisor

Professor Aladin Zayegh

ABSTRACT

Cross-linked Polyethylene (XLPE) underground cables are widely used in Victorian power distribution networks due to its lower Dielectric Dissipation Factor (DDF) over Ethylene Propylene Rubber (EPR) cable. Advancement in compounding technology led to the reduction of DDF in some EPR proprietary material.

This research investigated the viability of silane-cured low-DDF Tree-Retardant EPR (TR-EPR) cable as an alternative over standard XLPE cable in Victoria. The thermal ageing behaviour of TR-EPR was studied by means of laboratory-based experimentation using accelerated ageing test to observe the time variation of its mechanical properties: tensile strength and elongation at break. Measurements of Partial Discharge (PD) were also conducted prior and after cable heating at service temperature. The results of the thermal ageing test and PD measurements were visually presented through graphs and plots. For the thermal ageing, a theoretical life model was used with the parameters determined using Least Square Regression Method (LSRM). Data from the TR-EPR thermal ageing test were mathematically extrapolated to service temperature through the Arrhenius law to determine the extent of validity of the results. The economic viability of the TR-EPR was also analysed. The results obtained can be utilised by network operators and large industrial companies when designing their underground cable system and taking into consideration the reliability and economy of the power system.

DECLARATION

“I, **Fernando Esma Agustin**, declare that the PhD thesis entitled **The Investigation of Tree-Retardant Ethylene Propylene Rubber Insulated Medium Voltage Cables as an Alternative Underground Cable for Victorian Power Distribution Network** is no more than 100,000 words in length including quotes and exclusive of tables, figures, appendices, bibliography, references, and footnotes. This thesis contains no material that has been submitted previously, in whole or in part, for the award of any other academic degree or diploma. Except where otherwise indicated, this thesis is my own work.”



Signature

Date: 07/01/2021

ACKNOWLEDGEMENTS

Foremost, I would like to thank Victoria University, Footscray Campus, Victoria, Australia for granting the scholarship for this research project and by giving me the opportunity to continue my PhD degree.

I would like to express my sincere gratitude to my Principal Supervisor, Professor Akhtar Kalam, Head of External Engagement and Leader of Smart Energy Research Unit of Victoria University, for his countless support and encouragement especially during those difficult times of my research journey. Prof. Kalam is the instrumental to the success of this research project. I would like to extend my gratitude to my Associate Supervisor, Professor Aladin Zayegh, for his valuable support and motivation during my study. I would also like to thank Associate Professor Juan Shi for her encouragement.

I would also like to express my gratitude to TriCab Australia for giving me an opportunity to work as Head of Technical and R&D Team from 2009-2019.

Most importantly, my deepest gratitude and appreciation to my wife Marjorie and my son Jofer for their love, understanding, patience and support throughout this research study.

AUTHORED PUBLICATIONS

This thesis contains works that have been published and accepted for publication:

Details of the work:
Agustin, F., Kalam, A., Zayegh, A., "Investigation of 22kV silane cure TR-EPR cable". <i>International Journal of Applied Power Engineering (IJAPE)</i> Vol. 10, No.1, March 2021, pp. 41~47
Location in the thesis:
Chapter 5 and 6
Student Contribution to work:
F. Agustin investigated the thermal characteristics of TR-EPR underground cable that aid in modelling the service life of cable using Arrhenius acceleration factor.

Details of the work:
Agustin, F., Kalam, A., Zayegh, A., "Calculation and Measurement of Ampacity for Class 5 Flexible Aluminium Cable at 110°C". <i>International Journal of Applied Power Engineering (IJAPE)</i> . Accepted on 16 Dec 2020 .
Location in the thesis:
Chapter 7
Student Contribution to work:
F. Agustin determined the ampacity ratings of Class 5 flexible Aluminium cables at 110°C by using various methodologists and verified through simulations.

TABLE OF CONTENTS

ABSTRACT	I
DECLARATION.....	II
ACKNOWLEDGEMENTS.....	III
AUTHORED PUBLICATIONS	IV
TABLE OF CONTENTS.....	V
LIST OF ABBREVIATIONS.....	X
LIST OF FIGURES	XIV
LIST OF TABLES	XVI
CHAPTER 1 INTRODUCTION AND OBJECTIVES OF THE RESEARCH.....	1
1.0 Introduction.....	1
1.1 Research	2
1.2 Methodology and conceptual framework.....	6
1.3 Conclusion.....	11
CHAPTER 2 LITERATURE REVIEW.....	12
2.0 Introduction.....	12
2.1 Power lines	13
2.2 Underground cable distribution systems	14
2.3 Power distribution cables	18
2.4 Components of a power distribution cable.....	19

2.5	Accessories in power distribution cable systems	24
2.6	Theoretical modelling of cable insulations	26
2.7	Conclusion.....	70
CHAPTER 3 CROSS-LINKED POLYETHYLENE AND ETHYLENE PROPYLENE RUBBER UNDERGROUND CABLE		
72		
3.0	Introduction.....	72
3.1	Design	73
3.2	Property	79
3.3	Breakdown history	86
3.4	Treeing phenomenon.....	88
3.5	Discussion about Cross-linked Polyethylene	96
3.6	Discussion about Ethylene Propylene Rubber	110
3.7	Conclusion.....	121
CHAPTER 4 METHODS OF TESTING THE MEDIUM VOLTAGE UNDERGROUND CABLE		
123		
4.0	Introduction.....	123
4.1	Tests as per IEC 60502-2	124
4.2	Tests as per AS/NZS 1429.1	150
4.3	Air oven ageing as per AS/NZS 1660.2.2	160
4.4	Withstand voltage test using Very Low Frequency (VLF) method	164
4.5	Conclusion.....	171

CHAPTER 5 ACCELERATED AGEING TEST FOR 22kV TREE RETARDANT-ETHYLENE PROPYLENE RUBBER CABLE.....	173
5.0 Introduction.....	173
5.1 Prolonged thermal ageing test setup.....	175
5.2 Prolonged thermal ageing results	176
5.3 Comparison with theoretical model	178
5.4 Extrapolation to service temperature using Arrhenius relationship	185
5.5 Correlation of tensile strength and elongation at break.....	187
5.6 Estimation of TR-EPR insulation life	189
5.7 Discussion	193
5.8 Conclusion.....	196
CHAPTER 6 ELECTRICAL AND NON-ELECTRICAL TEST FOR 22kV TREE RETARDANT-ETHYLENE PROPYLENE RUBBER CABLE	198
6.0 Introduction.....	198
6.1 PD Test.....	199
6.2 Bending test proceeded by PD test.....	203
6.3 Tan delta measurement.....	204
6.4 Heating cycle test proceeded by PD test	206
6.5 Impulse withstand test proceeded by HV test	206
6.6 HV test	208
6.7 Hot set test.....	209

6.8	Conclusion.....	211
CHAPTER 7 CALCULATION OF CURRENT CAPACITY OF FLEXIBLE ALUMINIUM CABLE 213		
7.0	Introduction.....	213
7.1	Review of conductors.....	214
7.2	Review of thermal expansion.....	215
7.3	Cable ampacity calculation	216
7.4	Heat dissipation test	222
7.5	Results of heat dissipation test	224
7.6	Conclusion.....	227
CHAPTER 8 ECONOMICS IN USING TR-EPR UNDERGROUND CABLE 228		
8.0	Introduction.....	228
8.1	Cable life cycle costs.....	229
8.2	LCCA parameters.....	235
8.3	Results of LCCA calculation.....	238
8.4	Conclusion.....	248
CHAPTER 9 CONCLUSION AND RECOMMENDATIONS FOR FUTURE WORK 249		
9.0	Conclusion.....	249
9.1	Recommendations for future work.....	252

REFERENCES 254

Appendix A 278

Appendix B 287

LIST OF ABBREVIATIONS

3P-ETM	3 Parameter Exponential Threshold Model
3P-IPTM	3 Parameter Inverse-Power Threshold Model
4P-ETM	4 Parameter Exponential Threshold Model
4P-IPTM	4 Parameter Inverse-Power Threshold Model
a.c.	Alternating Current
ANSI	American National Standard Institute
AS	Australian Standard
AS/NZS	Australian/New Zealand Standard
ASTM	American Society for Testing and Materials
CAM	Combined Analysis Method
CBD	Central Business District
CDF	Cumulative Distribution Function
CN	Concentric Neutral
CSPE	Chlorosulfonated Polyethylene
d.c.	Direct Current
DDF	Dielectric Dissipation Factor
DMA	Dynamic Mechanical Analysis
DSC	Differential Scanning Calorimetry
EDS	Energy Dispersive Spectroscopy
EHV	Extra High Voltage
EI	Elongation at Break
EPDM	Ethylene Propylene Diene Monomer

EPR	Ethylene Propylene Rubber
ES	Electric Strength
ESC	Environmental Stress Cracking
ETM	Exponential Threshold Model
EUAC	Equivalent Uniform Annual Cost
EVA	Ethylene-vinyl Acetate Copolymer
FEM	Field-Emission Model
GIL	Gas Insulated Lines
GRG	Generalised Reduced Gradient
HDPE	High Density Polyethylene
HEPR	Hard Grade Ethylene-Propylene Rubber
HIC	Halving Interval in Celsius/Centigrade
HMWPE	High Molecular Weight Polyethylene
HTS	High Temperature Superconductive
HV	High Voltage
IEC	International Electrotechnical Commission
IEEE	Institute of Electrical and Electronics Engineers
IEPS-W	Information Embedded Power System via Wide Area Network
IPM	Inverse Power Model
IPTM	Inverse Power Threshold Model
IRHD	International Rubber Hardness Degrees
ISO	International Organisation for Standardisation
LDPE	Low Density Polyethylene
LMWPE	Low Molecular Weight Polyethylene
LSRM	Least Square Regression Method

LV	Low Voltage
MDPE	Medium Density Polyethylene
MEC	Mechanical Endurance Coefficient
MLE	Maximum Likelihood Estimation
MLM	Maximum Likelihood Method
MV	Medium Voltage
NMN	Nomex-Mylar-Nomex
NPV	Net Present Value
OIT	Oxidation Induction Time
OMT	Oxidation Maximum Time
PD	Partial Discharge
PE	Polyethylene
PET	Polyethylene Terephthalate
PI	Polyimide
PILC	Paper Insulated Lead Covered
PP	Polypropylene
PTFE	Polytetrafluoroethylene
PVC	Polyvinyl Chloride
QTR	Quality Test Report
r.m.s.	Root Mean Square
SAFT	Scale-Accelerated Failure-Time
S	Standard Error of Regression
SAIDI	System Average Interruption Duration Index
SCI	Stress-compatibility Index
SDI	Single-core Double Insulated

SEM	Scanning Electron Microscopy
SG	Smart Grid
SSE	Sum of Squared Errors
THD	Total Harmonic Distortion
TI	Temperature Index
TR-EPR	Tree-retardant Ethylene Propylene Rubber
TR-XLPE	Tree-Retardant Cross-linked Polyethylene
TS	Tensile Strength
UHV	Ultra-High Voltage
ULDPE	Ultra-Low Density Polyethylene
VEC	Voltage Endurance Coefficient
VLF	Very Low Frequency
WDS	Wavelength Dispersive Spectroscopy
WTR-XLPE	Water Tree-retardant Cross-linked Polyethylene
XLPE	Cross-linked Polyethylene

LIST OF FIGURES

Figure 1.1: Bushfire in Victoria (credit: Toa55 iStock photo-1188418810).....	5
Figure 1.2: Conceptual framework.....	10
Figure 2.1: Cable parts (cross-sectional view).....	20
Figure 2.2: Cable parts (longitudinal view)	20
Figure 3.1: Types of water trees.....	90
Figure 4.4.1: Measurement of conductor resistance.....	127
Figure 4.2: Conditioning of sample for conductor resistance test.....	127
Figure 5.1: Longitudinal section of 22kV 1C120mm ² TR-EPR cable.....	175
Figure 5.2: Specific dimensions of dumbbell specimens	176
Figure 5.3: Longitudinal section of 22kV 1C120mm ² TR-EPR cable	176
Figure 5.4: Relative TS graph compared with relative TS measurements; relative EI points included.....	182
Figure 5.5: Plot of relative TS-relative EI points (red), regression line included (blue).....	188
Figure 5.6: Relative TS cubic graph compared with relative TS measurements	191
Figure 6.1: TR-EPR cables are subjected to heating.....	200
Figure 6.2: Measurement of PD	200
Figure 6.3: 125kV Reactor and Series Resonance PD test system.....	201
Figure 6.4: PD graph of 22kV TR-EPR cable before and after heating.....	201
Figure 7.1: Schematic diagram of heat dissipation test system.....	222
Figure 7.2: Measuring of test current using Fluke 435 Power Analyser.....	224
Figure 7.3: Graph of heat dissipated to termination, conductor, insulation, and sheath	227
Figure 8.1: Percentile of costs for 22kV 1c630mm ² XLPE cable.....	243
Figure 8.2: Percentile of costs for 22kV 1c630mm ² TR-EPR cable	244

Figure 8.3: Percentile of costs for 66kV 1c630mm² XLPE cable..... 245

Figure 8.4: Percentile of costs for 66kV 1c630mm² TR-EPR cable 245

LIST OF TABLES

Table 2.1: Classification of Power Lines according to Voltage range	14
Table 2.2: Conductor Size	21
Table 3.1: Nominal Insulation thickness of XLPE and EPR as per AS/NZS 1429.1	75
Table 3.2: Nominal Insulation Thickness of XLPE and EPR as PER IEC 60502-2.....	76
Table 4.1: Number of samples for Sample Tests as per IEC 60502-2	128
Table 4.2: Sample Test Voltages as per IEC 60502-2	131
Table 4.3: Impulse Voltages as per IEC 60502-2	134
Table 4.4: Maximum Core Temperatures of Sheathing materials as per IEC 60502-2	137
Table 4.5: Non-electrical Type Tests as per IEC 60502-2	138
Table 4.6: Test requirements for mechanical properties of Insulation as per IEC 60502-2.....	140
Table 4.7: Test requirements for mechanical properties of Sheathing as per IEC 60502-2.....	140
Table 4.8: Test requirement properties for PVC Sheath materials as per IEC 60502-2.....	142
Table 4.9: Test requirement properties for PVC Insulation material as per IEC 60502-2	142
Table 4.10: Test requirement properties for PE sheathing materials as per IEC 60502-2	143
Table 4.11: Test requirement for thermoset Insulation materials as per IEC60502-2	144
Table 4.12: Test requirement properties for Elastomeric sheathing materials as per IEC60502-2	145
Table 4.13: Basis for number of samples as per AS/NZS 1429.1	151
Table 4.14: Partial Discharge Voltage levels as per AS/NZS 1429.1	152
Table 4.15: Test Voltages for 5 and 15-minute HV Test AS PER AS/NZS 1429.1	154
Table 4.16: Impulse Withstand Voltages as per AS/NZS 1429.1	159
Table 4.17: Test Voltage for 4 hour HV tests as per AS/NZS 1429.1	159
Table 4.18: VLF Test Voltage.....	166

Table 5.1: Tensile Strength Measurements of TR-EPR Insulation from Prolonged Thermal Ageing Test	177
Table 5.2.: Elongation at Break Measurements of TR-EPR Insulation from Prolonged Thermal Ageing Test	177
Table 5.3: Comparison of tensile strength values from experiment and theoretical model (Simoni)	183
Table 5.4: Comparison of tensile strength values from experiment and theoretical model (Cubic).....	192
Table 6.1: Measured PD values of TR-EPR cables from third party validation	203
Table 6.2: Measured $\tan\delta$ of TR-EPR cables	204
Table 6.3: Various $\tan\delta$ measurement of TR-EPR cables	205
Table 6.4: Cross-linking development of TR-EPR at ambient temperature	210
Table 6.5: Cross-linking development of TR-EPR at 60°C heating.....	211
Table 7.1: Construction of Class 5 flexible Aluminium conductor (Class 2 conductor referenced for d.c. resistance)	215
Table 7.2: Calculated conductor d.c. resistance	217
Table 7.3: Calculated conductor a.c. resistance	218
Table 7.4 : Calculated dielectric loss	219
Table 7.5: Calculated Thermal resistances (T_1 and T_4).....	220
Table 7.6: Calculated Ampacities at 110°C based on IEC 60287 and AS/NZS 3008.1.1.....	221
Table 7.7: Current and temperature measurements at calculated Ampacity rating.....	225
Table 7.8: Conductor-to-connector cross-sectional area ratio.....	226
Table 8.1: General LCCA parameters.....	236
Table 8.2.: Insulation and U_0 parameters	237
Table 8.3: LCCA OF 22kV 1C630mm ² XLPE AL cable	239

Table 8.4: LCCA of 22kV 1C630mm ² TR-EPR AL cable	240
Table 8.5: LCCA of 66kV 1C630mm ² XLPE AL cable	241
Table 8.6: LCCA of 66kV 1C630mm ² TR-EPR AL cable	242
Table 8.7: LCCA Summary	247
Table 8.8: LCCA Summary for same service life	248

CHAPTER 1 INTRODUCTION AND OBJECTIVES OF THE RESEARCH

1.0 Introduction

With the advent of technology, there is an ever-increasing demand for electrical power. In this aspect, the role of electricity sector is indispensable in ensuring that electrical power is delivered to the end users in the most efficient, economic, and environmental way. Reliable source of electrical power is becoming necessitated in some regions of the world. In addressing the issue regarding reliable and safer means of delivering electrical power to end users, overhead lines are being turned into underground cable systems. The change in configuration of the cable system affected the considerations in design of cables especially of the insulation. The most common insulation materials being used in underground cables are the Cross-Linked Polyethylene (XLPE) and Ethylene-Propylene Rubber (EPR). EPR generally has better electrical characteristics than XLPE except in the aspect of the Dielectric Dissipation Factor (DDF). XLPE cable has a low DDF than standard EPR cable, which corresponds to low dielectric loss [1]. Yet the dielectric loss of material is less significant in Medium Voltage (MV) level where all power distribution networks operate. These are the areas where EPR can be utilised and since the dielectric loss angle of EPR can be lowered due to modern compounding technology, the loss due to insulating material becomes less relevant when the life cycle analysis is considered as depicted in (1.1):

$$W_d = \omega \cdot C \cdot U_o^2 \cdot \tan\delta \quad (1.1)$$

where W_d refers to the dielectric loss, ω indicates the angular frequency in $\frac{\text{radian}}{\text{s}}$ and is equivalent to $2\pi f$ where f indicates frequency in Hz , C corresponds to capacitance per unit length, U_o denotes voltage to earth, and $\tan\delta$ pertains to the dielectric loss angle of material or DDF.

1.1 Research

1.1.1 Aims of the project

In addressing the issue regarding the higher DDF of EPR, this research aims to introduce an improved version of the dielectric material called Tree-Retardant Ethylene-Propylene Rubber (TR-EPR) which features a significantly lower DDF than EPR and even to XLPE for power cable industry. This research investigated the viability of low DDF silane cross-linkable TR-EPR as an alternative underground cable for Victorian Power Distribution Network. Victoria is the second smallest state in southeastern Australia. There is also an emphasis regarding the application of undergrounding in all bushfire zones and other specialised installation. This project will seek to determine whether TR-EPR insulation material has reliability and economic advantage over XLPE cable when used in Victorian Power Distribution Network. In lieu of this, the properties of TR-EPR are studied pertinent to service condition. This research study investigated the cross-linking behaviour of TR-EPR insulation. It also aims to learn about the partial discharge characteristics of TR-EPR insulated cables pertinent to heating condition. This research focused on determining the expected service condition of silane cross-linkable TR-EPR compared to XLPE. Furthermore, the aim of this research is to contribute to the body of knowledge that can

be utilised by network operators and industrial companies in designing a reliable and cost-effective underground cabling system.

1.1.2 Contribution to knowledge

There is an increased need for more research in the reliability of electric distribution network due to ageing of overhead distribution and underground cable lines. The study and investigation conducted by Al-Khalidi [2] suggested the need of undergrounding due to the reliability of underground cable system compared to overhead lines.

The quality of insulation plays a vital role in the reliability of underground cable system as it is subjected to thermal, mechanical, and electrical stress throughout its service life. The insulation should be able to withstand changes in temperature, load cycles, voltage surge, and water penetration during its operation.

In Victoria, network operators and large industrial companies preferred XLPE over EPR for their MV underground cable requirement as stated in [3] and [4] and this is the reason why there were no studies conducted on EPR cable in Australian condition.

This research intends to build more data and understanding of the performance of TR-EPR for the use in MV underground cable in Australia and to develop more innovative practices of ensuring long term stability and reliability of TR-EPR use by engaging the various sector in order to monitor and maintain its electrical performance and cost effectiveness with the support of manufacturers, engineers, and the public sector.

Results from the laboratory experiments contribute to the following body of knowledge:

- Introduction of an alternative EPR-based dielectric material relevant to application of cables for power industry.
- Understand the physical, thermal, and electrical properties of TR-EPR cables in comparison with XLPE. A comprehensive review of the accelerated thermal ageing behaviour of TR-EPR over XLPE insulation pertinent to endurance characterisation can be established. This will be used to determine the suitable cable with respect to its intended application.
- Presentation of the correlation of $Tan\delta$ of TR-EPR and XLPE is presented. This is contributed to the power loss analysis of underground cable system.
- Recommendation for supplemental revision of existing standard.
- Re-establishing economic consideration of XLPE cables and consideration through cost-effective analysis of TR-EPR cables in the implementation of new underground cable system.
- Application of silane dry curing as a method of cross-linking of insulation material.
- Ampacity calculation and simulation of Class 5 flexible Aluminium conductor pertinent to IEC 60228 and AS/NZS 1125.

1.1.3 Statement of significance

This research contributes to the promotion of the transitioning from overhead to underground cable system for the Victorian Power Distribution System. This is achieved by considering the heightened reliability of operation for network operators and industrial sectors. The reliability of underground cables is of extreme importance in power utility and large industrial companies. Power outages due to premature cable failure have severe economic impact due to high cost of

repair and in worst case, replacement of the whole cable system. Poor cable design and ageing overhead lines have been a factor to big economic loss and sometimes leads to safety and risks of the community at large.

Victoria is very prone to bushfires due to its environment and eco-system. The climate change is expected to further increase the likelihood of bushfire occurrence in Victoria. The 2009 Black Saturday bushfires as shown in Figure 1.1 in Kilmore East, Coleraine, and Horsam, Victoria which were considered to be the deadliest bushfire ever occurred in Australia were found to be caused by ageing power lines [5].



Figure 1.1: Bushfire in Victoria (credit: Toa55 iStock photo-1188418810)

The analysis of the overall cost of underground cable system is very important in distribution network design as much as its reliability. Initial cost of cable, operating voltages, dielectric loss, and operating cost are the most essential factors affecting the overall costs over the life of underground cable system. By utilising the ageing characteristics and phenomena by means of accelerated ageing test, the service behaviour of TR-EPR underground cables can be predicted that could benefit to the economics of power system.

The other benefit of reliable underground cable is the replacement of overhead lines in bushfire zone areas. This will eliminate the risk of losing properties and life due to fire and associated incidents caused by overhead lines. Although there is a report from Putting Cables Underground Working Group [6], it only discussed the use of standard XLPE cables and did not discuss the possibility of using other type of underground cables.

The excellent flexibility of TR-EPR cables is another advantage over XLPE cables when the installation in a very tight and highly populated area is to be carried-out. This will also improve the work safety by minimisation of the injury that can be sustained by the cable installer and jointer caused by the bending of a very rigid underground cable like XLPE.

1.2 Methodology and conceptual framework

Qualitative approach through series of experimentation were employed to determine the service performance of TR-EPR underground cable. Experimental data were transformed to graphical modelling of mechanical properties (tensile strength and elongation at break) of TR-EPR material over the period of accelerated thermal ageing and then mathematically interpreted to service temperature. Computational analysis was performed to represent the correlation between power

loss due to dielectric dissipation factor, reliability of power distribution network, and the thermal stability of material that will be the key factors in determining the economic impact of TR-EPR underground cables to Victorian distribution network.

This research is divided into two categories:

- Laboratory experiments, and
- Economic analysis

The experiments performed are categorised into two: those particular to the TR-EPR insulation and those pertinent to the Aluminium conductor. The experiments performed on the TR-EPR insulation include the hot set test for the determination of the cross-linking behaviour in ambient and service condition, cable heating for the partial discharge behaviour, and accelerated thermal ageing test for the time behaviour of the mechanical properties. On the other hand, regarding the Aluminium conductor, the a.c. resistance, d.c. resistance, dielectric loss, thermal resistance, and current capacities measurements were carried out.

A third-party accredited testing laboratory was also assigned to perform testing on the TR-EPR insulation in compliance with AS/NZS 1429.1, IEC 60092-350 and IEC 60092-354.

1.2.1 Hot set test

The hot set test serves to determine the ultimate cross-linking stage of the insulation. This cross-linking or curing period is attained by subjecting TR-EPR insulated cable samples under ambient temperature, hence corresponded to the practically longest cross-linking period. For appreciable comparison, the experiment for the determination of cross-linking of TR-EPR was also performed

under service temperature which was considerably higher than the ambient temperature which will also demonstrate the effect of temperature in the rate of cross-linking process.

1.2.2 Accelerated thermal ageing test

The thermal ageing experimentation was carried out in two phases.

- The first phase of this experimentation was the preparation of samples from TR-EPR insulated cable. These samples were subjected to thermal ageing. Ageing test was carried out for 30 months period.
- The second phase was the analysis of experimental data using Arrhenius Statistical model in order to establish a correlation and comparison between various samples. Arrhenius relationship is a widely used model to predict the effect of temperature to reaction rate of certain material to the accelerated ageing [7].

The focus of the investigation on thermal ageing is to predict the tendency of the service life of cable under thermal stress with the aim of determining the time behaviour of the TR-EPR with respect to its mechanical properties. Fifty-five dumbbell-shaped insulation specimens were placed inside the oven at 90°C. Five specimens were taken out in the oven and were subjected to tensile strength and elongation at break test of material in every third month for the total period of up to 30 months.

Data are presented to compare the results obtained by the study conducted by previous researchers and the new data on thermal ageing obtained from this research.

1.2.3 Economic analysis

The economic analysis considers the comparison of the TR-EPR insulated cable with XLPE-insulated cable pertinent to application in underground cable system. Among the various ways of comparing alternatives in engineering economics, the annual cost method is used as it is suitable for comparison of two projects with unequal lives. For the annual cost method, the total cost of each project (which include initial, periodic, and end of life costs) is evaluated to its present worth value called the Net Present Value (NPV). The present values obtained are then evaluated to their respective annual costs called Equivalent Uniform Annual Cost (EUAC) using the annuity formula. For this method, the price difference between the TR-EPR and XLPE insulated cables is reflected on the initial cost while their conductor and dielectric losses is translated in the periodic costs. Various parameters and resulting cost calculations are presented through tables while the proportions of the major costs of each project with respect to their NPV are interpreted using figures.

1.2.4 Conceptual framework

In this research, there are several information that are meant to be obtained. These information are pertinent to the variables considered for the research and the corresponding processes involved in treating or obtaining them. The map of the concepts involved in this research study along with the links of the variables and processes under consideration are shown in Figure 1.2.

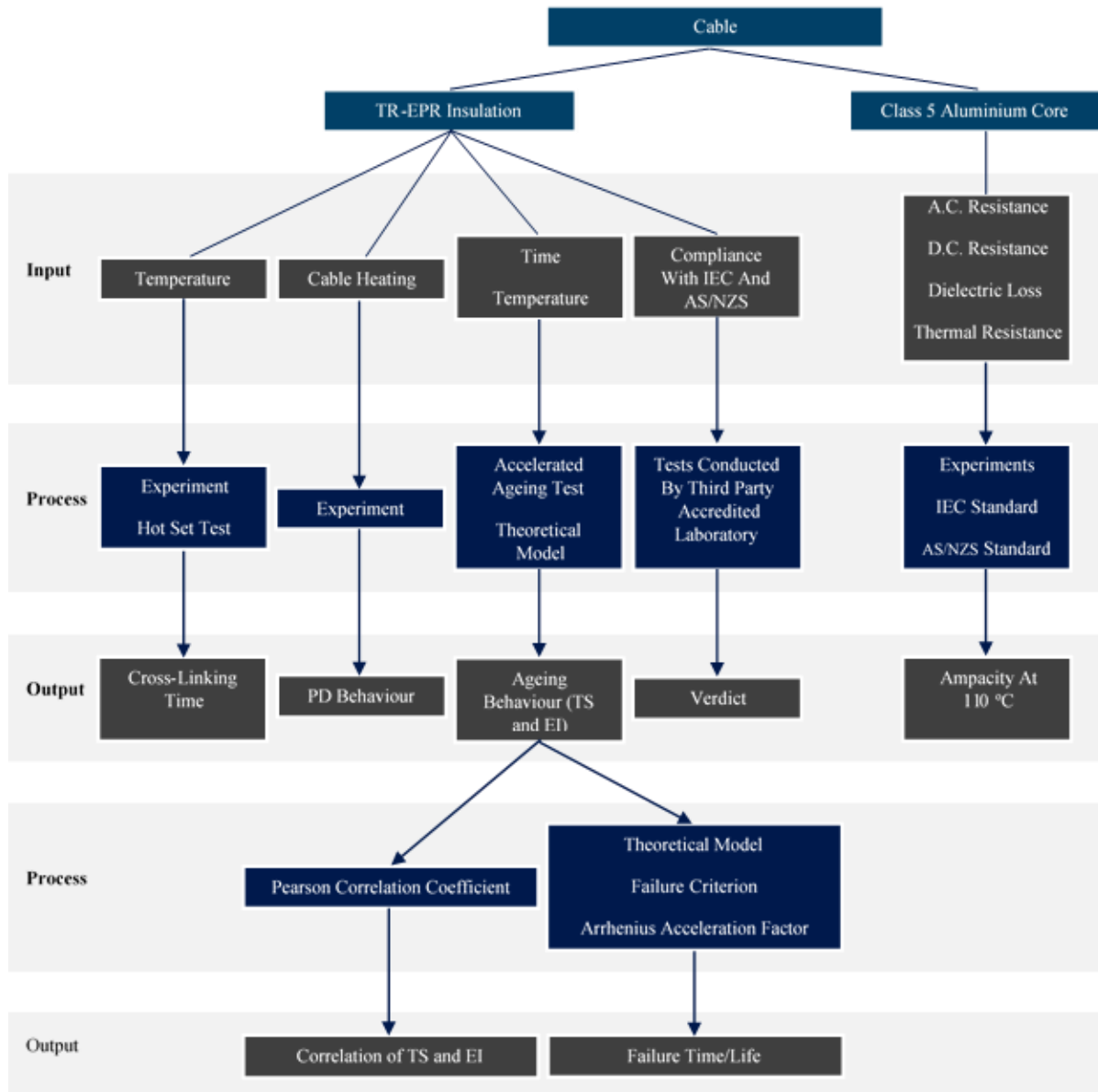


Figure 1.2: Conceptual framework

The boxes pertain to the concepts involved in this research study which include the head topics, variables, and processes. These boxes are linked through lines and arrows. The lines connect boxes that are linked by category. For instance, under the category of cables are categories pertinent to its components including insulation and conductor (TR-EPR insulation and Class 5

Aluminium conductor in this case). This research study encompasses information about cables with primary focus on insulation (TR-EPR insulation) and supplement research involving conductor (Class 5 flexible Aluminium conductor). On the other hand, arrows connect boxes pertinent to the direction of concepts involved considering causal relationships on a chronological basis. This helps in tracing the necessary means of achieving the desired information. The framework also features horizontal classification of the concepts which are the input, process, and output. The input generally corresponds to the independent variable while the output generally corresponds to the dependent variable. The process refers to the manner by which the information is treated to obtain the output. The specific paths defined in the conceptual framework will be further elaborated in the latter part of this thesis.

1.3 Conclusion

The underground cable system is one of the measures of the power distribution network due to continuous technology of polymeric insulated medium voltage underground cable taking into consideration its reliability and economic factor. This is in-line with the growth of populations and businesses in the urban and central business around the world.

This research provides an opportunity to understand the behaviour of TR-EPR cables that could potentially improve the reliability and life of underground power distribution network system. This also contributes to the theoretical and practical knowledge in the field of underground cable system.

CHAPTER 2 LITERATURE REVIEW

2.0 Introduction

In the previous chapter, the discussion focused on introducing the vital points of this research pertinent to the promotion of movement from overhead lines to underground cables and the selection of alternative insulation material TR-EPR over XLPE. The latter was of prime consideration in this thesis. Specific means of evaluating the viability of TR-EPR was also revealed which involved testing and analysis. The shown conceptual framework also provided guidance in tracing the chronological flow of concepts pertinent to variables considered. To sum it up, Chapter 1 aimed at providing a quick overview of the things that tackled in this thesis.

In order to gain a better grasp of the concepts being considered in this research, it is essential to gain a comprehensive background of the topic. In this way, a systematic and organised understanding can be found to pinpoint the location of the prime topic from its corresponding hierarchal network of knowledge. To be more specific, TR-EPR may then be recognised as an alternative insulation material being introduced in MV underground cable distribution system in which:

- TR-EPR pertains to a type of insulation (in contrast with XLPE)

- insulation denotes a component of a power cable (which also include conductor, conductor screen, insulation screen, metallic screen, and outer sheath)
- MV corresponds to a voltage rating of cables systems (which also include low, high, extra-high, and ultra-high)
- underground refers to cable configuration (which may also be overhead)
- distribution corresponds to transport of electrical power from substation to end users (in contrast with transmission pertinent to transport from source to substation)

More particular discussion has been done in the differentiation between overhead and underground cable configurations and between XLPE and EPR in terms of their advantages and disadvantages. The most comprehensive discussion was made on the various theoretical models developed relevant to the prediction of insulation life through considerations in the degradation mechanisms in relation to other parameters.

2.1 Power lines

Power lines are responsible for the transport of electricity. They can be categorised into two types: transmission and distribution. Transmission lines transport electricity from the power source to the substations and involve higher voltage levels. On the other hand, distribution lines transport electricity from the substations to end users and involve lower voltage levels. A summary of the voltage classifications and ratings as per ANSI C84.1-2011 [8] are presented in Table 2.1. It should be noted however that classification of voltage (aside from low voltage) may vary from country to country, hence may cause confusion. To deal with this, it is advised to define the cable in terms of its actual voltage rating [9].

Table 2.1: Classification of Power Lines according to Voltage range

Voltage Classification	Voltage Range (kV)
Low Voltage (LV)	Up to 1
Medium Voltage (MV)	1-100
High Voltage (HV)	100-230
Extra High Voltage (EHV)	230-1000
Ultra-High Voltage (UHV)	1000 above

2.2 Underground cable distribution systems

Based on how the cables are laid, the means of supplying electrical energy can either be overhead or underground. In the selection of these, various factors are considered including but not limited to cost-effectiveness, geography, environmental impact, and capacity limitations. Preference of overhead lines over underground cables is greatly considered due to the disadvantages possessed by underground cables which include:

- higher initial cost (taking into account insulation and property restoration);
- longer line outage, difficulty in implementing line modifications;
- harder to locate faults, costly repair, and lower power carrying capacity.

Despite the given disadvantages, underground cables systems are selected for reasonable factors. In terms of safety, underground cable systems have the advantage since there is no risk of contact with the lines. The cable systems appear tidier for underground cable systems as no visible lines and posts are present. Supply interruptions also become rare as the cables are protected below from possible environmental dangers like hurricanes, lightning strikes, falling trees, debris, vehicle accidents, wind load, and snowstorms. Based on Mohammad, Kalam, and Akella [10],

Victoria is confronting issues regarding reliability supported by occurrence of power outages due to storm, high temperature, and bushfires which affected nearly half million of Victorians.

Operations and maintenance costs are also reduced in line with the fewer interruptions and being free from executing tree trimming activities. Some special circumstances also impose necessity for applying underground cable systems like installation across river crossings and on congested urban sites (considering space limitations), and issues regarding aesthetics like national parks. Hence, underground cable distribution systems are becoming more significant in power delivery distribution networks [11-17]. This becomes more significant especially when considering high reliability of power supply [18]. In lieu of this, continuous development lead to improvements regarding the reliability aspect of distribution networks like in the case of electrical grid which are turned into Smart Grids (SG) [19]. Samples of improvement pertinent to information technology include Information Embedded Power System via Wide Area Network (IEPS-W) introduced by Oo, Kalam, and Zayegh [20] and real-time publisher/subscriber communication model proposed by Ozansoy, Zayegh, and Kalam [21]. Additionally, Al-Khalidi and Kalam [22] provided an elaborate discussion regarding the various cable technologies in undergrounding including XLPE cable, Gas Insulated Lines (GIL), and High Temperature Superconducting (HTS) cables as well as the impact of underground cable system in Australia in terms of reliability, economical, and environmental aspects.

In the case of Cox et al. [23], earlier in history, Paper Insulated Lead Covered (PILC) cables were used. However, due to cost and inconvenient installation time, High Molecular Weight Polyethylene (HMWPE) were used. In 1973, the rate of failures of HMWPE insulated cables with HMWPE was 2.63 annual failures per 100 km length i.e., 2.63f/100 km-yr. After 3 years, the rate of failure of HMWPE insulated cables increased to 9.94 f/100 km-yr. On the other hand, in 1980,

XLPE insulated cables was recorded to have a failure rate of 1.86f/100 km-yr. The highest rate of failure recorded for HMWPE insulated underground residential distribution cables was 54.06f/100 km-yr which occurred in 1983 while for XLPE insulated cables, the peak failure rate was 6.84f/100 km-yr. Owing to the significantly high and increasing rate of failure of HMWPE insulated cables, transition to the use of XLPE as insulation for cables occurred. Since both HMWPE and XLPE insulated cables showed failure rates that were significantly high and increasing, decision was made in which instead of choosing to minimise the cost initially incurred, the cost of economic life cycle was considered. This decision translated to the selection of another insulation material called Ethylene Propylene Rubber (EPR) which offered greater reliability proven by more than 30 years of service life. The recorded failure rate for EPR insulated cables was 0.1f/100 km-yr which was at least a magnitude lower compared with cables insulated with HMWPE and XLPE.

Afotey and Aliadeh [24] presented from literature some of the common encountered failures in underground MV cable systems. In general, thermal, electrical, and mechanical stresses lead to cable degradation. Furthermore, stresses from voids, existence of water trees, presence of chemical contaminants, improper practices in cable installation, and electrical surges induced by switching operation cause deterioration of the insulation material resulting to occurrence of breakdown. Another factor leading to failure of cable was the harmonic distortion. Referring to IEEE 519 standard, 15% Total Harmonic Distortion (THD) corresponded to 15% reduction in the life of cable.

From a survey carried out by Maggioli, Leite, and Morais [25] with data relevant to underground MV cable system in Portugal between 2001 and 2013, 68% of cable failures were associated to failure of equipment from which 84% were due to insulation faults and 15% due to degradation

of material. The MV distribution networks were divided into four categories according to voltage rating: 6kV, 10kV, 15kV, and 30kV. The failure rates were highest for the two lower voltage ratings (i.e., 6kV and 10kV) which were 6.1f/100 km-yr and 6.5f/100 km-yr respectively. For the 15kV and 30kV underground cable networks, the corresponding failure rates were 2.2f/100km-yr and 1.7f/100 km-yr. Based from the research of Calcara et al. [26] involving an Italian network pertinent to the years 2012 to 2017, 64% of the failures in underground cable systems were attributed to the joints, 24% associated to the cables, and 12% pointed to the terminals.

In lieu of the failures encountered in underground cable systems, various methods of identifying the location of cable faults were developed. An example of such method was through the measurements of voltage in which Fourier analysis was applied. Yet the model lacked accuracy and robustness. Another cable fault method involves the impedance of fault loop with the location identified by section. In this case, the realised sections of faults were simply ranked. There is also a cable fault locating method which was an improvement of traditional means which involved the determination of the cable apparent impedance. This method was performed in faults for three-phase and faults for single phase to ground which takes into account the capacitive property of cables. Further improvements compared with traditional methods were made which involved sequence impedance models in which the capacitance of cables was taken into account. An appropriate method for degraded cables was also developed which utilised an algorithm for locating faults based on multiple terminal input. This takes into account that degradation of cables significantly affects the sequence capacitances and relative permeability. In this method, phasor measurements are taken from various cable terminals. Naidu, George, and Pradhan [27] introduced an improved algorithm in locating faults of underground cables which involved measurements of voltage and current from a single terminal where the locator is set. This

algorithm takes into account sheath currents, sheath capacitances, and ground modes which allowed accurate locating of cable faults.

2.3 Power distribution cables

A cable can be simply defined as a core (conductor) covered with insulation. Power distribution cables are fashioned to transmit and distribute electrical energy. The history of cables can be traced back in Russia during the early 1800 where it was used for the detonation of ores [28]. Half a century later, natural rubber was introduced as insulation for cables. A notable contribution in the development of the power distribution system took place in New York City during 1882 when Thomas Edison introduced economic model for the generation and distribution of electrical energy which involves d.c. cables using Copper rods with jute as insulation [29]. In England, during the 1890s, Sebastian Ziani de Ferranti developed one of the first flexible paper insulated cables (featuring concentric cable construction at a working voltage of 11kV) alongside advancement in the establishment of a.c. distribution networks and power stations [30]. Screen cables were introduced in 1917. Then 8 years later, pressurised paper cables were developed. In 1942 which is 5 years after its invention, Polyethylene (PE) insulation was marketed. This was followed by the Polyvinyl Chloride (PVC) insulation for cables and eventual progress in the development of catalysts applied for the co-polymerisation of ethylene and propylene resulting to Ethylene Propylene Rubber (EPR) in the 1950s. In 1963, EPR insulation has already been widely used in low and medium voltage applications alongside the development of Cross-Linked Polyethylene (XLPE). Some of the important features of EPR were the resistance against water and weathering, flexibility, and high temperature rating but owing to being more expensive than XLPE, its application was limited to those requiring high reliability like submarine cables and coal mines [31]. Utilities in the US began utilising XLPE in 1968 in medium voltage applications.

Special features of XLPE include low dielectric loss and high dielectric strength [32]. In the following years, further developments in material science were made in efforts to improve the performance of cables especially in high and extra high voltage applications. One development made is the introduction of water tree retardant XLPE [33].

Underground cables are usually classified according to number of cores, voltage rating, cable construction, insulation type, and manner of installation. Number of cores includes but not limited to single core or triple core. Voltage ratings are categorised into five types: low tension cable (up to 1kV), high tension cable (1 to 11kV), super tension cable (11 to 33kV), extra high-tension cable (33 to 66kV), and extra super voltage cable (above 132kV). Regarding the construction of the cable, it may either be belted, screened, or pressured. Common types of insulations used in cables are paper, rubber, PVC, and PE. The manner of installing and laying out of cable may either be direct buried, channels, trough, and gas insulated lines [34].

2.4 Components of a power distribution cable

Additional components were introduced to handle the challenges emerging from the significant voltage increase in power distribution. Hence, it becomes beneficial to look into a detailed description of the cable components. This is especially essential in the case of underground power distribution cables in emphasising the extra considerations taken in its design.

The parts of a power distribution cable include the core, core screen, insulation, insulation screen, and outer sheath as seen on Figure 2.1 and Figure 2.2.

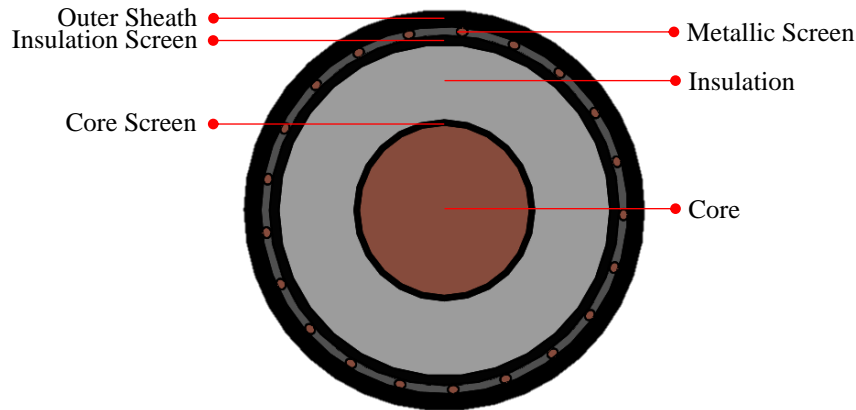


Figure 2.1: Cable parts (cross-sectional view)

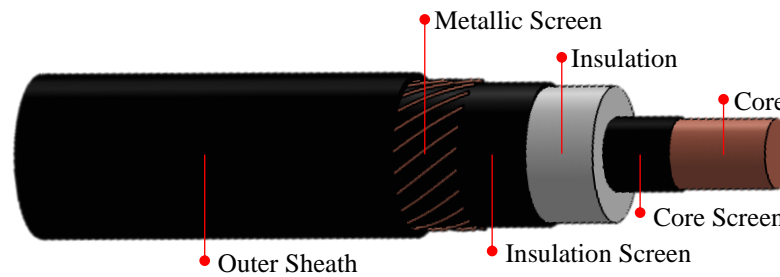


Figure 2.2: Cable parts (longitudinal view)

2.4.1 Core

The core (or conductor) is a conductive material which serves to carry electric current. The core is commonly round [35] and may be a solid one or in multi-strand form. A solid core is tougher but less flexible (hence lower endurance strength) while a multi-strand core offers better flexibility (hence higher endurance strength) but with less durability. In material selection, despite silver being the best core, Copper and Aluminium are more preferred since they are significantly cheaper. Considering the same volume, the conductivity of Aluminium is around 61% of Copper but due to significantly lower density, it only weighs about 30% of the Copper. With these

variation in properties, the selection of the size of a core, configuration, and material is critically observed depending on various factors like flexibility, toughness, voltage drop requirement, cost, and weight [36]. In sizing of cores, the length (of diameter) and area (of cross-section) are mostly considered. Typical size of copper and Aluminium conductors (stranded compacted) are shown in Table 2.2 based on IEC 60228 [37] and Nexans Olex [38].

Table 2.2: Conductor Size

Nominal Conductor Area	Diameter (Stranded Compacted)		
	(mm)		
	IEC 60228	Nexans Olex	
mm ²	Copper & Aluminium	Copper	Aluminium
10	3.6-4.0	-	-
16	4.6-5.2	4.8	-
25	5.6-6.5	5.8	-
35	6.6-7.5	6.8	6.9
50	7.7-8.6	8	8.1
70	9.3-10.2	9.6	9.6
95	11.0-12.0	11.5	11.4
120	12.3-13.5	13.1	12.8
150	13.7-15.0	14.5	14.2
185	15.3-16.8	16.1	15.7
240	17.6-19.2	18.5	18
300	19.7-21.6	20.7	20.1
400	22.3-24.6	23.6	23
500	25.3-27.6	26.5	26.5
630	28.7-32.5	29.9	29.9
800	-	35.9	34.2
1000	-	40.2	40.2
1200	-	43.8	43.8

2.4.2 Core screen

Core screen is the interface between a core and insulation to prevent damage caused by partial discharges. The partial discharge occurs when high electric fields concentrate on gaps with air in

which energised ions cause degradation of the insulation material. The insulation then becomes vulnerable to water tree formation which leads to the eventual failure of the insulation; hence the manufacturing process of the core screen should be carefully performed as to ensure that the surface of the core screen has a smooth texture, round geometry, and well contacted with the insulation [35]. The application of core screen is greatly considered in medium and high voltage applications starting at around 3.3kV [39]. Usually, the material used for the core screen is similar to the polymeric insulation used but with added feature of being impregnated with carbon black. This causes the core screen material to act as a semiconductor and allows for the even radial distribution of the stress due to the electric field at the interface to prolong the life of the cable [40-42].

2.4.3 Insulation

In the discussion of the development of power distribution cables, the insulation (also referred to as dielectric) is commonly an emphasis. Insulation is a non-conductive material that prevents the flow of electric current. It also helps conserve the electrical energy delivered by preventing it to dissipate into the environment. Insulation can be classified into two types: laminated and extruded. Laminated insulation is one of the earliest types of insulation which is exclusive to PILC cables. This insulation is made by stacking layers of oil or gel impregnated paper. Lead sheath is used to enclose the insulation. Despite its application in cables for more than a century, there has been a decreasing number in the use of PILC which can be attributed to its weak moisture resistance and complications in splicing and terminating [43]. The primary reason for this decline can be attributed to its environmental impact with the use of lead and impregnators. For the extruded insulation, it can be further divided into two types: thermoplastic and thermoset. Both thermoplastics and thermosets exhibit softening by heating and retain shape by cooling. The difference is that thermoplastics can be repeatedly heated and cooled, hence recycled, and reused

while thermosets can only perform the heating and cooling once due to the effects of polymerisation. With the transformation of thermosets into more rigid structure due to higher molecular weight via cross-linking, their melting point is significantly higher than thermoplastics. Examples of thermoplastics include PVC and PE which may be HMWPE which is also referred to as High Density Polyethylene (HDPE) or Low Molecular Weight Polyethylene (LMWPE) which is also referred to as Low Density Polyethylene (LDPE). On the other hand, example of thermosets includes XLPE, Water Tree Retardant Cross-Linked Polyethylene (WTR-XLPE) also more shortly referred to as Tree Retardant Cross-Linked Polyethylene (TR-XLPE), and EPR [36].

2.4.4 Insulation screen

Similar to the core screen, the insulation screen allows smooth cylindrical interface between the insulation and the metallic screen. It also provides even radial distribution of electric field around the insulation, hence relieving high voltage stress concentrations. Additionally, it maintains ground potential for the voltage outside the cable in which fault currents are directed to the earth [43-45]. The application of insulation screen is required in voltage applications starting at 3.3kV [39].

2.4.5 Metallic screen

Metallic screen serves as a metal path around the insulation screen to ground and carry the cable's capacitive charging current to avoid the cable to act as a capacitive divider [35]. The metallic screen may comprise of drain wires, metal tape, or Concentric Neutral (CN) wires. To make the outside of the insulation earth, the primary screen is earthed. The primary screen usually uses bare Copper, but it may also be coated with tin or lead. Other materials used for the screen include Aluminium and lead. The concentric neutral is placed helically around the primary screen and

serves two functions. The first one is to act as the metallic component of the insulation screen. The second function is to act as a conductor for the neutral return current [45].

2.4.6 Outer sheath

The outer sheath is an external covering which encloses the insulation and screen. It serves to protect them against mechanical, thermal, and chemical damages from the environment like infiltration of water leading to corrosion. Thermoplastics are the usual materials used for the outer sheath like PVC and PE including Chlorosulfonated Polyethylene (CSPE), LDPE, Medium Density Polyethylene (MDPE), and HDPE [36, 40].

2.5 Accessories in power distribution cable systems

Due to limits in lengths, combining two or more cables are necessary to act as a single cable to affect the transfer of electrical energy. Two cables are joined by joints or splices with appropriate jointing tools. Aside from connecting cables, joints serve other functions which include: controlling electrical stress using Faraday cage, replacing insulation using tubes or moulds, replacing earthing using metal canister or Copper braid and stocking, permitting the single core cables to be cross bonded, avoiding infiltration of moisture through seals, and ensure provision of mechanical strength [46].

For each end of the power distribution cable, termination is performed to connect them to their corresponding terminals [36]. The termination comprises of the cable end seal, connector (compression, soldered and welded, bolted, and set screw), and materials for the electric stress relief and electro-chemical track resistance [47]. Goulsbra [46] listed the various functions of terminations with the corresponding means of achieving them which include: making sure that

air is not present in particular crucial points through tapes or putties, avoiding electric stress concentrations using moulded earth with conical geometry or stress control tube made from material with high permittivity and low resistivity, preserving the quality of cable insulation from external surrounding through application of mould or tubes resistant against erosion and tracking, performing earthing, avoiding infiltration of moisture by application of sealant at termination ends, providing link to certain electrical equipment using lugs, and covering bare connections using bushing boots.

In power distribution cable system, the joints and terminations are referred to as accessories. In the design of accessories, there are three primary considerations. The first one is the electrical performance which considers the radial and longitudinal electrical stress experienced by the accessories to be designed to acceptable limits. The radial electrical stress takes into account the various relative permittivities of insulation layers used. For polymeric cables, high permittivity can decrease the electrical stress by 3 to 8 times while presence of void in the form of air or gas may increase to some factor. Therefore, it is very important to ensure that the insulation is sufficiently smooth enough to avoid the formation of voids especially prior to being tampered by another joint insulation. The second consideration is the thermal performance which emphasises the tensile and compressive forces generated due to the cooling and heating of the cable system which the accessories must be capable to handle. The last but not necessarily the least consideration is the mechanical performance which, aside from the thermo-mechanical performance previously discussed, is applied to joints buried under the ground being able to withstand the vertical loading of the soil [48].

Calcara et al. [26] conducted a research regarding faults in joints of underground cables. As have been discussed, 64% of the failures was associated to joints while 12% associated to the

terminations and the remaining 24% to the cables. They also performed analysis of the joint's failures with respect to the months. Data showed that there are significant number of joints failures during hot months for the years 2015 and 2017 which were quadruple of that of the annual average. Hence, overheating was pointed to be a major factor in the occurrence of joints failures in line with significantly high ambient temperatures during summer periods, not enough dissipation of heat in the surroundings, and anomalies in the cable joints.

Trends in jointing and termination involve skill requirement, performance time, and tool simplification. Skill requirement addresses early failures caused by improper core settings of jointers. For the performance time, the quicker the installment can be performed, the more time can be saved which reflects lesser cost. Simplification reduces the required tools to perform the jointing and terminations which equates to reduction in purchase and corresponding transportation cost [49].

2.6 Theoretical modelling of cable insulations

Several studies have been performed in efforts to predict insulation life by investigating the ageing mechanisms involved in the degradation process resulting to breakdown. Properties are selected which will most likely give good correlation to the ageing and breakdown phenomenon. Models are formed to relate the variables selected and statistical methods are applied to come up with the best fit between the data from the mathematical model and those obtained from experimentation. Some notable publications regarding the study of ageing and breakdown of insulations are presented in chronological manner to emphasise developments.

In 1973, Simoni [50] began an examination of theories regarding thermal and electrical ageing life tests which involved the fundamental ageing law, Arrhenius equation, Weibull distribution, and Eyring equation. He then proposed an extension of these by applying a phenomenological approach which involved neglecting the mechanism of deterioration and considering the only the effects. Investigation of the electrical ageing led to understanding of the relationship between short-time and long-time dielectric strength suggesting new approach for voltage-endurance test which involved measurements of dielectric strength of pre-stressed samples.

It was described that voltage life tests involved subjecting the test specimen to constant a.c. voltage gradient until breakdown occurs. This allowed characterisation of the life of the test specimen for a corresponding stress or vice versa through the plotted voltage lifeline. On the contrary, the thermal life tests involved the plot between a selected property and ageing time. When the selected property dropped to a predetermined value called the failure criterion, the ageing time was regarded as the ageing life or end of life of the test specimen. The appropriate selection of property considered the degradation process. For the thermal life test considering a chemical approach, it was essential to be knowledgeable of the connection of the property P , temperature T in which the test specimens are subjected, and the exposure time t to be able to arrive at the t values when P drops to the particular predetermined failure criterion value, hence an estimation of the ageing life for a particular temperature. Simoni [50] referenced the work done by Dakin and Mamlow for the equation of the fundamental ageing law as shown in (2.1) to (2.7):

$$\frac{dP}{dt} = -K \cdot P^\alpha \quad (2.1)$$

where P was referred to the property, K referred to the velocity coefficient of chemical process, and α referred to the reaction order. The coefficient K was expressed in terms of the Arrhenius law equation as shown in the following:

$$K = A \cdot e^{-\frac{E}{R \cdot T}} \quad (2.2)$$

where A and E were referred to as characteristic material constants (E being the activation energy), R referred to the gas constant, and T referred to the temperature in absolute scale. Algebraic manipulation followed by integration was performed on (2.1) as shown in the following:

$$\int_{P_0}^P \frac{dP}{P^\alpha} = - \int_0^t K dt \quad (2.3)$$

where P_0 was referred to the initial property value corresponding to $t = 0$. An assumption was made in which the temperature and K were considered constant which allowed (2.3) to become:

$$\int_{P_0}^P \frac{dP}{P^\alpha} = f(P) - f(P_0) = -K \cdot t \quad (2.4)$$

Then (2.2) was substituted to (2.4) as follows:

$$f(P_0) - f(P) = A \cdot e^{-\frac{E}{R \cdot T} \cdot t} \quad (2.5)$$

Boundary condition was set in which it became failure time or material life l when P drops to the predetermined failure criterion value P_F which were applied in (2.5) as shown in the following:

$$f(P_0) - f(P_F) = A \cdot e^{-\frac{E}{R \cdot T} \cdot L} \quad (2.6)$$

Logarithm was then applied to (2.6) which revealed the famous thermal life-law as shown in the following:

$$\ln\left(\frac{L}{t_0}\right) = C + \frac{B}{T} \quad (2.7)$$

where t_0 was referred to the appropriate reference time which was usually 1 hour, C equivalent to $\{\ln[f(P_0) - f(P_F)] - \ln(t_0 \cdot A)\}$, and B equivalent to $\left(\frac{E}{R}\right)$. A semi-log plot of (2.6) between log of life and inverse of temperature yielded a straight line which allowed a simple extrapolation of the test data to lower temperatures considering that the Arrhenius law applies; otherwise, the life line would be a curve. It was addressed that the most significant trouble for the test was the

selection of the property pertaining to the degradation phenomena. The property used was dielectric strength which presented a drawback of being virtually constant for a significant period. Literature referenced to Moses by Simoni [50] presented dielectric strength measurements of insulating wrappers (silicon bond glass cloth-backed mica paper, silicone-varnished glass cloth, organic bond glass cloth-backed mica wrapper, organic-varnished cotton cloth, and organic-varnished glass cloth) versus ageing time at 175°C. Results showed decreasing value of dielectric strength with increasing ageing time in the form of downward curvature for all insulations. From another literature referenced to Montsinger by Simoni [50] which involved percent tensile strength versus ageing time (up to 68 weeks) of yellow varnished cloth both in air and oil at temperatures of 90°C, 100°C, and 110°C. Results showed a general decrease of the percent tensile strengths with increasing ageing time in the form of downward curvatures in air and upward curvatures in oil. In the quantification of material degradation, non-destructive properties were usually preferred including weight loss, resistivity, and dielectric loss. A new type of analysis by thermogravimetric means was also tackled which involved continuous measurement of weight with time and temperature allowing significantly shorter test times. The selection of end-point criterion was necessary to define the event of inability of insulation to function anymore (failure point). The dielectric strength served to be the best option for such consideration since breakdown was characterised by the dropping of this property to the value of the voltage applied. This became the basis of the point that the dielectric strength being a reference for the other properties and that endpoint value was determined through breakdown tests [50].

For the voltage-endurance test, a probabilistic approach was applied. The performance of the voltage-endurance test involved the application of constant a.c. voltage requiring no property measurements. A particular applied a.c. voltage corresponded to a particular breakdown time with tendency for large dispersion causing various breakdown times even for significantly similar test

specimens. There were also incidents where no breakdown occurred even for a significant period of time that the test was stopped prior to failure. Even so, determination of failure for a percentage of the specimens can be done by resorting to a probabilistic approach. The percentage expressing the failure probability Φ was treated as a function of time and applied voltage. The distribution of the probability failure was defined using the Weibull function expressed as follows:

$$\Phi(t, G) = 1 - e^{-c \cdot t^a \cdot G^b} \quad (2.8)$$

where Φ was referred to as failure probability, t referred as time, G referred as effective voltage gradient applied, and a , b , and c referred as the material constants. By letting G be a constant value, the equation became:

$$\Phi(t, G) = 1 - e^{-c' \cdot t^a} \quad (2.9)$$

where c' is equivalent to $c \cdot G^b$. By performing natural logarithm on the equation twice, the following equation was obtained:

$$\ln \left\{ \ln \left[\frac{1}{1 - \Phi(t)} \right] \right\} = k' + a \cdot \ln \left(\frac{t}{t_0} \right) \quad (2.10)$$

where k' was equivalent to $\ln(c' \cdot t^a)$ and t_0 referred to appropriate reference time value. Equation (2.10) produces a straight line in a Weibull plot between cumulative percent and logarithm of time with $\frac{1}{a}$ as slope. An inverse relationship between coefficient a and standard deviation of the logarithm of time was also declared by the observation that interval associated to predetermined failure probability values decrease with increasing slope. By having assumed a constant value of t in (2.8), a straight-line Weibull plot was produced between cumulative percent and logarithm of voltage gradient having a slope of $\frac{1}{b}$ that is inversely proportional to the logarithm of the voltage gradient. For equal probability failure $\Phi = \bar{\Phi}$ in which (G, t) pair values were considered, a straight line was also formed in a bi-log plot based from the equation:

$$\ln \left[\ln \left(\frac{1}{1 - \bar{\Phi}} \right) \right] = b * \ln \left(\frac{G}{G_0} \right) + a \cdot \ln \left(\frac{t}{t_0} \right) + k'' \quad (2.11)$$

where G_0 was referred to as appropriate reference voltage gradient value and k'' equivalent to $\ln(c \cdot G^b \cdot t^a)$. Different values of probability $\bar{\Phi}$ corresponded to group of parallel lines (described as endurance lines) with $\frac{a}{b}$ as slope. By setting a 50% probability value ($\bar{\Phi} = 0.5$), endurance line called median endurance/lifeline was derived having an equation of:

$$\ln\left(\frac{L}{t_0}\right) = k - n \cdot \ln\left(\frac{G}{G_0}\right) \quad (2.12)$$

where k is equivalent to $\left[\ln(\ln 2) - \frac{k''}{a}\right]$ and n equivalent to $\frac{b}{a}$. Equation (2.12) was also described in linear coordinates as follows:

$$L = \frac{\gamma}{G^n} \quad (2.13)$$

where γ and n were referred to as constant insulation characteristics varying with manufacture method, temperature, and environmental factors. Various literatures were cited by Simoni [50] agreeing with (2.13) where n values were determined: 15-20 for mica-asphalt according to Starr and Endicott, 9 for polyethylene according to Kreuger, 9 for polystyrene according to Artbauer and Griac, and 15 for plastic insulated MV cables according to Occhini. The inverse relationship between n and slope of the straight graph in a bi-log plot was also emphasised. It was also noted that lower isothermal breakdown voltage gradients scatter and greater breakdown times scatter at constant voltage correspond to the larger n values. There were literatures cited which do not agree with (2.13). For instance, experiment of polyester foil (laminated sheets) by Meyer revealed non-parallel straight lines which indicated that the ageing mechanism changed and consequently also n too.

After the discussion of the two insulation life laws corresponding to thermal and electrical ageing treatments, a combined treatment of both was discussed. The investigation began by introducing an equation similar to (2.4) as shown in the following:

$$F(P) = K \cdot t \quad (2.14)$$

where K was denoted as the deterioration rate or rate of chemical reaction being a function of both thermal and electrical stress. Instead of applying the Arrhenius law, the Eyring law was applied expressed as follows:

$$K = k_1 \cdot T^w \cdot e^{-\frac{B}{T}} \cdot e^{(k_2 + \frac{k_3}{T}) \cdot f(S)} \quad (2.15)$$

where k_1 , w , B , k_2 , and k_3 denote material constants that do not vary with stress, temperature and time while $f(S)$ referred to electrical stress dependent function. Hence by equating $f(S)$ to zero, the equation was reduced to thermal ageing model as shown:

$$K = k_1 \cdot T^w \cdot e^{-\frac{B}{T}} \quad (2.16)$$

which was similar to the Arrhenius equation except for the additional term T^w . But since w is usually near 1, for usual test temperatures (most probably particular to test temperatures with small intervals), the term T^w was characterised by slight changes as opposed to the term $e^{-\frac{B}{T}}$, hence (2.16) and (2.2) were almost compatibly the same. The Arrhenius law was usually preferred owing to better fitting of the data from experiments. Considering T as constant, (2.15) was expressed as follows:

$$K = \mu \cdot e^{m \cdot f(S)} \quad (2.17)$$

where μ is equivalent to $(k_1 \cdot T^w \cdot e^{-\frac{B}{T}})$ and m is equivalent to $k_2 + \frac{k_3}{T}$. Having assumed that $f(S)$ is equivalent to $\ln(S)$, (2.17) was then expressed as:

$$K = \mu \cdot e^{m \cdot \ln(S)} = \mu \cdot S^m \quad (2.18)$$

Having considered (2.14) in which the property P decreased to the property failure criterion value P_F , then the time t became life of material L which was applied to form the life equation as shown:

$$F(P_F) = K \cdot L \quad (2.19)$$

With the assumption that $F(P)$ at failure is a characteristic constant with respect to the material, the life equation was then interpreted as follows:

$$K \cdot L = \text{constant} \quad (2.20)$$

By equating (2.18) to (2.20), the following equation was derived (note that the absence of μ was due to its arbitrary nature, hence simply merged to the constant of the following equation):

$$S^m \cdot L = \text{constant} \quad (2.21)$$

It was observed that (2.18) was simply the same as (2.13) in which $G = S$, $m = n$, and $\gamma = \text{constant}$. Hence, an equation which covered both thermal and electrical ageing was derived by substituting (2.15) to (2.14) with the assumption that $f(S)$ is equivalent to $\ln(S)$ [50].

Then a new phenomenological theory was proposed. This involved the introduction of a general ageing equation for insulations that related property, stress, and time. Since three variables indicate a three-dimensional geometric presentation of the equation, two variables were taken at a time to produce a plot with the other one variable being held as a parameter. $P(t)$ represented degradation curves at constant stress while $S(t)$ represented endurance curves at constant property. For a property failure criterion value P_F , the endurance line produced was called the lifeline. The general ageing law was based on (2.1) including its integrated form (2.4) having emphasised that K was dependent to stress, particularly thermal stress in the form of temperature. Considering relative property value p equivalent to $\frac{P}{P_0}$ and ranging from 1 (corresponding to time at 0) to p_F (corresponding to time at failure or life L), (2.1) was written as follows:

$$\frac{dp}{dt} = -K \cdot p^\alpha \quad (2.22)$$

having noted that the same symbol for the degradation rate was used despite change in its dimension (owing to the use of relative property instead of the property). Having considered a constant stress, integration of (2.22) lead to the following form:

$$\int_1^p \frac{dp}{p^\alpha} = -K \cdot t \quad (2.23)$$

The general ageing law was also based on (2.14) with more specification regarding stress dependence of the degradation rate and the use of the relative property as shown in the following:

$$F(p) = K(s) \cdot t \quad (2.24)$$

A more explicit expression of $F(p)$ was used based on (2.23) in which

$$F(p) = - \int_1^p \frac{dp}{p^\alpha} \quad (2.25)$$

By evaluating the definite integral in (2.25) and considering different exponent α values, the following were derived:

First case where $\alpha = 0$ yielded a linear type

$$1 - p = K \cdot t \quad (2.26)$$

Second case where $\alpha = 1$ yielded an exponential type

$$\frac{1}{p} = e^{K \cdot t} \quad (2.27)$$

which was equivalent to

$$\ln\left(\frac{1}{p}\right) = K \cdot t \quad (2.28)$$

Third case where $\alpha > 1$ yielded a general type

$$\left(\frac{1}{p}\right)^{\alpha-1} - 1 = (\alpha - 1) \cdot K \cdot t \quad (2.29)$$

Although (2.29) was actually mathematically valid for $\alpha \neq 1$, the only considered values were 0 and those greater than 1 owing to the chemical-reaction law. However, in actual experiments, data plot revealed otherwise in which downward curvatures were observed. For this reason, it was advised to follow (2.24) instead. To come up with better fitting with results from experiment, (2.22) was considered but in this case, α was taken to be treated for any values, hence including negative values. This consequently violated the chemical hypothesis from which the equation was based but this was taken as a necessary step in order to arrive at a general law compatible not only

with thermal stress but also with electrical and mechanical stress. By considering only the effects and neglecting the degradation mechanism, the theory was classified as phenomenological. Degradation curves for electrical ageing were observed to reveal monotonic trend suitable on (2.22) but considering negative α . Hence, a new variable β equivalent to $-\alpha$ was introduced in (2.23) as shown:

$$\int_1^p p^\beta dp = -K \cdot t \quad (2.30)$$

Evaluation of the integral in (2.30) lead to the following:

$$1 - p^{\beta+1} = (\beta + 1) \cdot K \cdot t \quad (2.31)$$

Sample graphs of (2.31) were presented which revealed monotonic trend of lines having downward curvatures for all positive values of β while a straight plot was produced by $\beta = 0$ [50].

For constant stress equation, (2.24) called the general behaviour law and the general life equation as shown in the following were recalled:

$$F(p_F) = K \cdot L \quad (2.32)$$

where it can be observed that (2.32) was simply (2.19) in which relative property p was used instead of property P and that K denoted ageing rate instead of chemical reaction rate that was a function of stress and not of time. The function $F(p)$ denoted the ageing quantity which increased linearly as time increased which can be expressed as (2.25). A parallel investigation was performed between (2.32) and (2.13) with the latter denoted as inverse power law which resulted to direct proportionality relations between K and G^n as shown in the following:

$$K = K_1 \cdot G^n \quad (2.33)$$

where K_1 was referred to as material characteristic constant. By substituting (2.33) into (2.24), the following equation for constant stress was derived [50]:

$$F(p) = K_1 \cdot G^n \cdot t \quad (2.34)$$

For variable stress, K was defined as a function of time-dependent stress as shown in the following:

$$F(p) = \int_0^t K[S(t)] dt \quad (2.35)$$

Considering the occurrence of failure when relative property p drops to p_F , the time becomes life L_v with the subscript v denoting variable stress. Having applied these failure conditions, (2.35) became:

$$F(p_F) = \int_0^{L_v} K[S(t)] dt \quad (2.36)$$

Having considered a linear variation of stress which was also known as progressive stress, a linear relation was established as follows:

$$S = \lambda \cdot t \quad (2.37)$$

Equation (2.36) was then substituted to (2.35) to arrive at the following equation:

$$F(p_F) = \int_0^{L_p} K(\lambda \cdot t) dt \quad (2.38)$$

where L_p was referred to the life under progressive stress. To be able to evaluate the integral (2.38), the function K was substituted with (2.33) having considered $G = S = \lambda \cdot t$ as follows:

$$F(p_F) = \int_0^{L_p} K_1 \cdot \lambda^n \cdot t^n dt = \frac{K_1 \cdot \lambda^n \cdot L_p^{n+1}}{n + 1} \quad (2.39)$$

Equation (2.39) was also equivalent to:

$$F(p_F) = \frac{K_1 \cdot G_F^n \cdot L_p}{n + 1} \quad (2.40)$$

where G_F was also equivalent to $\lambda \cdot L_p$ which corresponded to the voltage gradient at failure for the test under progressive stress. Having considered constant gradient voltage at failure for (2.34), the following equation was derived:

$$F(p_F) = K_1 \cdot G_F^n \cdot L \quad (2.41)$$

By equating (2.40) and (2.41), a relationship between the lives at constant stress and progressive stress was derived as shown in the following:

$$\frac{L_p}{L} = n + 1 \quad (2.42)$$

Equation (2.41) was used by other literatures in the conversion of constant stress data to progressive stress data and vice versa. It was noted that progressive stress answered the trouble of having highly scattered data from tests conducted under constant stress.

The equation of the dielectric strength as a function of time was also investigated where the study of voltage life was deemed essential. By considering the characteristic constant γ at initial and general conditions from (2.13) which was the inverse-power law now treated as the life law, the following relationship was derived:

$$\frac{L}{t_0} = \left(\frac{G_{F0}}{G} \right)^n \quad (2.43)$$

where G_{F0} corresponded to gradient at life t_0 . By expressing the ratio of the gradient variables as relative gradient value g with G_{F0} as reference, the following equation was derived:

$$\frac{L}{t_0} = \frac{1}{g^n} \quad (2.44)$$

With reference to (2.34), the ageing amount for a pre-stressed material was defined by:

$$F(p_F) = K_1 \cdot G^n \cdot L = K_1 \cdot G_{F0}^n \cdot t_0 \quad (2.45)$$

The ratio of ageing amount to failure value χ was then derived by dividing (2.34) to (2.45) as follows:

$$\chi = \frac{F(p)}{F(p_F)} = g^n \cdot \frac{t}{t_0} \quad (2.46)$$

For a particular time t , the remaining life was represented as $L - t$. These two variables were explicitly solved from (2.44) and (2.46) respectively as shown in the following:

$$L - t = \frac{t_0}{g^n} - \frac{t_0 \cdot \chi}{g^n} \quad (2.47)$$

By dividing both sides by t_0 , the following was derived:

$$\frac{L - t}{t_0} = \frac{1 - \chi}{g^n} \quad (2.48)$$

Having considered that time t at which dielectric strength equals stressing gradient equivalent to $L - t_0$ i.e. $t_0 = L - t$, substitution was performed on (2.48) resulting of the following:

$$\frac{1 - \chi}{g_F^n} = 1 \quad (2.49)$$

Algebraic rearrangement of (2.49) lead to the following equation:

$$\chi = 1 - g_F^n \quad (2.50)$$

Having equated (2.46) and (2.50), the following relationship was arrived:

$$1 - g_F^n = g^n \cdot \frac{t}{t_0} \quad (2.51)$$

Equation (2.51) provided a mathematical relations between relative dielectric strength for the property, relative voltage gradient for the stress applied, and time. A semi-log plot between relative dielectric strength and relative time based from (2.51) for some paired values of g and n showed curves tending towards sharp decrease which were identified to be in good agreement with literature by Simoni [50] like that of Meyer (breakdowns tests on insulated bars subjected to 13.8kV and pre-stressed at 50kV) considering $n = 15$. Another literature cited was that of Koikow who performed a.c. short time dielectric strength test on Polytetrafluoroethylene (PTFE) film subjected to 1.2kV stress showed curve shape in perfect agreement with (2.51). The deterioration curves produced from (2.1) by considering negative value of exponent showed a similar trend compared to those produced by (2.51). Analysis of the exponents with (2.31) produced the following relations:

$$n = \beta + 1 = 1 - \alpha \quad (2.52)$$

Having substituted (2.52) on (2.31) and applied relations with (2.24), the following equation was derived:

$$F(p) = F(g_F) = \frac{1 - g_F^n}{n} \quad (2.53)$$

By equating (2.51) to (2.53), the following equation was derived:

$$F(p) = \frac{1 - g_F^n}{n} = \frac{g^n}{n} \cdot \frac{t}{t_0} \quad (2.54)$$

From (2.54), the rate of ageing K was defined as follows:

$$K = \frac{g^n}{n \cdot t_0} \quad (2.55)$$

Having considered (2.44) and (2.55), an interesting relationship was derived as shown:

$$F(p_F) = K \cdot L = \frac{1}{n} \quad (2.56)$$

It was shown in (2.56) that coefficient n that represents the reciprocal of the slope of lifeline in a bi-log plot, serves to be a parameter that characterised material ageing. It was also noted that (2.51) held only valid if the life law followed the form of an inverse-power law [50].

The presented ageing function (2.24) provided a means of predicting expected life through evaluation of ageing like thermal tests. It was also shown that dielectric strength associated well with life law making it possible to learn about the insulation life using known values of dielectric strength. Guidelines in conducting the test of dielectric strength were given. This involved sufficiently large number of test specimens that were arranged into few groups where each were subjected under equal voltage of differing duration. For each time a group reached the pre-determined voltage stress duration, each specimen from the group were subjected to dielectric strength test. The measured dielectric strength from each group with their respective ageing time served as a coordinate or point in the plotting of the degradation curve. Upon completion of the plotting of the degradation curve, the derived line was compared with the theoretical model. If

good agreement was observed, n (life coefficient) shall be computed. Compared to other tests, several advantages were pointed out. First was that this test ends prior to the failure of specimens. Hence, considering the same duration of test time, the stress was lower which was near actual service value. Next was that, assuming that thickness of test specimens was not too small, the G_F values were less scattered owing to the less scattered values of isothermal breakdown gradient compared to the breakdown times at constant voltage. Another advantage was the feasibility of checking lifeline shape experimentally which may either be through the degradation curve of dielectric strength or comparison of life coefficient n for various stresses. It was reminded that in the case of statistical tests, coefficient n was known through the slope of the regression line in a bi-log plot. Lastly, property measurements may be performed prior to the test specimens being punctured which in turn provides wide knowledge about the electrical behavior of insulation material. The experiment performed involved numerous spherical ageing electrodes and a dielectric strength measuring equipment. The ageing cell selected was in air to avoid degrading effects when subjected to other fluids. The configuration of the electrode with respect to the specimen was made to effect high ionisation (by the induced electric field) along the circumference of the central area to allow analysis of the corona resistance as well. On the contrary, the short-time dielectric strength test was performed in oil to prevent surface flashover on the test specimen. Progressive voltage test was performed with an average duration of 1 minute. About 8 to 15 specimens of 1mm to 1.5mm thick each were contained in each group. Every specimen was punctured in the areas subjected to electric field (central area) and corona (around the central area) each treated separately. The dielectric strength measurements showed low scatter having standard deviation not exceeding 10%. The first results were those obtained from PVC at electric stress of 12.8kV/mm which was enough to produce heat due to dielectric losses that contributed to the insulation ageing. The plot of dielectric strength versus ageing time showed good agreement with the proposed theory with estimated values of n between 12 and 14.

It was noted that this result was particular to the measurement in the central area only whereas on the area subjected to corona showed significantly lesser decrease which proved that PVC has high corona resistance. The next result involved PE subjected to electrical stresses of 18kV and 24kV in which the dielectric loss was not enough to produce significant heating that affected ageing, hence solely considered electrically aged ones. No significant increase was observed on lower stresses which lead to the consideration of increasing the gradient to 20kV/mm. The high voltage gradient caused significant decrease in the dielectric strength both in the central area and the area subjected to corona where the former showed monotonic behaviour while the latter showed non-monotonic behaviour. The estimated n was 10 for the 6 specimen groups. Last result involved EPR subjected to 14kV/mm electrical stress which showed a more linear decrease in dielectric strength which did not agree with (2.51). The reason for such was associated to two reasons. One was that the bi-log plot may have been concaved upward indicating variability of n which increased as stress decreased. Another was that at constant stress, n is dependent on time due to the cross-linking of EPR where the settlement of its structure occurs after few hours of ageing stress in which afterwards n would be constant and a downward curvature of the curve will be observed [50].

In 1981, Simoni [51] investigated a life model compatible for multiple stresses particularly thermal and electrical stress and with added modification in line with threshold for better data fitting. The study of insulation can be performed by considering changes in time behavior referred to as ageing. Suitable properties of insulation were considered in the quantification of these changes. Ageing at a certain end point led to the breakdown phenomenon which was characterised as inability of the insulation to perform designated work. Breakdown was determined when the insulation property strength reached the applied stress value. The effect of changes in strength translated to changes in the insulation structure, hence affecting other insulation properties as

well. A function $F(p)$ was introduced with variation rate R that was constant when stress was constant. The $F(p)$ function was referred to as the ageing, cumulative degradation, or total damage function equivalent to $R \cdot t$ where t denotes time. For the failure boundary condition, when the property dropped to the failure criterion value p_L , the ageing time t becomes life L , hence modified the ageing function as $F(p_L) = R \cdot L$. When $F(p_L)$ was considered, an inverse relationship between ageing rate and life was observed. The discussion then began from the models for single stress namely thermal and electrical stress. Tracing back history, Montsinger acquired a connection between ageing life and temperature but it was Dakin who developed the thermal ageing relations based on the chemical reaction theory. The theory proposed that increase in temperature accelerated the rate of chemical reaction (which was translated to rate of ageing) that lead to thermal ageing. This empirical relationship was defined by the so-called Arrhenius equation as shown in (2.57):

$$R_t = A \cdot e^{-\frac{B}{T}} \quad (2.57)$$

where R_t was referred to as thermal ageing rate, A and B referred as constants where B was equivalent to the ratio of activation energy and Boltzmann's constant, and T referred as temperature in absolute scale. Based on inverse relationship between ageing rate and life, the following equation was derived:

$$L_t = k_t \cdot e^{\frac{B}{T}} \quad (2.58)$$

where L_t was referred to as the thermal life and k_t was equivalent to $\frac{1}{A}$. By applying ambient conditions on (2.58), k_t (assumed constant) was expressed as follows:

$$k_t = L_0 \cdot e^{-\frac{B}{T_0}} \quad (2.59)$$

where L_0 corresponded to life at room temperature T_0 . The room temperature was then replaced by a more convenient temperature ΔT equivalent to the following:

$$\Delta T = \frac{1}{T_0} - \frac{1}{T} = \frac{T - T_0}{T \cdot T_0} \quad (2.60)$$

Substitution of this temperature lead to the following equation:

$$L_t = L_0 \cdot e^{-B \cdot \Delta T} \quad (2.61)$$

The purpose of this was to express the limit of ΔT as temperature T approached infinity to be equal to $\frac{1}{T_0}$. Both (2.58) and (2.61) produced a straight plot for logarithm of life versus reciprocal of temperature. For the electrical ageing model corresponding to voltage endurance of insulation, two models were considered namely inverse power law and exponential law. The inverse power law was represented as follows:

$$L_e = c \cdot G^{-n} \quad (2.62)$$

where L_e denoted electrical life particularly at room temperature, c and n referred as constants, and G denoted electrical stress. Equation (2.62) produced a straight graph in a bi-log plot with slope n . On the other hand, the exponential law was represented as follows:

$$L_e = k \cdot e^{-h \cdot G} \quad (2.63)$$

where k and h were referred as constants. For this equation, a straight graph was also produced in a bi-log plot of logarithm of life versus electrical stress with h as slope. From a statistical basis, the inverse power law was more preferred than the exponential type due to its conformity with Weibull statistics. For the agreement of the boundary condition of the thermal and electrical life model, by observation that $L_e = L_0$ when $G = 0$, the constant k from (2.63) was replaced with L_0 as follows:

$$L_e = L_0 \cdot e^{-h \cdot G} \quad (2.64)$$

Having performed logarithm of (2.61) and (2.64), the following equations were derived:

$$\begin{cases} \ln \frac{L_t}{L_0} = -B \cdot \Delta T \\ \ln \frac{L_e}{L_0} = -h \cdot G \end{cases} \quad (2.65)$$

It was observed that the two equations from (2.65) showed parallel format of the variables in which the logarithm of the relative life was negatively in direct proportion with their respective stress. Contrary to the thermal ageing equation, for the inverse power law, the equation followed that zero electrical stress corresponded to life tending infinity. This was adjusted by introducing electrical stress G_0 below which no ageing occurred, hence, for $G \leq G_0$, life was only associated to thermal ageing and equal to L_0 . This was represented by the following function:

$$L_e = L_0 \cdot \left(\frac{G}{G_0}\right)^{-n} \quad (2.66)$$

with the conditions that $G > G_0$, otherwise $L_e = L_0$ (when $G \leq G_0$). These modifications allowed compatibility of (2.66) with the Arrhenius law and with the more correct interpretation with regards to the life L_0 denoting life at room temperature with electrical stress involved no greater than G_0 . By performing logarithm on (2.61) and (2.66), the following equations were derived:

$$\begin{cases} \ln \frac{L_t}{L_0} = -B \cdot \Delta T \\ \ln \frac{L_e}{L_0} = -n \cdot \ln \frac{G}{G_0} \end{cases} \quad (2.67)$$

which were observed to be the same as (2.65) except that $\ln \frac{G}{G_0}$ was used instead of G . Another condition was also tackled about the value of voltage gradient G_S in which the insulation life approached infinity. It was described that electrical stress value no greater than G_S corresponded to absence of electrical ageing. Distinction between G_0 and G_S was made in which the former tended to life approaching L_0 while the latter tended to life approaching infinity. Dakin was referenced by Simoni [51] for a model depicting breakdown voltage to be dependent of failure time as shown in the following:

$$L_e = \frac{\alpha \cdot e^{-h \cdot G}}{G - G_S} \quad (2.68)$$

where α was denoted as constant corresponding to constant frequency. The validity of (2.68) was restricted to values of $G > G_S$ and it can be observed that as G tended toward G_S , life approached

infinity. It was confirmed that (2.68) agreed well with data from experiments but had the drawback of being incompatible with the Arrhenius model. With (2.68) being valid, (2.61) was proposed for modification in line with (2.68) [51].

The study was then focused on the combined stress condition considering thermal and electrical stress. The investigation began by considering the relationship of the ageing rates of the two stresses. An additive relationship which considered superposition effects expressed in the following:

$$R = R_e + R_t \quad (2.69)$$

was rejected since an additive relationship provided smaller combined ageing rate R value which was contrary to the results of the experiments. The ageing rate equation by Eyring was introduced which was presented as follows:

$$R = A \cdot e^{-\frac{B}{T}} \cdot e^{-(a+\frac{b}{T}) \cdot f(G)} \quad (2.70)$$

where A , B , a , and b were depicted as constants that do not vary with temperature, electrical stress, and time and $f(G)$ denoted a particular function dependent on electrical stress. When considering only the thermal ageing rate, $f(G) = 0$ which yielded (2.57). On the other hand, when considering only the electrical ageing rate, $f(G) = G$ based on the exponential model. By applying the inverse relationship of ageing rate and life, the following equation based on (2.70) was derived:

$$L = \frac{1}{A} \cdot e^{\frac{B}{T}} \cdot e^{-(a+\frac{b}{T}) \cdot G} \quad (2.71)$$

Further modifications were applied which involved considering room temperature conditions which yielded life L_0 (under no electrical stress), substitution of $\frac{1}{T}$ with ΔT , and $a + \frac{b}{T_0} = h$ by analysis with (2.64). These yielded the following equation based on (2.71):

$$L = L_0 \cdot e^{-B \cdot \Delta T - h \cdot G + b \cdot \Delta T \cdot G} \quad (2.72)$$

Equation (2.72) involved three variables including life, thermal stress, and electrical stress, hence representing a three-dimensional model of life under combined stress conditions. The three-dimensional surface (2.72) was also able to provide the thermal lifeline (when $G = 0$) and electrical life line (when $\Delta T = 0$). By performing logarithm operation, (2.72) became:

$$\ln L = \ln L_0 - B \cdot \Delta T - h \cdot G + b \cdot G \cdot \Delta T \quad (2.73)$$

Mathematically, the thermal and electrical life lines produced were straight when a coordinate system $(\ln L, \Delta T, G)$ was used for (2.73). By considering (2.61) and (2.64), (2.73) was alternatively expressed as follows:

$$L = \frac{L_t \cdot L_e}{L_0} \cdot e^{b \cdot G \cdot \Delta T} \quad (2.74)$$

which was described to provide a more understandable point regarding the incorporation of the ageing rates. Since L_0 denoted the largest value of life, it then followed that L was smaller compared to L_t and L_e . The term $b \cdot G \cdot \Delta T$ (from the exponent of the equation) served as a corrective term which compensated for the too short life values produced since the term increases with increasing thermal and electrical stress. A substitution was then introduced where $k_c = \frac{b}{h \cdot B}$ and applied to (2.74) and also considered (2.65) which led to the following equation:

$$L = \frac{L_t \cdot L_e}{L_0} \cdot e^{k_c \cdot \ln\left(\frac{L_0}{L_t}\right) \cdot \ln\left(\frac{L_0}{L_e}\right)} \quad (2.75)$$

Equation (2.75) was able to relate the insulation life of combined stresses. Alternatively, having considered inverse power law instead of exponential law on (2.70) so that $f(G) = \ln\left(\frac{G}{G_0}\right)$ and applying similarly the room temperature conditions in which life for no electrical stress was L_0 and substitution of $a + \frac{b}{T_0} = n$ and $\frac{1}{T} = \Delta T$, a life equation was derived based from (2.70) as follows:

$$L = L_0 \cdot e^{-B \cdot \Delta T} \cdot \left(\frac{G}{G_0}\right)^{-(n-b \cdot \Delta T)} \quad (2.76)$$

which was equivalent to (2.61) when $G = G_0$ and to (2.66) when $\Delta T = 0$ ($T = T_0$). Having considered placement of the terms in (2.76) as exponents, the following equivalent equation was derived:

$$L = L_0 \cdot e^{-B \cdot \Delta T - n \cdot \ln\left(\frac{G}{G_0}\right) + b \cdot \Delta T \cdot \ln\left(\frac{G}{G_0}\right)} \quad (2.77)$$

By performing logarithm on (2.77), the equation became:

$$\ln L = \ln L_0 - B \cdot \Delta T - n \cdot \ln\left(\frac{G}{G_0}\right) + b \cdot \Delta T \cdot \ln\left(\frac{G}{G_0}\right) \quad (2.78)$$

It was observed that (2.77) and (2.78) were identical with (2.72) and (2.73); differed only by the use of $\ln\left(\frac{G}{G_0}\right)$ instead of G [51].

In 1993, Montanari and Simoni [52] analysed the phenomenology of insulation ageing, and the various life models considered for the ageing. Despite the various research available for the last decade about the phenomenology of ageing, efforts regarding the phenomenology of ageing and life models for ageing were pushed to address the issues concerning the development of new insulations, requirement for greater stress characteristics, and reliability of insulation performance taking into account degradation processes like water treeing. As per standards of IEC and IEEE, ageing refers to any irreparable and damaging changes in the insulation influencing its capability to render required service performance. Ageing was caused by enforced stresses and various influencing factors leading to physical and chemical changes. Therefore, it became important to consider ageing-reactive properties as bases of the recognition and assessment of ageing. Mathematically, this would mean defining ageing as a function of the considered property or more specifically, the specific property that was failure related. The rate of ageing was then represented as the derivative of ageing with respect to time. The rate of ageing was taken as a function of

stress and independent of time which was associated with the monotonic behaviour of property with variation in time. The rate of ageing was also considered additive for serially applied stresses while multiplicative nature was considered for application of combined stresses. The general equation of insulation ageing was then derived by integration in which ageing was the product of ageing rate (function of stress) and time. Considering time to failure, ageing became the ageing limit while the general equation of insulation ageing became the general equation of insulation life. In the general equation of insulation ageing, the number of dimensions is two more than the number of stresses considered while for the general equation of insulation life, the number of dimensions is one more than the number of stresses considered. Hence, when only a single stress is considered (which may be due to assumption of dominance over other stresses), the ageing equation produced a three-dimensional surface having coordinates of stress, specific property, and time while the life equation produces a two-dimensional plane having coordinates of stress and life which could be produced by intersecting the life equation surface with the plane where specific property equals specific property limiting value. In the case of two stresses applied like thermo-electrical stress, the ageing equation produced a four-dimensional display of no visual equivalence having the two stresses, specific property, and time as coordinates while the life equation produced a three-dimensional surface having the two stresses and life as coordinates. The three-dimensional life surface was compatible in deriving the stress equations by equating one of the stresses to zero. Also, considering a constant value of life (which can be equal to expected insulation service life), the stress-versus stress plane can be derived allowing evaluation of the insulation endurance under multiple stress in the form of Stress Compatibility Index (SCI). Single stress models were available for electrical, thermal, and mechanical stress. Common models used were the exponential and inverse-power type (including constant stress and progressive stress) for the electrical stress and Arrhenius type for the thermal stress which were applicable considering amplitude to be constant. Eyring model was also used to derive models for

multiple stress. Curvilinear models for electrical life were also introduced which were applicable for thermo-electrical stress and takes into account the concept of electrical threshold where insulation life tended to infinity. The existence of electrical threshold had been earlier subjected to debate but is now accepted as supported by experiments. In actuality, even few thousand hours of experimental ageing were unable to show threshold tendencies except if the insulation exhibited unusually large threshold temperature and small activation energy. Distinguishing whether there is linear or curvilinear trend can be carried out at shorter times by resorting to multiple stress tests. In the case where linear trend was observed, the endurance coefficient may be used as reference for the insulation characterisation. If curvilinear trend was observed, the threshold value can be used as reference for the insulation characterisation. One trouble being considered in the application of life models with the experimental results was the determination of the parameters of the model including the confidence intervals. Apparently, more parameters equated to better determination of material behaviour but with consequence of greater uncertainty in the estimation of parameters and tendency of problems in convergence of estimation methods like maximum likelihood and least square regression. Owing to the stochastic nature of failure, broader confidence intervals were also produced. Ways of enhancing the accuracy of the estimation of parameter include increasing sizes of sample, increasing number of performed life tests, and decreasing the degree of censoring all of which will consequently increase test cycle cost. In line with this, it was argued that the selection of life model should be done first prior to data evaluation offering good fitting for stress ranges close to actual service conditions. It was also suggested that for newer ageing and life models, the treeing phenomenon should be associated by considering fractal approach.

In the derivation of the general phenomenological model for multi-stress conditions in insulation, experiments showed that the rate of ageing for multi-stress was significantly greater than additive

treatment of individual ageing rates but slightly below the multiplicative treatment. Hence, the latter was preferred but with the addition of a corrective term that is a function of the stresses. The equation related the specific life for multi-stress with the product of the individual specific life for each stress multiplied by the corrective term which was a function of the stresses. The equation offers compatible treatment for multiple stress capable of carrying out both the linear and curvilinear (associated with threshold) modelling of insulation life. In modelling electrical life (specific electrical life in this case), the common linear models used were the exponential model and inverse-power model. These linear models produced straight lines in semi-log and bi-log plots. The corresponding voltage endurance coefficients had inverse relationship with the slope of the lifeline and were used to characterise the endurance of insulation greatly considered in design for a reasonable range of stresses. For the modeling of thermal life (specific thermal life in this case), one of the usual models used was the Arrhenius model. A more favorable variation of the Arrhenius model was the substitution of the absolute temperature with the difference of reciprocals of reference temperature and absolute temperature and the substitution of the ratio between activation energy and Boltzmann constant with a single parameter. A straight line is produced when graphing the Arrhenius model in a semi-log plot. As per IEC 216, the determination of the Halving Interval in Celsius (HIC), Temperature Index (TI), and the 95% lower interval of confidence of TI was prescribed. The phenomenon called compensation effect was also recognised which was considered in thermal ageing. The compensation effect was associated with the activation enthalpy having linear relationship with entropy of degradation process that is actuated thermally. The single parameter in the Arrhenius model was then replaced with a binomial expression expressing linear relationship of the single parameter with the logarithm of insulation life. For the corrective function, the exponential and inverse-power model was used. The derived equations for the specific electrical life, specific thermal life, and corrective function were then substituted to the general phenomenological model for multi-stress yielding

to a four-parameter equation including the voltage endurance coefficient, reference multi-stress life, Arrhenius single parameter, and corrective function single parameter. Threshold was also recognised since there were evidences of asymptotic approach towards a stress value tending to infinite life. The adjustment for threshold was implemented by introducing quotients on the exponential and inverse-power model (for electrical life) which tended towards zero for electric stress tending towards reference electrical threshold and on the Arrhenius model (for thermal life) which tended to zero for thermal stress tending towards reference thermal threshold. Integrating the threshold adjustments in the general phenomenological model for multiple stress, the model now consists of six parameters in total having added two additional parameters namely reference electrical threshold and reference thermal threshold. The increased number of parameters produced a consequence of allowing greater uncertainty in the estimation of the parameters using methods like maximum likelihood method for the benefit of covering wide range of characterisation of endurance for single and multiple stress applications. Using the six-parameter model, the electrical lifeline can be derived by considering constant thermal stress (using temperature) while the thermal lifeline can be derived by considering constant electrical stress (using electric field) useful for determining criterion for insulation failure. It was emphasised that occurrence of failure was associated with the presence of electrical stress that introduced breakdown and the presence of thermal stress which introduced ageing and promoted shorter breakdown time when partnered with electrical stress. Additionally, lines of constant life (isochronal lifeline) may also be derived from the six-parameter model which could give the corresponding combinations of electrical and thermal stress for a particular insulation life especially life tending towards infinity. The isochronal lifelines also allowed an additional index for insulation characterisation called Stress Compatibility Index (SCI). Considering the threshold line equation where the denominator in the six-parameter model equals zero, a straight line is produced with SCI equal to 1 which does not agree with results of experiment showing curvilinear

line. Hence, the denominator was modified by introducing an additional term which involves one additional parameter that is a function of other parameters varying the plot from a straight line to a hyperbolic line. Variation of the six-parameter model involved replacing the difference of electrical stress with threshold to difference in their logarithm. To revamp the fitting of the Exponential Threshold Model (ETM) with experimental results, a shape factor as exponent of its denominator which transformed the electrical life equation into Four-Parameter Exponential Threshold Model (4P-ETM) [52].

In the derivation of the model for thermal-electrical-mechanical stresses, similar approach was adopted. For the specific mechanical life, the inverse-power model was used. The specific electrical, thermal, and mechanical life models were then substituted in the general phenomenological model of multiple stress. A hypersurface was produced when considering the plot of electrical, thermal, mechanical, and life parameters for a total of four variables. For thermal stress (considering temperature) equal to zero, electrical stress (considering electric field) equal to the electrical threshold, and mechanical stress equal to mechanical threshold, combined pair of stresses were obtained (electro-mechanical, thermo-electrical, and thermo-mechanical). Bi-log plot of stresses (except thermal since it is semi-log) versus insulation life produced straight lines while plots between two stresses (constant life) produced curvilinear lines. Constant insulation life gave a three-dimensional relationship between electrical, thermal, and mechanical stress. Mechanical threshold was also considered in the inverse-power model of mechanical stress. Another approach considered for the modelling of multiple stress was through a thermodynamic approach utilising the Eyring model and taking into account the reciprocal relationship between ageing rate and insulation life. Semi-log plot between the logarithm of insulation life and reciprocal of thermal stress gave a linear or straight graph. The compensation effect was also integrated to the model. The electrical and mechanical stresses were integrated with the

thermodynamic model in relation to thermal stress by a proposal that the two stresses decreased the free energy barrier leading to increased rate of the degradation process. The application of this concept led to the development of the Zhurkov (for thermo-electrical) and Crine (for thermo-electrical and thermo-mechanical) models of combined stresses. The semi-log plot of mechanical stress versus logarithm of insulation life of the Zhurkov model produced straight lines. The Crine models produced straight lines of electrical and mechanical life for high values of stress at a particular temperature in a semi-log plot and produced life tending towards infinity for electrical and mechanical stresses approaching zero value [52].

For easier determination of the parameters of electrical models, the threshold parameters (electrical stress and failure time) were instead associated to the largest valid range of electrical stress. This was also applied to three-parameter exponential and inverse-power threshold model. A satisfactory determination of the prolonged behaviour of electrical properties for vast range of temperatures was provided by the 4P-ETM (with electrical threshold stress substituted with largest valid range of electrical stress). For the inverse-power model, the voltage endurance coefficient was defined as a function of electrical stress. From literature, the fitting of the 4P-ETM and Four Parameter Inverse-Power Threshold Model (4P-IPTM) was satisfactory associated with proper range selection of electrical and thermal stress. The authors shared that a phenomenological study of insulation materials allows understanding of material behaviour but took into account also the impact of the technology used and the conditions of the test. This emphasised a goal of determining the intrinsic properties of the insulation materials. For instance where measurements of aged insulation were found to be close to measurements conducted on the same type of unaged insulation, the cause of failure can be strongly associated with inferior technology and not of the insulation material quality [52].

The discussed four-parameter models can be used in the modelling of multiple stress conditions. But due to the high number of parameters, accuracy and determination of their values. In line with this, it was discovered that the parameters of the model showed dependence on temperature (from literature on the study of XLPE and NMN) which could be represented by an exponential type[52].

With great consideration to time, insulated materials were commonly subjected to accelerated life tests at reasonable stress ranges ideally close to the service conditions. The frequency and magnitude of the stress may be considered for the acceleration of the test. In case of new insulations, the data of the experiments and life model considered should be compatible. The characterisation of the insulation performance may be referred to the parameters of the model. In doing so, it should be taken into account the validity in terms of the assumptions, type of test, representative samples, stress ranges, and processing of the data in line with actual service conditions. Application of statistics was necessary in holding the data of the experiment, the characterisation of insulation materials, and evaluation of the design. In the plotting of lifelines, Weibull distribution and lognormal distribution were usually applied in the experimental results for particular times and probability of failure. Fitting was considered to provide accurate presentation of models with respect to the experimental data. Good agreement of the model fitting with experimental data can be achieved by accurate determination of the model parameters by resorting to best estimation methods like maximum likelihood method and least square regression method. Parameter estimations usually became challenging especially for models considering large number of parameters like four parameters and above in which accuracy of the estimation decreased. Approach in graphing can help in the determination of the model indices and parameters. Sample of which was the use of the Combined Analysis Method (CAM) for multiple

stresses line thermo-electrical stress in which the graphs of the electrical, thermal, and isochronal lines can be plotted and used in the analysis of the endurance characteristics of the insulation [52].

From the introduced theory of phenomenological ageing, the model of ageing can be described with the action of the electrical stress in multiple stress selecting electric strength property in the evaluation of ageing. It was noted that electric strength decreased for single and multiple stress conditions more noticeably at a prolonged ageing period. A slight decrease in electric strength was generally followed by a dramatic decrease to zero value equating to failure. The tendency for sharp decrease in electric strength towards failure made 50% electric strength decrease a reasonable reference for the end points [52].

In 1995, Montanari [53] consolidated the latest ageing models for solid insulation under multiple stress conditions. The investigation of the models of insulation ageing was described to have been performed for four decades more particularly to thermal and electrical stress conditions. Some of the proposed insulation ageing models asserting to have physical meaning were labelled by Montanari as rather phenomenological models. The model of insulation ageing was defined to be a function of diagnostic property and should be described as a function of the stress applied and the ageing time. This was represented by the equation:

$$F(p) = K(S) \cdot t \quad (2.79)$$

where p referred to the diagnostic property under consideration, $K(S)$ referring to the rate of ageing with S as the stress applied, and t as the time of insulation ageing. Considering the criterion for failure which involved the selection of an endpoint in which the diagnostic property becomes failure diagnostic property ($p = p_L$), the ageing equation was transformed into an equation for life modelling in which the failure time was explicitly expressed as shown:

$$F(p_L) = K(S) \cdot t_L \quad (2.80)$$

$$t_L = \frac{F(p_L)}{K(S)} \quad (2.81)$$

where t_L referred to the time to failure, end-point time, or insulation life. The multiple stress insulation life models were commonly based on either the Arrhenius or Eyring models (in the case of ageing by thermal stress) which were based from the theory of reaction kinetics (taking into consideration the inverse relationship between insulation life and rate of ageing) expressed as:

$$t_L = A \cdot e^{\frac{B}{T}} - \text{Arrhenius model} \quad (2.82)$$

$$t_L T = \frac{h}{k} \cdot e^{\frac{DG}{kT}} - \text{Eyring model} \quad (2.83)$$

where A referred to the Arrhenius location parameter, B denoted Arrhenius endurance coefficient, T corresponded to temperature depicting thermal stress, h referred to the Planck constant, k referred to the Boltzmann constant, and DG corresponded to the free Gibb energy. On the other hand, ageing by electrical stress was based on the exponential power models and inverse-power models which were expressed as follows:

$$t_L = t_{L0} \cdot e^{-h \cdot (E - E_0)} - \text{Exponential model} \quad (2.84)$$

$$t_L = t_{L0} \cdot \left(\frac{E}{E_0}\right)^{-n} - \text{Inverse-power model} \quad (2.85)$$

where t_{L0} is the location parameter, h is exponential endurance coefficient, E is the electrical stress, E_0 is the ceiling value of electrical stress below which no electrical ageing happens (not a function of T), and n is the inverse-power endurance coefficient. The endurance coefficient of the ageing models was linked to the slope of the lifelines associated to the activation energy considered in the process of degradation. In suitable coordinate systems, the given models produce straight line graphs. But various experiments performed supported the existence of

thresholds in insulations. It was argued that insulations showed tendency towards threshold both in thermal and electrical sense and that results of the experiment were relevant to the linear or curvilinear aspect of the insulation lifelines depending on the insulation material and applied stress. A general approach was considered in the construction of phenomenological insulation life model under multiple stress conditions which may be additive or multiplicative in nature, both of which were integrated with a corrective term to take into account the synergism of the applied stresses. A multiplicative type of insulation life modelling was expressed as:

$$\frac{t_L}{t_{L0}} = \frac{t_L}{t_{L1}} \cdot \frac{t_L}{t_{L2}} \cdot \frac{t_L}{t_{L3}} \dots \frac{t_L}{t_{LN}} \cdot G(S_1 S_2 S_3, \dots S_N) \quad (2.86)$$

$$\frac{t_L}{t_{L0}} = \left(\prod_{i=1}^N \frac{t_L}{t_{Li}} \right) \cdot G(S_1 S_2 S_3, \dots S_N) \quad (2.87)$$

where t_L is the insulation life for multiple stress condition, $t_{L1}, t_{L2}, \dots t_{LN}$, are the insulation lives for single stress condition, $S_1, S_2, \dots S_N$ are the applied stresses with N depicting the number of stresses applied simultaneously, and $G(S_1, S_2, \dots S_N)$ is the corrective term or synergism term. Sample of the application of the phenomenological multiple stress model (particularly thermo-electrical stress) of multiplicative type was given as follows:

$$t_L = t_{L0} \cdot e^{-hE' - \frac{B}{T'} + b \cdot E' \cdot T'} \quad (2.88)$$

where $E' = E - E_0$ and $T' = \frac{1}{T_0} - \frac{1}{T}$, with T_0 referring to a determined reference temperature usually taken as the room or ambient temperature. The given sample model was based from an Arrhenius model and only provided a linear graph in a semi-log plot. A recently derived equation by Montanari was presented capable of holding both linear and curvilinear plot for tendencies towards threshold as follows:

$$L = L_0 \frac{e^{-h \cdot E' - \frac{B}{T'} + b \cdot E' \cdot T'}}{\left(\frac{E'}{E'_{t0}} + \frac{T}{T'_{t0}} - k_c \cdot \frac{E'}{E'_{t0}} \cdot \frac{T'}{T'_{t0}} - 1 \right)^{\mu(E', T')}} \quad (2.89)$$

which contained seven parameters including L_0 , h , B , b , E'_{t0} , T'_{t0} , and μ . The behaviour for linear or curvilinear insulation lifelines was defined based on the value of μ . The major reason pointed out in deriving models of insulation life was the characterisation of the insulations through indices. From the model presented, in the case of threshold materials, b , E'_{t0} , and T'_{t0} were the most significant indices considered while for no-threshold materials, E_0 , L_0 , h , B , and b were the most important indices considered. Additionally, the phenomenological insulation life models provided a basis for selecting designed range of stresses and the analysis of the mechanisms of degradation. Physical meaning in insulation life models aimed at providing relationship between the time to failure and applied stress in line with the degradation process in which parameters of the model were defined as function of applied stress and carry physical sense. There was also an emphasis regarding the importance of deriving estimations of the model parameters in a reasonably short period of time. For significantly high electrical stresses, the breakdown was usually caused by a dominant degradation process while at thermal and electrical stress conditions near the design operating conditions were usually caused by two or more degradation processes: one leading to emergence of microscopic cavities which may be accompanied by formation of electrical treeing and the other causing the maturation of the treeing towards occurrence of ultimate breakdown. Hence, it was proposed that two or more life models were necessary to illustrate the times to failure acquired from life tests performed at low electrical stress condition.

Mazzanti et al. [54] introduced model equation for life prediction taking into account electrical, thermal, and mechanical stresses and solved 7 parameters using Levenberg-Marquadt algorithm. The study of insulation behaviour under the influence of multiple stresses paved way for the complete characterisation of the endurance features and life comparable to actual operating conditions. An in-depth view for the life model of multiple stresses insulation was based on the phenomenological ageing theory. Having considered N number of general stresses S_1, S_2, \dots, S_N

under which a particular dielectric material was subjected, a satisfactory relationship of the dielectric properties was found as expressed in the following:

$$A(t) = f[p(t)] = \int_0^t R(S_1, S_2, \dots, S_N) dt \quad (2.90)$$

where A referred to amount of ageing, $p(t)$ corresponded to normalised specific property equivalent to $\frac{P(t)}{P_0}$ where P_0 denoted initial value of property, R referred to the ageing rate equivalent to $\frac{dA}{dt}$ and varied with stress not time. With the assumption of the non-variability of stress with time, R consequently became constant as well, hence (2.90) was evaluated as follows:

$$A(t) = R(S_1, S_2, \dots, S_N) \cdot t \quad (2.91)$$

Upon the specific property p reaching to a certain limiting value p_L referred to as endpoint value which corresponded to failure of insulation, time t became life L , $A(t)$ became $A(L)$, and $f[p(t)]$ became $f(p_L)$. By applying the failure condition on (2.91), the following explicit expression of life was obtained:

$$L = \frac{f(p_L)}{R(S_1, S_2, \dots, S_N)} \quad (2.92)$$

This was recognised as a life model for multiple stress but still contained generic functions of variables. A defined expression of the ageing rate will lead to a more defined expression of (2.92). The approach began by considering single stress conditions. By considering electrical stress alone i.e. $S = E$, the model for electrical life was obtained expressed by the application of the Inverse-Power Model (IPM) as shown in the following:

$$L_E = L_{0E} \cdot \left(\frac{E}{E_0}\right)^{-n} \quad (2.93)$$

where L_E was referred to as electrical life, L_{0E} corresponded to electrical life at E_0 , E denoted electrical stress, E_0 corresponded to lower electrical stress limit under which electrical ageing was negligible, and n referred to as Voltage Endurance Coefficient (VEC). By considering thermal

stress alone i.e., $S = T$, the model for thermal life was obtained expressed by the application of the Arrhenius model as shown in the following:

$$L_T = L_{0T} \cdot e^{-B \cdot T} \quad (2.94)$$

where L_T was referred to as thermal life, L_{0T} corresponded to thermal life at Θ_0 , B denoted coefficient that was directly related to activation energy of the principal degradation process, and T corresponded to conventional thermal stress equivalent to the expression $\frac{1}{\Theta_0} - \frac{1}{\Theta}$ where Θ_0 denoted reference temperature (like room temperature) and Θ denoted temperature both in absolute scale. By considering mechanical stress alone i.e. $S = M$, the model for mechanical life was obtained expressed by the application of the IPM (similar to the model for electrical life) as shown in the following:

$$L_M = L_{0M} \cdot \left(\frac{M}{M_0}\right)^{-m} \quad (2.95)$$

where L_M was referred to as mechanical life, L_{0M} corresponded to mechanical life at M_0 , M denoted mechanical stress, M_0 corresponded to lower mechanical stress limit under which mechanical ageing was negligible, and m referred to as Mechanical Endurance Coefficient (MEC). In lieu of compatibility of model for multiple stress life, for mechanical and electrical stresses below corresponding limit values, each respective life became equivalent to thermal life corresponding to reference temperature which were expressed as follows:

$$L_E(E \leq E_0) = L_{0E} = L_{0T} \quad (2.96)$$

$$L_M(M \leq M_0) = L_{0M} = L_{0T} \quad (2.97)$$

For simplification, $L_{0T} = L_{0E} = L_{0M}$ simply referred to as L_0 . Further simplification was made by considering substitution of stresses denoted by E' and M' where

$$E' = \log\left(\frac{E}{E_0}\right) \quad (2.98)$$

$$M' = \log\left(\frac{M}{M_0}\right) \quad (2.99)$$

By applying these substitutions, the part of the models for electrical and mechanical life were alternatively expressed as follows:

$$\left(\frac{E}{E_0}\right)^{-n} = e^{-n \cdot E'} \quad (2.100)$$

$$\left(\frac{M}{M_0}\right)^{-m} = e^{-m \cdot M'} \quad (2.101)$$

Proceeding to the multiple stress life model, the combination of the stresses were related by multiplicative assumption which provided a simplified treatment. This was shown in the following:

$$\frac{L}{L_0} = \left(\frac{L_E}{L_0}\right) \cdot \left(\frac{L_T}{L_0}\right) \cdot \left(\frac{L_M}{L_0}\right) \quad (2.102)$$

$$L = L_0 \cdot e^{-B \cdot T - n \cdot E' - m \cdot M'} \quad (2.103)$$

However, in the case of combined electrical and thermal stress, the life obtained by the multiplicative treatment resulted to overestimated synergism of the stresses which consequently resulted to underestimated value of life obtained more distinctly at greater stress conditions. To compensate this, a corrective factor G was introduced that was dependent on the stresses applied. This factor was meant to improve the fitting of the values of the experimental results. Considering double stress particularly electrical and thermal stresses, the corrective factor G was granted as follows:

$$G = e^{b \cdot E' \cdot T} \quad (2.104)$$

where b corresponded to the coefficient associated to the synergism of the electrical and thermal stresses. Similarly, considering triple stress, the corrective factor was defined as follows:

$$G = e^{b' \cdot E' \cdot T + b'' \cdot M' \cdot T + b''' \cdot E' \cdot M'} \quad (2.105)$$

where b' corresponded to the coefficient associated to the synergism of the electrical and thermal stresses, b'' denoted to the coefficient associated to the synergism of the mechanical and thermal stresses, and b''' corresponded to the coefficient associated to the synergism of the electrical and mechanical stresses. By applying the corrective factor in (2.103), the following was obtained:

$$L = L_0 \cdot e^{-B \cdot T - n \cdot E' - m \cdot M' + b' \cdot E' \cdot T + b'' \cdot M' \cdot T + b''' \cdot E' \cdot M'} \quad (2.106)$$

By performing logarithm on both side of the equation, (2.106) became

$$\log L = \log L_0 - (n - b' \cdot T) \cdot \log \left(\frac{E}{E_0} \right) - (m - b'' \cdot T) \cdot \log \left(\frac{M}{M_0} \right) - B \cdot T + b''' \cdot \log \left(\frac{M}{M_0} \right) \cdot \log \left(\frac{E}{E_0} \right) \quad (2.107)$$

It was emphasised that (2.107) was compatible when the conditions of the boundary were considered. In the case of $E \leq E_0$, the model became

$$L = L(M', T) = L_0 \cdot e^{-B \cdot T - m \cdot M' + b'' \cdot M' \cdot T} \quad (2.108)$$

For $M \leq M_0$, the model became

$$L = L(E', T) = L_0 \cdot e^{-B \cdot T - n \cdot E' + b' \cdot E' \cdot T} \quad (2.109)$$

In the case of $T = 0$, the model became

$$L = L(E', M') = L_0 \cdot e^{-n \cdot E' - m \cdot M' + b''' \cdot E' \cdot M'} \quad (2.110)$$

The suggested life model for multiple stress conditions expressed in (2.107) was identified to contain 10 parameters which include L_0 , n , b' , Θ_0 (from T), E_0 , m , b'' , M_0 , B , and b''' . However, the three parameters Θ_0 , M_0 , and E_0 can be excluded since they can already be determined through experimentation considering single stress conditions. This left 7 parameters to be solved from the equation which was still recognised to be quite many. Solving high number of parameters necessitated the use of complicated numerical iterations which in some instances presented problems in approaching divergence especially when the curve possessed great non-linearity. In

lieu of this, selection of suitable algorithm and good estimation of the guess values of the parameters aided in the determination of the parameters.

In 1997, Mazzanti and Montanari [55] compared XLPE and EPR insulations for high voltage cables. The selection of the insulation materials was based from the most common used in high voltage applications. To compare the two insulation materials, their endurance characteristics must be known corresponding to the stresses they experience during operation which include temperature and electric field. Such endurance characterisation required the performance of life tests, selection of valid life models, and use of suitable statistical tools. The life tests were performed on a sample portion of a cable with the aim of characterising the endurance properties of the insulation materials and for comparison with other dielectrics. The thermal and electrical stresses were recognised to be principal factors of degradation in high voltage cables with other ageing elements in the environment ignored. This study involved application of sole thermal and electrical stresses and their combinations which would take into account their synergism. Accordingly, electrical life tests, thermal life tests, and combined thermo-electrical life tests were conducted on EPR and XLPE insulated cables. In the performance of life tests, progressive censoring was conducted which allowed collection of data pertinent to failure of material and reduction of testing times. The method of progressive censoring involved removal of few test specimens that have not failed yet at predetermined period of times referred to as censoring times upon which diagnostic properties (like dielectric strength and tensile strength) were measured. The data gathered from both specimens that did and did not fail were handled by suitable statistical treatments. In doing so, information for both failure and time-analysis of the properties under consideration were produced. The significance in carrying out the life tests was described which was to characterise the endurance properties of the insulation material within a range of stress near actual operating condition. Naturally, the tendency for more valid observation of property

behaviour of insulating materials increases as testing conditions were closer to actual operating conditions but consequently leads to impractical long times. Hence, the optimum consideration between testing times and test validity was recognised. The totality of the tests were partitioned into two portions: characterisation of short-term endurance properties and long-term properties. The first one involved greater stress conditions compared to actual operating conditions. This was beneficial by providing knowledge of the unaged insulation material as well as aid in the planning of the long-term tests. For the long-term endurance tests, lower stresses compared to the short-term tests were applied. In lieu of these endurance tests, an analysis called Combined Analysis Method (CAM) aided in the selection of optimum levels of stresses which lead to lesser number of life tests performed, hence saving time and money. The CAM follows the assumption that under thermo-electrical stresses, insulation life can be represented by a three-dimensional surface where the thermal and electrical lifelines can be obtained by considering intersections with planes of constant thermal and electrical stress. Additionally, CAM allowed the graphing of the constant insulation lines which provide combinations of thermal and electrical stress for a certain insulation life value. In order to produce the stress life lines, constant-life lines, determine endurance indices, and conduct extrapolation of data based on actual operating conditions, appropriate life models should be considered. The models also play a significant role in the determination of the probability of insulation failures through statistical means like the Weibull function. For the experiment, in order to produce more valid comparison of the XLPE and EPR insulation materials, identical size and geometry were taken into account. The dimensions of the test specimens were considered in such way as to produce numerically equal values of applied voltage and electric field. The temperatures for each insulation were not equal (100°C, 110°C, 130°C, and 150°C for XLPE while 120°C, 130°C, 150°C, and 160°C for EPR). The properties considered for measurement were electric strength, tensile strength, density, and weight. Arrhenius plot at 50% probability of failure was considered in graphing the thermal lifelines and 50% reduction of

electric strength was considered as the failure criterion. The Arrhenius equation which served as the basis of the plot was expressed as follows:

$$L_T = L_{T_0} \cdot e^{-B \cdot cT} \quad (2.111)$$

where L_T was referred to as the thermal life corresponding to time when failure occurs for the specified thermal stress, L_{T_0} corresponded to thermal life for the given reference temperature T_0 (like room temperature), B denoted coefficient directly related to activation energy of deteriorating mechanism, and cT referred to as conventional thermal stress equivalent to $\frac{1}{T_0} - \frac{1}{T}$ where T corresponded to applied temperature. Results showed that for XLPE at 100°C, the failure criterion was not met even after 25,000 hours of testing (which led the testers to withdraw the specimens and proceeded to the measurements). This was associated to the possibility of a threshold for the thermal lifeline near 100°C. In the case of EPR, threshold at 110°C was observed. Additionally, results showed that at the same temperature, EPR corresponded to longer life than XLPE. Further treatment with assumed linearity of the data points lead to the calculation of the Temperature Index (TI) which corresponded to the temperature when the endpoint was reached for a test duration of 20,000 hours and the Halving Interval in Celsius (HIC) which corresponded to the increase in temperature from the TI which will half the failure time. For XLPE, the TI and HIC values obtained were 101 and 7.8 while for the EPR, the values obtained were 111 and 8.4 respectively. The results showed that EPR exhibited larger, hence better TI, HIC, and thermal threshold values compared with XLPE. The thermal lifelines of EPR and XLPE also showed identical slopes which denoted seemingly equal values of activation energies. On the other hand, the electrical life tests were conducted at room temperature of 20°C, power frequency of 50Hz, and in both water and air. In the case of low stresses, the electrical life tests were also performed at high frequencies as high as 900Hz in order to study the behaviour of the electrical lifeline at prolonged time. In lieu of high voltage rating of cables, results of the dry test were considered.

The obtained initial value of the electric strength on XLPE was a bit higher compared with EPR (80kV/mm versus 75kV/mm respectively). The tests involved application of constant voltage values between 12kV and 75kV for XLPE insulated cables and between 30 to 70kV for the EPR insulated cables. Similarly, the graphs were presented at 50% probability of failure in a semi-log fashion. Results revealed that the data points were in good agreement with the electrical lifelines based from exponential model expressed as follows:

$$L_E = L_{EH} \cdot e^{-h \cdot (E - E_H)} \quad (2.112)$$

where L_E was referred to as the electrical life or the time to failure, L_{EH} denoted the electrical life at E_H , h corresponded to the coefficient linked to the slope of the electrical lifelines, E denoted electrical stress applied, and E_H referred to as the ceiling value of electrical stress. The data points also showed good fitting with the Inverse-Power Model (IPM) expressed as:

$$L_E = L_{EH} \cdot \left(\frac{E}{E_H} \right)^{-n} \quad (2.113)$$

where n corresponded to the coefficient linked to the slope of the electrical lifelines (similar to h in the exponential model). The correlation coefficient R obtained from both exponential and inverse-power model was more than 0.99 which indicated good fitting with data points of the electrical lifelines in semi-log coordinates for the former and bi-log coordinates for the latter. In the case of XLPE, a threshold was observed at about 11.5kV/mm which corresponded to stress below which electrical ageing was negligible and life tended towards infinity. Having observed the existence of a threshold in the plotted electrical lifeline, threshold models were considered including the Four Parameter Exponential Threshold Model (4P-ETM) expressed as

$$L_E = L_{EH} \cdot e^{-\frac{h \cdot (E - E_H)}{\left(\frac{E - E_T}{E_H - E_T} \right)^\mu}} \quad (2.114)$$

and the Four Parameter Inverse-Power Threshold Model (4P-IPTM) expressed as

$$L_E = L_{EH} \cdot \left(\frac{E}{E_H}\right)^{-n(E)} \quad (2.115)$$

in which

$$n(E) = \frac{n_i}{\left(1 - \frac{E_H - E}{E_H - E_T}\right)^\mu} \quad (2.116)$$

where E_T corresponded to the threshold electrical stress, μ denoted shape parameter dependent on the approach of threshold, and n_i corresponded to the voltage endurance coefficient when applied stress equals ceiling electrical stress. The parameters h and n were also referred to as the Voltage Endurance Coefficients (VEC). The higher the VEC, the lower the slope of the electrical lifelines and the better the endurance characteristics of the insulation material. Results showed that despite the bit lower value of the dielectric strength of EPR, its VEC was higher compared to XLPE indicating better endurance characteristics. Owing to the linearity of the voltage endurance line obtained for EPR, models of probabilistic life were needed to be able to deduce from the results the design stresses for a selected probability and to correspond to other sizes of cables. On the other hand, for XLPE since the electrical threshold was higher than the design stress, the probability of failure was virtually zero and not affected by size. It was stated that for EPR, the VEC and initial value of electric strength were the important indices while for XLPE, it was the electrical threshold. In order to obtain a more accurate basis for the design of cables, it was pointed out that electrical stress should not be the only stress considered but also the thermal stress including the synergistic effect of both. This demanded to the endurance characterisation of the insulation materials under multiple stresses i.e., thermo-electrical stress. In lieu of this, experiments were performed which corresponded to XLPE and EPR insulation [55].

For the XLPE, the test involved electrical stress values ranging from 4kV to 30kV at temperatures ranging from 60°C to 110°C. The results were reported at 50% probability of failure and 95%

confidence intervals. CAM points were also included coinciding the lifelines which were derived by considering the thermal lifelines and constant life lines [55].

For the EPR, the life tests were performed at electrical stresses of 10kV to 50kV at temperatures ranging from 60°C to 150°C. The electrical lifelines derived were drawn in a semi-log plot at 50% probability of failure. From the results, it was observed that at electrical stresses higher than 30kV/mm, the electrical lifelines at each temperature showed linear trend. It was also observed that for temperatures above 90°C, the electrical lifelines showed downward curvatures. Thermal life tests performed with zero electrical stress applied corresponded to E_0 value of 6kV/mm. The plots of the linear part of electrical lifelines at electrical stresses ranging from 30kV/mm to 60kV/mm were performed using the IPM () expressed in parametric form considering temperature and probability of failure as parameters shown as follows:

$$L_E(T) = L_{EH}(T, P) \cdot \left(\frac{E}{E_H}\right)^{-n(T)} \quad (2.117)$$

The parameters of this model were determined by resorting to least square method and CAM points for every temperature. The VEC values obtained for EPR were notably high even at maximum operating temperatures and above which corresponded to excellent endurance performance under multiple stress condition. The temperature variation of VEC was described as follows:

$$n = n_0 - b \cdot cT \quad (2.118)$$

where n_0 corresponded to initial VEC value i.e., at reference temperature and b depicted coefficient pertinent to slope. Application of this equation to the results of endurance coefficients at different temperatures revealed good fitting which proved the suitability of using linear models for multiple stress condition particularly between 30kV/mm to 60kV/mm and ranging from 20°C

to 100°C applicable for insulation materials showing no tendency of thresholds expressed as follows:

$$L(E, T) = L_0 \cdot \left(\frac{E}{E_0}\right)^{-(n-b \cdot cT)} \cdot e^{-B \cdot cT} \quad (2.119)$$

This equation was described to be phenomenological but can be obtained from the principle of thermodynamics. The parameters of the model were calculated using least square regression method except B which was based on the HIC value determined from the thermal lifelines subject to no electrical stress. Results showed that parameters of (2.119) do not vary with temperature except L_0 . Furthermore, application of (2.119) for the electrical lifelines at various temperatures with the experimental data and CAM points plotted in bi-log coordinates showed satisfactory fitting. Going back from the semi-log plot of the electrical lifelines, no tendency towards threshold were identified below 90°C. But from a separate literature by Montanari, Mazzanti, and Simoni [50-55] showed tendency of electrical lifelines in semi-log plot to be concaved upward for insulation life of 100,000 hours at temperature of 20°C obtained in bi-log coordinates. However, this was not enough to determine the threshold. It was also noted that at temperatures no less than 100°C, the value of VEC could be high enough to such degree that the threshold tendency was hardly observable and would require prolonged duration of tests to verify the presence of upward concavity of the lifelines when considering slight values of electrical stress. Further observations pertinent to threshold tendencies were done by considering Arrhenius plots of thermal lifelines (at various electrical stresses) and isochronal lines (at various failure times) both at 50% probability of failure and 95% confidence interval. The fittings were performed in line with experimental data and CAM points. Thermal thresholds were identified in the thermal lifelines which were 105 °C for no electrical stress and 90°C for electrical stress of 20kV/mm. Conversely, it was speculated that the electrical threshold for 90°C was 20kV/mm. This meant that thermal threshold should be evident and increasing for lower temperatures but restricted only down to

20°C and electrical stresses between 20kV/mm and 30kV/mm based on the graph of thermal lifelines. This led to the characterisation of the electrical lifelines below high temperatures which showed upward concavity at low electrical stress, downward concavity in the case of medium electrical stress, and straight plot for high electrical stress. The existence of electrical threshold was also noted to vanish at temperatures above 105°C [55].

2.7 Conclusion

This chapter provided a general introduction about power lines. The power lines were classified into various ways according to some basis. In the basis of power delivery, the power lines were classified as either transmission or distribution. Between the two, this research study has focused on the distribution power lines. In the basis of voltage levels, the power lines were classified as LV, MV, HV, EHV, and UHV. Among the voltage levels, the MV power lines were given greater emphasis. Based on the manner of laying, the power lines were categorised as overhead or underground in which the latter was concentrated upon. Comparison between overhead and underground cable distribution systems were made in lieu of selection considerations by discussion of their corresponding advantages and disadvantages. The discussion was then led to the power distribution cable itself revealing its rich historical development in design and material especially the insulation. The basic components of power distribution cables were then discussed which included the core, core screen, insulation, insulation screen, metallic screen, and outer sheath. For each component, discussions about their functions, materials, and types were discussed. Additionally, accessories in power distribution cable systems which were the joints and terminations were tackled regarding their functions and other important considerations. Lastly, various theoretical models were presented in chronological manner in order to emphasise time development. The theoretical models took into account considerations in approach (like

phenomenological, stochastic, and statistical), natures of stresses under consideration (including thermal, mechanical, electrical, and combinations of such), asymptotic tendencies (threshold and no-threshold), consideration of endurance coefficient (constant or variable), manner of plotting curve (regular, semi-log, or bi-log), estimation methods including Maximum Likelihood Estimation (MLE) and Least Square Regression Method (LSRM), properties considered (including but not limited to ageing time, insulation life, electric strength, temperature, and tensile strength), and number of parameters considered. Models particular to thermal stress are based on Arrhenius or Eyring laws. On the other hand, models particular to electrical and/or mechanical stress are based on exponential or inverse-power laws. The models were also subject to adjustments for satisfaction of boundary conditions to support their physical meaning. In some cases, the physical meaning of the models is sacrificed upon consideration of actual behaviour of curves based on experimental results.

CHAPTER 3 CROSS-LINKED POLYETHYLENE AND ETHYLENE PROPYLENE RUBBER UNDERGROUND CABLE

3.0 Introduction

In the preceding chapter, various information from literature were presented. Section 2.1 discussed about the power lines including their types according to stage of electricity delivery and voltage rating. Distinction between overhead lines and underground cables in their positive and negative aspects were tackled in Section 2.2. Section 2.3 provided a brief history of power cables which included the comparison between XLPE and EPR while Section 2.4 focused on the components or parts of the cables. Cable accessories which refer to the joint and terminations were also discussed in Section 2.5. The last section provided an extensive discussion of theoretical models introduced in history pertinent to the prediction of the life of dielectric materials.

Since this research study involves the introduction of TR-EPR insulation in underground cabling system, it is crucial to have suitable knowledge about the well-considered insulation material in underground cables which is XLPE alongside EPR. This includes the various design considerations of the cables pertinent to their components especially the insulation and properties which may serve as reference for comparison. Additionally, due to the nature of underground cabling, it is significant to determine the various factors relevant to the failure mechanisms of insulation which directly affect insulation life with special emphasis to recognise treeing phenomenon.

3.1 Design

For the design criterion of cable components, the Australian/New Zealand Standard (AS/NZS) and International Electrotechnical Commission (IEC) standards were used as references.

3.1.1 Core

For normal operation and short circuit condition, both [39] and [56] consider the same maximum core or conductor temperature which depends on the insulation material and type of operation. Under normal operation, the maximum core temperature is 90°C for both XLPE and EPR. For 5 seconds short-circuit condition, the maximum core temperature is 250°C for both XLPE and EPR. However, for the emergency operation temperatures exclusive to [39], the core has a higher rating of 130°C when using EPR compared to 105°C when using XLPE. The core shall have a circular profile [39] and may be solid or stranded [56]. Core material shall either be Aluminium (plain or alloy) or Copper (plain, tinned, or metal-coated annealed) in accordance with AS/NZS 1125 [39] or IEC 60228 [56]. Actions may be taken to attain water tightness (especially for stranded cores).

When screening is required, single-core and three-core cables shall have conductor screen and insulation screen. Exceptions include unscreened EPR insulated cables at rated voltage of 3.8/6.6 (7.2) kV following nominal insulation thickness prescribed in Table 3.2 [56].

3.1.2 Core screen

An extruded, cross-linked, and non-metallic semiconductive screen is required to cover the core or conductor directly or cover the core indirectly through a semiconducting tape applied in between. The semiconductive compound is required to be tightly bound with the insulation [56]. The surface irregularities of the interface between the core screen and insulation are limited to 0.25mm protrusion. The minimum thickness of the core screen at any point should be no less than 0.30mm. The core screen should also be made readily removable from the core [39].

3.1.3 Insulation

For the insulation, it is required that the material used is either XLPE including its variant TR-XLPE or EPR (although PVC is also a choice as per IEC 60502-2:2005 [56]) complying with AS/NZS 3808 [39]. The bonding between the insulation and the core screen should be in such way that damage in the interface is induced when separation is performed between the two [39]. The nominal and minimum thickness of the insulation is based on the insulation material used (XLPE or EPR), nominal cross-sectional area of the core ($16-1600\text{mm}^2$), and the rated voltages expressed in U_o/U (U_m) where U_o indicates the designed r.m.s. power frequency voltage to earth, U the r.m.s. power frequency voltage between phases, and U_m the designed maximum r.m.s. power frequency voltage between any two-phase cores.

As per AS/NZS 1429.1 [39], referring to Table 3.1, higher nominal and minimum insulation thickness is required for EPR than XLPE at voltage rating of 1.9/3.3 (3.6) kV at every core area.

For the remaining voltage ratings 3.8/6.6 (7.2) kV, 6.35/11 (12) kV, 12.7/22 (24) kV, and 19/33 (36) kV, for every corresponding core area, the nominal and minimum insulation thickness required for XLPE and EPR are the same. It can also be observed that for the higher rated voltages starting from 6.35/11 (12) kV to 19/33 (36) kV, the thickness required is independent of the core area. For the concentricity defined as the ratio of the thickness range ($t_{max} - t_{min}$) and the maximum thickness (t_{max}), it should not exceed 0.15 i.e., $\frac{t_{max}-t_{min}}{t_{max}} \leq 0.15$ in mathematical expression. Shrinkage should not exceed 4% when heated between temperatures 127-133°C for 1 hour. No voids should be present that are greater than 0.08mm while contaminants should be no more than 0.15mm. For XLPE, size of discoloured translucent should not exceed 1.25mm. Void concentrations should not be greater than 30 per 16cm³ while contaminants concentration should be no more than 15 per 16cm³.

Table 3.1: Nominal Insulation thickness of XLPE and EPR as per AS/NZS 1429.1

Nominal cross-sectional area of core mm ²	Nominal insulation thickness at rated voltage U _o /U (U _m)						
	1.9/3.3 (3.6) kV		3.8/6.6 (7.2) kV	6.35/11 (12) kV	12.7/22 (24) kV	19/33 (36) kV	
	XLPE mm	EPR mm	Both XLPE and EPR				
16	2	2.2	2.5	3.4	5.5	8	
25							
35							
50							
70							
95		2.4	2.6	3.2	3.4	5.5	8
120							
150							
185		2.6	2.8	3.2	3.4	5.5	8
240							
300		2.8	3	3.2	3.4	5.5	8
400							
500		2.2	2.8	3.2	3.4	5.5	8
630	2.4						
800	2.6						
1000	2.8						
1200	-	-	-	-	-	-	
1600	-	-	-	-	-	-	

As per IEC 60502-2:2005 [56] referring to Table 3.2 similar to Table 3.1, higher nominal and minimum insulation thickness is required for unscreened EPR than XLPE at voltage rating of 3.6/6 (7.2) kV at every core area. For the remaining voltage ratings 6/10 (12) kV, 8.7/15 (17.5) kV, 12/20 (24) kV, and 18/30 (36) kV, for every corresponding core area, the nominal and minimum insulation thickness required for XLPE and EPR are the same. It can also be observed that for all voltage ratings except 3.6/6 (7.2) kV, the thickness required is independent of the core area (ignoring the unindicated values represented by the “-“symbol). For core cross-sectional areas smaller than 10mm², the core diameter may be increased by either the conductor screen or insulation. For cores with cross-sectional area larger than 1000mm², nominal insulation thickness may be increased to prevent mechanical damage when installing and servicing.

Table 3.2: Nominal Insulation Thickness of XLPE and EPR as PER IEC 60502-2

Nominal core cross-sectional area of core mm ²	Nominal insulation thickness at rated voltage U _o /U (U _m)						
	3.6/6 (7.2) kV		6/10 (12) kV	8.7/15 (17.5) kV	12/20 (24) kV	18/30 (36) kV	
	XLPE mm	EPR		Both XLPE and EPR mm			
		Unscreened mm	Screened mm				
10	2.5	3	2.5	-	-	-	
16				-	-	-	
25				3.4	4.5	5.5	8
35							
50 to 185							
240	2.6	2.6					
300	2.8	2.8					
400	3	3					
500 to 1600	3.2	3.2	3.2				

Cross linking grants advantages in the improvement of the mechanical and thermal properties of polypropylene while retaining its electric properties. The two commonly used cross linking methods are the peroxide method and silane method [1].

Peroxide method involves the addition of dicumyl-peroxide to the polymer. Immediately after the extrusion in a particular tube at high pressure and temperature, the dicumyl-peroxide compound is activated. The high pressure and high temperature were formerly attained using steam, hence the term steam curing for the method. Later on, it was found out that the use of steam causes high concentrations of water and the emergence of void in the insulation which encourages the occurrence of partial discharge resulting to breakdown, hence a new method was developed called dry curing. Dry curing involves the use of nitrogen gas for pressurising the insulation and curing tube (electric heating element) which supplies heat by convection and radiation. Gas or water is used for the cooling process of this method [1].

On the other hand, the silane method involves curing done on the different step in production instead of being done immediately after the extrusion. The curing process uses silane compound that attaches to polyethylene chains during extrusion. Cooling is performed slowly after the extrusion where the cable is placed in an 85°C water tank while reeled. [1].

3.1.4 Insulation screen

Similar to the core screen, the insulation screen is also required to be comprised of an extruded, cross-linked, and non-metallic semi-conductive layer to cover the insulation. As per IEC 60502-2:2005 [56], for the non-metallic layer, it is necessary that it is directly extruded for the insulation of each core. It is needed also that it consists of bonded or strippable semi-conducting material. Each core or core assembly may then be covered with a layer of semi-conducting compound or tape. The metallic layer may then be applied over each core or over the core assembly. The minimum thickness of the insulation screen at any point should be not less than 0.60mm [39].

3.1.5 Metallic screen

For the metallic screen, it shall consist of one or more tapes, braid, a concentric layer wires, or a combination of wires and tapes [56]. Material required is Copper conforming to AS/NZS 1125 which can either be plain or tinned annealed [39] taking into account resistance against corrosion [56]. The metallic screen may also be a sheath or an armour [56].

As per AS/NZS 1429.1 [39], wires used should be of equal sizes not smaller than 0.60mm in nominal diameter with at most 5% size variation. Placement shall be performed in a helical manner with lay length no more than 10 times the pitch circle diameter of the wire over the core. Spacing for each wire shall be no more than 4mm. Each core should contain equal number of wires in the case of three-core cables. In the case of metal sheathed single core cables, the metallic screen should cover the semi-conductive tape covering the metal sheath. The tape should be non-hygroscopic if not water-blocking.

3.1.6 Outer sheath

For all cables, an outer sheath is required [56]. The outer sheath may either be made of thermoplastics (PVC, polyethylene, LDPE, MDPE, HDPE), elastomeric materials (cross-linked elastomeric compounds, CSPE, polychloroprene), or reduced fire hazard cable materials which should be in compliance with AS/NZS 3808. Chemical additives applied on the outer sheath for essential purposes, should cause no harmful consequences to man or the environment [56]. The outer sheath shall be applied tightly in such way that it can be readily removed from the cable incurring no harm to other components [39]. The outer sheath should also be coloured black unless stated otherwise like when a chosen colour is in accordance with the manufacturer and purchaser's agreement under suitable reasons [56]. For the nominal thickness (t_s) of the outer sheath, the following formula shall be applied:

$$t_s = 0.035D + 1 \quad (3.1)$$

where D refers to the fictitious diameter immediately under the outer sheath in mm unit rounded off to the nearest tenths place [56]. As per AS/NZS 1429.1 [39], at any point of the outer sheath, the minimum thickness shall be expressed as:

$$\text{minimum thickness} = 0.8t_s - 0.2 \quad (3.2)$$

The nominal thickness of the inner layer for composite sheaths is required to sit between 30% and 50% of the total nominal thickness but should never be below 1mm. On the other hand, the remainder of the total nominal thickness shall be the nominal thickness of the outer layer but should never be less than 1mm for single-core and three-core cables and 1.8mm for phase cable to be bundled.

As per IEC 60502-2:2005 [56], for cases like unarmoured cables with outer sheath indirectly applied over metallic screen, armour, or concentric conductor, the nominal outer sheath thickness is required to be at least 1.4mm for single-core cables and at least 1.8mm for three-core cables. For cables with outer sheath directly applied over metallic screen, armour, or concentric conductor, the nominal outer sheath thickness is required to be at least 1.8mm.

3.2 Property

Several studies support the idea that for both XLPE and EPR, their properties are a function of temperature especially the physical properties in contrast with electrical properties. Mechanical properties are also affected by temperature with XLPE being more sensitive to temperature compared to EPR. Considerations in the mechanical properties is of great importance taking into account that more than 90% of failures in underground cables are associated with mechanical damage during installations and dig-ins [57]. Generally, temperature produces a greater effect

than applied voltage for both EPR and XLPE [58]. Overvoltage can also influence the values of the properties of insulation material. Uydur et al. [59] conducted a study regarding the effect of overvoltage in 20kV XLPE insulated cable. The test performed involves subjecting 5 m long XLPE insulated cables under 60kV stress for a duration of 15 minutes for 80 cycles of ageing. Dielectric loss, DDF, and partial discharge were measured for each ageing cycle. In the case of dielectric loss and DDF, the measurements were performed at three voltages i.e., 2kV, 6kV, and 12kV at power frequency of 50Hz. Results showed increasing trends for all voltage measurements of the dielectric loss and DDF with increasing ageing cycles. The results also showed that graphs produced by dielectric loss and DDF are completely identical with respect to the same voltage measurement. Similar findings were also found for the partial discharge which showed increasing partial discharge activity with increasing ageing cycles.

Qi and Boggs [60] performed measurements of the thermal and electrical properties of four EPR compounds (EPR1, EPR2, EPR3, and EPR4) and one TR-XLPE ranging from room temperature (20°C) up to 140°C pertinent to the thermal conductivity, heat capacity, thermal expansion, and thickness properties.

3.2.1 Thermal conductivity

Thermal conductivity refers to how well a certain material can conduct heat [61]. EPR showed stability in its thermal properties where there has only been slight decrease in the thermal conductivity as temperature increases. EPR1 was measured to have a thermal conductivity ranging from 0.36 to 0.4W/m-K while EPR2, EPR3, and EPR4 thermal conductivity values ranged from 0.29 to 0.34W/m-K. The greater thermal conductivity of EPR1 compared to the other EPR's by about 10% is associated with the presence of more inorganic filler content. On the other hand, the thermal conductivity of TR-XLPE can be discussed into three distinct changes with

corresponding temperature ranges. Between 20 to 80°C, the thermal conductivity of TR-XLPE varied from 0.29 to 0.33W/m-K similar to EPR (2, 3, and 4). Between 80 to 100°C, its thermal conductivity increased from 0.33 to 0.39 W/m-K. From 100 to 140°C, the thermal conductivity significantly dropped from 0.39 to 0.25W/m-K. For the temperatures between 80 to 120°C, the thermal properties of the TR-XLPE are greatly influenced by melting. Beyond 120°C, the thermal conductivity of TR-XLPE becomes lower than EPR from which it is described as amorphous. From the results of the thermal conductivity measurements, the analysis of the thermal resistivity can be concluded taking into account the reciprocal relationship between thermal conductivity and resistivity [60].

3.2.2 Heat capacity

For heat capacity, EPR shows a very steady value all throughout the temperatures between -50 to 150°C attributed to its being amorphous. The heat capacity for EPR ranged between 1 to 2.5J/g-K. For TR-XLPE, the heat capacity steadily increases from 1.5 to 3J/g-K between -50 to 50°C. From 50 to 105°C, the heat capacity spiked from 3 to 12.6J/g-K. Between 105 to 120°C, the heat capacity dramatically decreased from 12.6 to 2.5J/g-K. From 120°C beyond, the heat capacity stabilised at 2.5J/g-K. The spike in heat capacity for TR-XLPE is associated with its crystallinity [60].

3.2.3 Thermal expansion

Generally, the thermal expansion of both EPR and TR-XLPE increases with temperature. EPR shows a slight gradual increment with increasing temperature. The thermal expansion of EPR increases from 0 to 4.2% from the temperature of 20 to 150°C. For the TR-XLPE, the thermal expansion linearly increases from 0 to 2.5% between the temperatures 20°C and 80°C. From 80

to 120°C, the thermal expansion drastically increases from 2.5 to 12%. From 120 to 150°C, the thermal expansion returns to the linear increase [60].

3.2.4 Stiffness

The stiffness is measured in terms of the stress required to produce a determined displacement via Dynamic Mechanical Analysis (DMA). Generally, the stress decreases with increasing temperature. For EPR, the stiffness shows a uniform decrease by a factor of about 100 from -40°C to 150°C. In the case of TR-XLPE, the stiffness decreases by a significantly larger factor of 10,000. Compared to EPR, the stiffness of TR-XLPE is greater by some order of magnitudes for lower temperatures while being lesser by some order of magnitudes for higher temperatures around 140°C. Since simultaneous properties of having high thermal expansion and low stiffness is undesirable for cable accessories, the operating temperatures are limited for XLPE (90°C or 105°C) and EPR (140°C) [60].

3.2.5 Partial discharge

Despite lack of general agreement for the definition of partial discharge taking into account its tendency to being associated and used interchangeably with other phenomenon like corona and local breakdown [62], IEC 60270:2000 [63] will be used to provide the general meaning for it. Partial discharge is a term used for the local electrical discharge which causes only partial bridging of insulation between conductor which may or may not exist adjacent to a conductor [62-63]. Partial discharge diagnostic test is usually applied in detecting defects along the cable system [36]. Detection may involve use of systems like a series resonance system. As per AS/NZS 1429.1 [39], the partial discharge for cables is required to be no more than 20pC partial discharge magnitude for the particular voltage designated on the second column of Table 4.14 or no more

than 5pC partial discharge magnitude for the particular voltage designated on the third column of Table 4.14.

3.2.6 Tensile strength and elongation

As per IEC 60502-2 [56], the minimum tensile strength is 4.2MPa for EPR and 12.5MPa for XLPE cable insulation used. As per AS/NZS 1429.1 [39], in line with the compatibility test of air oven aged samples, the measured tensile strength of insulation should not be lower than 75% of the tensile strength of unaged sample.

As per IEC 60502-2 [56], the minimum elongation at break is 200% for both EPR and XLPE cable insulation used. As per AS/NZS 1429.1 [39], in line with the compatibility test of air oven aged samples, the measured elongation at break should not be lower than 65% of the elongation at break of unaged sample.

3.2.7 Dielectric strength

The dielectric strength also referred to as the withstand field strength and breakdown field strength is a property of insulation material particular to value of the electric field in which breakdown of interelectrode occurs. The dielectric strength can be calculated by dividing the breakdown voltage with the electrode distance. For non-homogenous electric field, a factor called degree of homogeneity is introduced in the denominator of the formula previously stated. Various factors are considered which affect the measured value of the dielectric strength of insulation materials which include thickness of test specimen, mechanical strain, pretreatment, moisture, gas inclusions, structure of the molecules of material, fillers, purity, type of voltage applied, voltage waveform, voltage frequency, duration of the application of stress, surrounding pressure, humidity, and temperature, electrode geometry like distance and curvature, stressed volume, and

quality of surface. There are three recognised mechanisms associated with solid insulation breakdown which include electrical, thermal, and partial discharge effects. Since the dielectric strength is particular to the electrical breakdown mechanism alone, the thermal and partial discharge factors are taken into account as to not influence the measured dielectric strength in the test. In order to do this, the test for measuring dielectric strength is made short and the material structure is made homogeneous. In line with the dielectric strength test, the IEC 60243 [66] is one of the most usual reference used. The tests were designed for solid insulations at power frequencies ranging from 48 to 62Hz. The dielectric strength test from the standard is only intended for observing changes from usual material characteristics caused by ageing or other factors. The dielectric strength test is not applicable on evaluation of the insulation behaviour for actual operating conditions. The test usually involves oil immersion in which a 1-3mm flat dielectric material is placed between two plate round-edged electrodes parallel to each other at a coaxial position. The high voltage electrode situated at the top has a diameter of 25mm while the ground electrode situated at the bottom has a diameter of 75mm corresponding to 2mm alignment tolerance or 25mm corresponding to 1mm alignment tolerance. The round edge of the electrodes follows a certain curvature called Rogowski profile in order to reduce the enhancement of electric field due to finite size of the parallel electrodes. However, an issue still arises regarding the triple point (intersection of an electrode, test insulation specimen, and surrounding medium) where intensity of electric field is the highest in the test configuration associated to the difference in permittivity of the sample insulation and the oil surrounding it. This is due to the ignition of partial discharges at this point prior to the interelectrode breakdown i.e., an earlier failure occurs due to partial discharges referred to as boundary field breakdown. Since a premature failure is induced, the measured value of dielectric strength is an underestimation of the actual dielectric strength. The measured dielectric strength values usually range from 15kV/mm to 30kV/mm [64-67].

3.2.8 Dielectric Dissipation Factor (DDF) / $\tan\delta$

The Dielectric Dissipation Factor (DDF) also known as the $\tan\delta$ is a means of measuring the amount of power dissipated by an insulation material equating to power losses [36]. For underground cables, the DDF measurement is representative of the general losses instead of local defects. Measurement of DDF involves application of a.c. voltage and determination of the difference in the phase of voltage and current waveform. The DDF can be illustrated by an electric circuit composed of a resistor and capacitor in parallel connection in which an a.c. voltage is applied. In this case, the DDF is equivalent to the ratio of the current passing through the resistor termed as the loss current I_R to the current passing through the capacitor termed as charging current I_C expressed in the following equation:

$$DDF = \frac{I_R}{I_C} \quad (3.3)$$

Another way of representing DDF is by considering the complex permittivity ε in F/m of the form:

$$\varepsilon = \varepsilon' - j \cdot \varepsilon'' \quad (3.4)$$

where ε' refers to the real part of the complex permittivity (pertinent to insulation material), j denotes imaginary unit value of $\sqrt{-1}$, and ε'' corresponds to the imaginary part of the complex permittivity (pertinent to the losses in insulation). From [36], DDF is expressed as:

$$DDF = \frac{\varepsilon''}{\varepsilon'} \quad (3.5)$$

With the relationship of conductivity σ in S/m and ε'' expressed as

$$\sigma = \omega \cdot \varepsilon'' \quad (3.6)$$

where ω refers to the angular frequency in rad/s, DDF can be furthermore expressed as follows:

$$DDF = \frac{\sigma}{\omega \cdot \varepsilon'} \quad (3.7)$$

As per AS/NZS 1429.1 [39], test for the measurement of DDF at higher temperature is performed for rated voltages higher than 3.8/6.6 (7.2) kV. Criterion involves $\tan\delta$ not exceeding 0.008 for XLPE and 0.04 for EPR between 95 to 100°C. Measurement is performed using power frequency voltages of $0.5 U_0$, U_0 , and $2 U_0$ at similar temperatures with deviation of $\pm 5^\circ\text{C}$. Heating of the sample is done in a liquid tank, oven, or through heating current passed through the metallic screen or through current loading of cores. Measurement of the core temperature is determined through measurement of core resistance or through other appropriate methods. The core temperature is raised until it reaches the prescribed temperature range of 95 to 100°C. Measurement of DDF is then performed by applying 2kV power frequency voltage to the sample. Experiments on XLPE show that DDF increases with temperature [68].

3.3 Breakdown history

As time progresses, power distribution cables are subject to the ageing process. This in turn causes degradation on the quality of the insulation material used which eventually leads to breakdown [36].

The breakdown mechanisms of insulation materials can be categorised into four types [1]:

- Electric,
- Thermal,
- Electromechanical, and
- Partial discharge

Electric breakdowns or intrinsic breakdown occurs when a free electron accelerates at a very high electric field strength around 500kV/mm which causes electron avalanche leading to a breakdown. Although in reality such magnitude of electric field strength is not attained, the breakdown still occurs attributed to the imperfections of the material [1, 36]. For PE, electric breakdown caused by discharge was greatly recognised and was subject to various studies. The significantly severe discharge corrodes the fine channels of the PE resulting to failure. The corrosion may be in the form of chemical decomposition, melting, and formation of microscopic cracks in the insulation [9].

Thermal breakdown takes place when there are net concentrations of heat losses in particular areas of the insulation due to insufficient heat dissipation. This causes the electrical conductivity of the material to increase as well as the current density which contributes to increased heating effect until such time that thermal runaway occurs [1]. Thermal breakdown usually occurs in cables using PVC and paper insulations. It was associated to a number of failures for insulation materials having low DDF in which contaminants brought by the processing and compounding cause appearance of localised areas with higher DDF. Detection of the presence of such localised areas is impracticable since DDF measurements are only particular to predominant low DDF figure of insulation, hence inundating the fewer numbers of high DDF areas [9].

Electromechanical breakdown takes place when the insulation is thinned out by attraction of the electrostatic forces with the electrodes. The thinning of the insulation leads to further increase of attraction. Heating contributes to speeding of the process which eventually leads to breakdown [1].

Partial discharge breakdown takes place when partial discharges occur in void filled with gas like air which leads to the formation of electrical trees. As the partial discharge keeps on going, the electrical tree continues to grow until breakdown occurs [1].

3.4 Treeing phenomenon

3.4.1 History

In the 1960s, upon application of polymer insulated cables especially XLPE in MV power networks, the water treeing phenomenon was not yet known. After about a decade, early faults were associated to the not yet known treeing phenomenon. In the case of USA, many early failures of cables were associated to the water treeing phenomenon emerging from protrusions and edges of semiconducting screens that were taped. Although more known to occur in polyethylene, water trees also have verified occurrence in other materials including EPR, PVC, PP, and Ethylene-Vinyl Acetate copolymer (EVA). The occurrence of water trees was not only restricted to conditions under high stress. There were also water trees discovered in electrical stresses less than 1kV/mm [9].

In the present, the phenomenon of water-treeing was recognised as the most significant degradation mechanism in polymer insulated MV cables. Water trees are tree-like or bush-like structures (as revealed by microscopy) found in polymeric insulation materials. Water trees comprise of tiny channels and microscopic voids through which penetration of the water occurs due to electric field. Their growth can be induced by the presence of water which can correspond to air at 70% relative humidity and electric field. Presence of contaminants can also contribute to the occurrence of water trees. Presence of water trees especially of vented type in polymers cause

decrease in the electric withstand of the material which consequently leads to greater failure probability. Dielectric properties also vary depending on whether the water tree is wet or dry. For wet water trees, the dielectric properties show non-linear behaviour while for dry water trees, their dielectric properties were identical with the dry insulation. Wet water trees were also determined to have relative dielectric permittivity values ranging from 2.3 to 3.6 and being 9.2 at the tip. Wet water trees were also found to have higher conductivity values than the polymer insulation, hence water trees tend to have greater permittivity, conductivity, and capacitance [1, 36].

3.4.2 Types of water trees

There are generally two types of water trees: vented type and bow-tie type (see Figure 3.1).

Vented Type: The vented type of water trees are those that initiate along the surface or boundary of the insulation i.e. at interfaces of the insulation and semi-conductive screens (insulation screen and core screen). Between the two types of water trees, the vented type of water trees are considered the most dangerous associated to major cause of failures of water-treed specimens. The vented type water trees growing from the core screen are considered as critical vented water trees which may grow long based on design of the cable and conditions upon service [1, 4, 36].

Bow-tie Type: On the other hand, a bow-tie type of water tree refers to those growing inside the insulation which may be from a void, contaminant that is soluble to water, and others. Types of water trees identical to the look of bowtie (hence the name) can extend up to a few thousands of micrometers and even to but with eventual tendency to have a fixed size. There is also the possibility of several bow-tie type water trees combining into a single long water tree or reaching either of the screen boundaries and transforming into

a vented-type water tree. Various factors are considered for the possibility of occurrence of such instances including the number and distribution of the bow-tie type water trees and the condition of the environment. In majority of instances, the bow-tie type water trees do not cause breakdown. Bow-tie water trees have lesser impact in the reduction of the electrical withstand of the insulation owing to being significantly shorter than vented-type water trees [1, 4, 36].

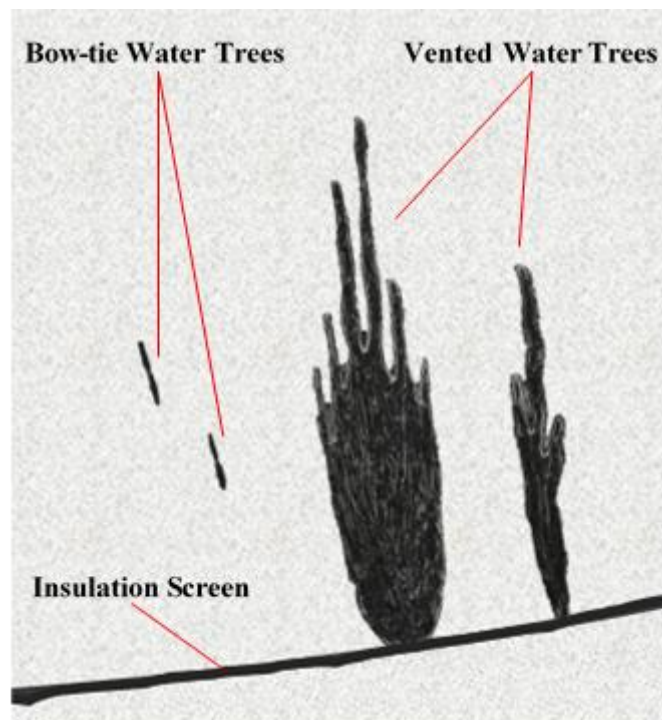


Figure 3.1: Types of water trees

3.4.3 Stages of water tree growth

Two or three stages are associated to the growth of the water trees. The first one pertains to early inception of the water tree described by swift growth but with decreasing growth rate. The inception of water trees is associated to presence of impurity in the insulation which may be in the form of salt inclusion or transition metal ions. This is followed by emergence of hydrophilic

path usually containing salt indicating development of the water trees. The second stage is characterised by an even further decrease in growth rate. Vented-type water trees may take about half a decade or above in order to fully grow throughout the insulation. The third stage is referred to as the final breakdown stage. This stage begins when the water tree transforms into an electrical tree. Detection of carbon in water trees suggests this transition into electrical trees. The rate of propagation of electrical tree is more than 1000 times greater compared to water tree. Upon initiation of electrical tree from water tree, the occurrence of breakdown may take into place even in just few hours under usual stress condition of 2kV/mm. The transition into electrical tree usually occurs from the tip of water tree where the gradient of electrical field is maximum. In rare cases as reported by other literatures, electrical trees may also form from the base of water trees. Either ways in time, the electrical trees will propagate the insulation, bridging the insulation resulting to failure. Various factors lead to the transition of water trees into electrical trees. These include transient overvoltage, value of voltage, design of cable, and oxidation in the insulation. Regarding the transient overvoltage, greater magnitude is required for shorter duration. Upon removal of water and voltage, the water trees were deemed to vanish and upon introduction of water and voltage again, the water trees revive. Temperature was also found to contribute to the transition of water trees into electrical trees. High temperature tends to decrease the transition time attributed to the increased oxidation activity in the insulation. Experiment by Bulinski et al. on XLPE insulations showed that the transition occurs when the vented type water trees have grown enough to reach the insulation screen or about 200 μm [1, 4, 36]. It also suggests that concentration or type of contaminants do not have direct effect on the tendency for the transition of the water tree to electrical tree.

3.4.4 Water tree inception and growth

Various theories regarding the inception and growth of water trees were discussed by Footitt [4]. He pointed out that the location of the water trees could help in the determination of their cause. For water trees showing consistent distribution all over the insulation, impurities may be the cause. In the case of chemical causes, the water trees may be found on a particular portion of the insulation. When the water trees are concentrated close to the core, the leading causes may be associated to electrical or thermal degradation. If the water trees are found on the outer radial portion of insulation, the dominant cause may be attributed to mechanical means.

Contamination: Despite the improvements in the characteristics of polymer insulation, there is almost an assurance that there is a certain amount of contaminant present which may induce chemical reactions detrimental to the life of the material. Example of usual contaminant is sodium chloride or salt. There are also other contaminants which have potentials of causing greater harm to the insulation [4]. Promvichai et al. [69] conducted a study regarding the effect of sodium chloride in the propagation of water tree in XLPE insulated cable for MV underground cable system. The test involves using an XLPE insulated cable in which group of pinned holes are made on the insulation. The test specimen was then subjected to 0.1 mol/L concentration of sodium chloride under rated voltage but of three sets of temperatures: ambient, 50°C, and 70°C. The test was also performed for two durations of 1,000 hours and 2,000 hours. Results showed the formation of water trees for all test parameter combinations but only of vented type. The water trees measured between 100µm to 300µm. For the 1,000 testing period, the average water tree length was found to be consistently decreasing with increasing temperature. However, for the 2000 hours testing period, the average water tree length showed non-monotonic increase peaking at 50°C.

Oxidation: Bond cleavage is pointed to be a possible agent of growth of water trees. Bond cleavage may be caused by mechanical malfunction or injection of electrons. With the polymer chains having been broken, oxygen free radicals are released causing the occurrence of further bond cleavage. Additionally, the derivative of oxidation is more hydrophilic compared to the polymer insulation. However, it was noted that even the lack of oxygen was not able to cease the development of water tree which is further supported by a study which found out that oxidation level are almost identical to both the water treed areas and the polymer [4].

Environmental Stress Cracking (ESC): The theory of ESC suggests that sufficient mechanical stress may induce cracking of the insulation promoting water tree growth. Considering insulation under electrical stress, an electrokinetic force may have been generated which tends to force expansion of the insulation. The expansion makes it easier for the penetration of water into the microscopic cracks of the insulation which consequently hastens the time of formation of the water trees [4].

Residual Stresses/Bending: Between the two axial stresses, tensile stress tends to cause the faster formation of water trees compared to the compressive stress. This is associated to the enlargement of microscopic cracks allowing more water to penetrate, hence support water tree inception. This can be induced by the bending of the cable in which the outer bend part experiences tensile stress. The increased rate of growth of water trees is found to be optimised under moderate magnitude of tensile stress. More specifically, development of water tree increased by 100%, hence doubling the rate for a 30% tensile stress while for above values, effect on growth is not remarkable [4].

Field-Induced Fracture: When an insulation is subjected under an electric field, various types of forces are induced. For instance, interfacial force is induced when two materials with unlike permittivities become in contact with each other. The amount of interfacial force depends upon the permittivities and orthogonal field components. Presence of cracks or voids filled with water will produce electric field concentrations on the void ends which is about two to five times greater than the electric field applied to the material. Consequently, low density regions are formed with microscopic voids leading to heightened water tree developments [4].

Fatigue: Under the influence of strong electric fields, drops of water tend to distort which makes a void filled with water to contract and expand repeatedly due to the alternating nature of the field. This action causes the insulation material to experience mechanical fatigue which in turn causes the development of microscopic cracks supporting the growth of water trees. On this basis, ageing increases with frequency on a logarithmic basis [4].

Dielectric Heating: With consideration to the effect of chemical processes in the growth of water trees, heat also hasten the development of water trees by boosting the chemical activities. Additionally, owing to the imperfection of the insulation regarding its homogeneity, there are regions where local intensification of electrical field occur. In the instances of impulse, the intense electrical field may give rise to overheating causing damage or deformation to the material [4].

Dielectrophoresis: Dielectrophoresis refers to the motion of polarised particle in a non-uniform electric field i.e., from low to high field area. Owing to water concentrations in

a water tree, diffusion causes movement of the water molecules away. Dielectrophoresis tends otherwise, maintaining the water molecules inside the water tree. When the dielectrophoretic force overcomes the diffusive force, water molecules are even pushed into the water tree site. The dielectrophoretic force depends on the particle geometry and electric field intensity. Comment on this theory is the validity of d.c. field to cause development of water trees. It was instead observed that greater frequency corresponds to rise of water tree growth but to the decline of dielectrophoretic force. The dielectrophoresis theory proposes that under the influence of d.c. field, brief changes in morphology of XLPE with water trees takes place [4].

Electro-Osmosis: The existence of intrusion, inclusion, or void in the dielectric material induces local electric field intensification. Water molecules in the dielectric material will likely evacuate from low to high electric field regions which in turn result to hydrostatic pressure providing a pool from which water trees can draw from [4].

Electrostriction: This is also referred to as Maxwell forces in which there is a proposal that a pressure change takes place when a dielectric fluid is under the influence of electric field. The pressure change depends on the electric field and permittivity of insulation. In the case of electric field that varies with time, water droplet will exhibit indefinite contraction and expansion causing cracking and fatigue in the material [4].

Condensation: Despite absence of insulation anomalies (e.g., inclusions, voids), hydraulic pressure may still be imposed upon condensation of water vapour between strands of the polymer insulation. For instance, 2.5MPa of hydraulic pressure is imposed with 2% supersaturation of air. Such magnitude of pressure is near the XLPE rupture

point. Presence of ions soluble in water will reduce the vapour pressure of the water resulting to the greater condensation rate, hence faster development of water trees. At 75% relative humidity conditions, condensation becomes suitable for inclusions of sodium chloride. By virtue of thermodynamics, regions of high electric field like voids promote the condensation of water. Therefore, condensation of water is almost a guarantee in humid environments like in cables that are directly buried [4].

Osmosis: By the principle of osmosis, considering the semi-permeability of polymer like XLPE, water will show natural tendency to evacuate towards the dielectric material until balance of concentration is achieved. Presence of water-soluble inclusions in the dielectric material will cause attraction of water particles which consequently leads to building up of osmotic pressure. The osmotic pressure may cause formation of cracks in the insulation, hence promoting growth of water trees [4].

3.5 Discussion about Cross-linked Polyethylene

It was in the 1930s that LDPE was first developed. PE is a thermoplastic material made up of long chains of hydrocarbon molecules. The manufacture of PE involves pressure by polymerisation of ethylene. Compared with the earlier paper insulation, PE provided flexibility at low temperature, ease of manufacturing, better electrical properties, resistance from chemical and moisture, and minimal cost. However, its temperature rating was only 75°C compared with paper insulation which was about 80 to 90°C [28].

In 1963, General Electric Company invented XLPE which can be produced by compounding LDPE with a cross-linking agent (e.g., dicumyl peroxide). The cross-linking of the long chains of

PE molecules was induced through vulcanisation or curing process. The cross-linked material acquired improvements in its mechanical properties while preserving its electrical properties. The development of XLPE allowed the operating temperature to be increased to 90°C. The use of XLPE insulated cables in medium voltage applications began in 1968 [28].

However, in 1972, there was a significant increase in the rate of failures of the cables installed. The failures were attributed to the water trees caused by localised high electrical stress points formed by ingress of moisture and imperfections in the cable. In response to this, several measures were taken which include use of dry curing method to prevent moisture and void, application of semiconductive screens, and introduction of WTR-XLPE [28].

At low temperatures like 20°C, XLPE insulation was described to be stronger than EPR insulation. Then as the temperature approached 90°C which reflects maximum operating condition, the tensile strength values of both insulations tend to be equal. With the temperature further increased to 130°C which reflects overload condition, 63% reduction in tensile strength value of XLPE was observed. This was attributed to the transformation of XLPE from crystalline to amorphous at melting point of 110°C. XLPE then showed stable values from the overload temperature to the short circuit condition of 250°C. On the other hand, EPR showed stability throughout the entire range considered. XLPE was also described to be very stiff which makes it difficult to handle [70].

Various research were conducted with the aim of predicting the behaviour of the properties of XLPE with respect to various parameters like time and stress. Life models were also developed in an attempt to predict the life of XLPE by considering the changes in its properties with respect to selected parameters.

Montanari, Pattini, and Simoni [71] performed test cycles on XLPE insulated cable taking into account the thermal, electrical, and combined thermal-electrical stresses using Combined Analysis Method (CAM). Insulation life was represented as a function of electrical and thermal stress. Intersection of life surface with the planes parallel to the corresponding coordinates resulted to graphs of constant temperature electrical life at, constant electrical stress thermal life, and voltage vs temperature at constant life. Pretreatment of the samples was performed by heating at 90°C for a duration of 100 hours to remove the by-products of cross-linking. The electrical life curve plotted at room temperature was in agreement with the one obtained by Bahder where the lines approached a threshold value (about 11kV/mm for the Author's and 13kV/mm for Bahder). Combined-stress tests for every corresponding constant temperature showed convergence of line to threshold voltage (like 11kV at room temperature and 4kV at temperatures a bit lower than 110°C) with increasing life. For corresponding constant voltage, the line showed convergence towards threshold temperature (like 100 °C for 4-5kV electrical stress) with increasing life. For the constant life curves which depicted plots of voltage-temperature for every corresponding life, lines showed linear behaviour and parallel pattern from room temperature of 20 to 90°C from which a sharp and almost vertical drop occurs.

Motori, Sandrolini, and Montanari [72] performed measurements of the d.c. electrical conductivity of XLPE insulated cables subjected to various ageing times. The electrical test and combined-stress tests were conducted with at temperature range between 20 to 110°C and voltage range between 4kV and 28kV in air while the thermal life tests were conducted between 100 to 150°C as per IEC 216. Prior to performance of life tests, the specimens were pretreated at 90°C for a duration of 90 to 100 hours to compensate variety in manufacturing backgrounds. Progressive censoring was also applied which involved taking out samples prior to failure with the remaining ones aged to breakdown. The progressive censoring allowed the author to examine

the behaviour of properties as a function of time. Results showed significant increase in the value of electrical conductivity for temperatures 110°C and 130°C by several magnitudes while 100°C aged samples showed slight increase of the said property which supported the idea of thermal threshold at 100°C. The decrease of electrical conductivity at 130°C aged samples was associated with the phenomena of thermooxidative degradation with the appearance of macroscopic cracks.

Montanari and Cacciari [73] used two parameter Weibull Cumulative Distribution Function (CDF) as the probabilistic life model for XLPE insulated cables. The parameters of the Weibull CDF were assumed to be functions of electrical and thermal stress. The electrical lines considered for the new model showed upward curvature and threshold for both electrical and thermal for low stress values at different temperatures. The upward curvature of the lifeline in bi-log paper was associated with the changes in the value of the Voltage Endurance Coefficient (VEC) for the inverse power model. The authors also introduced an equation for the expression of the VEC as function of electrical stress. The electrical life tests were conducted at 20°C, 60°C, 90°C, and 110°C with 50Hz supply frequency and at room temperature for low voltages (11.5kV and 15kV) at frequency of 450Hz for determination of electrical threshold. For the higher frequency, life values were acquired by taking the ratio of frequencies as the acceleration factor. Results showed satisfactory agreement of the inverse power threshold model proposed where the plot of life model tended towards an electrical threshold value of 11.5kV/mm at 450Hz. There was also satisfactory agreement of the CAM model with the four test temperatures especially for 60°C and 90°C where there was clear convergence towards their respective threshold values. It was also observed that the statistical model gave unique electrical threshold value regardless of the failure percentiles which was in agreement with the threshold's physical meaning.

Montanari and Motori [74] studied the breakdown and time variation of the properties of XLPE insulated cables particular to thermo-electrical stress condition. Prior to testing, the test specimens were subjected to pretreatment. Electrical life tests were conducted at ambient temperature while thermo-electrical life tests were conducted in an oven. There were also few tests conducted at high frequency of 500Hz both in air and water to investigate the existence of an electrical threshold. The author also applied progressive censoring procedure for the electrical and thermo-electrical life tests to acquire information about the percentiles of failure time and the time variation of the important properties (including electrical stress, voltage, temperature, density, melting enthalpy, and electrical conductivity) under consideration. Results showed that synergism between electrical and thermal stress occurred considering the significant decrease in the electrical threshold with increase in temperature. Also, the thermal threshold was hypothesised to be around 100°C in which the thermal ageing was negligible. The plots between electrical stress and insulation life for a set of constant temperatures showed that increase in electrical stress and/or decrease in temperature corresponded to increase in insulation life and with each electrical lifeline having electrical threshold. It was observed as well that density, melting enthalpy and electrical conductivity increased with insulation life more significantly with both electric and thermal stress applied. The incremental tendency of density and melting enthalpy was associated with the phenomenon of recrystallisation amplified by the combined effects of temperature and electric field. Still, weaker degradation phenomena like thermo-oxidation may dominate the recrystallisation phenomena, hence producing opposite effect on the density and melting enthalpy (tending to decrease with ageing time). In the case of electrical conductivity, a non-monotonic display was observed. The initial increase in the value of the electrical conductivity was associated with increase in the motion of charge carriers while the decrease in its value was associated with the depletion of the average free path and the enhanced trapping upon degradation of the insulation bulk. But since the breakdown of the insulations took place prior to detection of the

bulk degradation, it was argued that in the condition of multiple stress, the failure or breakdown is to be associated with the local phenomena instead of the bulk degradation. The synergism of thermal and electrical stress decreased the activation energy which contributed to the occurrence of degradation processes which were not observed for single stress conditions. Observations by scanning electron microscopy revealed heterogeneous areas increasing in both number and size as ageing time increased under thermo-electrical stress while there were hardly any of such in the case of thermally aged specimens even for prolonged ageing durations.

Motori et al. [75] studied the time and stress variation of the chemical-physical properties (including density and melting enthalpy) and electrical properties (including d.c. electrical conductivity and electric strength) of XLPE insulated cables. Prior to testing, the test specimens were subjected to pretreatment by heating at 90°C for a duration of 90-100 hours for the stabilisation of the insulations taking into account the variety in the manufacturing backgrounds pertinent to the curing process. As per IEC 216, the thermal life tests were performed at temperatures 100°C, 110°C, and 130°C. Progressive censoring was applied in which a certain number of test specimens were taken periodically for the measurements of properties pertaining to the characterisation of thermal endurance (dielectric strength, tensile strength, and weight loss) and the said chemical-physical properties. As per ASTM Standard D257, measurement of the d.c. charging currents or the conductivity was performed using the voltmeter ammeter method in air between the temperatures 55°C and 90°C and at constant voltages reaching 3kV (equivalent to 3kV/mm application of electric field). Measurement of d.c. discharging currents was performed by electrode shorting, allowing detection of dielectric relaxation at frequencies below 0.01Hz using the Hamon method. Measurements of a.c. in obtaining the frequency and time variation of the relative dielectric constant and dielectric loss factor were performed as per ASTM Standard D150 in air at frequencies between 0.01Hz and 10,000Hz and temperatures between 55°C and

90°C. Results showed that for the pretreated cables at temperature of 90°C and thermally aged cables (at 110°C for 8074 hours and at 130°C for 4863 hours), the charging current tended to approach a quasi-steady state as evidenced by the almost constant values observed (very slight decrease) for each corresponding temperature for the whole test duration. On the other hand, the discharging currents decreased in value by up to three magnitudes based on the endpoints of the test time for both the pretreated and aged cables. For the 1 minute, 10 minutes, 60 minutes, and 120 minutes test durations, results showed linear increase in the electrical conductivity with the reciprocal of the increasing temperature in absolute scale for both pretreated and aged cables which conformed to the Arrhenius law. It was also observed that the electrical conductivity of the aged specimens were about two magnitudes higher than the pretreated specimens. This increase was associated to the increased density and mobility of charge carriers and the occurrence of process of thermo-oxidation. It was noted that the pretreated cables at 100°C produced almost the same data for the conductivity with minimal variations even with the prolonged time of ageing. The observation of constancy of the average apparent activation energy supported the idea that the conduction mechanism was not majorly influenced by thermal ageing. From the results, it was also shown that dielectric loss factor was non-monotonic (initially decreasing then increasing) with respect to the increase in frequency which was more evident for the aged specimens. The increased dielectric loss factor was associated with the dominance of thermo-oxidation as the degradation process for temperatures above 100°C.

Motori, Sandrolini, and Montanari [76] performed electrical, thermal, and electro-thermal tests on XLPE insulated cables for a comprehensive discussion of the effects and mechanisms of insulation ageing. Characterisation of the electrical, physical, chemical, and microstructural aspect of the insulation was also performed in line with the endurance tests. Before the ageing tests, the test specimens were thermally pretreated at a temperature of 90°C for a duration of

90hours for the stabilisation of the insulation materials taking into account the various manufacturing backgrounds. As per IEC 216, for the tests of thermal life, the test specimens (400mm long) were placed in an oven at temperature between 100°C and 150°C. Considered properties for the characterisation of the thermal endurance include tensile strength, tensile modulus, electric strength, density, weight, and melting enthalpy. For the electrical and thermo-electrical stress tests, the test specimens 40 to 2000mm long were subjected to temperatures between 20 to 110°C and voltage ratings between 4 to 28kV in air. The electrical and thermo-electrical stress tests were conducted until breakdown or failure while in some, progressive censoring procedure was applied where test specimens are taken out in between the ageing duration prior to failure. These procedures allowed a complete characterisation of the failure times and the time variation of properties under consideration. For the electric strength, measurements were conducted with voltage rise between 10 to 30kV/min.

In line with the thermal stress tests, the initial values for the properties considered for the characterisation of thermal endurance are as follows: density = 0.916g/cm³, melting enthalpy = 84J/g, and electric strength = 82kV/mm. Results showed that there was dramatic increase in the density for the temperatures 110°C and 130°C (about 5% increase after 9,000hours and 5,000 hours respectively) while density was almost constant at 100°C (noting that it was below the determined melting point of 106°C) for about 20,000 hours ageing time. The melting enthalpy at 100°C also showed almost no change for the whole ageing time while about 70% reduction after 9,000 hours and 90% reduction after about 8,000 hours was observed for temperatures 110°C and 130°C, respectively. There was also observed 50% reduction in the electric strength after 9,500 hours at 110°C and 1600 hours at 130°C while only 20% reduction was observed at temperature of 100°C at 20,000 hours ageing time. For the property analysis by radial position, it was revealed that density showed linear increase from inner to outer for both 110°C (almost constant for 554

hours ageing time, 1.5 to 2.5% increase for 5633 hours, 2 to 3% increase for 7695 hours, and 3 to 6% increase for 9,017 hours) and 130°C (almost constant for 92 hours ageing time, 0.5 to 4% increase for 830 hours, 2 to 5.7% for 2,730 hours, and 2.5 to 7% for 4,863 hours). Considering again the property analysis by radial position, the melting enthalpy showed almost linear decrease for both 110°C (0 to 15% decrease for 554 hours ageing time, 50 to 55% decrease for 5,633 hours, 55 to 60% decrease for 7,695 hours, and 88 to 95% decrease for 9,017 hours) and 130°C (almost constant for 92 hours, 12 to 30% decrease for 830 hours, 40 to 75% decrease for 2,730 hours, and 80 to 85% decrease for 4,863 hours). Scanning electron microscopy showed microscopic cracks in the pretreated insulation at various temperatures and time of ageing. The cracks showed negligible change for the ageing temperature of 100°C. However, at temperatures 110°C and 130°C, the cracks showed size growth and heterogeneities at prolonged times of ageing. Energy dispersive spectrometry and wavelength dispersive spectrometry showed existence of contaminants including sodium, chlorine, calcium, potassium and silicon [76].

In line with the electrical and thermo-electrical stress conducted at 12kV at temperatures 20°C, 60°C, and 90°C, results showed similar increasing trend for the density (0.2%, hence almost constant at 20°C, 1% at 60°C, and 0.5% at 90°C for 1000 hours ageing time) and melting enthalpy (1%, hence almost constant at 20°C, 18% at 60°C, and 5% at 90°C for 1.000 hours of ageing time). The electric strength showed non-monotonic behaviour characterised by spiked increase and decrease in the value for all temperatures. Considering radial position, the density and melting point showed very small increase from inner to outer and with longer ageing time (about 1% max difference of density between inner and outer for both 60°C and 90°C ageing temperature at 12kV). Scanning electron microscopy revealed discontinuities concentrated in areas with microstructures that were highly heterogeneous. Wavelength dispersive spectrometry showed presence of sulphur in the areas which tend to decrease with ageing time. Impurities including

sodium, chlorine, potassium, and silicon were detected associated with the manufacturing process, taper water-cooling proceeding steam curing, or impurities in semiconducting screen. For 20°C at 12kV, the microscopic cracks showed negligible change with ageing time. But for both 60°C and 90°C at 12kV, the cracks showed size growth at prolonged time of ageing [76].

The constancy of melting enthalpy and density in electrical ageing below 20°C and thermal ageing below 100°C in contrast with significant increase for thermo-electrical ageing suggested a synergism between electrical and thermal stress which was associated to the phenomena of recrystallisation. Greater density increases for 60°C at 12kV compared to 90°C at 12kV was associated to the dominance of thermal processes including thermo-oxidation and crystallisation which opposed the property increase and inhibited the synergism of temperature and electric field. The non-monotonic behaviour of the electric strength, particularly for the dramatic decrease was associated with being caused by slow diffusion in the bulk of the insulation and diffusion, consumption, and migration (towards outer surface of insulation) of the antioxidant taking into account that temperature amplified the diffusion causing hastened expelling of the antioxidant leading to decline in the stabilisation of voltage. The heterogeneity of areas from the analysis of microstructure was attributed to the clustering of antioxidant. It was argued that in the course of ageing, partial consumption and partial diffusion (towards outer layer) of the antioxidant took place alongside migration of contaminants towards the heterogeneous areas. The existence of heterogeneous areas in the insulation lead to susceptibility in treeing and partial discharge phenomenon when water and significantly high voltage was introduced [76].

Motori, Sandrolini, and Montanari [77] investigated the behaviour of the d.c. electrical conductivity, charging currents, and discharging currents under thermo-electrical stress of XLPE insulated cables. As per ASTM Standard D257, measurement of the d.c. charging currents or the

conductivity was performed on 40mm long cables using the voltmeter ammeter method in air between the temperatures 55°C and 90°C and at constant voltages reaching 3kV (equivalent to 3kV/mm application of electric field). Measurement of d.c. discharging currents was performed by electrode shorting, allowing detection of dielectric relaxation at frequencies below 0.01Hz using the Hamon method. Results showed that for 12kV at 60°C ageing condition at ageing times of 626 hours, 1134 hours, and 1367 hours, decreasing absolute difference between the charging and discharging current densities was observed with decreasing temperature. The measurements of the d.c. electrical conductivity considered voltage application times of 1 minute, 10, minutes, and 60 minutes plotted against reciprocal of temperature. For varied ageing time, plots at 60 minutes voltage application time showed notable linear behaviour, hence in agreement with Arrhenius law while at 1 minute and 10 minutes voltage application times, the plots showed fair linearity. Results also showed a non-monotonic behaviour of conductivity with respect to ageing time peaking at about 1134 hours for about 5.5 times compared to pretreated cables. There was also an observed dielectric relaxation process in cables aged at 12kV and 60°C for 1134 hours between the frequencies 0.00001Hz and 0.01Hz plotted in a dielectric loss factor versus frequency graph for temperatures 70°C, 80°C, and 90°C. The spike in the electrical conductivity was attributed to the development of heterogeneous areas in the insulation. The rising of the electrical conductivity was associated with the mobility of charge carriers due to synergism of temperature and electric field and their movement towards areas with low density. On the other hand, the decrease in the electrical conductivity was attributed to the heterogeneous areas confining the charge carriers. The sensitivity of the electrical conductivity with regards to degradation process was greatly considered for potential tool of diagnosis in cable monitoring.

Montanari [78] investigated various electrical life models which all considered threshold value. The first models introduced were 3 parameter models including Exponential Threshold Model

(ETM), Inverse-Power Threshold Model (IPTM), and Field Emission Model (FEM). These models were limited to the particular electrical and thermal conditions in which the considered degradation or breakdown was prevalent. This was an important consideration since there are times that the models do not provide good fitting with the results of the experiments conducted. Then phenomenological life models were introduced having 4 parameters for characterisation and were based on the previous 3 parameter models given. The Four-Parameter Exponential Threshold Model (4P-ETM) was derived from the ETM with an added shape parameter to enhance fitting of data. The Four-Parameter Inverse-Power Threshold Model (4P-IPTM) was derived from the IPTM by considering the voltage endurance coefficient as a function of the stress applied with an added shape parameter. For the evaluation of the time to failure for a particular failure probability, a two-parameter Weibull cumulative distribution function was introduced for obtaining the probabilistic life models. For the estimation of the model-parameters, the Least Square Regression Method (LSRM) was selected over the Maximum Likelihood Method (MLM). In the calculations of the confidence interval, methods like Fisher matrix, Monte Carlo, and Bootstrap were considered. For the comparison among the presented life models, the error function was used. Insulation materials considered include XLPE, Nomex-Mylar-Nomex^R, Epoxy Bisphenolic Resin (EPOXY), Polyethylene Terephthalate (PET), Polyimide (PI), and Polypropylene (PP) with data based on literature. Results showed that the error function values were generally lower in the four-parameter life models compared to three-parameter life models supporting the idea that four-parameter life models provided better agreement with the experimental results. Also, the exponential model gave better fitting than the inverse-power model for both the four-parameter and three-parameter life models. For some instances like XLPE and NMN, results revealed good agreement of the four-parameter and three-parameter life models with the Arrhenius law.

Cacciari and Montanari [79] proposed a Weibull-based general approach to probability distribution functions which took into account various stresses (thermal and electrical) considering tendency towards threshold. The life models considered were assumed to be functions of time to failure and stresses applied in which a probabilistic approach was necessary to evaluate the time to failure corresponding to probabilities of failure. The two-parameter Weibull distribution function was introduced as a function of failure time, electrical stress, and thermal stress with the aim of making it valid for particular range of electrical and thermal stresses. The scale and shape parameters were both assumed to be functions of electrical and thermal stress. The expression of the scale parameter may be based on life models with times to failure at 63.2% probability since the scale parameter corresponds to failure time at 63.2% probability. An explicit derivation of the failure time from the two-parameter Weibull distribution function was obtained for the percentiles of time to failure. The life models from literature which include the Four-Parameter Exponential Threshold Model (4P-ETM) and Four-Parameter Inverse-Power Threshold Model (4P-IPTM) were used in equivalence of failure life with scale parameter for explicit expression. Hence, the explicitly defined scale parameter based on the four-parameter models was substituted to the two-parameter Weibull distribution function: becoming a Gumbel distribution for the 4P-ETM. Using the hazard curve or bathtub curve, the shape parameter was expressed as ratio of shape parameter of breakdown voltage Weibull distribution and corresponding endurance coefficient, all of which were considered constant. However, the shape parameter actually showed variations in actual experiments and so the mean value was used considering a linear life model. In the case of curvilinear life models, the expression of the shape parameter was not valid anymore, hence the author proposed a solution in which the shape parameter was considered constant for particular temperatures (shape parameter was independent of electrical stress at a certain temperature). To define the generalised probabilistic life models in terms of temperature, it was proposed to conduct linear regression or multiple regression in

approximating the values of the parameters of the model from the life tests conducted at every temperature. This was also applicable in the case of the three-parameter models including the Field Emission Model (FEM), Inverse-Power Threshold Model (IPTM), and Exponential Threshold Model (ETM). For the estimation of parameters, the faster and simpler Least Square Regression Method (LSRM) was selected over the Maximum Likelihood Method (MLM) with Newton-Raphson method. The calculation of the confidence interval may be performed using the Fisher matrix, but the Monte Carlo or Bootstrap was the preferable choice. Regarding the estimation of the model parameters, it was taken into account the accuracy depended on the fitting of the model used, the accuracy of the statistical procedure selected in the estimation of the parameters, the procedure of the test, and the number of parameters being considered. The improvement of the fitting of the data may be done by considering more parameters and data (by increased number of performed life tests, size of sample, and censoring degree). The range of stresses considered in the probability distribution functions were as follows: for XLPE (electrical stress between 4kV/mm and 28kV/mm at temperatures between 20°C and 110°C), Nomex-Mylar-Nomex™ or NMN (electrical stress between 7kV/mm and 72kV/mm at temperatures between 20°C, and 180°C), epoxy bisphenolic resin or EPOXY (electrical stress between 10kV/mm to 20kV/mm at temperatures of 20°C and 40°C), and polyimide or PI (electrical stress between 3kV/mm to 30kV/mm at temperature of 180°C). The generalised probability distribution function in the thermal stress domain was mainly considered on XLPE and NMN since they cover multiple test temperatures (20°C, 60°C, 90°C, and 110°C for XLPE and 20°C, 50°C, 105°C, 180°C, and 180°C for NMN). Plots of NMN (at 50% probability based from 4P-ETM, 4P-IPTM, Three-Parameter Exponential Threshold Model (3P-ETM), and Three-Parameter Inverse-Power Threshold Model (3P-IPTM) for temperatures 50°C and 105°C), XLPE (at 10% and 90% probability failure based from 4P-ETM and 4P-IPTM at temperature of 20°C), PI (at 10% and 90% probability failure based from 4P-ETM at temperature of 180°C), and XLPE (at 10% and

90% probability failure based from 3P-ETM and 3P-IPTM at temperature of 20°C) were presented to compare model fitting. Logarithm of the parameters versus conventional thermal stress (in accordance with Arrhenius relationship) were also plotted which supported validity of linear regression in estimation of model parameters for other temperatures. Good fitting was observed for the 4P-ETM and 4P-IPTM of NMN and XLPE with respect to the results of the experiments. Even for extreme probability failures of 10% and 90%, the lifelines were significantly near life points, hence, accurate estimation of failures times can be obtained for other electrical stresses at extreme values of percentiles. The dispersion of experimental points with the life points was attributed to assuming the value of shape parameter to be constant for every temperature. Poorer fitting was observed for the three-parameter models compared to the four-parameter models but still showed good fitting with respect to the experimental points especially at values near threshold considering extreme probability values of 10% and 90%. Comparison of the models was statistically performed using the error function of LSRM method considering 10%, 50%, and 90% failure probabilities. Results showed error function values of almost the same order for the exponential and inverse-power models considering the given failure probabilities for all insulation materials. Generally, the exponential model provided lower error function values compared to inverse-power model, hence offered a bit better fit. It was also observed that the electrical threshold was not dependent with the probability of failure.

3.6 Discussion about Ethylene Propylene Rubber

According to Brown [61], in the view of polymer chemists, the term EPR pertains to ethylene and propylene copolymers. On the other hand, EPDM corresponds to terpolymers based on ethylene, propylene, and diene monomer. But in the context of electrical cable industry, EPR pertains to any polymers of ethylene and propylene regardless of whether a diene monomer is used or not.

It was observed that the electrical properties (particularly DDF and dielectric constant) of unfilled EPR (i.e., having no parts of clay or oil) are very similar to that of XLPE. This was explained by that fact that both materials possessed similar structure of hydrocarbons. It was also noticed that the DDF and dielectric constant showed decrease in values as less parts of clay and oil are introduced. This means that in order to derive EPR with lower losses, the amount of filler and plasticiser used should be reduced. Earlier around the 1970s this was deemed not practical owing to manufacture processing restrictions. Later on with the developments of EPR, it became possible to process it without the use of oil and plasticiser [61].

In lieu of the overloading problems, tests were conducted at ambient temperature and at 130°C which correspond to the overload temperature. It was observed that EPR maintained stable values of its electrical properties throughout the range of temperature. EPR has also significant resistance against deformation which also translates to greater cross-link density. The high deformation resistance of EPR allows it to greatly retain its shape within the limits it was designed for. The lesser 100% modulus value of EPR compared with XLPE corresponds to greater flexibility which translates to lower installation cost and ease of splicing and termination [61].

As thermal conductivity pertains to the measure of how well heat is conducted by a material, it is preferable in the case of cables that its value is high. High conductivity equates to improved dissipation of heat of the insulation which helps in the prevention of thermal breakdown. The thermal conductivity of EPR is about 20% (at 90°C temperature) higher compared with XLPE which becomes more significant at elevated temperatures (30% higher at 130°C) [61].

Several tests were also performed in which it observed that EPR has excellent resistance against tree inception and growth even with no additive or compounding materials used. This makes EPR

suitable for conditions where cycling loading and water ageing is evident like underground cable systems [61].

Although EPR insulation is less considered in comparison with XLPE, there has been some studies conducted aimed at determining the endurance characteristics of EPR as well as its suitability with respect to the developed life models. The following are some of the research conducted pertinent to EPR with some considering XLPE as well.

Montanari, Pattini, and Simoni [80] performed test cycles on EPR insulated cables with the aim of determining the life model and Voltage Endurance Coefficient (VEC). Prior to ageing, the samples were pretreated at 100°C for 100 hours to remove the by-products of the curing process. The tests were carried out in air and water. Complete tests were applied for high stresses while progressive censoring tests were performed for the majority of the test with the goal of analysing the time variation of properties of EPR insulation aside from the failure/breakdown time. Statistical method was applied for the treatment of the results. Results showed negligible time to failure of tests carried in water or air. VEC value obtained was 20 which was in agreement with the values obtained from HV cables by other laboratories.

Montanari [81] performed thermal (in compliance with IEC 216), electrical and combined-stress life tests on EPR insulated cables. The test temperatures selected range between 160°C and 100°C with interval of 10°C (excluding 140°C). By-products of curing process were removed by pretreating the samples at 90°C for 100 hours. Properties considered for the thermal characterisation of the EPR insulated cables include electric strength, weight loss, and tensile strength. The electric strength was selected as the basis for the thermal endurance characterisation. It was also pointed out that electric strength does not drop to zero when only the thermal stress is

in effect since thermal stress is non-destructive. However, sharp decrease in electric strength may reflect changes in the microstructure of the insulation and of ageing leading to treeing growth and eventual breakdown if under superimposition of voltage. The results showed monotonic decrease of the electric strength, weight loss, and tensile strength with increasing time at constant temperature. At constant temperatures 160°C, 150°C, and 130°C, a 50% drop in electric strength corresponded to the same 50% drop in tensile strength and 3% weight loss. For temperatures lower than 130°C, correspondence of failure criteria did not hold. Due to prolonged period of testing, after about 20,000 hours, the tests at 110°C and 100°C were stopped and extrapolation was performed. Extrapolation at 110°C was observed reasonable while it was depicted unreliable for 100°C owing to the deviation of the test times and the extrapolation times. Results also verified a linear relationship between the regression coefficients a and b for each of the properties which supported the ageing compensation effect.

Montanari [82] performed thermal life tests on EPR insulated cables in accordance with IEC 216 at temperatures between 110 to 160°C incremented by 10°C (140°C not included). The test samples were 200mm long and properties that were measured include weight loss, electric strength, density, tensile strength, and strength modulus. Observations via Optical and Scanning Electron Microscopy (SEM), microanalysis via Energy and Wavelength Dispersive Spectroscopy (EDS and WDS respectively), and measurements of crystallinity, conductivity, and dielectric properties were conducted. Prior to testing, the test specimens were first pretreated at 90°C for 100 hours for the removal of the cross-linking by-products. The selection of properties was based from the dominant stresses (weight loss for thermal stress, electric strength for electrical stress, and tensile strength for mechanical stress). The plots were pertinent to property endpoints versus time for various constant temperatures. The trouble in the choice of the end points of properties was handled by relating the end points to the electric strength in which selection of objective

failure was made possible. It was noted that upon application of voltage, the failure becomes the breakdown. When only the thermal stress is in effect, the electric strength does not drop to zero due to the non-destructive nature of thermal stress. But dramatic change in electric strength may indicate changes in the microstructure paving way for the development of trees leading to breakdown upon superimposition of voltage. For the criterion of objective failure, the selected end point value for the electric strength was 40% to 60% of initial value. Results showed a general decrease in the values of the electric strength, tensile strength, and weight with increasing time. Results also showed that 50% drop of electric strength corresponded to 50% drop in tensile strength and 3% drop in weight. These figures were then selected as the criterion for objective failure plotted as test life versus temperature. The results of these curves showed almost linear relationship between the test life and temperature for the corresponding failure criteria of electric strength (50% of initial value), weight (3% drop), and weight loss (3% drop). The slight non-linearity was associated with the errors in the Fisher test. Results also supported the idea of the compensation effect as confirmed by the linear plot of regression coefficients a (ordinate intercept) and b (slope) and by the existence of the isokinetic point for the properties especially of the weight and tensile strength for the test life versus conventional temperature curves at corresponding end points. The ageing compensation effect was also supported by the values of the correlation coefficient R near 1 for the properties under consideration (electric strength, weight, and tensile strength).

Cacciari et al. [83] performed life tests on both steam cured XLPE and EPR insulated cables for the characterisation of endurance of the insulations under electrical stress. The electrical life tests were performed at 20°C room temperature and 50Hz supply frequency. To study the resistance of the insulations to water-treeing, tests under water were also conducted. In an effort to study the existence of electrical threshold and seek the value of multiplicative factor associated with failure

times to the supply frequency, tests up to 900Hz high frequency were conducted at both dry (air) and wet (water) conditions. Aside from determining the percentiles for time-to-failure, to shorten the duration of the test and study time variation of insulation properties, method of progressive censoring was applied to samples. Properties considered include residual electrical strength, a.c. losses, conductivity, density, microstructural, and crystallinity analysis to direct a study towards degradation processes. Pretreated XLPE insulation showed initial electric strength of 80kV/mm from the test performed in water to avoid damage to cable by surface discharge. Results showed that for XLPE, curves of the electrical life tests at 20°C showed increasing insulation life with decreasing electrical breakdown stress. The curve also showed that as life approached infinity, the electric breakdown stress asymptotically approached towards a threshold value at about 11.5kV/mm. The linear behaviour of the electrical life curve from 30kV/mm and sudden curvature corresponding to tendency towards a threshold may be approximated by three or four parameter life models. Plots of both four-parameter inverse-power model and four-parameter exponential model showed good fitting with the data of the life test at 20°C. The high value of the electrical threshold as per the results of the tests and of the two models equates to high reliability in the design of cables with less consideration to statistics. Between the two models used, the exponential version showed greater accuracy compared to the inverse-power one in terms of least square method. The initial value of electric strength measured for EPR was about 70kV/mm. Measurement of initial value of electric strength and constant electric stress down to 60kV/mm was also performed in water for the same reason of avoiding breakdown due to surface discharge. Results showed greater increase in EPR insulation life at 20°C with decreasing electric breakdown stress compared to XLPE. The bi-log and semi-log plot of EPR life curve showed linear trend. The characterisation of EPR was suggested to be based on initial electric strength value and VEC with estimation of life aided by probabilistic model. On the other hand, the characterisation of XLPE was suggested to be based on electrical threshold.

Montanari and Cacciari [84] investigated the characterisation of the electrical endurance of insulations by the generalised probability distribution of the times to failure acquired from constant stress tests and progressive stress tests. The guidelines of IEC supported the constant stress tests over the progressive stress tests. A major advantage of constant stress tests was the significantly reduced test times compared to progressive stress tests while the latter has the advantage of the data being less dispersed, hence better confidence interval. Insulations considered for the experiments include flat XLPE specimen and EPR insulated cables. Models considered for the characterisation of electrical endurance were the exponential and inverse-power models which provided linear graphs on a semi-log and bi-log plot with inverse relationship of slope and endurance coefficient. Additionally, threshold and curvilinear models were considered especially in cases where there was significantly longer life at low stress tests compared to the linear model attributed to the variation of the activation energy of a particular process of degradation. The life model considered was a modified version of the inverse-power model with electrical stress components adjusted to the electrical threshold for particular temperatures taking into account the occurrence of breakdown by partial discharges in the voids of the insulation. The progressive stress tests may then be conducted considering a linear increase in applied electrical stress starting from 0 or from a predetermined initial electrical stress value. For both the constant stress tests and progressive-stress tests, the generalisation of the probability function was obtained using the two-parameter Weibull distribution with the shape parameter held constant and verified for constancy by methods like McCool test. The parameters of the generalised distribution can be approximated using maximum likelihood method. The tests involved five levels of voltage rise rate (between 0.01kV/min and 50kV/min) or constant electrical stress (between 54kV/mm and 87kV/mm for XLPE and between 32 to 40.9kV/mm for EPR). In the case of the progressive-stress tests, the electrical stresses were increased linearly from zero. Plots of electrical stress versus breakdown time are shown for both exponential and

inverse-power model and both XLPE and EPR insulation, each plot displaying results of constant stress test and progressive-stress test. Results showed good fitting of the two models with the data of the experiments. The graphs showed clear distinction of constant stress test having significantly lower time to failure compared with progressive-stress test by up to two orders. The parameters of the generalised probability distribution were also estimated based on the experimental results categorised by insulation type (XLPE and EPR), model used (exponential and inverse-power model), and nature of test (constant and progressive-stress test) using the maximum likelihood method at 95% probability for the confidence interval.

Montanari and Motori [85] investigated the validity of the ageing compensation effect in EPR insulated cables using measurements of oxidation time under single (electrical and thermal) and multiple stress. It was recognised that there were already various properties in insulation considered for ageing diagnosis including electric strength, partial discharge, tensile strength, dielectric losses, and conductivity. Issues considered in line with the said properties for ageing diagnosis include the length of cable required to perform the tests and the use of destructive tests (in the case of electric strength): rendering the cable samples unusable after the experiment. Oxidation was one of the most prevailing mechanism of ageing in polymers under electrical and thermal stress conditions. At service conditions, bulk oxidation was the dominant degradation mechanism while localised electric fields can cause localised oxidation. Hence, it was proposed that information about the degradation of insulation may be given by the measurement of the oxidation time. The Eyring and Arrhenius models were used to provide the plot of times for oxidation corresponding to various ageing times. The geometry of the cable specimens was chosen such that voltage applied provided the same numerical equivalence of the applied maximum electric field in the core. Progressive censoring method was also applied to allow measurements for various ageing times and with selection based from electric strength and tensile

strength with reference to their initial value. Seven test numbers (with three test specimens each for confidence intervals at 90% probability) were reported with ageing time up to 6930 hours, voltage of 0kV and 30kV (applied on to two test specimens subjected to 130°C), and temperatures 90°C, (two) 120°C, (three) 130°C, and 150°C. The measurement of the oxidation time (Oxidation Induction Time or OIT and Oxidation Maximum Time or OMT) at constant temperature was conducted using Differential Scanning Calorimetry (DSC). For instance where OIT measurements are too small, the OMT was referred. Measurements of OMT were conducted at five temperatures ranging between 165°C and 190°C. Using the Arrhenius or Eyring model, the activation energy was calculated. The compensation effect was also explained which suggested linearity between activation enthalpy and activation entropy. Literature showed validity of the ageing compensation effect for XLPE.

Results showed linear fitting of the compensation effect lines (activation entropy versus activation enthalpy graph) verified by the correlation coefficient of 0.998 which was extremely close to 1: the reference for perfect positive correlation. It was observed that greater ageing severity provided farther distance from the reference pretreated test samples in a compensation line. Hence, the compensation effect line can be used as a tool for describing the degree of degradation of insulation subjected to ageing [85].

Montanari, Motori, and Leonelli [86] proposed an accelerated endurance test as replacement to IEC 216 to address the long significant amount of hours required (100-5000 hours) in attaining thermal endurance indices like Temperature Index (TI) and Halving Interval in Centigrade (HIC). The fast-paced development in materials technology resulted in introduction of new insulation materials of varying properties and composition, hence the call for more rapid testing procedures for endurance characterisation. The method presented was based on IEC 1026 from which average

failure time should be no more than 300 hours. Since oxidation was recognised as the dominant degradation process in PE and EPR, the activation energy was considered in line with oxidative stability measurement. The measurement of oxidative stability was conducted for at least three temperatures until the Oxidation Induction Time (OIT) or the Oxidation Maximum Time (OMT) was achieved. The selection of the temperatures was based on duration of test not exceeding few days and the value of calculated activation energy compatible for maximum operating temperature on insulation (between 160°C and 190°C in the case of XLPE and EPR). The data of the times for the oxidation were based on either Eyring or Arrhenius models (with the latter considered). Selection of the conventional temperature should be such that end-point time is sufficiently small for accurate estimation of the TI but not too big like those from IEC 216. The formula for TI was based on the Arrhenius equation which was equal to the temperature corresponding to time failure criterion of 20,000 hours at a selected conventional temperature. The approximate formula for Halving Interval in Celsius (HIC) was derived by algebraic manipulation of the Arrhenius equation and the TI equation which in the end considered only the temperature index and coefficient of conventional temperature. Three insulation materials were used in the test, two of which were based on EPR (one of which having contaminants) and an Ultra-Low Density Polyethylene (ULDPE). The test was performed at 150°C considering Elongation at Break (EI), Tensile Strength (TS), and Electrical Strength (ES). Results showed non-monotonic behaviour described as decreasing and increasing of the electric strength and tensile strength in a graph of specific property (ratio of property to initial value) versus ageing time. Results regarding measurement of oxidative stability showed differences in the activation energy of each material specifically between the contaminated and reference materials. The results of the thermal endurance characteristics were better (higher TI and lower HIC) in the reference materials than the contaminated ones. It was also mentioned that EPR-based insulations had similar thermal endurance characteristics with ULDPE and those reported in other literatures.

Mazzanti, Montanari, and Simoni [87] studied the synergism between thermal and electrical stresses on EPR insulation. A synergism factor was introduced as the ratio between the rate for multi-stress ageing and the sum of individual rates of stress ageing (electrical and thermal). The multi-stress ageing rate (thermo-electrical) was derived from the multi-stress model developed by Simoni. The individual ageing rates were derived from the multi-stress ageing rate: setting conventional temperature to zero yielding the electrical ageing rate and setting electric strength to zero yielding the thermal ageing rate. Tests were then performed to EPR-insulated cables for temperatures 30°C, 50°C, 70°C, and 90°C and electric field magnitude from 30kV/mm to 60kV/mm. Results showed that the synergism factor tended to increment with increasing temperature at the same electric field magnitude (synergism factor of 50 at 30kV/mm at 90°C). Additionally, the synergism factor tended to decrease (towards unity for low temperatures) with increasing electric field magnitude at constant temperature.

Montanari, Mazzanti, and Simoni [88] conducted an investigation of the thermo-electrical endurance characteristics of EPR insulation to address the limited information known about the subject in contrast with XLPE which was associated with the numerous numbers of life tests required for the characterisation of endurance properties equating to time consuming and costly activity. Combined Analysis Method (CAM) was applied in the processing of the data which permitted an in-depth understanding of the behaviour of insulation under multi-stress condition with limited data. The CAM involved the designation of the test life as a function of both electrical (with electric stress as parameter) and thermal stress (with temperature as parameter) leading to a three-dimensional representation with variables life, electric stress, and temperature. As per IEC 216, thermal life tests were conducted without application of voltage including temperatures of 120°C, 130°C, 150°C, and 160°C. The diagnostic properties considered for the reference are the tensile strength and electric strength. A decrease of 50% in the electric strength for the endpoint

was used in the determination of the Temperature Index (TI) and Halving Interval in Centigrade (HIC). On the other hand, the tests for electrical life were conducted at ambient temperature (20°C) in both water and air at constant a.c. voltage between 30kV to 70kV. The tests for thermo-electrical life were performed at voltages between 10kV and 50kV and at temperatures between 60°C and 150°C. Progressive censoring was also applied for the electrical and thermo-electrical life tests which allowed study of mechanisms of ageing at decreased test duration. Results showed a linear relationship for both the bi-log and semi-log plot of the electrical life (electric stress versus life) at corresponding constant temperatures and for the Arrhenius graph of thermal life (life versus temperature) at corresponding constant electric stresses. The criterion for the selection of the electrical threshold corresponding to electric stress value in which ageing due to electrical stress was negligible and breakdown caused by other stresses was based on the thermal life lines at which value at constant 10kV/mm showed very close fit to the thermal life line at constant zero electrical stress.

3.7 Conclusion

In this chapter, considerations of the design of EPR and XLPE cables were discussed. The cable designs were based on two standards: AS/NZS 1429.1 and IEC 60502-2. The cable designs were specific to the cable components including core, core screen, insulation, insulation screen, metallic screen, and outer sheath. The different considerations were particular to diameter, thickness, material, and service conditions (like voltage rating and temperature). The common materials considered for the core are Copper and Aluminium. For the sizing of the core in terms of diameter, discussion from Chapter 2 about conductor sizes should be referred. Similar to the table of conductor sizes for the core, the insulation thickness also follows certain tables based on insulation material, voltage rating, cross-sectional area, and in one particular case (as per IEC

60502-2 at 3.8/6.6 (7.2) kV voltage rating using EPR material) on whether it is screened or not. The common materials considered for insulation are XLPE and EPR. In some cases, tolerances of dimensions are also discussed which were expressed in mathematical form. For the core screens and insulation screens, the materials required are semi-conductive in nature. Among the types of metallic screens, the one used by Figure 2.1 and Figure 2.2 is the concentric layer wires also known as concentric neutral (CN) wires. For the outer sheath, wider class of materials are considered including thermoplastics, elastomers, and other reduced fire hazard cable materials. Next, properties particular to the insulation material were tackled which covered those found by experiments and dictated by standards. Most significant properties discussed are the partial discharge, tensile strength, elongation (at break), dielectric strength (breakdown voltage), and DDF. Various breakdown mechanisms were also discussed which include electric, thermal, electromechanical, and partial discharge breakdown. Lastly, a thorough discussion of the treeing phenomenon was made particular to the water trees and electrical trees. The discussion includes information about their history, definition, types, and growth stages. The treeing phenomenon is a very important consideration in underground cabling systems utilising polymer insulations.

CHAPTER 4 METHODS OF TESTING THE MEDIUM VOLTAGE UNDERGROUND CABLE

4.0 Introduction

The increasing demand for the reliability of power transmission and distribution calls for the performance assessment of the cables. There have been several methods of testing that were developed in order to characterise the conditions of cable system including fault identification and predicting their performance and remaining life. This can help the utility to come up with cost-effective solutions in the repair and replacement of the cable system components. There are generally two ways to perform the testing of cable system:

- Offline method
- Online method

Offline method refers to the testing of the cable system by taking it outside of service while online method is performed when the cable system is still in service.

Cable system testing can be categorised according to the properties involved. This includes mechanical testing, electrical testing, and thermo-electrical testing. One type of mechanical testing is the accelerated ageing test. The accelerated ageing test evaluates the changes in the mechanical properties of the cable particularly the insulation and sheathing material. The idea for accelerated ageing test is to simulate the test samples under an environment with severe case scenarios including wet condition, high temperature, and electrical surges. The mechanical properties being observed include elongation at break, tensile strength, and compressive modulus. Procedure in accelerated ageing test involves use of an air oven where samples are subject to prolonged exposure to heat or water tanks where they are submerged underwater at controlled conditions of water, temperature, and voltage [89].

4.1 Tests as per IEC 60502-2

For the conditions of the test, as per IEC 60502-2 [56], ambient temperature conditions in conducting tests are required to be $20 \pm 15^{\circ}\text{C}$ unless stated otherwise. For the power frequency test voltages, the frequency is required to be between 49Hz and 61Hz with a sinusoidal waveform. With reference to IEC 60230, the virtual front time of the impulse wave shall range from $1\mu\text{s}$ to $5\mu\text{s}$ while the nominal time shall be 50% of peak value measured from $40\mu\text{s}$ to $60\mu\text{s}$. Otherwise, IEC 60060-1 is followed.

4.1.1 Routine tests

Routine tests performed to each length of manufactured cables include electrical resistance measurement, PD tests for cables with core and insulation screen, and voltage test [56].

Regarding the electrical resistance, measurement is performed on the core and concentric neutrals (if any) of each cable. Test of conductor resistance can also be done on the finished conductor prior to extrusion process as shown in Figure 4.1. The conductor or cable length is placed in a test room for a minimum of 12 hours as shown in Figure 4.2. When it is uncertain that cable has attained thermal equilibrium with the room air, the electrical resistance is measured after 24 hours in the test room. Another option is to place the cable in a temperature-controlled bath and proceed on measuring the electrical resistance after 1 hour. The resistance measure is required to be corrected to the value corresponding to 20°C temperature and a length of 1 km in compliance with the factor and formulas in IEC 60228. For each core, the d.c. resistance at 20°C is required to be no more than the intended maximum value as per IEC 60228. The resistance for concentric neutrals shall be in compliance with national standards and/or regulations [56].

PD test is performed according to IEC 60885-3 but following a sensitivity of 10pC. In the case of three-core cables, PD test is performed to each core, with the voltage applied between the core and the screen. Test voltage is incremented moderately to $2 U_0$ and held for 10 seconds then steadily decremented to $1.73 U_0$ [56].

Voltage test at power frequency is performed at ambient temperature using alternating voltage. Voltage test for single core cables involves application of test voltage for 5 minutes between the core and metallic screen. Voltage test for three core cables with individually screened cores involves application of test voltage for 5 minutes between each core and metallic layer. Voltage test for three core cables without individually screened cores involves consecutive application of test voltage for 5 minutes between every insulated core and other cores and collective metallic layers. Testing of three-core cables in single operation may be done using a three-phase transformer. The power frequency test voltage is required to be 3.5 times of U_0 . For standard rated

voltages, the rated voltage (in kV) with corresponding test voltage (in kV) enclosed in parenthesis shall be as follows: 3.6 (12.5), 6 (21), 8.7 (30.5), 12 (42), and 18 (63). In the case of three-core cables, if three-phase transformer is used to perform voltage test, the test voltage is required to be 1.73 times the original. Voltage tests should not cause breakdown of insulation [56].



Figure 4.1: Measurement of conductor resistance



Figure 4.2: Conditioning of sample for conductor resistance test

4.1.2 Sample tests

Sample tests considered in [56] include:

- examination of the core,
- examination of dimensions,
- voltage test for 3.6/6 (7.2kV) voltage rated cables
- hot set test particular to insulations made up of XLPE, EPR, and Hard Grade Ethylene-Propylene Rubber (HEPR) and sheaths made from elastomers.

Regarding the sample test frequency, examination of core, insulation and sheath thickness measurement, and measurement of overall diameter is done on single piece taken from every batch manufactured of identical material and equal cross-section not exceeding 10% in length numbers for any reduction. As part of requirement, samples of manufactured cables are subjected to electrical and physical tests in accordance with conventional procedures of quality control. However, if no agreement is made, and cable length involved is above 4 km for single-core cables and above 2 km for three-core cables, Table 4.1 shall be used as guide for the number of samples in conducting the sample tests [56].

Table 4.1: Number of samples for Sample Tests as per IEC 60502-2

Cable length (km)		Number of samples
Single-core cables	Multicore cables	
$4 < \text{Length} \leq 20$	$2 < \text{Length} \leq 10$	1
$20 < \text{Length} \leq 40$	$10 < \text{Length} \leq 20$	2
$40 < \text{Length} \leq 60$	$20 < \text{Length} \leq 30$	3
etc.	etc.	etc.

Regarding test repetition, when any samples failed in the sample tests, an additional two samples will be taken from the same group and be subjected to the same test. If the two additional samples passed the test, all samples from the same batch are considered passed. Otherwise, in the case that either of the two additional samples failed, all samples from the same batch are as well considered failed [56].

Regarding the examination of core constructed as per IEC 60228, inspection and measurement are performed when feasible for the checking [56].

Method for measurement of insulation thickness and non-metallic sheaths (which includes separation sheaths that are extruded but does not include inner coverings that are extruded) is required to comply with IEC 60811-1-1 clause 8. Every length of cable chosen for the sample test is required to be represented by one piece of cable that has been taken from an end after discarded which can be a damaged part if essential. For every core, the minimum thickness of the insulation is required to comply with the following two inequalities:

$$t_{min} \geq 0.9t_n - 0.1 \quad (4.1)$$

$$\frac{t_{max} - t_{min}}{t_{max}} \leq 0.15 \quad (4.2)$$

where t_n pertains to nominal thickness inmm, t_{min} depicts minimum thickness inmm, and t_{max} refers to maximum thickness inmm. For cables without armour and cables with indirectly applied outer sheaths over concentric neutral, metallic screen, or armour, the minimum value for the thickness of the non-metallic sheath is required to comply with the following inequality:

$$t_{min} \geq 0.85t_n - 0.1 \quad (4.3)$$

For separation sheath and cables with directly applied outer sheaths over concentric neutral, metallic screen, or armour, the minimum value for the thickness of the non-metallic sheath is required to comply with the following inequality [56]:

$$t_{min} \geq 0.8t_n - 0.2 \quad (4.4)$$

The measurement of the minimum thickness of a lead sheath is performed by either strip method or ring method. The minimum thickness of a lead sheath should also be based on the manufacturer and is guided by the following inequality:

$$t_{min} \geq 0.95t_n - 0.1 \quad (4.5)$$

The strip method involves the use of a micrometer with 4mm to 8mm diameter place faces with accuracy of ± 0.01 mm. Measurement is performed from an approximately 50mm long sheath taken from a cable. The sheath longitudinally cut and should be cautiously laid flat and cleaned.

Along the sheath's circumference, adequate number of measurements are performed which should be at least 10mm from the edge to ascertain that the dimension being measured is the minimum thickness. The ring method also involves the use of a micrometer with one flat nose and one ball nose or a flat rectangular nose (0.8mm by 2.4mm) and one flat nose with accuracy of ± 0.01 mm. The flat rectangular nose or ball nose is required to be applied inside the ring. The measurement is performed from a cautiously cut sheath in the form of a ring. Adequate number of measurements are performed around the sheath ring's circumference to ascertain that the dimension being measured is the minimum thickness [56].

The measurement of tape involves the use of a micrometer with two flat noses having estimated diameters of 5mm and an accuracy of ± 0.01 mm. Measurement of tapes with width of 40mm below is performed at the width centre. For tapes with width above 40mm, measurements are taken 20mm from the tape's edge in which the thickness shall be the average of the measurements. The measurement of the diameter of round armour wires and thickness of flat armour wires involves the use of micrometer with two flat noses having an accuracy of ± 0.01 mm. In the case of round wires, there will be two measurements to be performed where the wires are oriented with the same position at right angles to each other where the diameter is taken as the average between the two values measured [56].

For the external diameter of cable, measurements are required to be in compliance with IEC 60811-1-1 clause 8 [56].

For the voltage test for 4 hours, it can only be applied to cables with a rated voltage above 3.6/6 (7.2) kV. Cable for sample voltage test is required to be no less than 5 meter long between the terminations of the test. The power frequency voltage is required to be applied at ambient

temperature for a duration of 4 hours between the core and metallic layers. The test voltage is required to be $4U_0$. Refer to Table 4.2 for the test voltage values applied for each corresponding standard voltage rating. The test voltage is required to be applied gradually until it reaches the specified value and is sustained for 4 hours. The voltage test should not cause breakdown of the insulation [56].

Table 4.2: Sample Test Voltages as per IEC 60502-2

Rate Voltage U_0 kV	6	9	12	18
Test Voltage kV	24	35	48	72

For insulations made up of XLPE and EPR and sheaths made up of elastomers, hot set tests are performed in compliance with IEC 60811-2-1 clause 9. The hot set test air temperature with a tolerance of $\pm 3^\circ\text{C}$ is 200°C for XLPE and 250°C for EPR. Both XLPE and EPR have a time under load of 15 minutes. For the mechanical stress, both XLPE and EPR are subject to 200kPa. Maximum elongation when under load for both XLPE and EPR shall be 175% while maximum permanent elongation upon being cooled for both materials shall be 15%. For the hot set test elastomeric sheaths, oil temperature shall be 100°C with a tolerance of $\pm 3^\circ\text{C}$ with a time under load of 15 minutes under a mechanical stress of 200 kPa. The maximum elongation when under load of the elastomeric sheath shall be 17% and the maximum permanent elongation upon being cooled is 15%.

4.1.3 Electrical type tests

For successful type tests on a cable type, in compliance with IEC 60502-2 for a particular rated voltage and cross sectional area, other cables of the same type will also be considered valid for the same particular rated voltage and cross sectional area if: (1) identical materials (like for semiconducting screens and insulation) and manufacturing means are used, (2) if the cross-

sectional area of the core is no greater than the cable tested except for cross-sectional area no more than 630mm² are approved provided that the tested cable has a cross-sectional area ranging from 95 to 630mm², and (3) if the rated voltage is no greater than the cable tested. Such approval will not be affected by the material of the core [56].

In the case of three cores, every measurement and test is required to be performed to each core on the cables with core screens and insulation screens. The usual sequence of the tests is required to be in the following order: bending test to be proceeded by PD test, measurement of $\tan\delta$, heating cycle test to be proceeded by PD test, impulse test to be proceeded by the voltage test, and 4-hour voltage test. Sample cable with lengths ranging from 10 m to 15 m are required to be subjected to the given tests. $\tan\delta$ measurement can be performed on another sample which were used in the stated tests sequence. For cables having rated voltage less than 6/10(12) kV, $\tan\delta$ measurement will not be required. For the 4-hour voltage test, another sample can be taken for the condition that the sample is previously submitted to bending test (proceeded by PD test) and 4-hour voltage test [56]. The bending test involves bending the sample around a test cylinder which may be a drum's hub no less than one full turn at ambient temperature. The sample will then be unwound and the whole procedure will be repeated besides that the direction of the bending is reversed without rotation with respect to the axis. This cycle is required to be repeated three times. Cable samples with longitudinally applied metal foil that is overlapped or with lead sheath shall be tested using a test cylinder with diameter equal to: $25 \cdot (d + D) \pm 5\%$ for cables with single core and $20 \cdot (d + D) \pm 5\%$ for cables with three cores. For other cables, shall be tested using a test cylinder with diameter equal to: $20 \cdot (d + D) \pm 5\%$ for cables with single core and $15 \cdot (d + D) \pm 5\%$ for cables with three cores. From the formulas given, D refers to the sample cable's external diameter inmm while d refers to the core's actual diameter inmm. For cases of cables with non-circular core, d shall be calculated using the following formula:

$$d = 1.13 \sqrt{S} \quad (4.6)$$

where S refers to the nominal cross section expressed in mm^2 . Upon completion of the bending test, PD test is performed on the sample. In compliance with IEC 60885-3, PD test is performed with sensitivity of 5pC (or better). There will be incremental increase in the test voltage until it reaches $2U_0$ and will be maintained for 10 seconds and afterwards steadily decreased to $1.73U_0$. No discharge shall be detected which exceeds the selected sensitivity of the sample at $1.73U_0$. It should be noted that the partial discharge involved in the test sample may cause harm. For the measurement of $\tan\delta$ for rated voltage no less than 6/10 (12) kV, the cable sample is required to be heated by any of the following means: placing the sample in an oven or liquid tank, or passing heating current through the core, metallic screen, or both. The heating is performed until the temperature of the core reaches 5 to 10°C higher than the maximum core normal operation temperature. Determination of the temperature of the core may use the core resistance or using an appropriate temperature reading device in the oven, bath, screen's surface, or on a reference cable that is identically heated. At least 2kV alternating voltage shall be used in the measurement of the $\tan\delta$. For EPR, $\tan\delta$ should not exceed 0.04 while for XLPE, $\tan\delta$ should not exceed 0.004. For the heating cycle test, it involves laying the previously tested sample on the floor and heating the core by passing current through the core until the temperature stabilises 5 to 10°C above the maximum core normal operation temperature. In the case of cables with three cores, current is required to be passed through all core for heating. The heating cycle is required to last for 8 hours: no less than 2 hours of maintaining the temperature to the stated limits and followed by no less than 3 hours of ambient air cooling to a core temperature within 10°C of the ambient temperature. The whole cycle is repeated 20 times. PD test shall be performed on the sample upon finishing the last cycle. For the impulse test, the sample is required to be 5 to 10°C higher than the maximum core normal operation temperature. Application of the impulse voltage is required to be in

compliance with IEC 60230 with a peak value corresponding the rated voltage as shown in Table 4.3.

Table 4.3: Impulse Voltages as per IEC 60502-2

Rated voltage $U_o/U (U_m)$ kV	3.6/6 (7.2)	6/10 (12)	8.7/15 (17.5)	12/20 (24)	18/30 (36)
Peak test voltage kV	60	75	95	125	170

Each of the cable core must be able to withstand positive and negative impulses of voltage (10 each) without failure. After performing the impulse test, power frequency voltage test is performed to the cable cores for a duration of 15 minutes at ambient temperature. For the test voltage, is it required to follow the same specification of the test voltage for the routine test. For the impulse test, it should not cause breakdown of the insulation. For the 4-hour voltage test, it involves application of power frequency voltage between the conductor/s and screen/s of the sample for a duration of 4 hours under ambient temperature. The test voltage is required to be $4U_o$. The applied voltage is gradually incremented to the value specified. The 4-hour voltage test should not cause breakdown of the insulation. For cables with conductors and insulation covered with extruded semiconducting screens, resistivity is required to be determined by taking test sample from core of cable as made and from a cable that underwent ageing treatment. Measurement of resistivity is required to be performed at maximum core normal operation temperature with $\pm 2^\circ\text{C}$ deviation (refer to Annex D of IEC 60502-2 regarding the early procedures for the electrodes pertinent to measurement of resistivity). The electrodes are connected using appropriate clips. When connecting the electrodes to the core screen, it is required to be certain that clips are well insulated with respect to the insulation screen test sample outer surface. The assembly is then put inside an oven where it is preheated to a predetermined temperature for a duration of no less than 30 minutes after which the resistance is measured between the electrodes via circuit with a power no greater than 0.1W. Following the measurement of resistance, at

ambient temperature, the thicknesses of the core and insulation screen and the diameters over the core and insulation screen are measured six times in which the average is used. The core screen volume resistivity (ρ_c) is calculated using the following formula:

$$\rho_c = \frac{\pi \cdot R_c \cdot (D_c - T_c) \cdot T_c}{2L_c} \quad (4.7)$$

where ρ_c corresponds to the volume resistivity of core screen in Ω -m, R_c pertains to measured resistance in Ω , L_c refers to distance between potential electrodes in m, D_c depicts outer diameter over the core screen in m, and T_c refers to the average thickness of core screen in m.

The insulation screen volume resistivity (ρ_i) is calculated using the following formula:

$$\rho_i = \frac{\pi \cdot R_i \cdot (D_i - T_i) \cdot T_i}{L_i} \quad (4.8)$$

where ρ_i pertains to volume resistivity of insulation screen in Ω -m, R_i corresponds to measured resistance in Ω , L_i depicts distance between potential electrodes in m, D_i refers to outer diameter over the insulation screen in m, and T_i corresponds to the average thickness of insulation screen in m.

For both unaged and aged condition, the resistivity shall be no greater than 1000 Ω -m for the core screen and 500 Ω -m for the insulation screen [56].

Regarding cables with unscreened insulation at rated voltage of 3.8/6.6 (7.2) kV, sample cable cores that are between 10m to 15m long are required to undergo the following test performed consecutively: measurement of insulation resistance at ambient temperature, measurement of insulation resistance at maximum core normal operation temperature, and 4-hour voltage test. On a separate sample of cables that are between 10m to 15m long, the cables are also required to undergo impulse test. The measurement of insulation resistance at ambient temperature is required

to be performed prior to other electrical tests. Outer coverings are required to be taken off and the core to be submerged in water no less than 1 hour at ambient temperature prior the test. The d.c. test voltage about 80V to 500V is required to be applied for an adequate amount of time by which the measurement is stabilising from 1 to 5 minutes. The measurement is performed between each core and water. Upon request, the measurement may be verified at $20 \pm 1^\circ\text{C}$ temperature. From the insulation resistance that is measured, the volume resistivity is the calculated using the following formula:

$$\rho = \frac{2\pi \cdot l \cdot R}{\ln \frac{D}{d}} \quad (4.9)$$

where ρ refers to the volume resistivity of insulation in $\Omega\text{-cm}$, R depicts measured resistance of insulation in Ω , l pertains to cable length in cm, D corresponds to outer diameter of insulation screen in mm, and d refers to the inner diameter of insulation screen in mm. K_i (referred to as insulation resistance constant in $\text{M}\Omega\text{-km}$) can also be computed using the following formula:

$$K_i = \frac{l \cdot R \cdot 10^{-11}}{\lg \frac{D}{d}} = 0.367 \cdot 10^{-11} \cdot \rho \quad (4.10)$$

It should be noted that the D/d for shaped cores is equivalent to insulation perimeter over core perimeter. For PVC/B, the volume resistivity is required to be no less than $10^{14} \Omega\text{-cm}$ at 20°C . For PVC/B, the insulation resistance constant K_i is required to be no less than $367\text{M}\Omega\text{-km}$ at 20°C . For the measurement of insulation resistance at maximum core temperature, the core is required to be submerged in water for no less than 1 hour at maximum core normal operation temperature with deviation of $\pm 2^\circ\text{C}$. The d.c. test voltage about 80V to 500V is required to be applied for an adequate amount of time by which the measurement is stabilising from 1 minute to 5 minutes. Calculation of the volume resistivity and/or insulation resistance constant is calculated using the same calculation procedures for measurement of insulation resistance at ambient temperature. For PVC/B, the volume resistivity is required to be no less than $10^{11}\Omega\text{-cm}$ at

maximum core normal operation temperature of 70°C. For EPR/HEPR, the volume resistivity is required to be no less than $10^{12}\Omega\text{-cm}$ at maximum core normal operation temperature of 70°C. For PVC/B, the insulation resistance constant K_i is required to be no less than 0.37 M $\Omega\text{-km}$ at maximum core normal operation temperature of 70°C. For EPR/HEPR, the volume resistivity is required to be no less than 3.67M $\Omega\text{-km}$ at maximum core normal operation temperature of 70°C. For the 4-hour voltage test, the core is required to be submerged in water for no less than 1 hour at ambient temperature. The power frequency voltage equivalent to $4U_o$ is required to be applied gradually until it reaches the specified value and is sustained for 4 hours between each core and water. The 4-hour voltage test should not cause breakdown of the insulation. For the impulse test, the sample is required to be 5°C to 10°C higher than the maximum core normal operation temperature. Application of the impulse voltage is required to be in compliance with IEC 60230 with a 60kV peak value. Every impulse series are applied between the core phases and other cores connected with each other and to the earth. Each of the cable core must be able to withstand positive and negative impulses of voltage (10 each) without failure [56].

4.1.4 Non-electrical type tests

The designations and type of sheathing materials are stated in Table 4.4 that shows its maximum operating temperature. For determining the required non-electrical type tests, refer to Table 4.5.

Table 4.4: Maximum Core Temperatures of Sheathing materials as per IEC 60502-2

Sheath Material		Abbreviated Designation	Maximum core normal operation temperature °C
Thermoplastic	PVC	ST1	80
		ST2	90
	PE	ST3	80
		ST7	90
Elastomeric	Polychloroprene, CSPE, or similar polymers	SE1	85

Table 4.5: Non-electrical Type Tests as per IEC 60502-2

Designation of compounds	Insulations				Sheaths				
	PVC/B	EPR	HEPR	XLPE	ST ₁	ST ₂	ST ₃	ST ₇	SE ₁
<i>Dimensions</i>									
Measurement of thicknesses	x	x	x	x	x	x	x	x	x
<i>Mechanical properties</i> (tensile strength and elongation at break)									
Without ageing	x	x	x	x	x	x	x	x	x
After ageing in air oven	x	x	x	x	x	x	x	x	x
After ageing of pieces of complete cable	x	x	x	x	x	x	x	x	x
After immersion in hot oil	-	-	-	-	-	-	-	-	x
<i>Thermoplastic properties</i>									
Hot pressure test (indentation)	x	-	-	-	x	x	-	x	-
Behaviour at low temperature	x	-	-	-	x	x	-	-	-
<i>Miscellaneous</i>									
Loss of mass in air oven	-	-	-	-	-	x	-	-	-
Heat shock test (cracking)	x	-	-	-	x	x	-	-	-
Ozone resistance test	-	x	x	-	-	-	-	-	-
Hot set test	-	x	x	x	-	-	-	-	x
Flame spread test on single cables (if required)	-	-	-	-	x	x	-	-	x
Water absorption	x	x	x	x	-	-	-	-	-
Thermal stability	x	-	-	-	-	-	-	-	-
Shrinkage test	-	-	-	x	-	-	x	x	-
Carbon black content*	-	-	-	-	-	-	x	x	-
Determination of hardness	-	-	x	-	-	-	-	-	-
Determination of elastic modulus	-	-	x	-	-	-	-	-	-
Strippability test**	-	-	-	-	-	-	-	-	-
Water penetration test***	-	-	-	-	-	-	-	-	-
NOTE x indicates that the type test is to be applied									
* For black outer sheaths only									
** To be applied to those designs of cable where the manufacturer claims that the insulation screen is strippable									
*** To be applied to those designs of cable where the manufacturer claims that barriers to longitudinal water penetration have been included									

For the measurement of insulation thickness, single sample is required to be taken for every insulated cable core. Performance of the measurement is required to be in compliance with 8.1 of IEC 60811-1-1. For every core, the minimum thickness of the insulation is required to comply with the following two inequalities [56]:

$$t_{min} \geq 0.9t_n - 0.1 \tag{4.11}$$

$$\frac{t_{max} - t_{min}}{t_{max}} \leq 0.15 \tag{4.12}$$

where t_n pertains to nominal thickness in mm, t_{min} depicts minimum thickness in mm, and t_{max} refers to maximum thickness in mm. For the thickness measurement of non-metallic sheaths (includes extruded separation sheaths but excludes inner coverings), a single cable is taken for

sample. Performance of the measurement is required to be in compliance with 8.1 of IEC 60811-1-1. For cables without armour and cables with indirectly applied outer sheaths over concentric neutral, metallic screen, or armour, the minimum value for the thickness of the non-metallic sheath is required to comply with the following inequality:

$$t_{min} \geq 0.85t_n - 0.1\rho = \frac{2\pi \cdot l \cdot R}{\ln \frac{D}{d}} \quad (4.13)$$

For separation sheath and cables with directly applied outer sheaths over concentric neutral, metallic screen, or armour, the minimum value for the thickness of the non-metallic sheath is required to comply with the following inequality [56]:

$$t_{min} \geq 0.8t_n - 0.2 \quad (4.14)$$

Regarding the tests in the determination of mechanical properties of unaged and aged insulation, the sampling and preparation of test pieces are required to be performed in compliance with 9.1 of IEC 60811-1-1. Ageing treatments are required to be performed in compliance with 8.1 of IEC 60811-1-2 and Table 4.6.

Conditioning and mechanical properties measurement is required to be performed in compliance with 9.1 of IEC 60811-1-1. The test results obtained from test before and after ageing is required to be in compliance with Table 4.6 [56].

For the tests in the determination of mechanical properties of unaged and aged non-metallic sheaths, the sampling and preparation of test pieces are required to be performed in compliance with 9.2 of IEC 60811-1-1. Ageing treatments are required to be performed in compliance with 8.1 of IEC 60811-1-2 and Table 4.7 [56].

Table 4.6: Test requirements for mechanical properties of Insulation as per IEC 60502-2

Designation of materials	PVC/B	EPR	HEPR	XLPE
Maximum core normal operation temperature (°C)	70	90	90	90
<i>Without ageing</i>				
Tensile strength (N/mm ²), minimum	12.5	4.2	8.5	12.5
Elongation at break (%), minimum	125	200	200	200
<i>After ageing in air oven</i>				
After ageing without core				
Treatment:				
- temperature (°C)	100	135	135	135
- tolerance (°C)	±2	±3	±3	±3
- duration (h)	168	168	168	168
Tensile strength:				
a) value after ageing, minimum (N/mm ²)	12.5	-	-	-
b) variation*, maximum (%)	±25	±30	±30	±25
Elongation at break:				
a) value after ageing, minimum (%)	125	-	-	-
b) variation*, maximum (%)	±25	±30	±30	±25
* Variation difference between the median value obtained after ageing and the median value obtained without ageing expressed as a percentage of the latter				

Table 4.7: Test requirements for mechanical properties of Sheathing as per IEC 60502-2

Designation of materials	ST ₁	ST ₂	ST ₃	ST ₇	SE ₁
Maximum core normal operation temperature (°C)	80	90	80	90	85
<i>Without ageing</i>					
Tensile strength (N/mm ²), minimum	12.5	12.5	10	12.5	10
Elongation at break (%), minimum	150	150	300	300	300
<i>After ageing in air oven</i>					
After ageing without core					
Treatment:					
- temperature (°C)	100	100	100	110	100
- duration (h)	168	168	240	240	168
Tensile strength:					
a) value after ageing, minimum (N/mm ²)	12.5	12.5	-	-	-
b) variation*, maximum (%)	±25	±25	-	-	±30
Elongation at break:					
a) value after ageing, minimum (%)	150	150	300	300	250
b) variation*, maximum (%)	±25	±25	-	-	±40
* Variation difference between the median value obtained after ageing and the median value obtained without ageing expressed as a percentage of the latter					

Regarding further ageing test on finished cables, the purpose of this test is to verify that non-metallic sheaths and insulation are not accountable to degrade while under operation owing to being in contact with the other cable components. This test shall be applicable for all types of cable. The samples are required to be taken from a cable in compliance with 8.1.4 of IEC 60811-1-2. Treatment for the ageing of the cable pieces is required to be performed in an air oven in compliance with 8.1.4 of IEC 60811-1-2 with a temperature $10 \pm 2^{\circ}\text{C}$ higher than the maximum core normal operation temperature for a duration of 7 x 24 hours. Prepared of insulation and outer sheath test pieces from aged cables are required which shall undergo mechanical tests in compliance with 8.1.4 of IEC 60811-1-2. Variations of the measured tensile strength and elongation at break median values between aged and unaged samples should be no higher than air oven aged values based from Table 4.6 (in the case of insulations) and Table 4.7 (in the case of non-metallic sheaths) [56].

For the loss of mass test on ST₂ sheaths, sampling and procedure of the test is required to comply with 8.2 of IEC 60811-3-2. Test results are required to be in compliance with Table 4.8 [56].

In line with the high-temperature pressure test on non-metallic sheaths and insulation, this test is required to be in compliance with Clause 8 of IEC 60811-3-1 with test conditions employed in test method and Table 4.8 to 4.10. Test results are required to be in compliance with Clause 8 of IEC 60811-3-1 [56].

In line with low temperature PVC sheaths and insulation test, sampling and procedure of the test is required to comply with Clause 8 of IEC 60811-1-4 with test temperature employed from Table 4.8 and 4.9. Test results are required to be in compliance with Clause 8 of IEC 60811-1-4 [56].

Table 4.8: Test requirement properties for PVC Sheath materials as per IEC 60502-2

Designation of material	ST ₁	ST ₂
Use of PVC material	Sheath	
<i>Mass loss in air oven</i>		
Treatment:		
- temperature (± 2 °C)	-	100
- duration (h)	-	168
Maximum mass loss (mg/cm ²)	-	1.5
<i>Pressure test at high temperature</i>		
- temperature (± 2 °C)	80	90
<i>Behaviour at low temperature</i>		
Test to be performed when unaged:		
Cold bending test (diameter < 12.5 mm)		
- temperature (± 2 °C)	-15	-15
Cold elongation test (on dumb-bells)		
- temperature (± 2 °C)	-15	-15
Cold impact test		
- temperature (± 2 °C)	-15	-15
<i>Heat shock test</i>		
- temperature (± 3 °C)	150	150
Duration (h)	1	1
* In line with climate conditions, lower temperature may be necessitated by national standards		

Table 4.9: Test requirement properties for PVC Insulation material as per IEC 60502-2

Designation of material	PVC/B
Use of PVC material	Insulation
<i>Pressure test at high temperature</i>	
- temperature (± 2 °C)	80
<i>Behaviour at low temperature</i>	
Test to be performed when unaged:	
Cold bending test (diameter < 12.5 mm)	
- temperature (± 2 °C)	-5
Cold elongation test (on dumb-bells)	
- temperature (± 2 °C)	-5
<i>Heat shock test</i>	
- temperature (± 3 °C)	150
Duration (h)	1
<i>Thermal stability test</i>	
- temperature (± 0.5 °C)	200
Minimum time (min)	100
<i>Water absorption test</i>	
Electrical method:	
- temperature (± 2 °C)	70
Duration (h)	240
* In line with climate conditions, lower temperature may be necessitated by national standards	

Table 4.10: Test requirement properties for PE sheathing materials as per IEC 60502-2

Designation of material	ST ₃	ST ₇
Density *		
<i>Carbon black content (only for black outer sheaths)</i>		
Nominal value (%)	2.5	2.5
Tolerance (%)	±0.5	±0.5
<i>Shrinkage test</i>		
- temperature (± 2 °C)	80	80
- duration of heating (h)	5	5
- cycles of heating	5	5
- maximum shrinkage (%)	3	3
<i>Pressure test at high temperature</i>		
- temperature (± 2 °C)	-	110
* Density measurement is only necessary if stated in other tests		

Regarding the PVC sheaths and insulation cracking resistance test (also referred to as heat shock test), sampling and procedure of the test is required to comply with Clause 9 of IEC 60811-3-1 with the temperature and duration of the test employed from Table 4.8 and 4.9. Test results are required to be in compliance with Clause 9 of IEC 60811-3-1 [56].

For the ozone resistance test of insulations made from EPR and HEPR, sampling and procedure of the test is required to comply with Clause 8 of IEC 60811-2-1. The duration of the test and ozone concentration shall be referred to Table 4.11. Test results are required to be in compliance with Clause 8 of IEC 60811-2-1 [56].

In line with the XLPE, EPR and HEPR insulations and elastomeric sheaths hot set tests, it should be based on IEC 60811-2-1 clause 9. The hot set test air temperature with a tolerance of ±3°C is 200°C for XLPE and 250°C for EPR. Both XLPE and EPR have a time under load of 15 minutes. For the mechanical stress, both XLPE and EPR are subject to 200kPa. Maximum elongation when under load for both XLPE and EPR shall be 175% while maximum permanent elongation upon being cooled for both materials shall be 15%. For the hot set test elastomeric sheaths, oil

temperature shall be 100°C with a tolerance of $\pm 3^\circ\text{C}$ with a time under load of 15 minutes under a mechanical stress of 200kPa. The maximum elongation when under load of the elastomeric sheath shall be 17% and the maximum permanent elongation upon being cooled is 15% [56].

Table 4.11: Test requirement for thermoset Insulation materials as per IEC60502-2

Designation of material	EPR	HEPR	XLPE
<i>Ozone resistance test</i>			
- ozone concentration by volume (%)	0.025-0.030	0.025-0.030	-
- test duration w/o cracks (h)	24	24	-
<i>Hot set test</i>			
Treatment:			
- temperature ($\pm 3^\circ\text{C}$)	250	250	200
- time under load (min)	15	15	15
- mechanical stress (N/cm^2)	20	20	20
- maximum elongation under load (%)	175	175	175
- maximum permanent elongation after cooled (%)	15	15	15
<i>Water absorption test</i>			
Gravimetric method:			
- temperature ($\pm 2^\circ\text{C}$)	85	85	85
- duration (h)	336	336	336
- maximum mass increase	5	5	1*
<i>Shrinkage test</i>			
- distance L between marks (mm)	-	-	200
- temperature ($\pm 3^\circ\text{C}$)	-	-	130
- duration (h)	-	-	1
- maximum shrinkage (%)	-	-	4
<i>Determination of hardness</i>			
- minimum IRHD**	-	80	-
<i>Determination of elastic modulus</i>			
- minimum modulus at 150% elongation (MPa)	-	4.5	-
* More than $1 \text{ mg}/\text{cm}^2$ increase is considered for XLPE with density more than 1			
** IRHD refers to international rubber hardness degreee			

In line with the oil immersion test of sheaths made from elastomers, sampling and procedure of the test is required to comply with Clause 10 of IEC 60811-2-1 with conditions employed from Table 4.12. Test results are required to be in compliance with Table 4.9 or Table 4.11 [56].

Table 4.12: Test requirement properties for Elastomeric sheathing materials as per IEC60502-2

Designation of material	SE ₁
<i>Oil immersion test proceeded by mechanical properties measurement</i>	
Treatment:	
- oil temperature (± 2 °C)	100
- duration (h)	24
- maximum tensile strength variation* (%)	± 40
- maximum elongation at break variation* (%)	± 40
<i>Hot set test</i>	
Treatment:	
- temperature (± 3 °C)	200
- time under load (min)	15
- mechanical stress (N/cm ²)	20
- maximum elongation under load (%)	175
- maximum permanent elongation after cooled (%)	15
* Variation denotes difference between median of treated and untreated test specimen which is expressed as parentage of the untreated test specimen	

Regarding the test of flame spread for single cables; application is limited to ST₁, ST₂, or SE₁ and is performed when required. Methods of the test and requirements are required to be in compliance with IEC 60332-1-2 [56].

For the measurement of the amount of black carbon of black PE outer sheaths, sampling and procedure of the test is required to comply with Clause 11 of IEC 60811-4-1. Test results are required to be in compliance with Table 4.10 [56].

In line with the XLPE insulation shrinkage test, sampling and procedure of the test is required to comply with Clause 10 of IEC 60811-1-3 with conditions employed from Table 4.11 [56].

In line with the PVC insulation test for thermal stability, sampling and procedure of the test is required to comply with Clause 9 of IEC 60811-3-2 with conditions employed from Table 4.9. Test results are required to be in compliance with Table 4.9 [56].

Regarding the HEPR insulation hardness determination, test piece is required to be a sample cable, with all coverings that are external to HEPR insulation carefully removed. Insulated core sample can also be used as alternative. The test is in compliance with ISO 48 except for the guidelines to follow. In the case of surfaces having high radius of curvature, the instrument used complying with ISO 48 is required to be configured such that it is firmly rested on the insulation (HEPR) and allows the indenter and presser foot to perform contact with surface vertically. This can be performed in two ways. The first way is that the instrument has feet that is capable of moving through its universal joints causing self-adjustment with respect to the curved surface. The second way is the instrument's base is equipped with two rods that are parallel to each other at a certain distance dependent upon the surface curvature.

The mentioned two ways can be performed to surfaces with at least 20mm radius of curvature. For HEPR insulation measured thickness of 4mm below, instrument from the method described in ISO 48 applied for small and thin test pieces is used. In the case of surfaces having low radius of curvature, identical firm base is used to support the test piece in a manner that minimises the movement of the body of the HEPR insulation when there is applied indenting force increment upon the indenter that is above the test piece axis. Proper instruction includes: test piece rested in trough or groove in metal jig and test piece conductor ends rested upon V-blocks.

For the given methods, the part of the surface having the lowest radius of curvature is required to be no less than 4mm. For cases of smaller radii, instrument from the method described in ISO 48

applied for small and thin test pieces is used. For the conditioning and temperature of the test, the minimum duration between manufacturing (like vulcanisation) and testing is required to be 16 hours. The required temperature is $20 \pm 2^{\circ}\text{C}$ and maintained at such temperature for no less than 3 hours prior to testing. For each three or five various distributed points on the test specimen surrounding, one measurement is performed. The median is then calculated and be designated as the test piece hardness, rounded off to closest whole number which indicates International Rubber Hardness Degrees (IRHD). Test results are required to be in compliance with Table 4.11 [56].

For the measurement of the HEPR insulation elastic modulus, sampling, preparation, and procedure of the test is required to comply with Clause 9 of IEC 60811-1-1. Measurement of loads for 150% elongation shall be required. The stresses are determined by the ratio of the measured loads to the areas of the cross section of unstretched test specimens. Elastic moduli for an elongation of 150% are then calculated by dividing the stresses to the strains. The median value is determined as the elastic modulus. Test results are required to be in compliance with Table 4.11 [56].

In line with the PE outer sheaths shrinkage test, sampling and procedure of the test is required to comply with Clause 11 of IEC 60811-1-3 with conditions employed from Table 4.10. Test results are required to be in compliance with Table 4.10 [56].

In line with the insulation screen strippability test, this test is performed upon claim of the manufacturer of the strippability of extruded insulation screen made up of semiconducting material. The test is required to be conducted three times for sample with and without ageing, either by using a single cable piece positioned at three points along the circumference having equal measure of 120° or by using three separate cable pieces. Length of core no less than 250mm

is required to be taken from unaged and aged cable. For each sample, two longitudinal cuts are made on the insulation screen from end-to-end and radially going down the insulation, with the cuts that are parallel relative to each other and 10 ± 1 mm apart. After having the 10mm strip removed its 50mm length by pulling in parallel direction with respect to the core at 180° stripping angle, the core is vertically mounted on a tensile machine where one core end is gripped while the 10mm strip on the other. The required force in the separation of no less than 100mm length of 10mm long strip from insulation is measured with 250 ± 50 mm/min speed of pulling at an approximately 180° stripping angle. The temperature in the performance of the test is maintained at $20 \pm 5^\circ\text{C}$. For both sample with and without ageing, the values of the stripping force is recorded continuously. For both aged and unaged samples, the required force in the separation from the insulation of the extruded semiconducting screen is required to be between 4N to 45N. The surface of the insulation is required to incur no damage and the insulation screen left no trace [56].

Regarding the test for water penetration, test for water penetration is required to be applied for cable designs with included barriers for water penetration (longitudinal) as claimed by the manufacturer. Designed of the test is based on buried cables and not suited for submarine cables application. The application of the test includes designs with included barrier securing water penetration (longitudinal) along the core and/or metallic layers region. Sample cable no less than 6m which have not underwent any electrical type test is required to undergo bending test with exclusion of the test of partial discharge. From the sample cable which underwent bending test, 3m cable length is cut and horizontally positioned. From the length's centre, a 50mm wide ring is taken which consist of layers outside the insulation screen. If there is also a barrier for the core, layers outside the core is then included in the ring. No less than two barriers is required for the cable sample if the longitudinal water penetration barriers are intermittent where the ring is taken

off between barriers. For such case, sample cable length and average barrier distance is required to be determined. Cutting of the surface is performed to expose the interfaces to water considering their longitudinal watertight property. Interfaces that are not considered being longitudinally watertight are required to be sealed with appropriate material or removal of the outer coverings is performed. Sample of such cases include core being the only one with barrier and if interface is between the metallic sheath and outer sheath. A tube with diameter no less than 10mm is sealed to the outer sheath's surface while vertically positioned over the ring which is exposed. The seals is required to not apply any cable mechanical stress on the exit location of the cable on the apparatus. It should be noted that unless stated otherwise, tap water is used. Within 5 minutes at $20 \pm 10^{\circ}\text{C}$ ambient temperature, water is filled at a height of 1m with respect to the centre of the cable for a duration of 24 hours. The sample is then required to undergo 10 cycles of heating through current passed through the core until it stabilises at temperature 5°C to 10°C higher than the maximum core normal operation temperature but in any case, no greater than 100°C . The cyclic heating is performed for a duration of 8 hours. For every period of heating, the temperature of the core is maintained for a duration no less than 2 hours to be proceeded by no less than 3 hours of ambient cooling. The head of the water is preserved at 1m. While the test in under effect, water should not emerge from the test piece ends [56].

4.1.5 Site tests

The type tests were also referred to as electrical tests following installation [9]. After cable and accessories installation, d.c. voltage test of outer sheath is recommended and if required, insulation test is performed. If only the d.c. voltage test is performed, insulation test can be substituted by quality assurance test performed while the accessories are being installed [56].

Regarding the D.C. voltage test of outer sheath, magnitude and duration of the voltage applied between the ground and each metallic screen or metallic sheath is required to be in compliance with IEC 60229. For the effectivity of the test, the ground should essentially have good contact with the external surface of the outer sheath which can be assisted by a conductive layer [56].

Regarding the insulation test, for the a.c. testing, upon the contractor and purchaser's agreement, a.c. voltage test at particular power frequency in compliance with the following may be performed: 5-minute test with application of the system's phase to phase voltage between core and metallic sheath or screen, or 24 hours test under system's normal operating voltage. On the other hand, for the d.c. testing, 15-minute d.c. test using voltage of $4 U_0$ may be used as substitute for a.c. testing. It should be noted that d.c. testing can cause damage to tested insulation. In case of used installations, lower level of voltage and/or lower time durations may be considered [56].

4.2 Tests as per AS/NZS 1429.1

There are three types of tests: routine tests, sample tests, and type tests. For the selection of sample for the sample tests, refer to Table 4.13. Repetition of type tests are not required except when there are changes in the materials of the cable or the means of the manufacturing process which may alter the characteristics of the performance parameters. The following type tests are required to be performed in sequence for a 10m to 15m length cable sample: bending test proceeded by PD test, measurement of DDF dependent on voltage (only for cables using EPR as insulation), measurement of DDF for higher temperatures, heat cycling test proceeded by PD test, impulse withstand test proceeded by HV test, and 4-hour HV a.c. test. New sample is allowed to be taken and undergo 4-hour HV a.c. test for the condition that it has underwent bending test proceeded by PD test and heat cycling test proceeded by PD test.

Table 4.13: Basis for number of samples as per AS/NZS 1429.1

Production Length (km)	Number of Samples	
	Thickness Tests	Other Sample Tests
$PL \leq 2$	1	0
$2 < PL \leq 10$	2	1
$10 < PL \leq 20$	3	2
$20 < PL \leq 30$	4	3
etc.	etc.	etc.

Upon request in line with cable supply for commercial purpose, the supplier presents a Qualification Test Report (QTR) to prove compliance of cable with tests. The QTR effects qualification of range of core sizes. Cables with core sizes no more than 800mm² are qualified by QTR covering core sizes between 50mm² and 500mm². Furthermore, QTR covering core sizes between 1000mm² and 1600mm² qualifies core sizes for the same range. For a particular voltage rating, QTR qualifies all those cables no greater than that particular voltage rating. Single-core and triplex cables are qualified by QTR which covers three-core cable. Separate QTR is required for changes in the design including change of insulation material and metallic sheath. QTR is independent for design changes in other components like core material [39].

4.2.1 Routine tests

PD Test: PD test is performed in compliance with AS/NZS 1660.3 for rated voltages higher than 1.9/3.3 (3.6) kV. Criterion involves maximum value of 20pC partial discharge magnitude for the particular voltage designated on the second column of Table 4.14 or maximum of 5pC particular discharge magnitude for the particular voltage designated on the third column of Table 4.14 [39].

Table 4.14: Partial Discharge Voltage levels as per AS/NZS 1429.1

Cable voltage rating kV	200% U_0 kV r.m.s.	150% U_0 kV r.m.s.
3.8/6.6 (7.2)	7.6	5.7
6.35/11 (12)	13	10
12.7/22 (24)	25	19
19/33 (36)	38	29

As per AS/NZS 1660.3 [90] applicable to cables with voltage rating higher than 1.9/3.3 (3.6)kV, the apparatus required to perform partial discharge include HV power supply with sufficient kVA capacity, voltmeter suitable for high voltage, and device for measuring PD and a calibrator of discharge which should all have adequately minimum level of noise for the required sensitivity. The test circuit of the device for measuring PD is required to have oscilloscope that is coupled with an indicating instrument, voltmeter being connected to HV side of power supply (which is calibrated so as to indicate the r.m.s.), and amplifying equipment that is used with oscilloscope, adequate to verify presence of PD and detect every charge pulses. Calibration is performed using the charge transfer method as per AS 1018. In the case of long cables (referred to the cables in which variation of the response of the device for measuring PD with that of a charge that is predetermined, which was in turn injected at near and far ends of cable, is more than 20% considering that termination is performed upon the characteristic impedance of the cable), connection is performed in turn on each of the cable's ends under test causing injection of preset amount of charges in the test sample. The charge for calibration must be in turn injected at each end of the cable with termination performed upon the characteristic impedance of cable in order to quantify the value of the apparent charge attenuation coefficient. Otherwise, connection is performed on either of the cable's end to effect injection of predetermined charge amount in test specimen. The calibrating pulse characteristics is required to be in compliance with AS 1018. Test circuit sensitivity for a certain instrument described as minimum charge that is detected and seen with noise is required to be no more than 4pC. In the case of routine tests, adjustment of the

amplifier is performed such that in 20pC of charge transfer, the deflection of the oscilloscope should be at least 10mm, the deflection of the X-Y recorder should be at least 20mm, and deflection of charge transfer metre should be at least 20% of the full scale. Provisions for long cables are required for the prevention of errors produced by the superposition of the travelling waves. Prior the energisation of the HV test transformer, disconnection of the main calibration circuit is required except if calibrator capacitor rating is suitable with the involved test voltages. Unless there is an available continuous visual display of corresponding signal for calibration for the test duration, readjustment of the amplifier should not be performed. The provision of continuous visual display of corresponding is part of primary calibration circuit rated at full voltage in which disconnection prior the energisation of the HV test transformer is not required or secondary capacitor is utilised that is connected to the detector's input in which case pre-calibration of the secondary pulse response amplitude with respect to primary calibrating circuit is required prior the disconnection of the latter circuit and energisation of the HV test transformer. Application of the test voltage is performed between the core and screen. The test voltage is then incremented and then maintained at constant value not exceeding 1 minute at voltage $0.25U_0$ higher than the highest voltage at which measurement of partial discharge is performed. Test voltage is then gradually reduced to the voltage required by cable standard from which measurement of partial discharge is performed. Each cycle of the partial discharge is required to be no more than 3 minutes. PD test cannot be performed within 7 days if a PD test is performed for more than 3 minutes. Retest of cable is required to be conducted with the near end and far end interchanged. For each level of voltage, discharge (q_{max}) is computed using the formula:

$$q_{max} = \sqrt{q_1 \cdot q_2 \cdot a} \quad (4.15)$$

where q_1 corresponds to the measured cable discharge from one end in pC, q_2 refers to the measured cable discharge from the other end in pC, and a depicts the apparent charge attenuation coefficient.

5-minute HV test: For the 5-minute HV test, application of voltage is performed between the core and earthed metallic screens. Alternating voltage is applied with frequency range of 40 to 62Hz having a sine waveform with similar half cycles (refer to AS 1931). Voltage is incremented moderately and kept constant upon reaching full value referring to Table 4.15 for a duration of 5 minutes. Criterion involves no incident of breakdown occurs [39].

Table 4.15: Test Voltages for 5 and 15-minute HV Test AS PER AS/NZS 1429.1

Cable voltage rating kV	Test voltage kV r.m.s.
1.9/3.3 (3.6)	6.5
3.8/6.6 (7.2)	12.5
6.35/11 (12)	21
12.7/22 (24)	42
19/33 (36)	63

1-minute HV a.c. test on separation sheath: The 1-minute HV a.c. test is performed in compliance with AS/NZS 1660.3. Criterion involves no incident of breakdown upon application of 3.5kV between adjacent layers divided by the sheath [39].

4.2.2 Sample tests

Measurement of insulation thickness: The nominal insulation thickness (t_i) for XLPE and EPR are provided in Table 3.1 for voltage ratings between 1.9/3.3 (3.6) kV and 19/33 (36) kV and nominal cross-sectional areas of core ranging from 16mm² to 1600mm². The minimum thickness (in mm) for any point in the insulation is equivalent to $0.90t_i - 0.10$. The test method is referred to AS/NZS 1660.2.1 [39].

Determination of insulation concentricity: For the concentricity defined as the ratio of the thickness range ($t_{max} - t_{min}$) and the maximum thickness (t_{max}), it should not exceed 0.15 i.e. $\frac{t_{max}-t_{min}}{t_{max}} \leq 0.15$ in mathematical inequality [39].

Determination of insulation shrinkage: Shrinkage should not exceed 4% when heated between temperatures 127-133°C for 1 hour [39].

Determination of the size of voids, contaminants and discoloured translucents (applicable to XLPE only) and the number of voids and contaminants: No voids should be present that are greater than 0.08mm while contaminants should be no more than 0.15mm. For XLPE, size of discoloured translucent should not exceed 1.25mm. Void concentrations should be no greater than 30 per 16cm³ while contaminants concentration should be no more than 15 per 16cm³ [39].

Hot set test: For the hot set test performed for 15 minutes, at a temperature of $200 \pm 3^\circ\text{C}$ for XLPE or $250 \pm 3^\circ\text{C}$ for EPR, and under a load of 200 kPa, the maximum elongation when under load should be 175% while the maximum residual elongation upon being cooled is 15% [39]. In compliance with AS/NZS 1660.2.2:1998 [91], two test samples are tested from each sheath or core is required to undergo the hot set test after their preparation and measurement of their cross-sectional area (as per AS/NZS 1660.2.1). Cable insulations more than 1kV shall have their dumbbells taken from the inner part of insulating wall after any present ridges and/or semiconducting layer are removed. An oven is required to be use for the test, held at a certain temperature for a particular material as per cable standard. A viewing window is required for the oven. Provision of grip is required, allowing every test specimen to be suspended from the upper grip in oven with

attached weight to the lower grip that is fastened to the test sample. Test specimens are hang inside the oven with weights that are fixed to the jaws on the bottom to effect force exertion for the particular material as per cable standard. For a particular temperature as per cable standard, after 15 minutes, with the oven door closed, measurements of distance between marker lines and percent elongation computations to nearest 5% are performed. The weight is then separated from the test specimen which may be through cutting at lower grip, leaving the test specimen for a duration of 5 minutes for recovery at the corresponding temperature. The test specimens are then withdrew from the oven and cooled at ambient temperature proceeded by measurements of distance between marker lines to nearest 0.5mm and computations of percent elongation. The average of the pair of values measured is required to be reported considering elongation under load and after cooling.

4.2.3 Type tests

Bending test proceeded by PD test: Bending test is performed for rated voltages higher than 1.9/3.3 (3.6) kV. Finished cables undergo this test with exception of triplex cables where one phase cable from finished cable is subjected to bending and PD test. Cable samples with longitudinally applied metal foil (overlapped) or with metallic sheath shall be tested using a test cylinder with diameter equal to: $25 \cdot (d + D) \pm 5\%$ for cables with single core and $20 \cdot (d + D) \pm 5\%$ for cables with three cores. For other cables, shall be tested using a test cylinder with diameter equal to: $20 \cdot (d + D) \pm 5\%$ for cables with single core and $15 \cdot (d + D) \pm 5\%$ for cables with three cores. The PD test is performed in compliance with AS/NZS 1660.3 for rated voltages higher than 1.9/3.3 (3.6) kV. Criterion involves maximum value of 20pC discharge magnitude for the particular

voltage designated on the second column of Table 4.14 or maximum of 5pC discharge magnitude for the particular voltage designated on the third column of Table 4.14 [39].

Measurement of DDF dependent on voltage (only for insulation using EPR as insulation):

Test for the measurement of DDF of cable using EPR insulation is performed for rated voltages higher than 3.8/6.6 (7.2) kV. Criterion involves $\tan\delta$ no greater than 0.02 at U_o and increment no greater than 0.025 between $0.5U_o$ and $2U_o$. Measurement is performed using power frequency voltages of $0.5U_o$, U_o , and $2U_o$ at equal temperatures with deviation of $\pm 5^\circ\text{C}$ [39].

Measurement of DDF for higher temperatures:

Test for the measurement of DDF at higher temperature is performed for rated voltages higher than 3.8/6.6 (7.2) kV. Criterion involves $\tan\delta$ not exceeding 0.08 for XLPE and 0.04 for EPR between 95 to 100°C . Measurement is performed using power frequency voltages of $0.5U_o$, U_o , and $2U_o$ at similar temperatures with deviation of $\pm 5^\circ\text{C}$. Heating of the sample is done in a liquid tank, oven, or through heating current passed through the metallic screen or through current loading of cores. Measurement of the core temperature is determined through measurement of core resistance or through other appropriate methods. The core temperature is raised until it reaches the prescribed temperature range of 95 to 100°C . Measurement of DDF is then performed by applying 2kV power frequency voltage to the sample [39].

Heat cycling test proceeded by PD test:

The heat cycling test is performed for rated voltages higher than 1.9/3.3 (3.6) kV. Heating of the sample is performed by supplying current through the core until temperature stabilises at range of 105 to 110°C for cables

using XLPE insulation and 130 to 135°C for cables using EPR insulation. In the case of cables with three cores, the current is supplied to all cores. The duration of the heating cycle is 8 hours. Core temperature is kept between the specified limits of temperature for a duration no less than 2 hours for each period of heating to be followed by no less than 3 hours of ambient cooling to a core temperature below 45°C. Sample is required to undergo 20 cycles. After finishing the whole cycle, the sample is required to undergo PD test. The PD test is performed in compliance with AS/NZS 1660.3 is performed for rated voltages higher than 1.9/3.3 (3.6) kV. Criterion involves maximum value of 20pC discharge magnitude for the particular voltage designated on the second column of Table 4.14 or maximum of 5pC discharge magnitude for the particular voltage designated on the third column of Table 4.14 [39].

Impulse withstand test preceded by HV test: The impulse withstand test is performed for rated voltages higher than 1.9/3.3 (3.6) kV. Criterion involves no incident of breakdown occurs. For the preparation, heating of the sample is performed by supplying current through the core until temperature stabilises at range of 95 to 100°C. Application of impulse test is performed between the cores and metallic screens consisting of positive and negative impulses of voltage (10 each) whose values are in compliance with Table 4.16 and AS/NZS 1660.3. After the impulse withstand test, the sample undergoes 15-minute power frequency voltage test applied between the core and earthed metallic screens at magnitude prescribed in Table 4.15 [39].

Table 4.16: Impulse Withstand Voltages as per AS/NZS 1429.1

Cable voltage rating kV	Impulse voltage kV peak
3.8/6.6 (7.2)	60
6.35/11 (12)	90
12.7/22 (24)	150
19/33 (36)	200

4-hour HV a.c. test: For the 4 hours HV a.c. test, criterion involves no incident of breakdown occurs. Application of voltage is applied between the core and earthed metallic screens. Alternating voltage is applied with frequency range of 40Hz to 62Hz having a sine waveform with similar half cycles (refer to AS 1931). Magnitude of applied voltage is required to be in compliance with Table 4.17. Voltage is incremented moderately and kept constant upon reaching full value referring to Table 4.15 for a duration of 4 hours [39].

Table 4.17: Test Voltage for 4-hour HV tests as per AS/NZS 1429.1

Cable voltage rating kV	Test voltage kV r.m.s.
1.9/3.3 (3.6)	8
3.8/6.6 (7.2)	15
6.35/11 (12)	25
12.7/22 (24)	50
19/33 (36)	75

Compatibility test on insulation, outer sheath, and separation sheath proceeding air oven ageing: As per AS/NZS 1429.1 [39], the test shall be performed at a temperature of $100 \pm 2^\circ\text{C}$. For each material, the measured tensile strength should not be lower than 75% of the tensile strength of unaged sample. Similarly, for each material, the measured

elongation at break should not be lower than 65% of the elongation at break of unaged sample.

4.3 Air oven ageing as per AS/NZS 1660.2.2

As per AS/NZS 1660.2.2:1998 [91], regarding the ageing in air oven, oven having flow of air by natural convection or pressure differential is required to be used. The entry of air in the oven requires flow over the test specimen surfaces leaving close to oven top. For specific ageing temperature, the oven is required to have 8 to 20 air changes per hour.

Regarding the preparation of the test pieces, ageing is performed in ambient air conditions. The test specimens are suspended in a vertical manner mainly in the central part of the oven each of which are no less than 20mm from other test pieces. The temperature and time duration for keeping the test specimens in the oven is required to be in compliance with cable standard. It should be noted that testing of more than one material type in the same oven at the same time is not allowed. Upon completion of ageing time, the test specimens are taken out of the oven and exposed at ambient temperature for a duration no less than 16 hours away from direct sunlight. Tensile test is then performed in compliance with AS/NZS 1600.2.1 [91].

Regarding completed cable pieces, three 200mm long complete cables are used favorably from the particular position similar to where the unaged samples subjected to tensile test are taken as per AS/NZS 1660.2.1. The test specimens are suspended in a vertical manner mainly in the central part of the oven each of which are no less than 20mm from other test pieces and occupying no more than 2% of the oven volume. The temperature and time duration for keeping the test specimens in the oven is required to be in compliance with cable standard. Upon completion of

ageing time, the test specimens are taken out of the oven and exposed at ambient temperature for a duration no less than 16 hours away from direct sunlight. The three cable pieces are then dismantled. Two test specimens are derived from insulation of every core (three cores maximum) and from sheath of every cable as per AS/NZS 1660.2.1, summing to six test specimens taken from every core and sheath. If the test specimens require cutting or grounding for thickness reduction not exceeding 2mm is needed, this procedure shall be performed on the farthest side possible not facing a different type of material in the cable that completed. If cutting or grounding of ridges on the side facing a material of different type, removed material of the side is required to be minimum suitable with sufficient smoothing. After having performed cross-sectional area measurements and conditioning, the test specimens are required to undergo tensile test in compliance with AS/NZS 1660.2.1 [91].

Regarding compatibility, three pieces of 200mm long completed cable are used, favorably from a location near the taken unaged samples. The test specimens are suspended in a vertical manner mainly in the central part of the oven each of which are no less than 20mm from other test pieces and occupying no more than 2% of the oven volume. The temperature and time duration for keeping the test specimens in the oven is required to be in compliance with cable standard. Upon completion of ageing time, the test specimens are taken out of the oven and exposed at ambient temperature for a duration no less than 16 hours away from direct sunlight. The three cable pieces are then dismantled. Where different type of materials is directly contacted to one another, the test specimens for tensile test is required to be taken from every material of each cable sample. Testing is only considered to the contacted materials; hence does not include barrier tapes, fillers, and binders. If the test specimens require cutting or grounding for thickness reduction not exceeding 2mm is needed, this procedure shall be performed on the farthest side possible not facing a different type of material. If cutting or grounding of ridges on the side facing a material

of different type, removed material of the side is required to be minimum suitable with sufficient smoothing. After having performed cross-sectional area measurements and conditioning, the test specimens are required to undergo tensile test in compliance with AS/NZS 1660.2.1 [91].

For the measurement of the air flow in the oven, there are two methods which can be performed: indirect method through power consumption and direct method (continuous type). For the indirect method through power consumption, the volumetric amount of air passing through the oven per unit time shall be based on the energy balance between the difference in power consumption required to maintain oven temperature with open and closed ports and the enthalpy difference between oven and room. Determination for average power (P_1 in watts) in maintaining oven temperature with opens shall be observed for at least 30 minutes. The same procedure shall be applied to determine (P_2 in watts) except that the ventilation ports (which may include the thermometer aperture if necessary) are closed. Oven and room temperature difference is required to be equal for both tests within 0.2°C. Measurement of the room temperature is required to be performed around 2 m away from oven about the same level with the oven base and no less than 0.6m away from solid objects. The mass rate (\dot{m}) and volumetric flow rate (\dot{V}) of air passing the oven with open ports are calculated using the following formulas:

$$\dot{m} = \frac{P_1 - P_2}{c_p \cdot (t_2 - t_1)} \quad (4.16)$$

$$\dot{V} = \frac{3600 * \dot{m}}{d} \quad (4.17)$$

where \dot{m} refers to the mass rate of air in grams per second (g/s), $P_1 - P_2$ corresponds to the power consumption difference in watts (W), c_p pertains to the specific heat of air at constant pressure equivalent to 1.003J/g-K, t_1 depicts the temperature of room in degrees Centigrade (°C), t_2 corresponds to the temperature of oven in degrees Centigrade (°C), \dot{V} refers to the volumetric flow rate of air in litres per hour (L/h), and d corresponds to the air density for the particular test in the

laboratory in grams per litre (g/L) equivalent to 1.20g/L at Normal Temperature and Pressure Conditions (760mm Hg at 2°C). Assumption for this method is that there is no occurrence of air leakage with closed ports. Adhesive tapes shall be used to seal air-tight door joints and closure of inlet port is to be observed. If wattmeter is used to measure power consumption, the total time (in seconds) the ovens are turned on is measured using a stopwatch with wattmeter readings taken once every time the ovens are on. Power for maintaining constant temperature is then calculated by multiplying the mean wattage readings by the ratio of the time recorded by the stopwatch and the time duration of the test. If watt-hour metre is used, power in watts is calculated by dividing the total consumption of energy in watt-hour by the time duration of test in hour. If power is derived using household electric metre, the reading shall be performed with the rotating disc serving as the indicator since the dial units are too big which impose insufficient accuracy of the reading. The metre is placed in operation until such time that index mark of disc is opposite the window centre; it is then removed from connection until the beginning of the test. For reduction of error, the duration of the test may be prolonged to allow 100-disc revolutions and stopped upon visibility of the mark on disc. In case the mark is not visible even after the test, approximated part of revolution is added. The test begins and ends at respective points of the on and off cycle of heating like upon switching the thermostat on. For the direct method (continuous type), equipment includes air pressure regulator, flowmeter, and air oven. The air pressure regulator is a device which regulates the low pressure required for feeding oven by decreasing the pressure of the supply. It consists of an adjustable valve which allows the downstream to be at constant pressure. The flowmeter is an instrument that measures mass or volume flow rate of air. It involves the principle of pressure difference with a (1) 2mm diameter and 70mm long capillary tube and (2) double-graduated manometric tube with pressure difference between 0 ± 300 mm of water filled with distilled water serving as the manometric liquid. Consideration for the flow meter include full reliability, ease of manufacturing and calibration, and available for involved air rate range.

The air oven should be well sealed including the perimeter of the inlet tube entering the oven bottom. Only the outflow hole is opened located at the oven top. It should be noted that in practice, the effect of weak forced convection is negligible when considering its effects on the homogeneity of temperature inside the oven [91].

4.4 Withstand voltage test using Very Low Frequency (VLF) method

The use of Very Low Frequency (VLF) is becoming accepted on a global scale as diagnostic tool in medium and high voltage applications for maintenance and commissioning works. Several reasons considered in the use of VLF include significant reduction in the size and weight of required testing equipment, ease of travelling across the field, significant efficiency in determination of defects in insulation, enhanced reliability for partial discharge measurements due to precise and sensitive measurements in comparison to power frequency, better efficiency of diagnosis of partial discharge measurements through true sinusoidal HV source, and more effective testing compared to d.c. [92].

As per IEEE Std 400.2-2004 [93], VLF testing involves application of a.c. signals at frequency between 0.01Hz to 1Hz. Withstand voltage test using VLF method involves the application of predetermined magnitude of voltage on a dielectric material for a particular amount of time without incurring breakdown or failure. In the case of failure due to adequate accumulated degradation of the insulation, repair can be performed and allow retest until the withstand voltage test is passed. The types of VLF withstand voltage test include cosine-rectangular waveform, sinusoidal waveform, bipolar rectangular waveform, and alternating \pm d.c. step voltages. All types of VLF withstand tests involve subjecting to predetermined voltage through a high voltage power

supply at a particular period of time under which no breakdown or failure occurs. Application of the VLF withstand method to two conditions of cable. The first condition is when there are few numbers of defects present with less serious damage. The second condition is when there are many numbers of defects present with more serious damage. For such cases, immediate replacement of cable is advised. VLF withstand voltage tests are also rated according to how useful they are for particular conditions of cable and/or insulation. In the case of cable with corroded metallic screen, the VLF withstand voltage test is regarded to be acceptable. If the cable is substantially water treed, VLF withstand voltage test is not recommended as it is anticipated to give rise to several failures. In the event of insulation having some large faults or electrical trees in localised regions, the usefulness of VLF withstand test is regarded to be very good. For cables with faulty terminations and splices, the VLF withstand voltage test is labelled to be acceptably good. In line with this, it was said that sensitivity of damped alternating voltage tests are greater than VLF tests in the detection of defects in interfaces as shown by both field tests and laboratory tests. However, in the case of detection of water trees, VLF is regarded as being more sensitivity. Usefulness is described to be very good in the case of cables having mixed insulations for laminated and/or extruded.

Generally, the VLF test compels full penetration of the insulation by an electrical tree. The initiation and growth of electrical trees depend on the amplitude and frequency of test signal. In order to affect the full insulation penetration of electrical tree, the magnitude of the applied voltage and the time span of test are customised for two test signals that are usually used which are the cosine-rectangular waveform and sinusoidal waveform. In reference to custom global practice, the voltage levels range from $2U_o$ and $3U_o$. In this case, U_o corresponds to voltage ratings ranging from 5kV to 35kV. It was estimated that level of maintenance test is about 80% of the level of acceptance test. This can be further reduced by 20% if the number of applied test cycles is

increased. For the levels of voltage in VLF withstand voltage test for both cosine-rectangular waveform and sinusoidal waveform, refer to Table 4.18. In the case of sinusoidal waveform, it is assumed that r.m.s. is equivalent to 0.707 times the peak value considering below 5% distortion. On the other hand, with regards to cosine-rectangular waveform, the r.m.s. is taken to be equivalent to the peak value.

Table 4.18: VLF Test Voltage

Waveform	Cable rating	Installation	Acceptance	Maintenance
	phase-phase	phase-ground		
	r.m.s. voltage in kV	r.m.s.(peak) voltage in kV		
Cosine-rectangular	5	12	14	10
	8	16	18	14
	15	25	28	22
	25	38	44	33
	35	55	62	47
Sinusoidal	5	9(13)	10(14)	7(10)
	8	11(16)	13(18)	10(14)
	15	18(25)	20(28)	16(22)
	25	27(38)	31(44)	23(33)
	35	39(55)	44(62)	33(47)

For cosine-rectangular waveform, r.m.s. and peak voltage are assumed equal.

In line with the installation and acceptance, field tests performed by Moh on more than 15,000 cable circuits with XLPE insulation revealed that failure increases with testing time as follows: 68% within 12 minutes, 89% within 30 minutes, 95% within 45 minutes, and 100% within 60 minutes. The recommended time duration of the test is about 15 minutes to 60 minutes while results from the experiment by Moh suggests 30 minutes. In practice, the test time duration of the test is established by user and supplier and may also vary based on method of test, frequency of test, condition of insulation, cable system, and testing viewpoint. In the case of interruption of test, it is suggested to rest timer to original testing time. With regards to maintenance, it is recommended to have a test duration of 15 minutes for a frequency of 0.1Hz of the VLF withstand

voltage test. From the range of frequency of VLF test, the 0.1Hz frequency is usually utilised. In the performance of VLF withstand voltage test, various considerations are involved. One consideration is the availability of a route map to guide corresponding testing personnel regarding the cable, open points, accessibility of cables or joints, and cable constructions implemented. Another is have a test set enough to supply and recover the charging energy of the whole cable system for each cycle. In case of failure of cable, finding the location of the fault may be conducted. Finally, in case the test is interrupted, grounding should be immediately performed [93].

4.4.1 Cosine-rectangular waveform and bipolar pulse waveform

The setup consists of HV supply. A converter (comprising of rectifier and HV inductor) translates d.c. voltage to a.c. voltage with very low frequency. Every 5 seconds of polarity change, 0.1Hz frequency bipolar pulse waveform is produced. Testing of the cable may be conducted following an outage or for preventive maintenance measures. Repair and replacement may then be carried out on identified faults. IEC 60060-3 is referenced for the test voltage measuring system to be used. Degree of variation of peak voltage is limited to $\pm 5\%$ while the time it takes the measuring system to respond must not exceed half of a second. Regarding the procedure, it involves connection of cable system to VLF test. The voltage of cosine-rectangular form is stepped to the value provided in Table 4.18. Breakdown is induced by sinusoidal transitions at power frequency for cosine-rectangular waveform at 0.1Hz causing partial discharges in the imperfections of dielectric material. After just few minutes, this in turn results to development of breakdown channels. The bipolar waveform will be used as basis for the r.m.s. value with may not exactly be 0.707 times peak value. Upon passing the VLF withstand voltage test, applied voltage is set to zero and test setup is discharged and earthed. Afterwards, the cable system may be allowed to be back to operation. On the other hand, upon failure of the cable system, test voltage falls down as

in the case of d.c. HV test. The setup is shut off and the cable discharged and earthed. Afterwards, suitable equipment may be used to locate fault. One of the advantages of cosine-rectangular waveform is that the tendency for the development of space charges in the dielectric material is low associated to the sinusoidal transitions between switching polarities so as to avoid formation of travelling waves and the steady changes in the polarity. Another advantage is that this allows measurement of leakage currents. It is also possible to perform the cable test using a.c. test voltage that is about thrice of core-to-earth rated voltage with equipment of similar power rating, weight, and size compared to d.c. test setup. This VLF withstand test can also be carried out on cable systems having insulation that are laminated and extruded. Furthermore, using cosine-rectangular waveform for the VLF withstand test is suitable in removing fault of insulation that is in good condition. However, this test is limited when the cable has already severe deterioration due to water treeing or partial discharge. Also, the cable is required to be removed from operation in order to affect the test.

4.4.2 Sinusoidal waveform

For this test, the a.c. output voltages are provided with sine waveform for the testing of cables including capacitive loads. Similarly, IEC 60060-3 is used as reference for the test voltage measuring system to be used. Degree of variation of peak voltage is limited to $\pm 5\%$ while the time it takes the measuring system to respond must not exceed half of a second. Regarding the procedure, it involves connection of cable system to VLF withstand test. The voltage of cosine-rectangular form is stepped to the value provided in Table 4.18. Upon passing the VLF withstand voltage test, applied voltage is set to zero and test setup is discharged and earthed. On the other hand, upon failure of the cable system, test voltage falls down as in the case of d.c. HV test. The setup is shut off and the cable discharged and earthed. The failure is induced when the magnitude of localised electric field overcame the dielectric strength of the material in which partial

discharge initiates. It was noted that the magnitude of the localised electric field is dependent upon the magnitude of applied voltage, space charge, and the structure or geometry of the fault. Following the partial discharge inception, PD channels eventually become breakdown channels after few minutes of testing leading to failure. In this case, suitable equipment for locating faults is used. Testing of the cable may be conducted following an outage or for preventive maintenance measures. Repair and replacement may then be carried out on identified faults. Upon passing the VLF withstand test, the cable can then be placed back in operation. One of the advantages of it is that the tendency for the development of harmful space charges in the dielectric material is small. It is also possible to perform the test on cable using a.c. test voltage that is about thrice of core-to-earth rated voltage with equipment of similar power rating, weight, and size compared to d.c. test setup. This VLF withstand test can also be carried out on cable systems having insulation that are laminated, extruded, or mixed. Furthermore, using sinusoidal waveform for the VLF withstand test is suitable in removing fault of insulation that is in good condition. There is also available VLF test sets capable of measuring properties like dielectric spectroscopy, leakage current, and dielectric dissipation factor at 0.1Hz. Additionally, there are PD-free VLF HV generators available in the case of diagnostic testing. Lastly, VLF withstand combined with capability of measuring PD and DDF can be utilised to detect behaviour of PDF and DDF while 15 minutes to 60 minutes test is in progress. However, similarly, this test is limited when the cable has already severe deterioration due to water treeing or partial discharge. Partial discharge or other data from the diagnostic tests may not correspond to power frequency measurements. There is also a tendency for the development of space charges at significantly high voltage and very low frequency. Also, the cable is required to be removed from operation in order to affect the test.

4.4.3 Regulated \pm d.c. voltages

Besides the common sinusoidal VLF (at 0.1Hz) VLF test sets which have long been applied to electrical machines, other test sets are accessible in providing requirements in cable systems and with a different output waveform. In the case of cables with laminated and extruded dielectric material, HV generators are accessible with waveforms that are programmable. Features include bipolar waves at 0.1Hz with slew rate known, d.c. voltage that is regulated and time-variant \pm polarity, step voltage tests that are programmable and include \pm voltages, and \pm d.c. voltages with a.c. signals that are superimposed. In the assessment of the portion that is laminated insulation, data of leakage currents are compared with suitable data like historic records. For the extruded insulation part, leakage currents are not relevant. Similarly, IEC 60060-3 is used as reference for the test voltage measuring system to be used. Degree of variation of peak voltage is limited to $\pm 5\%$ while the time it takes the measuring system to respond must not exceed half of a second. For the procedure, connection of the cable system of mixed insulation type and the high voltage terminal of test set is performed after which voltage is supplied to the dielectric material. Voltage is regulated at maximum of $3U_o$ and documentation of measured leakage currents is done. Upon passing the withstand test or leakage current test, the voltage supplied is set to zero and the test set and cable system are discharged and earthed. The a.c. part of the test set is then connected to cable system. Voltage is regulated at maximum of $3U_o$. About 30 minutes to 60 minutes time of the test is advisable. Upon passing the VLF withstand voltage test, the voltage supplied is set to zero and the test set and cable system are discharged and earthed. On the other hand, upon failure on either d.c. or a.c. test, collapse of test voltage takes place. The setup is shut off and the test set and cable system are discharged and earthed. Afterwards, suitable equipment may be used to locate fault. The failure is induced when the magnitude of localised electric field overcame the dielectric strength of the material in which partial discharge initiates. It was noted that the magnitude of the localised electric field is dependent upon the magnitude of applied voltage, space

charge, and the structure or geometry of the fault. Following the partial discharge inception, electrical trees may develop and eventually become breakdown channels after few minutes of testing leading to failure. Testing of the cable may be conducted following an outage or for preventive maintenance measures. Repair and replacement may then be carried out on identified faults. Afterwards upon passing the VLF withstand voltage test, the cable system may be allowed to be brought back to operation. One the advantages of this test is that it is credited in the case of new cables having extruded insulation that are spliced with cable system that is mainly laminated dielectric material. Also, the test set offer the advantage of being mobile and requiring input power that is similar to existing equipment for locating faults. However, in line with the disadvantages, in the case of cables systems of mixed insulation type with extruded insulation that is aged by operation in humid environment, the d.c. part of test may lead to reduction of service life of the extruded insulation. Also, the cable is required to be removed from operation in order to affect the test.

4.5 Conclusion

This chapter dealt with various tests performed on cables based on IEC 60502-2 and AS/NZS 1429.1. In both standards, the tests were classified into four types: routine test, sample test, type test, and site tests. In the case of IEC 60502-2, a more distinct division of the type tests was made which are the electrical and non-electrical type tests. The routine tests are performed by the manufacturer on every single cable produced to guarantee compliance with standard requirements. The routine test common to both standards is PD test. On the other hand, the routine tests including measurement of core electrical resistance and the voltage test are particular to IEC 60502-2 while the 5-minute HV test, 1-minute HV a.c. test, and spark test are particular to AS/NZS 1429.1. The sample tests are periodically performed on a representative sample of cable

batches owing to impractical to be performed on every cable produced. The sample tests common to both include measurement of dimensions (which was focused on insulation), and hot set test. On the other hand, the sample tests including 4-hour voltage test is distinct to IEC 60502-2 while determination of insulation shrinkage, size of voids, contaminants and discoloured translucent, and number of voids and contaminants are distinct to AS/NZS 1429.1. The type tests are conducted whenever there are developments in insulation and the design of cable which may be repeated when significant alterations are made. The type tests common to both standards include measurement of volume resistivity of core screen and insulation screen, bending test proceeded by PD test, measurement of DDF depending on voltage, measurement of DDF for higher temperatures, heat cycling test proceeded by PD test, impulse withstand test proceeded by HV test, 4-hour HV a.c. test, water penetration test, and compatibility test proceeding air oven ageing. IEC 60502-2 included much more types tests including but not limited to mass loss test, high-temperature pressure test, low temperature test, cracking resistance test, ozone resistance test, hot set test, oil immersion test, oil immersion test, test for flame spread, measurement of the amount of black carbon, shrinkage test, test for thermal stability, hardness determination, measurement of elastic modulus, and strippability test. Notice that IEC 60502-2 included hot set test under both sample test and type test. The site tests are carried out after installation to confirm that proper installation of the cable along with its accessories is in effect. Example of site test is the voltage test: IEC 60502-2 proposes d.c. voltage while AS/NZS 1429.1 recommends a.c. voltage. The withstand voltage test was also discussed using VLF method with reference to IEEE standard.

CHAPTER 5 ACCELERATED AGEING TEST FOR 22kV TREE RETARDANT-ETHYLENE PROPYLENE RUBBER CABLE

5.0 Introduction

The most common types of solid insulation materials used in MV power distribution networks are the XLPE and EPR. XLPE was introduced by cross-linking of PE to increase the maximum operating temperature of the latter from 70°C (owing to the thermoplasticity of PE) to 90°C. However, for higher temperatures exceeding its crystalline melting point, the electric breakdown strength of XLPE sharply decrease. In such case of higher temperatures, EPR offers better electrical characteristics compared with XLPE. Additionally, EPR offers better flexibility and resistance to water and weathering. Study of dielectric materials by Montanari [52-56] revealed larger values of endurance coefficients for EPR which correspond to greater dielectric strength. However, EPR has higher Dielectric Dissipation Factor (DDF) compared with XLPE which corresponds to greater power losses. Also, EPR incurs relatively higher cost compared with XLPE; which made its use to be more usual on applications where safety and reliability are of utmost importance like in oil production and coal mining.

Great consideration of these reasons led to the development of an EPR-based insulation materials called Tree Retardant EPR (TR-EPR). TR-EPR offers significantly lower dielectric losses compared with XLPE [137].

Similar to XLPE, cross-linking of EPR is usually done either by peroxide method, silane method, or irradiation method. For the TR-EPR, silane method was used. Silane method requires low initial cost and can be performed using traditional PE extrusion machinery. The process involves the mixing into a hopper mixing station of the pellets with a 5% catalyst masterbatch. The mixture is then fed into an extrusion screw feeding zone. Contrary to the peroxide method in which cross-linking takes place in the chamber after the extrusion, the silane curing takes place at ambient condition (hence, can also be referred to as silane dry curing) for significant number of days. Therefore, the cross-linking of the extruded cables may be achieved by storing at ambient temperature. Additionally, dry curing was used in contrast with steam curing so as to avoid the introduction of water in the insulation which could lead to the formation of unwanted voids. These unwanted voids promote the occurrence of partial discharge and formation of water trees causing degradation and eventually leads to insulation breakdown.

A sample TR-EPR insulated cable used in this research study is shown in Figure 5.1. From inner to outer, the cable components emphasised are the core, semi-conductive core screen, TR-EPR insulation, semi-conductive insulation screen, metallic screen, binder tape, and PVC sheath. The cable has a voltage rating application of 22kV and a cross-sectional area of 120mm². The core is a Class 6 flexible plain annealed Copper made up of 1632 pieces of wires having a diameter of 0.3mm each. The core is enveloped with nylon semi-conductive tape of 0.2mm thickness and having an overlap of 15%. Simultaneous extrusion of the core screen, insulation, and insulation screen is performed using a 3-layered single extrusion head. This way, occurrence of voids in the

insulation and insulation screen is avoided as these could cause failure due to partial discharge when routine and qualification tests are conducted.

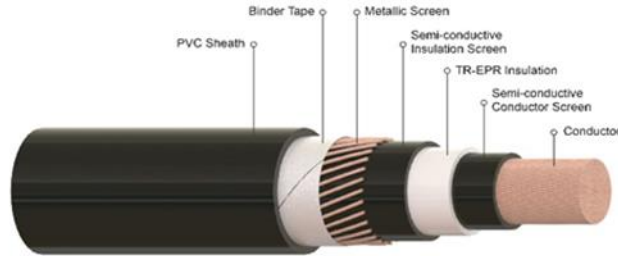


Figure 5.1: Longitudinal section of 22kV 1C120mm² TR-EPR cable

5.1 Prolonged thermal ageing test setup

Thermal ageing test was performed on the TR-EPR insulation for the simulation of effects of thermal stress corresponding to heightened temperature (equal to the maximum continuous operating temperature) in the physical properties of the insulation. This allows a time variation analysis of the properties considered particularly the mechanical properties. From the TR-EPR insulated cable sample, fifty-five test specimens are cut into dumbbell shapes as shown in Figure 5.2. Each of the test specimen are marked with designated specimen number from S1 to S55. The test specimens were then set inside a thermal oven at a temperature setting of 90°C for a test duration of 21,912 hours or about 30 months. Progressive censoring technique was employed for the testing in which every 12 weeks or 3 months, five test specimens were taken out of the thermal oven. The test specimens were then subjected to ambient temperature for about 24 hours to effect stabilisation of the insulation material and get rid of the possibility of heat in affecting the proceeding mechanical tests to be conducted. After the conditioning, the tensile strength and elongation tests were carried out. This was done by placing the test specimen one at a time onto

negligible degradation taking place in the insulation up to the 21,912 hours or 30 months of ageing time.

Table 5.1: Tensile Strength Measurements of TR-EPR Insulation from Prolonged Thermal Ageing Test

Time (hours)	Date	Tensile Strength (MPa)						Median
		Sample						
		1	2	3	4	5		
Initial	5-Oct-16	13.1	13.2	13.1	13.3	13	13.1	
2208	5-Jan-17	11.4	11.4	11.2	12	11.7	11.4	
4368	6-Apr-17	11.5	11.4	11.5	11.3	11.4	11.4	
6552	5-Jul-17	11.2	11.4	11.3	11.8	11.8	11.3	
8760	5-Oct-17	11.1	11.4	11.4	11.2	11.4	11.4	
10968	5-Jan-18	11.3	11.4	11.1	11.5	11.6	11.4	
13128	5-Apr-18	11.2	11.4	11.5	11.6	11.8	11.6	
15312	5-Jul-18	11.5	11.4	11.2	11.6	11.5	11.5	
17520	5-Oct-18	11.4	11.4	11.3	11.3	11.5	11.4	
19728	5-Jan-19	11.2	11.4	11.3	11.4	11.3	11.3	
21912	5-Apr-19	11.5	11.4	11.1	11.4	11.2	11.2	

Table 5.2: Elongation at Break Measurements of TR-EPR Insulation from Prolonged Thermal Ageing Test

Time (hours)	Date	Elongation (%)					Median
		Sample					
		1	2	3	4	5	
Initial	5-Oct-16	425	420	450	450	430	430
2208	5-Jan-17	397	386	388	381	372	386
4368	6-Apr-17	391	385	395	386	374	385
6552	5-Jul-17	378	384	379	390	387	384
8760	5-Oct-17	379	390	384	392	385	385
10968	5-Jan-18	386	380	390	386	379	386
13128	5-Apr-18	384	388	381	384	388	384
15312	5-Jul-18	381	387	381	384	378	381
17520	5-Oct-18	381	382	381	384	373	381
19728	5-Jan-19	384	380	376	377	377	377
21912	5-Apr-19	371	384	389	378	378	378

5.3 Comparison with theoretical model

From the literature, numerous theoretical models particular to the relationships of measurable characteristics of insulation materials were presented. The selection of theoretical model should take into account the availability of parameters required. In this paper, the study conducted on TR-EPR involved a time variation analysis of the mechanical properties (tensile strength and elongation) subjected to constant high temperature (corresponding to the thermal stress to effect accelerated ageing) for a prolonged period of time. Hence, the theoretical model should involve a time behaviour of insulation property. Simoni [50] presented a fundamental approach regarding test of thermal ageing through a chemical approach. It began from the investigation of relationship between property P , temperature T , and exposure time t . The selection of the property was pertinent to failure condition. Recalling the fundamental ageing law presented based on Dakin and Mamlow by Simoni [50], the equation took from:

$$\frac{dP}{dt} = -K \cdot P^\alpha \quad (2.1)$$

where the variation rate K was expressed in terms of the Arrhenius law equation

$$K = A \cdot e^{-\frac{E}{RT}} \quad (2.2)$$

Since the insulation material under consideration was subjected to constant temperature (particularly at 90°C), then K as well is constant. By rearranging (2.1), an integral form can be derived as follows:

$$\int_{P_0}^P \frac{dP}{P^\alpha} = - \int_0^t K dt \quad (2.3)$$

The lower limits of both integrals are pertinent to the initial conditions where P_0 is the initial value of property at $t = 0$. Since K is constant, hence independent of time, the integration operation can be proceeded resulting to the following:

$$\int_{P_0}^P \frac{dP}{P^\alpha} = f(P) - f(P_0) = -K \cdot t \quad (2.4)$$

Equation (2.4) can be rewritten as follows:

$$F(P) = K \cdot t \quad (2.14)$$

where $F(P) = f(P_0) - f(P) = -\int_{P_0}^P \frac{dP}{P^\alpha}$. Simoni proposed a new phenomenological theory

which involved the consideration of relative property p (equivalent to $\frac{P}{P_0}$) instead of property P ,

hence instead of $F(P)$, $F(p)$ is considered which is now equivalent to:

$$F(p) = -\int_1^p \frac{dp}{p^\alpha} \quad (2.25)$$

Notice that the lower limit was adjusted to 1 which is derived by recalling that initial property is

P_0 and relative property is $p = \frac{P}{P_0}$, hence the initial relative property $p_0 = \frac{P_0}{P_0} = 1$. Furthermore, K

was given a more general definition of being a function of stress instead of simply a function of

temperature (which was equivalent to the thermal stress). It should be noted that since K was

solely defined as a function of stress and not time, the integration performed in (2.4) still holds

valid. Application of the relative property p and stress dependence of K on (2.14) leads to the

following equation:

$$F(p) = K(s) \cdot t \quad (2.24)$$

By equating (2.25) and (2.24) and recalling the time independence of K , an explicit expression of

the relative property p is derived as follows:

$$\begin{aligned} -\int_1^p \frac{dp}{p^\alpha} &= K \cdot t \\ -\int_1^p p^{-\alpha} dp &= K \cdot t \\ -\left[\frac{p^{-\alpha+1}}{-\alpha+1} \right]_1^p &= K \cdot t \end{aligned}$$

$$\begin{aligned}
 \frac{1}{\alpha - 1} \cdot [p^{-\alpha+1}]_1^p &= K \cdot t \\
 [p^{-\alpha+1}]_1^p &= (\alpha - 1) \cdot K \cdot t \\
 \left[\frac{1}{p^{\alpha-1}} \right]_1^p &= (\alpha - 1) \cdot K \cdot t \\
 \left[\frac{1}{p^{\alpha-1}} - \frac{1}{1^{\alpha-1}} \right] &= (\alpha - 1) \cdot K \cdot t \\
 \frac{1}{p^{\alpha-1}} - 1 &= (\alpha - 1) \cdot K \cdot t \\
 \frac{1}{p^{\alpha-1}} &= 1 + (\alpha - 1) \cdot K \cdot t \\
 p^{\alpha-1} &= \frac{1}{1 + (\alpha - 1) \cdot K \cdot t} \\
 p &= \left[\frac{1}{1 + (\alpha - 1) \cdot K \cdot t} \right]^{\frac{1}{\alpha-1}} \tag{5.1}
 \end{aligned}$$

In this study, the property that will be considered for failure criterion is the tensile strength TS . Consequently, the relative property shall be the relative tensile strength $\frac{TS}{TS_0}$ where TS_0 pertains to the initial value of the tensile strength of the insulation material prior to ageing i.e., at $t = 0$, hence equation (5.1) becomes:

$$\frac{TS}{TS_0} = \left[\frac{1}{1 + (\alpha - 1) \cdot K \cdot t} \right]^{\frac{1}{\alpha-1}} \tag{5.2}$$

This equation provides the time variation of tensile strength (or relative tensile strength). On the basis of relative property which will first be focused, (5.2) contains five parameters which are $\frac{TS}{TS_0}$, p , t , α , and K . On the basis of property, (5.2) contains six parameters which are TS , TS_0 , p , t , α , and K . From the experimental results, TS_0 is equivalent to 13.1MPa. Time t (in hours) shall be the independent variable while TS shall be the dependent variable. As have been previously

discussed, K is constant. For α , it is assumed to be constant as well. The constants α and K are determined using the least square regression method.

The Least Square Regression Method (LSRM) is a statistical procedure used to determine the values of selected constant parameters of a defined function that will give the minimum sum of squared difference between the actual and the calculated values of the dependent variable. In mathematical form, the least square regression method involves the minimisation of the Sum of Squared Errors (SSE) expressed as follows:

$$SSE = \sum_{i=1}^n [(y_{actual})_i - (y_{calculated})_i]^2 \quad (5.3)$$

where y_{actual} refers to the value taken from the experiment, $y_{calculated}$ corresponds to the calculated value of the dependent variable based on the model function, and n denotes the number of data points. LSRM allows the determination of the function (of pre-defined form) that will give the best fit for the given set of data derived from the experiment. This was performed using the “Solver” function available in Microsoft Excel. Regarding the Solver function, the Generalised Reduced Gradient (GRG) Nonlinear method was selected which examines the gradient (slope) of the function while the decision variables or input values are changing until the partial derivative becomes 0 which corresponds to the optimal solution. The advantage of GRG Nonlinear is that it provides the optimal solution at a very short time which is almost instant. However, this method is very reliant on the initial conditions set in which the iteration stops when a local optimal solution is achieved which may not reflect the global optimal value. Additionally, this method best performs when the function under consideration is smooth: otherwise, algorithm problems may be encountered [95].

The results of LSRM applied in the experimental data from Table 5.1 provided the values of the constants α and K as follows:

$$\alpha = 639.294534139182$$

$$K = 9.406140891477090 \cdot 10^{31}$$

By substituting these constants into (5.2), the equation becomes:

$$\frac{TS}{TS_0} = \left[\frac{1}{1 + (639.294534139182 - 1) \cdot 9.406140891477090 \cdot 10^{31} \cdot t} \right]^{\frac{1}{639.294534139182 - 1}} \quad (5.4)$$

For simplification, $(\alpha - 1) \cdot K$ and $(\alpha - 1)$ were evaluated into their corresponding values resulting to the following:

$$\frac{TS}{TS_0} = \left[\frac{1}{1 + 6 \cdot 10^{34} \cdot t} \right]^{\frac{1}{638.29}} \quad (5.5)$$

The graph of (5.5) compared with the scattered plot of the experimental results in a relative tensile strength versus time coordinates ($\frac{TS}{TS_0}$ vs t) is shown in Figure 5.4.

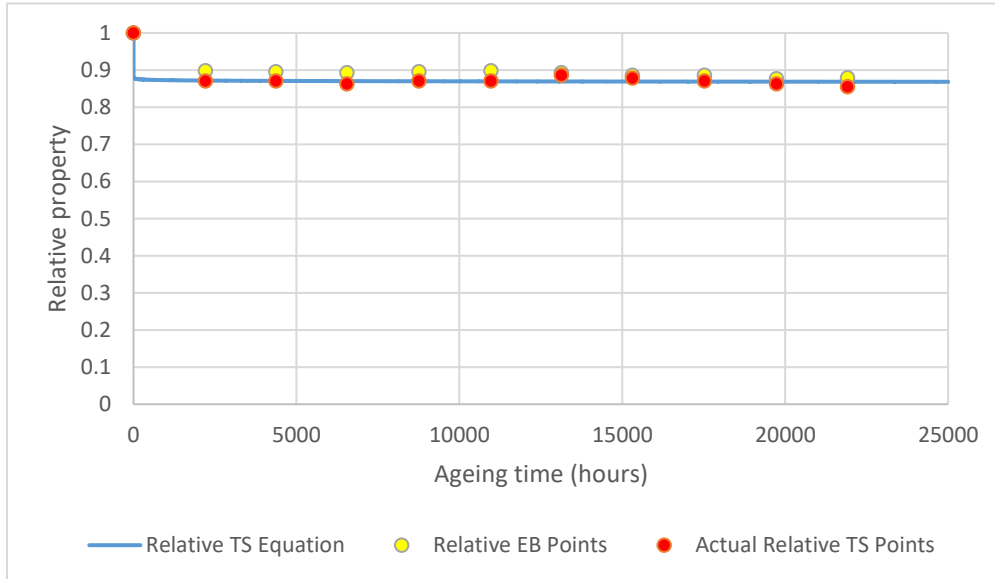


Figure 5.4: Relative TS graph compared with relative TS measurements; relative EI points included

It can be observed that the obtained equation for the time variation of relative tensile strength of TR-EPR subjected to constant 90°C showed good fitting with the experimental points. It can also be seen that the relative elongation at break points followed a similar trend with the relative tensile strength points.

The interpretation of the data can also be based on the tensile strength values instead of the relative tensile strength. Hence, by substituting $TS_0 = 13.1 \text{ MPa}$ in (5.5), the equation for time variation of tensile strength of TR-EPR subjected to constant 90°C is derived as follows:

$$TS = 13.1 \cdot \left[\frac{1}{1 + 6 \cdot 10^{34} \cdot t} \right]^{\frac{1}{638.29}} \quad (5.6)$$

The comparison between the tensile strength values obtained from the experiment and from (5.6) based on Simoni is provided in Table 5.3.

Table 5.3: Comparison of tensile strength values from experiment and theoretical model (Simoni)

Ageing time (hours)	Tensile Strength (MPa)	
	Experiment	Equation
0	13.1	13.1
2208	11.4	11.42
4368	11.4	11.4
6552	11.3	11.4
8760	11.4	11.39
10968	11.4	11.39
13128	11.6	11.38
15312	11.5	11.38
17520	11.4	11.38
19728	11.3	11.38
21912	11.2	11.38

From Table 5.3, it can be observed that the tensile strength values given by (5.6) show good fitting with the values measured from the experiment.

The goodness of fit of the model with experimental data through regression analysis can be quantified by resorting to statistical treatment. Given the non-linear nature of (5.6), the statistical measurement considered is the Standard Error of Regression (S). The standard error of regression gives the absolute measures of the interval of data points from the regression curve. A feature of the standard error of regression is that it has the same unit with the dependent variable. The formula used for the calculation of the standard error of regression is as follows:

$$S = \sqrt{\frac{SSE}{n - m - 1}} \quad (5.7)$$

In this case, y_{actual} refers to the tensile strength measurements from the ageing experiment (see Table 5.3), $y_{calculated}$ refers to the calculated values of the tensile strength based from (5.6) (see Table 5.3), $n = 11$ which corresponds to the number of data points (see Figure 5.4), and $m = 1$ which corresponds to the number of independent variables (in this case is the ageing time). From the computed SSE when the LSRM was applied, a low standard error of regression was calculated ($S = 0.1093$). An additional feature of the standard error of regression is that it is capable of providing an estimation of the 95% prediction interval (PI) [96]. This is mathematically expressed as:

$$95\% PI \approx \pm 2 \cdot S \quad (5.8)$$

Hence, the 95% PI is ± 0.2185 which indicates that around 95% of data points (particularly to measured tensile strength values) will deviate at about 0.2185MPa from the regression curve (5.6).

5.4 Extrapolation to service temperature using

Arrhenius relationship

As have been utilised in the literature, the Arrhenius relationship was one of the most common models referred with regards to the effect of temperature on the chemical reaction rate. From Escobar and Meeker [7], the Arrhenius equation may be expressed as follows:

$$R(T) = \gamma_0 \cdot e^{-\frac{E_a}{k \cdot T}} \quad (5.9)$$

where $R(T)$ depicted the rate of reaction dependent on temperature T , γ_0 referred to as the pre-exponential factor which is a characteristic parameter of the material, E_a corresponded to the activation energy which is also a characteristic parameter of the material, k denoted a constant which may either be the Boltzmann's constant (equivalent to $8.6171 \times 10^{-5} \frac{eV}{K}$ or $\frac{1}{11605} \frac{eV}{K}$) or universal gas constant (equivalent to $8.31447 \times 10^{-3} \frac{kJ}{mol \cdot K}$ or $\frac{1}{120.27} \frac{kJ}{mol \cdot K}$), and T corresponded to thermodynamic temperature expressed in Kelvin (K). In the case of k taken as the Boltzmann's constant, E_a takes the unit eV while for the case of k taken as the universal gas constant, E_a takes the unit $\frac{kJ}{mol}$. In a simple chemical reaction, which involves only a step, the activation energy represents the minimum energy necessary for the chemical reaction to take place. However, in actual, the chemical reactions are more complex which may involve multiple chemical deteriorating processes each having unique rate of reaction and activation energy. Therefore, the applicability of the Arrhenius relationship for the certain temperature range is limited to those whose overall reaction is governed by a dominant chemical reaction. From the Scale-Accelerated Failure-Time (SAFT) model, the ageing time $t(x)$ dependent on an explanatory variable x can be scaled by an acceleration factor $AF(x)$ expressed as follows:

$$t(x) = \frac{t(x_U)}{AF(x)} \quad (5.10)$$

where $t(x_U)$ corresponded to the ageing time for an explanatory variable at use condition x_U . For an explicit expression of the accelerating factor, (5.10) can be rewritten as:

$$AF(x) = \frac{t(x_U)}{t(x)} \quad (5.11)$$

In the case of thermal ageing, the explanatory variable can be taken as the temperature T . Considering this, (5.11) becomes

$$AF(T) = \frac{t(T_U)}{t(T)} \quad (5.12)$$

where T_U corresponds to the temperature at operating condition. Furthermore, by considering the inverse relationship between ageing time and rate of reaction, the acceleration factor from (5.12) can be further modified as:

$$AF(x) = \frac{R(T)}{R(T_U)} \quad (5.13)$$

where $R(T_U)$ corresponds to the rate of reaction at use temperature T_U . By applying (5.9) to (5.13), the following expression for the acceleration factor is derived:

$$AF(T) = e^{E_a \left(\frac{1}{k \cdot T_U} - \frac{1}{k \cdot T} \right)} \quad (5.14)$$

By taking the value of k as the universal gas constant, (5.14) can be further defined as

$$AF(T) = e^{E_a \left(\frac{120.27}{T_U} - \frac{120.27}{T} \right)} \quad (5.15)$$

In the case of TR-EPR, the service temperature is 60°C or equivalently 333K while the temperature constantly applied on the thermal ageing test was 90°C or equivalently 363K. According to Lei et al. [31], the activation energy of Ethylene Propylene Diene Monomer (EPDM) rubber with different grades ranges from 60 to 85 kJ/mol. However, according to the results obtained by Pourmand [97], the activation energy of EPDM rubber is around 110 kJ/mol. For conservative estimate, the middle value will be used which is 85 kJ/mol. By substituting this

value on (5.15), the accelerating factor derived is 12.64. This means that the every-three-months mechanical property values obtained at 90°C thermal ageing would correspond to every-38-months measurements obtained at 60°C, hence the thermal ageing results would correspond up to 31 ½ years of stable mechanical property measurements for a 60°C thermal stress.

5.5 Correlation of tensile strength and elongation at break

From Figure 5.4, it can be observed that the relative tensile strength and elongation at break have identical pattern of values. From this observation, it can be hypothesised that there exists a correlation between tensile strength and elongation at break. In statistics, correlation coefficients are used to measure the strength of relationship between two variables. In the case of linearity, one of the most common correlation coefficients used is the Pearson correlation coefficient r . In calculating the Pearson correlation coefficient, the following formula is used:

$$r = \frac{n \cdot [\sum_{i=1}^n (x_i \cdot y_i)] - (\sum_{i=1}^n x_i) \cdot (\sum_{i=1}^n y_i)}{\sqrt{[n \cdot \sum_{i=1}^n x_i^2 - (\sum_{i=1}^n x_i)^2] \cdot [n \cdot \sum_{i=1}^n y_i^2 - (\sum_{i=1}^n y_i)^2]}} \quad (5.16)$$

where n pertains to the number of observations, and x and y corresponds to the variables considered for the correlation. The value of r that can be obtained sits between -1 to 1. The closer the values to the extremities (-1 or 1), the stronger the correlation between the two variables is. Positive value of r corresponds to positive correlation which means that an increase in the value of one variable corresponds to an increase in the value of the other variable. This also means that a decrease in the value of one variable corresponds to a decrease in the value of the other variable. On the other hand, negative value of r pertains to negative correlation: an increase in the value of one variable corresponds to a decrease in the value of the other variable or vice versa [98].

For this research, $n = 11$ which corresponds to the number of median values obtained pertinent to either tensile strength or elongation at break as shown in Table 5.1 and 5.2. For the variables, x would pertain to relative elongation at break while y would pertain to the relative tensile strength. By substituting the values of relative tensile strength and relative elongation at break from Table 5.1 and 5.2 to equation (5.16), the Pearson correlation coefficient is obtained as $r = 0.9769$. This indicates a strong positive correlation between relative tensile strength and relative elongation at break. To visualise this correlation, the plot of relative TS-relative EI points is shown in Figure 5.5.

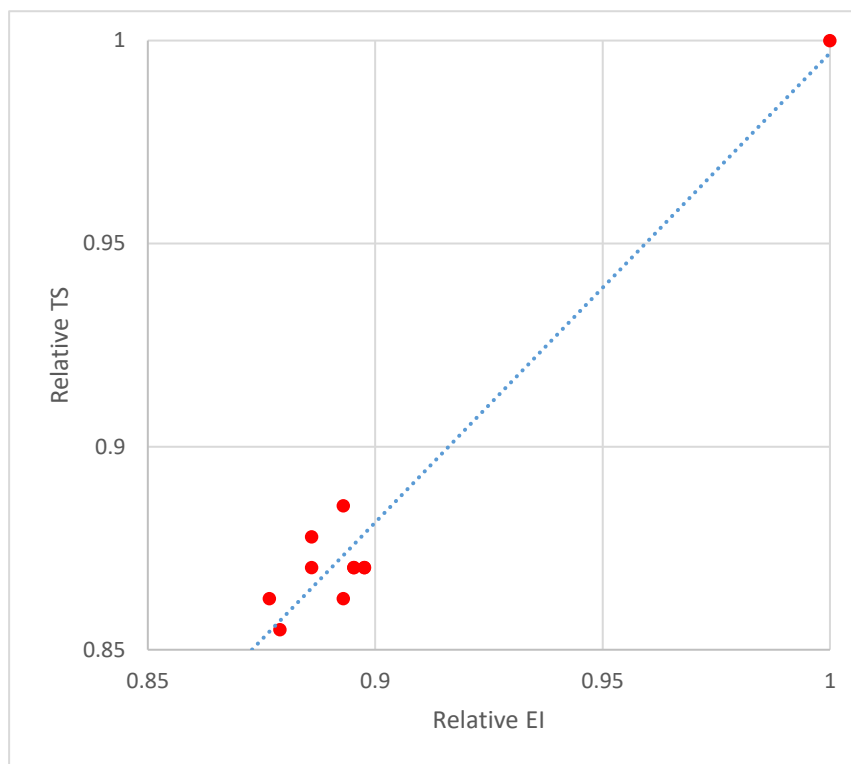


Figure 5.5: Plot of relative TS-relative EI points (red), regression line included (blue)

5.6 Estimation of TR-EPR insulation life

In the performance of accelerated ageing tests, one of the primary aims is the estimation of insulation life pertinent to the service condition. This is done by extrapolation of data gathered from the accelerated ageing experiment. It should be noted that in accelerated ageing tests, there exists a trade-off between severity of test and reliability of data pertinent to actual application. When considering more severe testing conditions e.g., higher stresses, the failure time is shortened which can possibly be within considered test duration. However, with greater test condition severity, the data deviates more from the measurements pertinent to service condition, hence, will require more careful handling when performing extrapolation to service condition. In other words, extrapolation to operating conditions becomes more critical and dangerous as the testing condition is made more severe. On the other hand, when the ageing test condition is less severe i.e., closer to service condition, the data gathered tends to become more comparable to actual measurements pertinent to operating conditions. Extrapolation tends to become safer and more reliable as well. However, the consequence of ageing test closer to service condition is the prolonged duration of the test which may go beyond considered testing time. This problem is greatly considered when the material under consideration has a considerably long service life which is the case of cable insulation.

In this research, the treatment of the accelerated ageing test data lead to the derivation of (5.5) which corresponded to the graph having suitable fitting with the experimental points (relative TR versus ageing time).

However as seen in Figure 5.4, the graph obtained would give extremely long insulation life value for a significant decrease in either mechanical properties (tensile strength and elongation at break)

pertinent to failure criterion. For instance, a 50% decrease in tensile strength corresponds to about 100 quinquagintillion hours or 10^{155} hours of ageing time which is very illogical. Hence, a more phenomenological picture of the obtained graph is necessary in which at some time, it will show a downward curvature indicating approach towards failure. Prior to this, it is important to establish a failure criterion first. Kashi and Moussaceb [99] used the 50% decrease in elongation at break for the failure criterion. In the case of Montanari [81], 50% decrease in electric strength was used for the failure criterion which corresponded to 50% decrease in tensile strength and 3% weight loss. For the sake of consistency, considering that the tensile strength and elongation at break are highly correlated, the 50% decrease in tensile strength will be considered for the failure criterion. Going back to the issue concerning the graph, it can be observed from Table 5.3 that the tensile strength values decreased from 13.1 to 11.3MPa, then increased from 11.3 to 11.6MPa and decreased again from 11.6 to 11.2MPa. The points pertinent to 11.3MPa and 11.6MPa served as reference points for the change in the slope of tensile strength values (negative-positive and positive-negative respectively). In analytic geometry, this can be described as change in the concavity of the graph where the point at 11.3MPa corresponds to upward concavity while the point at 11.6MPa corresponds to downward concavity. These reference points are referred to as points of inflection. In the case of two points of inflection, the equivalent polynomial graph would be a cubic equation in the form

$$\frac{TS}{TS_0} = a \cdot t^3 + b \cdot t^2 + c \cdot t + d \quad (5.17)$$

where $a, b, c,$ and d were simply coefficients of the cubic equation which will be all determined using the LSRM. This is the same format of equation used by Kashi and Moussaceb [99] for their graph of elongation at break versus ageing time. To optimise the determination of the equation coefficients pertinent to suitable fitting with experimental data, the ageing time t will be expressed

in years instead of hours (1 year = 8,760 hours). By applying LSM, the following values of the equation coefficients are derived:

$$a = -0.0606056545563823$$

$$b = 0.256075533445408$$

$$c = -0.314468395922584$$

$$d = 0.97472455337514$$

For simplicity, the coefficients were rounded to four significant figures so that the cubic equation for relative tensile strength can be expressed as:

$$\frac{TS}{TS_0} = -0.06061t^3 + 0.2561t^2 - 0.3145t + 0.9747 \quad (5.18)$$

The plot of the relative tensile strength cubic equation and actual relative tensile strength points are shown in Figure 5.6.

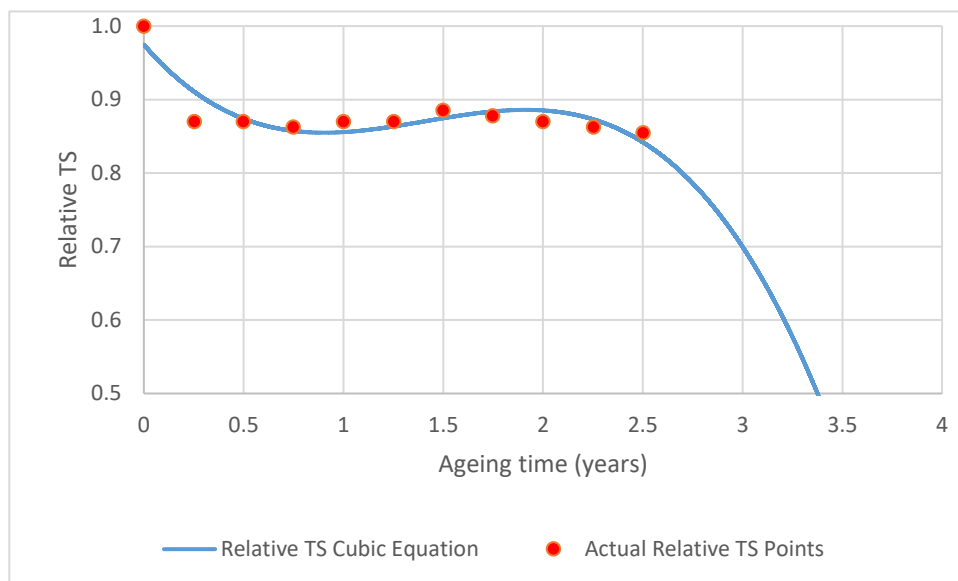


Figure 5.6: Relative TS cubic graph compared with relative TS measurements

It can be observed that the fittings of the cubic graph are fairly satisfactory but inferior to that obtained using Simoni-based theoretical model. Nevertheless, the cubic graph was capable of

providing the forecasted downward curvature pertinent to 50% drop in the value of relative tensile strength for the failure criterion. For comparison, the values of experimentally obtained tensile strength values and those calculated based on the Cubic graph are presented in Table 5.4.

Table 5.4: Comparison of tensile strength values from experiment and theoretical model (Cubic)

Ageing time (hours)	Tensile Strength (MPa)	
	Experiment	Equation
0	13.1	12.77
2208	11.4	11.93
4368	11.4	11.45
6552	11.3	11.23
8760	11.4	11.21
10968	11.4	11.31
13128	11.6	11.46
15312	11.5	11.58
17520	11.4	11.60
19728	11.3	11.44
21912	11.2	11.03

Except for the first two values, it can be observed that the differences between the experimental and graphical values are less than 0.2MPa. As have been previously performed, to statistically quantify the goodness of the fit of the cubic graph which falls under non-linear type, the standard error of regression can be used which can be calculated using (). Applying this using the graphical values, the standard error of regression was calculated as $S = 0.2486$ which corresponds to a 95% prediction interval of 0.4971 which indicates that about 95% of the tensile strength values derived from experiment will deviate no more than 0.4971MPa from the cubic regression curve corresponding to the ageing time.

By applying the 50% tensile strength decrease for the failure criterion, the corresponding failure time calculated at maximum operating temperature of 90°C is 3.376 years. By applying the computed Arrhenius acceleration factor of 12.64, the life of TR-EPR insulation pertinent to service temperature of 60°C is 42.68 years which can be roughly estimated to 45 years. This is 50% longer than the anticipated cable life of 30 years in actual experience. In the case where elongation at break is considered as reference instead of tensile strength, the calculated TR-EPR insulation life would be instead 46.85 years or roughly 50 years, hence TR-EPR insulation life of 45 years is as appropriate estimation as it is situated between the calculated values for the tensile strength and elongation at break reference.

5.7 Discussion

The fundamental Ageing law introduced by Dakin and Mamlow which was used by Simoni [50] considered the property to be associated with the failure of the insulation. In the research paper of Simoni, the property considered was the dielectric strength which is an electrical property. This was referred to as the best choice of property for the model since the occurrence of failure in electrical equipment is referenced when the value of dielectric strength measured dropped to the value of the applied voltage, hence other material properties were linked to dielectric strength especially when considering the breakdown phenomenon.

Regarding (5.1), Simoni found that the degradation curves produced by this equation showed upward curvatures for any positive values of α . This can be verified by the plot of the equation shown in Figure 5.4. He then argued that in actual, experimenters arrive at degradation curves that showed otherwise (i.e., downward curvatures). This was resolved by taking negative values of α which produced the desired curves having upward curvatures. However, in doing so, the

chemical hypothesis is rejected, hence the theory becomes phenomenological in which the effects only of the degradation is considered while the mechanism of degradation is ignored. It should be noted that the property considered for the degradation curve having downward curvatures was dielectric strength. On the other hand, the property considered in this research study was tensile strength which showed upward curvature. A research cited by Simoni in his same work [50] was that of Montsinger who performed tensile strength measurements with ageing time on yellow varnished cloth for three sets of temperatures (90°C, 100°C, and 110°C) in air and oil. The degradation curves of the tests performed in air at all temperatures produced downward curvatures; while degradation curves of the tests performed in oil at all temperatures produced upward curvatures. This shows that degradation curves based on tensile strength measurements may vary on curvatures tending towards the origin with higher temperature. The concavity of the degradation curves seems to be dependent on various factors which may be the property selected for failure criterion (dielectric strength, tensile strength, etc.), the insulation material, and medium of exposure (in air, oil, etc.). The upward concavity of the degradation curve for TR-EPR at 90°C that was derived in this research study is verified to be reasonable compared with the results of other literatures.

The results can also be compared to those obtained by various literatures presented earlier in the thesis. Prior to this, it is important to discuss first the effective electric field strength acting on the 22kV 120mm² TR-EPR insulation at service condition. A straightforward approach in the calculation of the electric field strength is by dividing the applied voltage to the thickness of the dielectric material. Pertinent to both IEC 60502-2 and AS/NZS 1429.1, the nominal insulation thickness for EPR with a voltage rating of 22kV and nominal cross-sectional area of 120mm² is 5.5mm. Hence, the electrical field experienced by the insulation is about 4kV/mm.

Montanari [81] presented a relative tensile strength versus life curve of EPR insulated cables for various temperatures in which 110°C is the lowest. Greater reduction of tensile strength for the same ageing time was observed with increasing temperature. The relative TS versus life curve at 110°C showed that relative tensile strength reduced to 75% after 20,000 hours of ageing time. Therefore, it is expected that the relative tensile strength should be above 75% when the temperature is lowered to 90°C. This is the case obtained in this research in which the relative tensile strength observed after 21,912 hours (a bit higher but close to 20,000 hours) of ageing time at 90°C is 85.5% which is in fact greater than 75%.

Montanari and Simoni [52] showed that from the electrical stress versus temperature curve of EPR insulated cables, the corresponding life of insulation at electrical stress between 0 to 6kV/mm and temperature at 90°C is greater than 100,000 hours. Since the TR-EPR insulation operates within the electrical stress range and at the same temperature, its failure time may similarly correspond to more than 100,000 hours (11 ½ years) as well.

Results of the thermal life tests conducted by Mazzanti and Montanari [55] on EPR insulated cables showed an electrical threshold value of 6kV/mm at 90°C. By definition, below the electrical threshold value (6kV/mm in the case of EPR), ageing due to electrical stress can be ignored and life tend to be so high that it can be considered to approach infinite. Since the calculated operating electrical stress of TR-EPR (4kV/mm) is below the electrical threshold, this means that accelerated thermal ageing test results obtained in this research can be extended to results that will be obtained when combined electrical and thermal ageing test is performed at service condition i.e., at 4kV/mm and 90°C. This thermo-electrical ageing test is actually further valid for electrical stresses between 0 to 6kV/mm. Additionally, based on Cao and Grzybowski [100], the

recommended value of electrical stress for EPR insulated cables in MV applications is 5kV/mm in which 4kV/mm is still below.

5.8 Conclusion

In this chapter, the insulation material TR-EPR was introduced after brief comparison of XLPE and EPR. The way TR-EPR cable was manufactured was also explained which involved the use of dry silane curing method to discourage the formation of voids. The components of a sample TR-EPR cable was also tackled which include the basic components of cable discussed in Chapter 2 (core, core screen, insulation, insulation screen, metallic screen, and outer sheath) but with the addition of binder tape located between the outer sheath and metallic screen. The core was made of Copper and the metallic screen was of concentric neutral type.

This chapter also focused on presenting the accelerated ageing test performed on the TR-EPR cable. This involved subjecting the test specimens in an ageing oven at elevated temperature equivalent to the maximum operating temperature of 90°C and applying progressive censoring method to gather test data (tensile strength and elongation at break) every 3 months. The whole ageing test lasted for 2 years without any of the samples attaining failure. The results showed almost constant values of tensile strength and elongation at break of the TR-EPR insulation for the whole test duration supporting the stability of the TR-EPR under high thermal stress. The only distinct change in the value of properties was observed in which there was a sudden slight drop of values for the first aged specimens compared to unaged ones. The next property measurements then showed slight deviations with respect to the measurements of the first aged specimens. The results were then applied to a model proposed by Simoni [50] with reference to Dakin and Mamlow which involved the fundamental ageing law and Arrhenius law. The parameters were

determined using LSM. The model showed satisfactory fitting with the results supported by statistical measure of fitting called standard error of regression. The estimation of TR-EPR insulation life was done which involved extrapolation to service temperature using Arrhenius acceleration factor, criterion failure of 50% decrease in tensile strength (and elongation at break), and alternative representation of fitting using cubic equation. This led to a conservative estimation of TR-EPR insulation life as 45 years.

CHAPTER 6 ELECTRICAL AND NON-ELECTRICAL TEST FOR 22kV TREE RETARDANT- ETHYLENE PROPYLENE RUBBER CABLE

6.0 Introduction

Electrical and non-electrical tests were performed on the TR-EPR cable samples for this research study. Similar tests were also carried-out by a third-party accredited laboratory (China National Centre for Quality Supervision and Test of Electric Wire and Cable) for verification. Hot set test is the only non-electrical test presented while the rest are classified as electrical tests. For the third-party accredited laboratory, two set of tests were performed corresponding to AS/NZS 1429.1, IEC 60092-350, and IEC 60092-354. The reference numbers were CT15-5627 for AS/NZS 1429.1 and CT15-5626 for IEC 60092-350 and IEC 60092-354.

6.1 Partial Discharge Test

Three TR-EPR cable samples of 10m length each as shown in Figure 6.1, were placed onto a cable tray and afterwards looped onto a current generator. Termination was performed on both ends of the cable via crimped Copper lug. A bolt was then used to connect two lugs which generates a short circuit loop which in turn causes an increase in the current. To be able to monitor the temperature of the cable core, thermocouples were secured to the core. Tuning of the load current was performed until the cores attain the operating temperature of 60°C and cross-linking of the insulation occurs. For every 24th hour interval of heating, insulation strips were taken out. At both events before and after heating, Partial Discharge (PD) tests as shown in Figure 6.2 using a 125kV Reactor and Series Resonance System as shown in Figure 6.3, were performed to compare the PD measurements between the initial and after heating. In compliance with AS/NZS 1660.3 [90], only one end is considered for the connection in which injection of charge was performed in the cable. Each cycle of the partial discharge was performed in no more than 3 minutes.

Measured PD values before and after heating of cable samples are shown in Appendix A. The summary of results of the PD tests performed on 25 test specimens are shown in Figure 6.4. It can be observed that before heating, the partial discharge values show large range from 2 to 163pC. But after heating, the partial discharge values show significant decrease ranging only to about 0 to 4pC. As per AS/NZS 1429.1 [39], the partial discharge values should not exceed 5pC for voltage level of 19kV r.m.s. (corresponding to 150% of U_0 referring to Table 4.14) for a cable designated voltage of 12.7/22 (24) kV. Since the partial discharge values obtained from the experiment are all lower than the required 5pC maximum partial discharge value, it follows that the TR-EPR cable conforms to the standard in terms of the PD test.

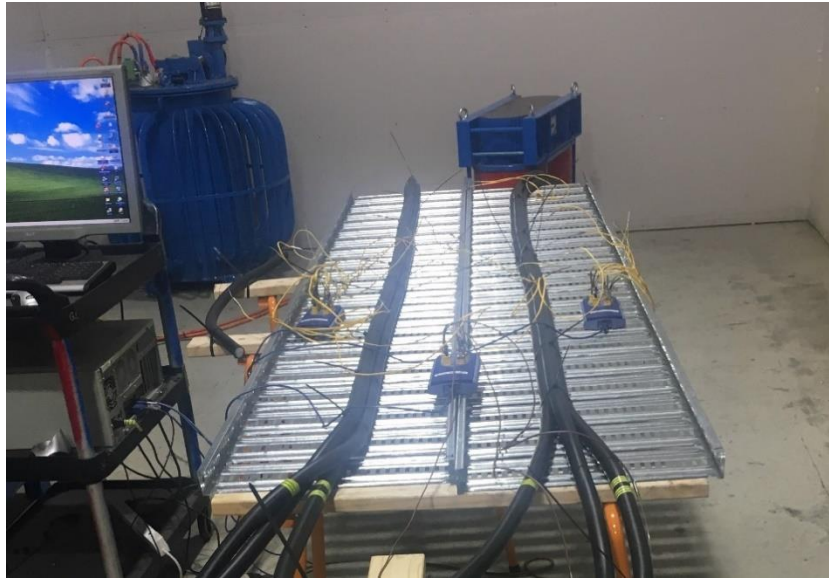


Figure 6.1: TR-EPR cables are subjected to heating



Figure 6.2: Measurement of PD



Figure 6.3: 125kV Reactor and Series Resonance PD test system

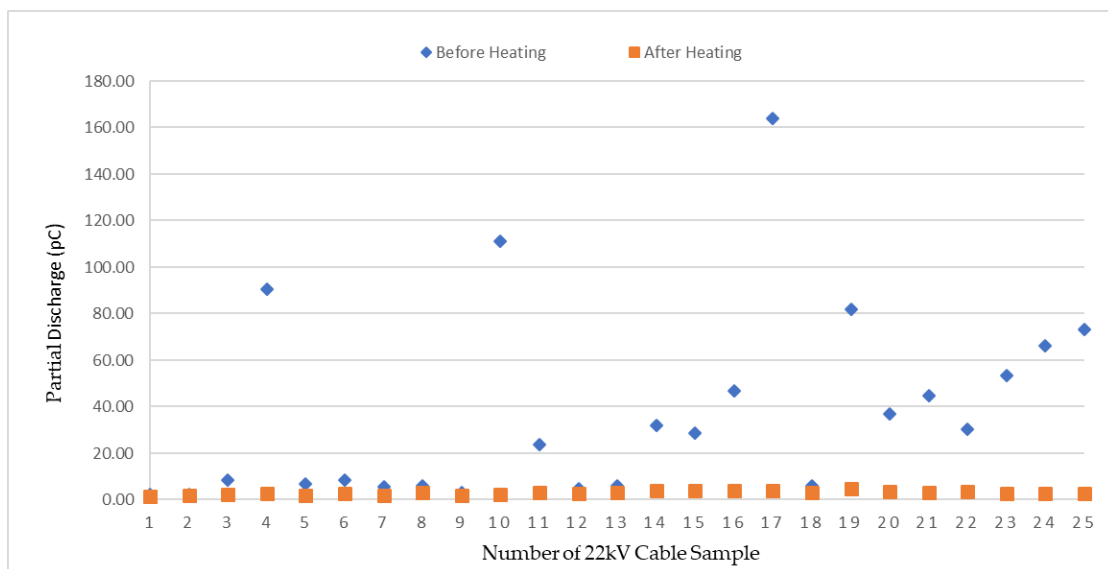


Figure 6.4: PD graph of 22kV TR-EPR cable before and after heating

6.1.1 PD test conducted by third party accredited laboratory as per AS/NZS 1429.1

As per AS/NZS 1429.1 [39], two partial discharge tests were performed: one at 25kV (corresponding to $2U_o$) and another at 19kV (corresponding to $1.5U_o$). The standard requires maximum partial discharge measure of 20pC for $2U_o$ and 5pC for $1.5U_o$ (refer to Table 4.14). For the test procedure, refer to discussion of PD test in compliance with AS/NZS 1660.3 [90]. The sensitivity of the PD test was declared as 1pC.

The PD test were performed to a newly manufactured cables with TR-EPR insulation using a 200kV series resonance system similar to the system describes in Figure 6.2. Both ends of cable were terminated by oil in which the one end connected to the PD tester and the other end to earth potential. The test voltage was regulated until it reached the voltage magnitude equivalent to the $2U_o$ and $1.5U_o$ of the cable voltage rating respectively.

Results as shown in Table 6.1 that for the 25kV ($2U_o$), the measured partial discharges were all less than 1pC compared to standard requirement of 20pC as maximum value. For the 19kV ($1.5U_o$), the measured partial discharges were also less than 1pC compared to standard requirement of 5pC as maximum value. This indicates a passing verdict of TR-EPR insulation on PD test both at $2U_o$ and $1.5U_o$ as per AS/NZS 1429.1 [39].

6.1.2 PD test conducted by third party accredited laboratory as per IEC 60092-350 and IEC 60092-354

As per IEC 60092-350 [101] and IEC 60092-354 [102], the partial discharge test should be conducted in compliance with IEC 60885-2 where it should be performed at discharge value of $1.73U_o$ where the closest voltage rating was adapted as 12/20kV. The standard requires a maximum partial discharge value of 5pC.

Results as shown in Table 6.1 that the measured partial discharge values were all less than 1pC compared to standard requirement of 5pC as maximum value. This indicates a passing verdict of TR-EPR insulation on PD test at $1.73U_o$ as per IEC 60092-350 and IEC 60092-354.

Table 6.1: Measured PD values of TR-EPR cables from third party validation

Cable Size (mm ²)	Voltage Rating (kV)	Test Standard	Test Voltage (kV)	Measured PD (pC)
95	22	AS/NZS 1429.1	25	1.0
95	22	AS/NZS 1429.1	19	1.0
95	20	IEC 60092-350	21	1.0

6.2 Bending test proceeded by PD test

6.2.1 Conducted by third party accredited laboratory as per IEC 60092-350 and IEC 60092-354

Bending test was performed proceeded by partial discharge at $1.73U_o$. As per IEC 60092-350 and IEC 60092-354, for the bending test, the test specimen at room temperature is bent as to encircle a suitable cylinder (like a drum hub) for a minimum of one revolution. Afterwards, the test specimen is unwound and bent again similar to the previous step completing a cycle which shall be repeated three times. In the case of cables with one core, the cylinder should have a diameter of $20 \cdot (\text{cable diameter} + \text{core diameter}) \pm 5\%$. The standard requires a maximum partial discharge value of 5pC.

Results show the measured partial discharges were all less than 1pC compared to standard requirement of 5pC as maximum value. This indicates a passing verdict of TR-EPR insulation on bending test at $1.73U_o$ discharge as per IEC 60092-350 and IEC 60092-354.

6.3 Tan delta measurement

Five trials of $\tan\delta$ measurement for various test voltages as shown in Table 6.2 were conducted on the TR-EPR cable samples. For the $\tan\delta$ value, the average of the results was considered. As per IEC 60502-2 [56] and AS/NZS 1429.1 [39] for EPR, $\tan\delta$ should not exceed 0.04.

Results show that TR-EPR insulation has a $\tan\delta$ measurement of 0.0003284 which is lower than the required value of 0.04 for EPR insulation as per IEC 60502-2 and AS/NZS 1429.1, hence in conformity with standards.

Table 6.2: Measured $\tan\delta$ of TR-EPR cables

Test Voltage (kV)	Measured $\tan \delta$
3.2	3.30×10^{-4}
3.2	3.30×10^{-4}
6.5	3.30×10^{-4}
12.9	3.26×10^{-4}
13.1	3.26×10^{-4}

6.3.1 Conducted by third party accredited laboratory as per IEC 60092-350 and IEC 60092-354

As per IEC 60092-350 and IEC 60092-354, tan delta measurements were performed as functions of voltage and as functions of temperature. For the function of voltage, after having performed the bending test, measurements were conducted at voltage U_o and increment from $0.5U_o$ to $2U_o$ both at power frequency. For EPR, the measured tan delta value should not exceed 0.02 for U_o and 0.0025 for increment from $0.5U_o$ to $2U_o$. For the function of temperature, the cable samples

may be heated in a tank filled with liquid, oven, or through heating current flowing in metallic insulation screen. For any method selected, the temperature reading of the core shall be known either through the measurement of core resistance, or through the use of thermometer in the tank, oven, or insulation screen surface. Heating is performed until temperature rating is attained with reference to IEC 60092-360 (as per IEC 60092-350) and IEC 60092-351 (as per IEC 60092-354). The measurement of tan delta is then carried out at 2kV voltage at power frequency and at specified temperature. For EPR, the measured tan delta value should not exceed 0.02 for room temperature and 0.04 for rated temperature of 90°C.

Results show that the tan delta measurement of TR-EPR were 0.00036 at U_o (compared with standard maximum value of 0.02), 0.00017 at increment from $0.5U_o$ to $2U_o$ (compared with standard maximum value of 0.0025), 0.00024 at ambient temperature (compared with standard maximum value of 0.02), and 0.00026 at rated temperature of 90°C (compared with standard maximum value of 0.04). This indicates a passing verdict of TR-EPR insulation on tan delta measurement as function of voltage (at U_o and increment from $0.5U_o$ to $2U_o$) and as function of temperature (at ambient temperature and rated temperature) as per IEC 60092-350 and IEC 60092-354. Various tan δ measurement of TR-EPR cables are presented in Table 6.3.

Table 6.3: Various tan δ measurement of TR-EPR cables

Author	Third Party	Third Party	Material Supplier
3.30×10^{-4}	3.60×10^{-4}	1.0×10^{-4}	1.60×10^{-4}

6.4 Heating cycle test proceeded by PD test

6.4.1 Conducted by third party accredited laboratory as per IEC 60092-350 and IEC 60092-354

As per IEC 60092-350 and IEC 60092-354, for the heating cycle test, the test specimen after having underwent the previous tests, was laid out on the test room floor and began to be heated through a.c. current passed through the core until it has reached a temperature that is 10°C more than that of maximum operating temperature. The heating is sustained for 2 hours and afterwards cooled for 4 hours at room temperature. The heating cycle test was performed three times proceeded by a partial discharge at $1.73U_o$. The standard requires a maximum partial discharge value of 5pC.

Results show the measured partial discharges were all below 1pC compared to standard requirement of 5pC as maximum value. This indicates a passing verdict of TR-EPR insulation on heating cycle test at $1.73U_o$ discharge as per IEC 60092-350 and IEC 60092-354.

6.5 Impulse withstand test proceeded by HV test

6.5.1 Conducted by third party accredited laboratory as per AS/NZS 1429.1

Impulse withstand test was performed at ± 125 kV impulse peak voltage (10 times) at 95°C to 100°C core temperature equal to standard requirement for voltage rating of 12.7/22 (24) kV based from AS/NZS 1429.1 [39] with reference from Table 4.16. This was proceeded by a 15-minute voltage test to power frequency of 50Hz at 42kV equal to the required standard test voltage for 12.7/22 (24) kV. For the test procedure, refer to discussion of impulse withstand test proceeded

by HV test in compliance with AS/NZS 1660.3 [90]. There must be no occurrence of breakdown of the test specimen.

Results show that the TR-EPR insulation experienced no breakdown when subjected to the consecutive impulse withstand test and 15-minute voltage test. This indicates a passing verdict of TR-EPR insulation on impulse withstand test proceeded by 15-minute voltage test as per AS/NZS 1429.1 [39].

6.5.2 Conducted by third party accredited laboratory as per IEC 60092-350 and IEC 60092-354

As per IEC 60092-350 and IEC 60092-354, the impulse withstand test was performed at 95°C core temperature (in compliance with standard requirement of 5°C higher than maximum core temperature which is 90°C in the case of EPR) and at $\pm 125\text{kV}$ peak voltage (10 times) (applicable for 12kV rated voltage U_o). This was proceeded by a 15-minute voltage test at 42kV equal to the required standard test voltage for 12kV rated voltage U_o . For the test procedure, refer to discussion of impulse withstand test in compliance with IEC 60230. There must be no occurrence of breakdown of the test specimen.

Results show that the TR-EPR insulation experienced no breakdown when subjected for the consecutive impulse withstand test and 15-minute voltage test. This indicates a passing verdict of TR-EPR insulation on impulse withstand test proceeded by 15-minute voltage test as per IEC 60092-350 and IEC 60092-354.

6.6 High Voltage test

The 5-minute HV test was performed with applied alternating voltage value of 45kV which is slightly higher, hence more severe compared to the standard requirement of 42kV for 12.7/22 (24) kV based from AS/NZS 1429.1 [39] with reference from Table 4.15. The test was conducted using a power frequency of 50Hz considering sine waveform. There must be no occurrence of breakdown of the test specimen.

Results show that the TR-EPR insulation experienced no breakdown when subjected to 45kV for 5 minutes. This indicates a passing verdict of TR-EPR insulation on 5-minute HV test as per AS/NZS 1429.1 [39].

6.6.1 Conducted by third party accredited laboratory as per AS/NZS 1429.1

The 4-hour HV a.c. test was performed with applied 50kV alternating voltage equal to the standard requirement of 50kV for 12.7/22 (24) kV based on AS/NZS 1429.1 [39] with reference from Table 4.17. The test was conducted using a power frequency of 50Hz considering a sine waveform. There must be no occurrence of breakdown of the test specimen.

Results show that the TR-EPR insulation experienced no breakdown when subjected to 50kV for 4 hours. This indicates a passing verdict of TR-EPR insulation on 4-hour HV test as per AS/NZS 1429.1 [39].

6.6.2 Conducted by third party accredited laboratory as per IEC 60092-350 and IEC 60092-354

IEC 60092-354 refers IEC-60092-350 for the performance of 4 hours HV test. As per IEC 60092-350, for the 4-hour HV test, the cable sample no less than 5 m long was subjected to 48kV (which corresponded to the required voltage of $4U_0$) at ambient temperature for 4 hours at power frequency. The voltage was applied between every core and metallic screens. There must be no occurrence of breakdown.

Results show that the TR-EPR insulation experience no breakdown when subjected to 48kV at ambient temperature for 4 hours. This indicates a passing verdict of TR-EPR insulation on 4-hour HV test as per IEC 60092-350 and IEC 60092-354.

6.7 Hot set test

The Hot set test was performed pertinent to the determination of the ultimate cross-linking time of the TR-EPR insulation at ambient temperature ranging from 0 to 15°C and service temperature of 60°C. The ambient temperature range is notably low since the experiment was conducted during the wintertime in Victoria. Since the cross-linking time is proportional to temperature and time, this indicates that the cross-linking time obtained for the ambient temperature will correspond to the longest period. Samples are composed of 10mm strips of insulation. The strips are polished by grinding the insulation surface to eliminate surface irregularities which may contribute to the breaking of test specimens when Hot set test is carried out. Prior to conducting the Hot set test, the grounded test specimens are first condition at ambient temperature for 16 hours. The size of dumbbell cuts from the sample is shown in Figure 5.2. After the test specimens are conditioned, they are hung inside an oven with each of them carrying a mechanical load

producing an equivalent of 20N/cm² tensile stress suspended at the bottom portion of each specimen. A test specimen is deemed to pass the test if it was capable of withstanding the mechanical load for a duration of 900 seconds without breaking and value of elongation and residual length relative to the original length is less than 175% and 15% respectively. The values of the Hot set time are taken every 96 hours interval for the ambient temperature and 24 hours interval for the service temperature.

Summary of the results of cross-linking development of TR-EPR at ambient temperature is presented in Table 6.4. It was observed that the molecules of the TR-EPR insulation began changing its physical and chemical properties forming new cross-link structure 24 hours after being extruded. The ultimate cross-linking was attained after 576 hours which is above the requirements as per IEC 60502:2018 [103].

Table 6.4: Cross-linking development of TR-EPR at ambient temperature

Number of hours exposed at ambient condition	Hot Set Test_Time after break (seconds)
24	28
96	35
192	88
288	335
384	590
480	744
576	900 (no break)

The results of the cross-linking development of TR-EPR at 60°C service temperature is presented in Table 6.5. Results showed that the ultimate cross-linking time was achieved after 120 hours under service temperature of 60°C. This will help in identifying the cross-linking time when there is not enough time for the TR-EPR insulation to cross-link when stored at room temperature.

Table 6.5: Cross-linking development of TR-EPR at 60°C heating

Number of hours exposed at 60°C	Hot Set Test_Time after break (seconds)
24	650
48	722
72	780
96	845
120	900 (no break)

6.8 Conclusion

This chapter discussed about the various tests performed by the author and third-party accredited laboratory in compliance with IEC 60092-350, IEC 60092-354, and AS/NZS 1429.1. The tests performed were PD test, bending test proceeded by PD test, tan delta measurement, heating cycle test proceeded by PD test, impulse withstand test proceeded by HV test, 5-minute HV test, and 4-hour HV test. The TR-EPR passed the sole PD test which showed values of partial discharge lower than the corresponding values required by both standards especially those obtained by the third-party accredited laboratory for $1.5U_o$, $1.73U_o$, and $2U_o$. Specifically, the author obtained partial discharge values below 4pC while those obtained from the third-party accredited laboratory were below 1pC which were all below 5pC. Similarly, the TR-EPR passed the bending test proceeded by PD test by having partial measurements below 1pC compared to IEC 60092-350 and IEC 60092-354 maximum of 5pC. The tan delta measurements performed on TR-EPR showed to be below those required for both conditions of voltage and temperature dependence, hence has been in compliance with both standards. The results of the heating cycle test proceeded by PD test on TR-EPR revealed a passing value of partial discharge measurements which were below 1pC compared to standard maximum requirement of 5pC. The TR-EPR also passed the

impulse withstand test by having no breakdown after the HV test performed afterwards for both standards. Lastly, the TR-EPR passed both the 5-minute (by the author) and 4-hour (by the third-party accredited laboratory) HV test by similarly experiencing no breakdown after being subjected to required voltage at power frequency. For the Hot set test, it was found that cross-linking of TR-EPR is achieved after 576 hours under ambient temperature and after 120 hours under 60°C service temperature.

CHAPTER 7 CALCULATION OF CURRENT CAPACITY OF FLEXIBLE ALUMINIUM CABLE

7.0 Introduction

The previous chapters were more particular to the insulation part of the underground cable. For Chapters 5 and 6, the discussion was focused on TR-EPR: more specifically the results of the tests performed on the insulation for the accelerated ageing, electrical, and non-electrical tests. In the light of providing a detailed analysis of economics between XLPE and TR-EPR insulation material, it becomes essential to allocate a discussion about the conductor part of the cable. This chapter presents a research study about cable ampacity calculation at 110°C in line with the issue of availability of ampacity values for Class 5 flexible Aluminium cable at maximum operating temperature. Sub-calculations including a.c. resistance, capacitance, and dielectric loss are explained; which will also be directly utilised for the economic analysis in the next chapter.

7.1 Review of conductors

As have been discussed in Chapter 2 by virtue of economics, the two most common choices for cable conductor material are Aluminium and Copper: but more specifically Class 2 stranded Aluminium and Copper. At room temperature (20°C), annealed copper has resistivity value of 17.24nΩ-m which is equivalent to 61.2% of that of Aluminium (28.03 nΩ-m). This translates to 1.6 times greater cross-sectional area for the Aluminium conductor to have the same resistance as the Copper conductor [104]. However, Aluminium becomes cost-effective since its density is less than one-third of Copper [105]. Conductors may be described pertinent to level of flexibility (solid, stranded, or flexible) and relevant to shape (circular, compacted, and sectioned) [37,106]. Considering low voltage rating, the stranded and flexible conductors are the common preferences. For Copper conductors, flexible types (classified as Class 5 or 6 depending on the wire count) are more usual owing to better tensile strength than Aluminium. Table 7.1 shows construction of Class 5 flexible Aluminium in LV application. There were also other related studies like those of Al-Khalidi et al. [107-108] regarding HTS cable that were conducted with the potential of improving power network reliability.

In determining the kind of cable to be used in a certain power installation, the operating temperature is taken into consideration in which 90°C rating is used in low voltage installation over long reaches while 110°C rating is utilised in high ampacity installation covering short range. For cable sizing, the parameters that are greatly considered include voltage drop, short-circuit temperature rating, and ampacity. In lieu of this, AS/NZS 3008.1.1 can be used as reference for the selection of cable based on temperature rating of the conductor and insulation [109]. Furthermore, the standard provides Copper and Aluminium cable ampacity values except at 110°C Aluminium cable which consequently limits the implementation of low-cost setup for cable

system at elevated temperature. Hence, the availability of ampacity values for Class 5 flexible Aluminium cable will allow electrical system designers to apply cost-effective but reliable cable system design. With regards to reliability, there is still an active issue concerning the connection of Aluminium conductor owing to greater thermal expansion than Copper. Regarding this issue, various research about Aluminium cable connection reliability were performed [110-116]. In line with the connection, thermal analysis of heat dissipation of the Class 5 flexible Aluminium cable was also conducted to determine appropriate connectors that can be utilised.

Table 7.1: Construction of Class 5 flexible Aluminium conductor (Class 2 conductor referenced for d.c. resistance)

Cross-Sectional Area (CSA) (mm ²)	Total Number of Wires	Diameter of Individual Wire (mm)	Maximum d.c. Resistance at 20 °C (Ω/km)
16	90	0.5	1.9100
25	133	0.5	1.2000
35	182	0.5	0.8680
50	231	0.5	0.6410
70	361	0.5	0.4430
95	494	0.5	0.3200
120	627	0.5	0.2530
150	760	0.5	0.2060
185	924	0.5	0.1640
240	1221	0.5	0.1250
300	1520	0.5	0.1000
400	2013	0.5	0.0778
500	1792	0.6	0.0605
630	2280	0.6	0.0469
800	2912	0.6	0.0367
1000	3640	0.6	0.0291

7.2 Review of thermal expansion

As current flows in the conductor, heat is produced which in turn raises the temperature of the material. The rise in temperature causes the conductor to experience elongation while decrease in temperature causes it to contract. This phenomenon of expansion and contraction of material

caused by temperature change is termed thermal expansion. Considering linear aspect for a certain length, the change in length experienced by a material has a direct proportional relationship with the change in temperature in which the constant of proportionality is labelled as coefficient of thermal expansion: a property [117] defined in (7.1):

$$\Delta\ell = \alpha \cdot \ell_0 \cdot \Delta T \quad (7.1)$$

where ℓ corresponds to the length, T refers to the temperature, and α is the coefficient of thermal expansion $(^\circ\text{C})^{-1}$ equivalent to $25 \times 10^{-6} (^\circ\text{C})^{-1}$ for Aluminium and $17 \times 10^{-6} (^\circ\text{C})^{-1}$ for Copper. It can be observed that the coefficient of thermal expansion of Aluminium is greater than that of Copper which indicate heightened sensitivity to temperature change. It should also be noted that it is important that the thermal expansion characteristics of materials involved in the termination are similar in ensuring connection reliability as the cable is subject to cycles of expansion and contraction (cyclic loading) throughout its operation. When the cable experiences stress relaxation, poor surface contact may occur resulting to higher resistance at the termination leading to overheating and eventual failure. Hence it is crucial to ensure that thermal expansion is minimum at the termination point by restricting the movement of connection as implemented in the thermomechanical design [9].

7.3 Cable ampacity calculation

For the calculation of ampacity ratings of Class 5 flexible Aluminium cable, two standards are referred: IEC 60287 and AS/NZS 3008.1.1 (clause 4.4). For IEC 60287, the calculation takes into account numerous considerations including conductor construction, insulation thermal resistivity, and configuration with respect to surroundings (e.g., trefoil formation). For AS/NZS 3008.1.1, the calculation is directly performed with known values of the initial rated ampacities.

7.3.1 Conductor resistance calculation [118]

The resistance of the conductor varies depending on the nature of current flowing which may either be direct (d.c.) or alternating (a.c.). The a.c. resistance of the conductor is larger than the d.c. resistance due to skin and proximity effect. The formulae for the d.c. and a.c. resistance of conductor are shown as follows respectively:

$$R = R' \cdot (1 + \gamma_s + \gamma_p) \quad (7.2)$$

$$R' = R_0 [1 + \alpha_{20} \cdot (\theta - 20)] \quad (7.3)$$

where R' refers to the conductor d.c. resistance at maximum operating temperature in Ω/m , R_0 pertains to the conductor d.c. resistance at 20°C in Ω/m , α_{20} corresponds to the constant mass temperature coefficient in $(^\circ\text{C})^{-1}$, θ pertains to the maximum operating temperature in $^\circ\text{C}$, R corresponds to the conductor a.c. resistance at maximum operating temperature in Ω/m , γ_s refers to skin effect factor, and γ_p corresponds to proximity effect factor. These equations will also be applied in the economic analysis of the cable in chapter 8. Applying these formulas, the d.c. and a.c. resistances of the conductor for various cross-sectional areas and maximum operating temperatures are calculated and summarised in Table 7.2 and Table 7.3.

Table 7.2: Calculated conductor d.c. resistance

CSA (mm ²)	d.c. Resistance (Ω/km)									
	20°C	25°C	40°C	50°C	60°C	70°C	80°C	90°C	100°C	110°C
16	1.910	1.948	2.064	2.141	2.218	2.295	2.372	2.449	2.526	2.603
25	1.200	1.224	1.297	1.345	1.393	1.442	1.490	1.539	1.587	1.635
35	0.868	0.885	0.938	0.973	1.008	1.043	1.078	1.113	1.148	1.183
50	0.641	0.654	0.693	0.718	0.744	0.770	0.796	0.822	0.848	0.873
70	0.443	0.452	0.479	0.497	0.514	0.532	0.550	0.568	0.586	0.604
95	0.320	0.326	0.346	0.359	0.372	0.384	0.397	0.410	0.423	0.436
120	0.253	0.258	0.273	0.284	0.294	0.304	0.314	0.324	0.335	0.345
150	0.206	0.210	0.223	0.231	0.239	0.248	0.256	0.264	0.272	0.281
185	0.164	0.167	0.177	0.184	0.190	0.197	0.204	0.210	0.217	0.223
240	0.125	0.128	0.135	0.140	0.145	0.150	0.155	0.160	0.165	0.170
300	0.100	0.102	0.108	0.112	0.116	0.120	0.124	0.128	0.132	0.136
400	0.078	0.079	0.084	0.087	0.090	0.093	0.097	0.100	0.103	0.106
500	0.061	0.062	0.065	0.068	0.070	0.073	0.075	0.078	0.080	0.082
630	0.047	0.048	0.051	0.053	0.054	0.056	0.058	0.060	0.062	0.064
800	0.037	0.037	0.040	0.041	0.043	0.044	0.046	0.047	0.049	0.050

Table 7.3: Calculated conductor a.c. resistance

CSA (mm ²)	a.c. Resistance (Ω/km)									
	20°C	25°C	40°C	50°C	60°C	70°C	80°C	90°C	100°C	110°C
16	1.910	1.949	2.064	2.141	2.218	2.295	2.372	2.449	2.526	2.603
25	1.200	1.224	1.297	1.345	1.394	1.442	1.490	1.539	1.587	1.635
35	0.868	0.886	0.938	0.973	1.008	1.043	1.078	1.113	1.148	1.183
50	0.641	0.654	0.693	0.719	0.745	0.770	0.796	0.822	0.848	0.874
70	0.444	0.453	0.479	0.497	0.515	0.533	0.551	0.568	0.586	0.604
95	0.321	0.327	0.347	0.359	0.372	0.385	0.398	0.411	0.424	0.437
120	0.254	0.259	0.274	0.285	0.295	0.305	0.315	0.325	0.335	0.346
150	0.207	0.212	0.224	0.232	0.240	0.249	0.257	0.265	0.273	0.282
185	0.166	0.169	0.179	0.185	0.192	0.199	0.205	0.212	0.218	0.225
240	0.127	0.130	0.137	0.142	0.147	0.152	0.157	0.162	0.167	0.172
300	0.103	0.105	0.111	0.115	0.119	0.123	0.127	0.131	0.134	0.138
400	0.082	0.083	0.088	0.091	0.094	0.097	0.100	0.103	0.106	0.109
500	0.065	0.066	0.070	0.072	0.074	0.077	0.079	0.081	0.084	0.086
630	0.053	0.054	0.056	0.058	0.060	0.062	0.063	0.065	0.067	0.069
800	0.044	0.045	0.047	0.048	0.049	0.050	0.052	0.053	0.054	0.056

7.3.2 Dielectric loss calculation [118]

In chapter 1, the dielectric loss was already introduced which represents the amount of heat loss in the insulation material and calculated using (1.1). In this equation, the capacitance can be calculated using the following equation:

$$C = \frac{\varepsilon}{18 \ln\left(\frac{D_i}{d_c}\right)} \cdot 10^{-9} \text{ (F/m)} \quad (7.4)$$

where ε corresponds to relative of insulation in F/m (3.0 F/m for X-HF-110), D_i depicts the external insulation diameter in mm, and d_c refers to the conductor diameter in mm. These formulas will also be utilised in the next chapter which is about cable economics. By applying these formulas, the dielectric loss of cable for different cross-sectional areas are obtained and are summarised in Table 7.4.

Table 7.4 : Calculated dielectric loss

CSA (mm ²)	W _d (W/m)
16	0.00025
25	0.00027
35	0.00031
50	0.00035
70	0.00036
95	0.00042
120	0.00043
150	0.00041
185	0.00040
240	0.00042
300	0.00045
400	0.00046
500	0.00049
630	0.00050
800	0.00056

7.3.3 Thermal resistances calculation [119]

There are various thermal resistances considered in the calculation of cable ampacity. First is the thermal resistance between the conductor and sheath (T_1) which can be calculated by conductive heat transfer in hollow cylinder as shown in the following:

$$T_1 = \frac{\rho_T}{2\pi} \cdot \ln \left[1 + \frac{2t_1}{d_c} \right] \quad (7.5)$$

where ρ_T pertains to the thermal resistivity of insulation (X-HF-110 in this case) in K·m/W, t_1 corresponds to the insulation thickness between the conductor and sheath in mm, and d_c refers to the diameter of conductor in mm. The next ones are the thermal resistance between the sheath and armour (T_2) and thermal resistance of the outer covering (T_3) which are both neglected since the cable samples under consideration are low voltage Single-Core Double-Insulated (SDI) having no metallic coverings. The last one is the external thermal resistance (T_4) which takes into account the thermal effects caused by the surroundings and is calculated using the empirical formula

$$T_4 = \frac{1}{\pi D_e \cdot h \cdot (\Delta\theta_s)^{1/4}} \quad (7.6)$$

where D_e^* pertains to the external diameter of cable in m, h corresponds to the heat dissipation coefficient in $W/m^2-K^{5/4}$, and $\Delta\theta_s$ indicates the temperature difference between the cable and the surroundings in K. The heat dissipation coefficient is calculated using the formula that is also empirical in nature as follows:

$$h = \frac{Z}{(D_e^*)^g} + E \quad (7.7)$$

where Z , E , and g correspond to constants determined depending on configuration of installation.

By applying these equations, the thermal resistance values are obtained which are summarised in Table 7.5.

Table 7.5: Calculated Thermal resistances (T_1 and T_4)

CSA mm ²	T_1	D_e m	Z	E	g	h	KA n=3	T_4 in Air
16	0.3851	0.0099	0.96	1.25	0.2	3.664	0.0441	6.112
25	0.3913	0.0120	0.96	1.25	0.2	3.573	0.0176	5.172
35	0.3437	0.0133	0.96	1.25	0.2	3.526	0.0169	4.731
50	0.2978	0.0156	0.96	1.25	0.2	3.455	0.0169	4.118
70	0.2835	0.0176	0.96	1.25	0.2	3.402	0.0178	3.707
95	0.2578	0.0198	0.96	1.25	0.2	3.352	0.0180	3.345
120	0.2477	0.0221	0.96	1.25	0.2	3.309	0.0189	3.051
150	0.2418	0.0241	0.96	1.25	0.2	3.273	0.0199	2.827
185	0.2347	0.0271	0.96	1.25	0.2	3.226	0.0215	2.550
240	0.2271	0.0295	0.96	1.25	0.2	3.193	0.0224	2.366
300	0.2107	0.0332	0.96	1.25	0.2	3.147	0.0230	2.132
400	0.2051	0.0376	0.96	1.25	0.2	3.101	0.0250	1.911
500	0.1903	0.0430	0.96	1.25	0.2	3.051	0.0261	1.697
630	0.1858	0.0478	0.96	1.25	0.2	3.014	0.0280	1.546
800	0.1848	0.0535	0.96	1.25	0.2	2.974	0.0308	1.399

7.3.4 Cable ampacity calculations [109,118]

For the cable ampacity, two standards can be referred: IEC and AS/NZS. By considering two standards, the ampacity values are further verified for validity of installation in air at 110°C including safety. As per IEC 60287, the following explicit formula is used:

$$I = \left[\frac{\Delta\theta - W_d [0.5T_1 + n \cdot (T_2 + T_3 + T_4)]}{R \cdot T_1 + n \cdot R \cdot (1 + \lambda_1) \cdot T_2 + n \cdot R \cdot (1 + \lambda_1 + \lambda_2) \cdot (T_3 + T_4)} \right]^{0.5} \quad (7.8)$$

where I pertains to the cable ampacity in A, n refers to conductors carrying load, λ_1 corresponds to ratio of metal sheath losses to total losses, and λ_2 indicates ratio of armouring losses to total losses. On the other hand, as per AS/NZS 3008.1.1, cable ampacity can be calculated using the following equation:

$$\left(\frac{I_0}{I_R} \right)^2 = \frac{\theta_0 - \theta_A}{\theta_R - \theta_A} \quad (7.9)$$

where I_0 corresponds to the operating current in A, I_R denotes to the rated current in A, θ_0 refers to the cable operating temperature at current I_0 in °C, θ_A pertains to the temperature of ambient air or soil in °C, and θ_R indicates the cable operating temperature of cable at current I_R in °C. The ampacity values calculated based on the two standards are summarised in Table 7.6.

Table 7.6: Calculated Ampacities at 110°C based on IEC 60287 and AS/NZS 3008.1.1

CSA mm ²	IEC 60287 Amps	AS/NZS 3008.1.1 Amps	Difference %
16	84	84	0
25	115	115	0
35	141	141	0
50	176	173	2.0
70	223	220	1.4
95	276	275	0.6
120	325	321	1.3
150	374	370	0.9
185	440	432	1.9
240	522	518	0.7
300	613	601	1.9
400	729	709	2.8
500	869	832	4.3
630	1020	975	4.4

7.4 Heat dissipation test

In order to verify the calculated ampacities at 110°C, a heat dissipation test was conducted using an automatic Induction Cable Heating System which is capable of providing prolonged heating of power cables (Copper and Aluminium) and corresponding cable connectors with load current of up to 6000A. The heating system includes a Cable Cycle Heating Test Unit (6000A), Pico Technology 8 Channels Thermocouple Data Loggers (including software component), 8 units of Type K Thermocouple assembly, current transformer (with sensor), Fluke 435 Power Analyzer, d.c. resistance metre, and Windows computer. The configuration of the test system is shown in

Figure 7.1

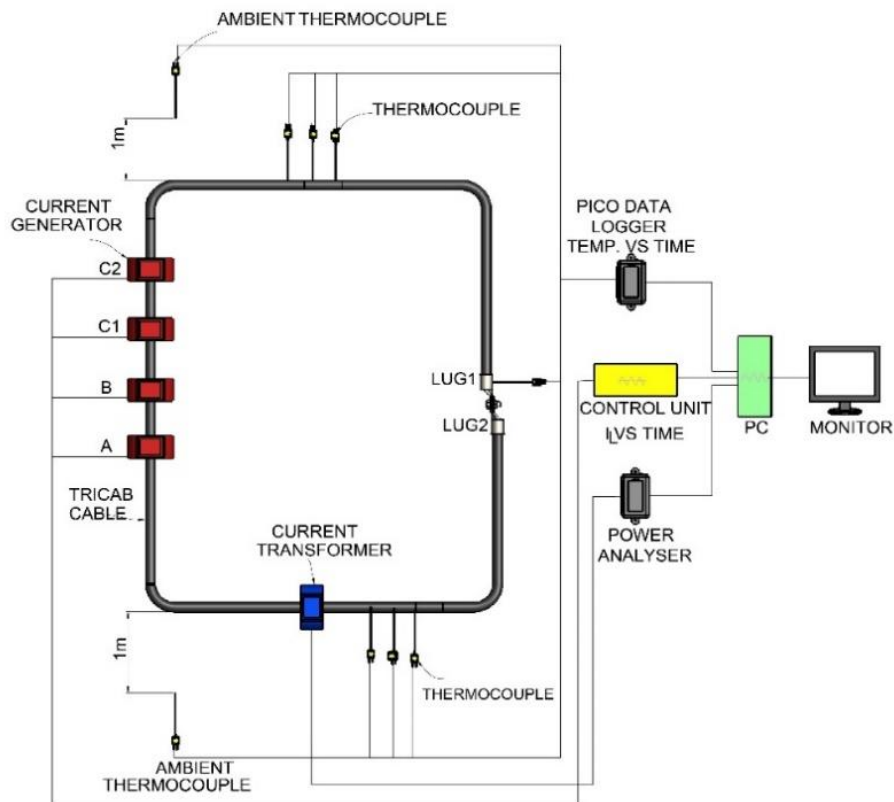


Figure 7.1: Schematic diagram of heat dissipation test system

The 12-metre cables used comprise of X-HF-110 insulation and PVC sheath. Three cables in parallel and trefoil formation were assembled with mechanical shear bolt connectors joined in series. 450mm cable ladder tray was used to hold the cables 650mm above ground with the aim of simulating installation condition of three cables in trefoil formation in free air. The cables were also looped and passed in a 6000/0.1 A current transformer. The mechanical shear bolts connectors allow termination of the cable in which they were sheared via torque wrench. Prior being inserted onto the connector, the conductors were first cleaned and polished with the use of steel wire brush. To avoid ingress of moisture within the contact point, conductive grease was applied between the conductor and inner connector barrel. To secure enough contact point, the palm of two mechanical connectors were attached with a bolt. The leads of the thermocouple were placed to the following parts: cable conductor, cable insulation, cable sheath, and mechanical connector body. To measure the ambient temperature, the other lead of the thermocouple was attached to a 1 metre conductor that was placed 1 metre from the unit being tested. Before the application of current, a d.c. resistance metre was used to measure the resistance of connections. The current generator from the heat dissipation test system was used to apply current which was tuned in line with the temperature of the surroundings inside the testing facility. As shown in Figure 7.2, Fluke 435 Power Analyser was used to verify the measure of induced currents supplied by the current generators.

The Thermocouple Data Logger records the measurement of temperature increases by the thermocouple leads. As per requirement, thermal equilibrium is established when the temperature reaches almost constant value indicated by not more than 1K/h of temperature change [120].



Figure 7.2: Measuring of test current using Fluke 435 Power Analyser

7.5 Results of heat dissipation test

With the application of current in the conductor, some power losses occur in the form of heat called conductor loss [121] which can be expressed as follows:

$$P_c = I^2 \cdot R \quad (7.10)$$

where P_c corresponds to the conductor loss in W, I refers to the current flowing to the conductor in A, and R pertains to the conductor d.c. resistance of in Ω/km . This phenomenon introduces temperature rise in the conductor which the thermocouple measures. In line with the ambient temperature rise, the current source was being tuned which eventually becomes complete when

$\pm 2^{\circ}\text{C}$ temperature stabilisation of the conductor and connection occurs for 15 minutes was attained [122]. The results of the average temperature of conductor are presented in Table 7.7. It can be observed that all measurements of conductor temperature are all below the 110°C maximum operating temperature rating with respect to the ampacity rating.

Table 7.7: Current and temperature measurements at calculated Ampacity rating

CSA	Ambient Temperature during testing	Rated Current at Ambient Temperature	Measured Current	Conductor Temperature at Equilibrium
mm^2	$^{\circ}\text{C}$	A	A	$^{\circ}\text{C}$
50	19	195	197	104
70	22	249	250	105
95	23	311	311	106
120	20	363	367	107
150	24	407	414	105
185	23	475	475	106
240	24	577	577	109
300	31	643	643	109
400	24	759	760	105
500	25	915	915	105
630	26	1073	1077	108

In the case of the terminations, the thermocouples provided temperature readings of connection points ranging from 62 to 72°C upon application of current in the conductor equivalent to the ampacity rating. This showed that the temperature of the mechanical bolt shear connectors was about 39°C lower compared to the conductors for all samples of cable. The highest temperature (72°C) measured on the connector occurred on the 240mm^2 and 630mm^2 conductor cross-sectional areas while low readings were taken for conductors ranging from 50mm^2 to 120mm^2 . The lower temperature of termination point is evident on the larger connector-to-conductor cross-sectional area ratio as shown in

Table 7.8.

As have been discussed, heat due to conductor losses is dissipated towards the conductor surrounding including the insulation, sheath, and metallic covers which in turn increases the ambient temperature and consequently affecting the cable ampacity rating reflected in the derating factor applied [123]. The profiles of the heat dissipation for the layers of the conductor as recorded by the Thermocouple Data Logger are presented in Figure 7.3. The complete data from data logger are presented in Appendix B. Results showed that the temperature readings of the insulation, sheath, and lug for all cross-sectional areas are all less than 90°C hence do not exceed the maximum operating temperature of PVC [123].

Table 7.8: Conductor-to-connector cross-sectional area ratio

Conductor Cross-Sectional Area	Connector Barrel Cross-Sectional Area	CSA Ratio
mm ²	mm ²	
50	324	6
70	419	6
95	419	4
120	541	5
150	541	4
185	575	3
240	575	2
300	1000	3
400	1000	3
500	1391	3
630	1656	3

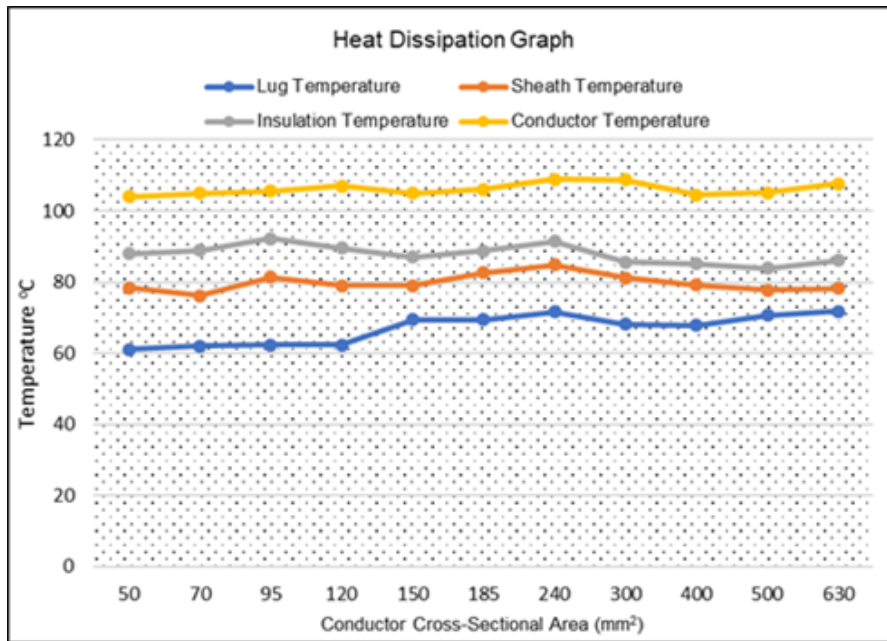


Figure 7.3: Graph of heat dissipated to termination, conductor, insulation, and sheath

7.6 Conclusion

This chapter focused with the discussion about the conductor part of the cable and the calculation of ampacity rating. There was also the reintroduction of concepts like d.c. resistance, a.c. resistance, and dielectric loss which were identified to be directly involved in the economic analysis as well in Chapter 8. Results support the applicability of (7.9) for ampacity calculations at 110°C maximum operating temperature. The simulated ampacity values as per AS/NZS 3008.1.1 compared to those calculated as per IEC 60287 showed acceptably small discrepancy of 5% most of which falling below 2% as seen in Table 7.6. The heat dissipation test results also support the applicability of mechanical shear bolts connector for the termination of Class 5 flexible Aluminium conductor attributed to the acceptable low joint temperature hence minimum expansion that is essential for ensuring the reliability of connection.

CHAPTER 8 ECONOMICS IN USING TR-EPR UNDERGROUND CABLE

8.0 Introduction

Recalling from the previous chapters, the discussion focused in providing information regarding two insulation materials: XLPE and TR-EPR. The former was primarily based on literature while the latter was based on both literature (based on EPR) and tests conducted. After having investigated the material characteristics and properties of the dielectric materials, it is suitable to perform economic analysis to quantify their cost-effectiveness. Prior to doing so, it is important to declare the working parameters.

The comparison of the XLPE and TR-EPR insulated cables is performed by evaluating their Equivalent Uniform Annual Cost (EUAC) using the present worth method in which their costs per unit length pertinent to their service life will be evaluated to their present value considering a discount rate. Aside from the insulation, the evaluation of the present worth is to be carried out on the basis of 22kV and 66kV design.

8.1 Cable life cycle costs

Based from [105], in lieu with the life cycle cost analysis (LCCA) of cable, the costs can be divided into four categories: initial cost, operation cost, failure cost, and discard cost. The initial costs include the cost of cable, accessories, and design and installation. The operation costs include the cost of inspection, maintenance, conductor losses, dielectric losses, and recondition. The failure costs include cost of repair, replacement, and energy not served. The discard costs include removal cost and treatment cost value with additional consideration for salvage value pertinent to the conductor material i.e., Aluminium.

8.1.1 Initial costs

Under initial costs, the cost of cable (${}_iC_c$ in AUD/km) greatly considers insulation and conductor material. The accessories and design and installation costs are represented by ${}_iC_a$ and ${}_iC_{d-i}$ respectively both in AUD/km. It should be noted that no multiplier for discount rate is used since all costs under initial costs are already expressed in present worth.

The present worth of the total initial cost ${}_iC$ in AUD/km is calculated as

$${}_iC = {}_iC_c + {}_iC_a + {}_iC_{d-i} \quad (8.1)$$

8.1.2 Operation costs

Under operation costs, the present worth of the inspection, maintenance, and recondition costs (${}_oC_i$, ${}_oC_m$, and ${}_oC_{rc}$ respectively all in AUD/km) are calculated respectively by uniform cost assumption applying annuity formula as follows [124]:

$${}_oC_i = {}_oC_{i/p} \cdot \frac{1 - (1 + i)^{-m \cdot L}}{i} \quad (8.2)$$

$${}_oC_m = {}_oC_{m/p} \cdot \frac{1 - (1 + i)^{-m \cdot L}}{i} \quad (8.3)$$

$${}_oC_{rc} = {}_oC_{rc/p} \cdot \frac{1 - (1 + i)^{-m \cdot L}}{i} \quad (8.4)$$

where ${}_oC_{i/p}$ refers to the cost of inspection per inspection period in AUD/km, ${}_oC_{m/p}$ refers to the cost of maintenance per maintenance period in AUD/km, ${}_oC_{rc/p}$ refers to the cost of recondition per recondition period in AUD/km, m is the number of inspection/maintenance/recondition times per year, L is the cable service life, and i is the discount rate calculated as

$$i = (1 + i_e)^{\frac{1}{m}} - 1 \quad (8.5)$$

where i_e pertains to the effective discount rate. It should be noted that for the sake of simplicity, m and i are not given any scripts for distinction, hence may depict different values corresponding to the cost under consideration.

For the present worth of the cost due to conductor loss (${}_oC_{cl}$ in AUD/km), the following formula is used [9,105,124]:

$${}_oC_{cl} = 9I_{max}^2 \cdot R_{a.c.} \cdot t \cdot LF \cdot C_E \cdot 10^{-3} \cdot \frac{1 - (1 + i_e)^{-L}}{i_e} \quad (8.6)$$

where I_{max} corresponds to the maximum current rating or ampacity in A, $R_{a.c.}$ refers to the a.c. resistance in Ω /km, t depicts annual operating time in hours/yr, LF pertains to load factor (ratio of average load to peak load), and C_E corresponds to energy cost in AUD/kWh.

For the present worth of the cost due to dielectric loss (${}_oC_{dl}$ in AUD/km), the following formula is used [9,105,124]:

$${}_oC_{dl} = 18\pi \cdot f \cdot C \cdot U_o^2 \cdot \tan\delta \cdot t \cdot LF \cdot C_E \cdot \frac{1 - (1 + i_e)^{-L}}{i_e} \quad (8.7)$$

where f is the frequency in Hz, C refers to the capacitance per unit length calculated using (7.4) in F/m, U_o corresponds to the phase to earth voltage in V, and $\tan\delta$ is equivalent to the dielectric

dissipation factor. Note that (8.6) and (8.7) are both multiplied to 9 which correspond to the three runs and three phase assumption. The present worth of the total operation costs (${}_oC$ in AUD/km) can be calculated as follows:

$${}_oC = {}_oC_i + {}_oC_m + {}_oC_{rc} + {}_oC_{cl} + {}_oC_{dl} \quad (8.8)$$

8.1.3 Failure costs

For the present worth of the cost of repair and replacement (${}_fC_{rpr}$ and ${}_fC_{rpl}$ respectively), a different treatment is considered. Consider the failure rate (f_{rate}) value of 0.1 failure/100 km-yr or equivalent to 0.001 f/km-yr. This indicates that for a cable length $l = 1 \text{ km}$, failures occur only once every 1000 years which is beyond the service life of cable causing inconvenient treatment in the economic analysis. However, if we consider $l = 100 \text{ km}$, this would result to 0.1f/yr which is equivalent to one failure every 10 years. Considering cable service life $L = 45 \text{ years}$, then the number of failures f_{number} throughout the cable service life can be calculated using the equation:

$$f_{number} = \lfloor f_{rate} \cdot l \cdot L \rfloor \quad (8.9)$$

Applying this formula, number of failures can then be calculated as $f_{number} = \lfloor 0.001 \cdot 100 \cdot 45 \rfloor = \lfloor 4.5 \rfloor = 4$. Note that the formula uses the floor function “ $\lfloor \]$ ” which forces the value calculated to be rounded down to the nearest lower integer since the number of failures should be expressed as a whole number but pertinent only within the cable service life. The obtained number of failures $f_{number} = 4$ corresponds to the failures for the 10th, 20th, 30th, and 40th years of cable service. Thus, for a certain $l \text{ km}$ length of cable, the present worth of the repair cost can be calculated by uniform cost assumption and applying annuity formula as

$${}_fC_{rpr} \text{ for } l \text{ km} = {}_fC_{rpr/p} \cdot \frac{1 - (1+i)^{-\frac{f_{number}}{f_{rate} \cdot l}}}{(1+i)^{\frac{1}{f_{rate} \cdot l}} - 1} \quad (8.10)$$

$${}_f C_{rpr} \text{ for } l \text{ km} = {}_f C_{rpr/p} \cdot \frac{1 - (1+i)^{-\frac{lf_{rate} \cdot l \cdot L}{f_{rate} \cdot l}}}{\frac{1}{(1+i)^{f_{rate} \cdot l} - 1}} \quad (8.11)$$

where ${}_f C_{rpr/p}$ corresponds to the repair cost per repair period [124]. Considering per unit length basis (per km), the present worth of the repair cost per unit length can be expressed as

$${}_f C_{rpr} = {}_f C_{rpr/p} \cdot \frac{1 - (1+i)^{-\frac{lf_{rate} \cdot l \cdot L}{f_{rate} \cdot l}}}{l \cdot \left[\frac{1}{(1+i)^{f_{rate} \cdot l} - 1} \right]} \quad (8.12)$$

The minimum value of the present worth of the repair cost per unit length can be obtained by evaluating the equation to $l \rightarrow 0$ while the maximum value is obtained when the equation is evaluated to $l \rightarrow \infty$. Prior to this, it should be observed that $[f_{rate} \cdot l \cdot L] = 0$ when $0 < f_{rate} \cdot l \cdot L < 1$ or $0 < l < \frac{1}{f_{rate} \cdot L}$. Considering this range, the value of (8.12) can be evaluated to

$$({}_f C_{rpr})_{0 < l < \frac{1}{f_{rate} \cdot L}} = {}_f C_{rpr/p} \cdot \frac{1 - (1+i)^{-\frac{0}{f_{rate} \cdot l}}}{l \cdot \left[\frac{1}{(1+i)^{f_{rate} \cdot l} - 1} \right]} = 0 \quad (8.13)$$

Hence, the minimum value of the present worth of the repair cost per unit length can be evaluated as

$$({}_f C_{rpr})_{min} = \lim_{l \rightarrow 0^+} {}_f C_{rpr/p} \cdot \frac{1 - (1+i)^{-\frac{lf_{rate} \cdot l \cdot L}{f_{rate} \cdot l}}}{l \cdot \left[\frac{1}{(1+i)^{f_{rate} \cdot l} - 1} \right]} = 0 \quad (8.14)$$

For the maximum value, it should be noted that for high values of l , $[f_{rate} \cdot l \cdot L] \approx f_{rate} \cdot l \cdot L$, hence $\lim_{l \rightarrow \infty} \frac{lf_{rate} \cdot l \cdot L}{f_{rate} \cdot l} = L$. The maximum value of the present worth of the repair cost per unit length can be obtained as follows:

$$({}_f C_{rpr})_{max} = \lim_{l \rightarrow \infty} {}_f C_{rpr/p} \cdot \frac{1 - (1+i)^{-\frac{l \cdot f_{rate} \cdot L}{f_{rate} \cdot l}}}{l \cdot \left[(1+i)^{\frac{1}{f_{rate} \cdot l}} - 1 \right]} \quad (8.15)$$

$$({}_f C_{rpr})_{max} = \lim_{l \rightarrow \infty} {}_f C_{rpr/p} \cdot \left[1 - (1+i)^{-\frac{l \cdot f_{rate} \cdot L}{f_{rate} \cdot l}} \right] \cdot \lim_{l \rightarrow \infty} \frac{1}{l \cdot \left[(1+i)^{\frac{1}{f_{rate} \cdot l}} - 1 \right]} \quad (8.16)$$

$$({}_f C_{rpr})_{max} = {}_f C_{rpr/p} \cdot [1 - (1+i)^{-L}] \cdot \lim_{l \rightarrow \infty} \frac{1}{l \cdot \left[(1+i)^{\frac{1}{f_{rate} \cdot l}} - 1 \right]} \quad (8.17)$$

$$({}_f C_{rpr})_{max} = {}_f C_{rpr/p} \cdot [1 - (1+i)^{-L}] \cdot \lim_{l \rightarrow \infty} \frac{\frac{1}{l}}{\left[(1+i)^{\frac{1}{f_{rate} \cdot l}} - 1 \right]} = \frac{0}{0} \quad (8.18)$$

Since the equation evaluates to indeterminate form, L'Hôpital's rule can be applied as follows:

$$({}_f C_{rpr})_{max} = {}_f C_{rpr/p} \cdot [1 - (1+i)^{-L}] \cdot \lim_{l \rightarrow \infty} \frac{\frac{d}{dl} \left(\frac{1}{l} \right)}{\frac{d}{dl} \left[e^{\frac{\ln(1+i)}{f_{rate} \cdot l}} - 1 \right]} \quad (8.19)$$

$$({}_f C_{rpr})_{max} = {}_f C_{rpr/p} \cdot [1 - (1+i)^{-L}] \cdot \lim_{l \rightarrow \infty} \frac{-\frac{1}{l^2}}{\left[-\frac{\ln(1+i)}{f_{rate} \cdot l^2} \right] \cdot e^{\frac{\ln(1+i)}{f_{rate} \cdot l}}} \quad (8.20)$$

$$({}_f C_{rpr})_{max} = {}_f C_{rpr/p} \cdot [1 - (1+i)^{-L}] \cdot \lim_{l \rightarrow \infty} \frac{1}{\left[\frac{\ln(1+i)}{f_{rate}} \right] \cdot e^{\frac{\ln(1+i)}{f_{rate} \cdot l}}} \quad (8.21)$$

$$({}_f C_{rpr})_{max} = {}_f C_{rpr/p} \cdot [1 - (1+i)^{-L}] \cdot \frac{1}{\left[\frac{\ln(1+i)}{f_{rate}} \right] \cdot e^{\frac{\ln(1+i)}{f_{rate} \cdot \infty}}} \quad (8.22)$$

$$({}_f C_{rpr})_{max} = {}_f C_{rpr/p} \cdot \frac{f_{rate} \cdot [1 - (1+i)^{-L}]}{\ln(1+i)} = {}_f C_{rpr} \quad (8.23)$$

where ${}_f C_{rpr/p}$ refers to the cost of repair per repair period in AUD/km.

In the case of replacement cost, it would be based on the initial cost of a cable segment. Metzinger [125] defined a cable segment to be around 140m to 150m in which the latter will be used as

reference i.e. 0.15km, hence similar to the repair cost, the present worth of the replacement cost per unit length would be

$${}_fC_{rpl} = 0.15 \cdot {}_iC \cdot \frac{r_{rate} \cdot [1 - (1 + i)^{-L}]}{\ln(1 + i)} \quad (8.24)$$

where r_{rate} corresponds to the replacement rate in times/km-yr. According to Burke [126], replacement is usually performed after 2 to 3 failures. Using the latter figure, this translates to $r_{rate} = \frac{f_{rate}}{3}$, hence (8.24) may be alternatively expressed as

$${}_fC_{rpl} = 0.05 \cdot {}_iC \cdot \frac{f_{rate} \cdot [1 - (1 + i)^{-L}]}{\ln(1 + i)} \quad (8.25)$$

The present worth of the cost of energy not supplied (${}_fC_{ens}$ in AUD/km) can be expressed as

$${}_fC_{ens} = \frac{450S \cdot SAIDI \cdot C_E}{3} \cdot \frac{1 - (1 + i_e)^{-L}}{i_e} \quad (8.26)$$

where S pertains to the apparent power in MVA and $SAIDI$ refers to the System Average Interruption Duration Index expressed in min/yr [124]. Note that (8.26) is multiplied by 9 which corresponds to the three runs and three phase assumption.

The present worth of the total failure costs ${}_fC$ in AUD/km can then be calculated as

$${}_fC = {}_fC_{rpr} + {}_fC_{rpl} + {}_fC_{ens} \quad (8.27)$$

8.1.4 Discard costs

Under discard cost, the present worth of the removal cost and treatment cost (${}_dC_r$ and ${}_dC_t$ respectively in AUD/km) are calculated as follows [124]:

$${}_dC_r = {}_dC_{r/l} \cdot (1 + i_e)^{-L} \quad (8.28)$$

$${}_dC_t = {}_dC_{t/l} \cdot (1 + i_e)^{-L} \quad (8.29)$$

where ${}_dC_{r/l}$ refers to the cost of removal per unit length in AUD/km and ${}_dC_{t/l}$ pertains to the cost of treatment per unit length in AUD/km.

On the other hand, the present worth of the salvage value (${}_dS$ in AUD/km) was obtained through the following equation [124]:

$${}_dC_s = -RP_{Al} \cdot W_{c/l} \cdot (1 + i_e)^{-L} \quad (8.30)$$

where RP_c refers to the recycling price of Aluminium in AUD/tonne and $W_{c/l}$ pertains to the weight of conductor per unit length in tonne/km.

The present worth of the total discard costs (${}_dC$ in AUD/km) can then be calculated as follows:

$${}_dC = {}_dC_r + {}_dC_t - {}_dS \quad (8.31)$$

8.1.5 Net present value and equivalent uniform annual cost

The Net Present Value (NPV in AUD/km) is then calculated as

$$NPV = {}_iC + {}_oC + {}_fC + {}_dC \quad (8.32)$$

Finally, the Equivalent Uniform Annual Cost (EUAC in AUD/km) is obtained as follows [124]:

$$EAUC = NPV \cdot \frac{i_e}{1 - (1 + i_e)^{-L}} \quad (8.33)$$

8.2 LCCA parameters

8.2.1 General parameters

The cable under consideration is 3 x 1c630mm² Aluminium cable in trefoil duct for three runs. From Deans [127], based on the report *Building Up and Moving Out*, the discount rate recommended by the House of Representatives Standing Committee on Infrastructure, Transport

and Cities is 4%. The apparent power $S = 25 \text{ MVA}$ along with the 22kV and 66kV voltage ratings are based on Jutrisa [128] involving the Gheringhap zone substation project in Victoria, Australia as example for calculation and analysis. The energy cost C_E is based on Baran [129]. The system average interruption duration index (*SAIDI*) is based on figures by Citipower [130] which is 16.83 min/yr (9.13 min/year for unplanned *SAIDI* and 7.7 min/yr for the planned *SAIDI*) pertinent to greater Central Business District (CBD). The recycling price of Aluminium RP_{Al} is based on Yi et al. [105] adjusted to their present value by considering the discount rate value used in their study. The parameters including frequency f , annual operation time t , load factor LF , and weight per unit length of Aluminium conductor $W_{c/l}$ are determined by the author. A summary of general LCCA parameters is presented in Table 8.1.

Table 8.1: General LCCA parameters

	Unit	Value
i_c		0.04
S	MVA	25
f	Hz	50
t	h/yr	8760
LF		1
C_E	AUD/kWh	0.2291
<i>SAIDI</i>	min/yr	16.83
RP_{Al}	AUD/t	21,726.00
$W_{c/l}$	t/km	1.785

8.2.2 Insulation and U_0 parameters

Based from various literatures including Takahashi et al. [131-132] and Sami, Gholami, and Shahrtash [133], the designed life of XLPE power cables is about 30 years. The $\tan\delta$ or dielectric dissipation factor of XLPE is based on [9] while that of TR-EPR is based on the results of $\tan\delta$ measurement presented in Chapter 6. The dielectric constant of XLPE is based on [9] while that of TR-EPR is taken from the measurement on the TR-EPR sample. From Hampton [134], the

failure rate of XLPE in MV application ranges from 0 to 0.3 f/100 km-yr. Based on Deschamps [135], the failure rates of 20kV and 30kV XLPE insulated cables are 0.13 f/100 km-yr and 0.84 f/100 km-yr respectively. From the given figures, the conservative value of 0.003 f/km-yr is chosen. In the case of EPR, it was already mentioned in Chapter 2 that the failure rate is 0.001 f/km-yr based on Cox et al. [23]. A summary of insulation and U_0 parameters is presented in Table 8.2.

Table 8.2:: Insulation and U_0 parameters

	Unit	Value
XLPE		
L	yr	30
DDF		0.004
ϵ		2.5
f_{rate}	failure/km-yr	0.003
TR-EPR		
L	yr	45
DDF		0.0003284
ϵ		2.3
f_{rate}	failure/km-yr	0.001
22 kV		
U_o	V	12700
I_{max}	A	219
D_c	mm	29.2
D_i	mm	42.7
R_{ac}	Ω/km	0.05281
66 kV		
U_o	V	38000
I_{max}	A	73
D_c	mm	29.9
D_i	mm	61.3
R_{ac}	Ω/km	0.05043

8.2.3 Initial cost parameters

The cost of accessories ${}_iC_a$ and cost of design and installation ${}_iC_{d-i}$ are based on Yi et al. [105] adjusted to their present value by considering the discount rate value used in their study. The cost of cable ${}_iC_c$ is also based on present cost.

8.2.4 Operation cost parameters

The cost of inspection per period ${}_oC_i$, cost of maintenance per period ${}_oC_m$, and cost of recondition per period ${}_oC_{rc}$ are obtained from Yi et al. [105] adjusted to their present value by considering the discount rate value used in their study.

8.2.5 Failure cost parameters

The cost of repair ${}_fC_{rpr/p}$ per period is based on Yi et al. [105] adjusted to its present value by considering the discount rate value used in their study.

8.2.6 Discard cost parameters

The cost of removal per unit length ${}_dC_{r/l}$ and cost of treatment per unit length ${}_dC_{t/l}$ are obtained from Yi et al. [105] adjusted to their present value by considering the discount rate value used in their study.

8.3 Results of LCCA calculation

The results of the life cycle cost analysis obtained are presented in Table 8.3 to 8.6. The LCCA of 22kV 1c630mm² XLPE Aluminium cable is presented in Table 8.3. It can be observed that for the 22kV XLPE cable, the highest cost is the operation cost proceeded by the initial cost, failure cost, and discard cost respectively.

Table 8.3: LCCA OF 22kV 1C630mm² XLPE AL cable

					Initial Cost Calculation		
					Unit	Value	
					iC_c	AUD/km	549,245.11
					iC_a	AUD/km	19,548.00
					iC_{d-i}	AUD/km	309,447.00
					iC	AUD/km	878,240.11
Operation Cost Parameters					Operation Cost Calculation		
m	i	Unit	Value		oC_i	AUD/km	251,002.67
$pC_{i/p}$	12	0.003274	AUD/km	1,188.00	oC_m	AUD/km	199,661.21
$pC_{m/p}$	12	0.003274	AUD/km	945.00	oC_{rc}	AUD/km	180,687.54
$pC_{rc/p}$	4	0.009853	AUD/km	2,574.00	oC_{cl}	AUD/km	791,079.44
C			F/m	3.660E-10	oC_{dl}	AUD/km	23,167.35
					oC	AUD/km	1,445,598.21
Failure Cost Parameters					Failure Cost Calculation		
m	i	Unit	Value		fC_{rpr}	AUD/km	3,083.15
$pC_{rpr/p}$			AUD/km	58,275.00	fC_{rpl}	AUD/km	2,323.25
					fC_{ens}	AUD/km	250,026.78
					fC	AUD/km	255,433.18
Discard Cost Parameters					Discard Cost Calculation		
m	i	Unit	Value		dC_r	AUD/km	22,193.39
$dC_{r/l}$			AUD/km	71,982.00	dC_t	AUD/km	4,478.64
$dC_{t/l}$			AUD/km	14,526.00	dC_s	AUD/km	(11,956.88)
					dC	AUD/km	14,715.15
					NPV and EUAC Calculation		
					NPV	AUD/km	2,593,986.65
					EUAC	AUD/km	150,010.50

The LCCA of 22kV 1c630mm² TR-EPR Aluminium cable is presented in Table 8.4. In the case of 22kV TR-EPR cable, the highest cost is the operation cost proceeded by the initial cost, failure cost, and discard cost respectively.

Table 8.4: LCCA of 22kV 1C630mm² TR-EPR AL cable

					Initial Cost Calculation		
					Unit	Value	
					${}_iC_c$	AUD/km	568,018.00
					${}_iC_a$	AUD/km	19,548.00
					${}_iC_{d-i}$	AUD/km	309,447.00
					${}_iC$	AUD/km	897,013.00
Operation Cost Parameters					Operation Cost Calculation		
m	i	Unit	Value				
				${}_oC_i$	AUD/km	300,761.93	
${}_pC_{i/p}$	12	0.003274	AUD/km	1,188.00	${}_oC_m$	AUD/km	239,242.44
${}_pC_{m/p}$	12	0.003274	AUD/km	945.00	${}_oC_{rc}$	AUD/km	216,507.39
${}_pC_{rc/p}$	4	0.009853	AUD/km	2,574.00	${}_oC_{cl}$	AUD/km	947,904.58
${}_C$			F/m	3.367E-10	${}_oC_{dl}$	AUD/km	2,096.78
					${}_oC$	AUD/km	1,706,513.11
Failure Cost Parameters					Failure Cost Calculation		
m	i	Unit	Value				
				${}_fC_{rpr}$	AUD/km	1,231.45	
${}_pC_{rpr/p}$			AUD/km	58,275.00	${}_fC_{rpl}$	AUD/km	947.77
					${}_fC_{ens}$	AUD/km	299,592.58
					${}_fC$	AUD/km	301,771.81
Discard Cost Parameters					Discard Cost Calculation		
m	i	Unit	Value				
				${}_dC_r$	AUD/km	12,323.20	
${}_dC_{r/l}$			AUD/km	71,982.00	${}_dC_t$	AUD/km	2,486.83
${}_dC_{l/l}$			AUD/km	14,526.00	${}_dC_s$	AUD/km	(6,639.23)
					${}_dC$	AUD/km	8,170.80
					NPV and EUAC Calculation		
					NPV	AUD/km	2,913,468.71
					EUAC	AUD/km	140,611.15

The LCCA of 66kV 1c630mm² XLPE Aluminium cable is presented in Table 8.5. In the case of 66kV XLPE cable, the initial cost is now the highest cost proceeded by the operation cost, failure cost, and discard cost respectively.

Table 8.5: LCCA of 66kV 1C630mm² XLPE AL cable

					Initial Cost Calculation		
					Unit	Value	
					${}_iC_c$	AUD/km	762,300.00
					${}_iC_a$	AUD/km	19,548.00
					${}_iC_{d-i}$	AUD/km	309,447.00
					${}_iC$	AUD/km	1,091,295.00
Operation Cost Parameters					Operation Cost Calculation		
m	i	Unit	Value		${}_oC_i$	AUD/km	251,002.67
${}_pC_{i/p}$	12	0.003274	AUD/km	1,188.00	${}_oC_m$	AUD/km	199,661.21
${}_pC_{m/p}$	12	0.003274	AUD/km	945.00	${}_oC_{rc}$	AUD/km	180,687.54
${}_pC_{rc/p}$	4	0.009853	AUD/km	2,574.00	${}_oC_{cl}$	AUD/km	83,941.46
C			F/m	1.937E-10	${}_oC_{dl}$	AUD/km	109,793.68
					${}_oC$	AUD/km	825,086.56
Failure Cost Parameters					Failure Cost Calculation		
m	i	Unit	Value		${}_fC_{rpr}$	AUD/km	3,083.15
${}_pC_{rpr/p}$			AUD/km	58,275.00	${}_fC_{rpl}$	AUD/km	2,886.85
					${}_fC_{ens}$	AUD/km	250,026.78
					${}_fC$	AUD/km	255,996.78
Discard Cost Parameters					Discard Cost Calculation		
m	i	Unit	Value		${}_dC_r$	AUD/km	22,193.39
${}_dC_{r/l}$			AUD/km	71,982.00	${}_dC_t$	AUD/km	4,478.64
${}_dC_{t/l}$			AUD/km	14,526.00	${}_dC_s$	AUD/km	(11,956.88)
					${}_dC$	AUD/km	14,715.15
					NPV and EUAC Calculation		
					NPV	AUD/km	2,187,093.50
					EUAC	AUD/km	126,479.83

The LCCA of 66kV 1c630mm² TR-EPR Aluminium cable is presented in Table 8.6. In the case of 66kV TR-EPR cable, the initial cost is now the highest cost proceeded by the operation cost, failure cost, and discard cost respectively. Percentile values of the initial, operation, failure, and

discard costs with respect to the NPV for all insulation and voltage rating combinations are presented in Figure 8.1 to 8.4..

Table 8.6: LCCA of 66kV 1C630mm² TR-EPR AL cable

					Initial Cost Calculation				
					Unit	Value			
					${}_iC_c$	AUD/km	816,228.00		
					${}_iC_a$	AUD/km	19,548.00		
					${}_iC_{d-i}$	AUD/km	309,447.00		
					${}_iC$	AUD/km	1,145,223.00		
Operation Cost Parameters					Operation Cost Calculation				
m	i	Unit	Value						
				${}_oC_i$	AUD/km	300,761.93			
${}_pC_{i/p}$	12	0.003274	AUD/km	1,188.00	${}_oC_m$	AUD/km	239,242.44		
${}_pC_{m/p}$	12	0.003274	AUD/km	945.00	${}_oC_{rc}$	AUD/km	216,507.39		
${}_pC_{rc/p}$	4	0.009853	AUD/km	2,574.00	${}_oC_{cl}$	AUD/km	100,582.18		
${}_pC$			F/m	1.782E-10	${}_oC_{dl}$	AUD/km	9,936.94		
					${}_oC$	AUD/km	867,030.88		
Failure Cost Parameters					Failure Cost Calculation				
m	i	Unit	Value						
				${}_fC_{rpr}$	AUD/km	1,231.45			
${}_pC_{rpr/p}$			AUD/km	58,275.00	${}_fC_{rpl}$	AUD/km	1,210.03		
				${}_fC_{ens}$	AUD/km	299,592.58			
				${}_fC$	AUD/km	302,034.06			
Discard Cost Parameters					Discard Cost Calculation				
m	i	Unit	Value						
				${}_dC_r$	AUD/km	12,323.20			
${}_dC_{r/l}$			AUD/km	71,982.00	${}_dC_t$	AUD/km	2,486.83		
${}_dC_{t/l}$			AUD/km	14,526.00	${}_dC_s$	AUD/km	(6,639.23)		
				${}_dC$	AUD/km	8,170.80			
					NPV and EUAC Calculation				
					NPV	AUD/km	2,322,458.75		
					EUAC	AUD/km	112,087.56		

Based on Figure 8.1 for the 22kV XLPE cable, the initial cost and operation cost represent the majority of the NPV: summing to a total of 90% contribution. In this case, the operation cost

exceeds the initial cost by 22%. Furthermore, the discard cost shows negligible contribution to the overall cable cost.

As shown in Figure 8.2, the 22kV TR-EPR cable shown similar results with the 22kV XLPE cable such that the operation cost and operation cost represent majority of the expense for a total of 90% of NPV. In this case, the operation cost exceeds the initial cost by 28%. Additionally, the discard cost showed negligible part of the overall cable cost.

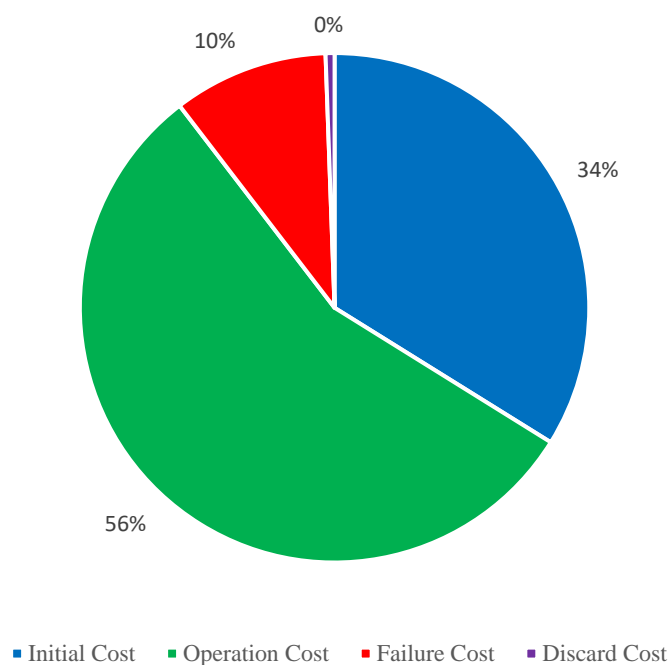


Figure 8.1: Percentile of costs for 22kV 1c630mm² XLPE cable

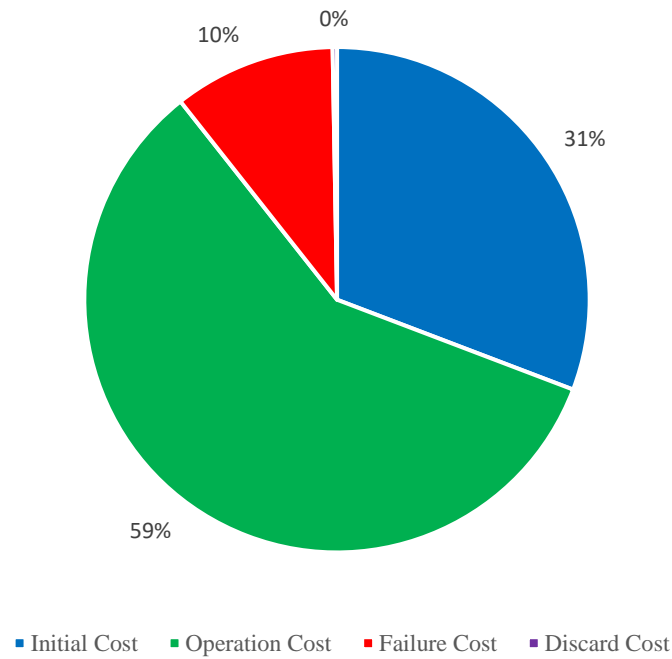


Figure 8.2: Percentile of costs for 22kV 1c630mm² TR-EPR cable

Figure 8.3 pertinent to the 66kV XLPE cable, the initial cost showed increase in percentile by about 16% and exceeding the operation cost by 12%. The initial cost and operation cost represent 88% of the overall cable cost. Additionally, the discard cost still showed negligible part of the overall cable cost.

As shown in Figure 8.4, it can be observed that for the 66kV TR-EPR cable, the initial cost has the largest percentile exceeding the operation cost by 12%. The initial cost and operation cost represent 86% of the NPV. Also, in contrast to other cable combinations, the discard cost showed slightly relevant share in the overall cost of the cable.

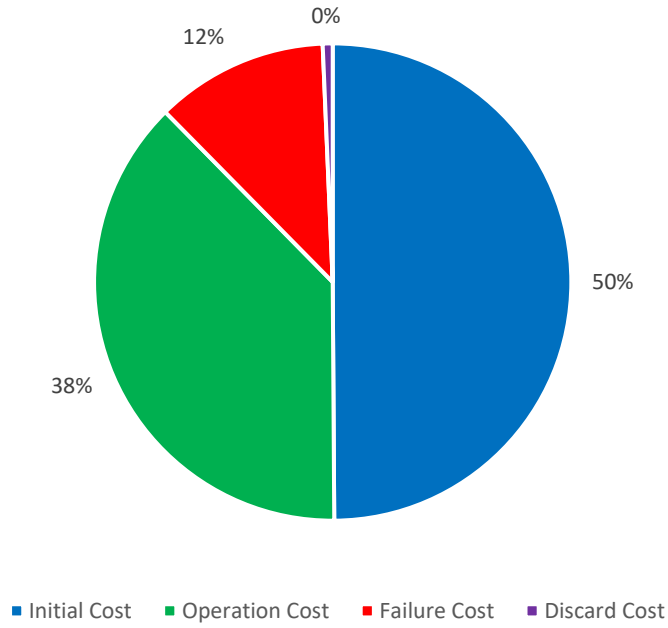


Figure 8.3: Percentile of costs for 66kV 1c630mm² XLPE cable

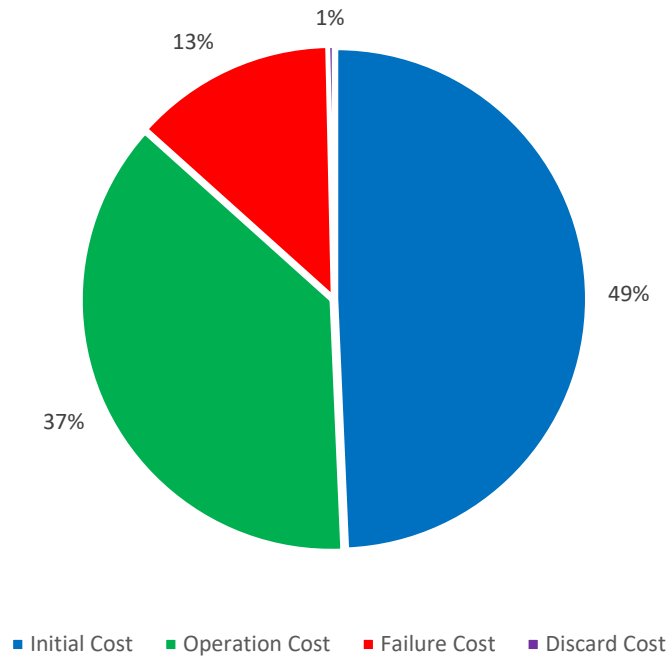


Figure 8.4: Percentile of costs for 66kV 1c630mm² TR-EPR cable

The summary of the LCCA results is presented in Table 8.7. It can be observed that at the same voltage rating, the initial, operation, and failure cost of TR-EPR is higher than that of the XLPE cable. Regarding the initial cost, 22kV TR-EPR is 2.14% higher than 22kV XLPE cable and 4.94% higher for 66kV voltage rating. This can be associated to the TR-EPR insulation being more expensive than XLPE insulation material. For the operation cost, the 22kV TR-EPR is 18.05% higher than 22kV XLPE cable and 5.08% for 66kV voltage rating. This can be attributed to greater number of annual costs considered for the accumulation caused by the longer life of TR-EPR. Owing again to having longer life, the accumulated failure cost of 22kV TR-EPR is 18.14% higher than 22kV XLPE cable and 17.98% higher for 66kV voltage rating.

On the other hand, for the same voltage rating, discard cost of TR-EPR cable is lower compared with XLPE cable. The lower discard cost of TR-EPR cable (44.47% for both 22kV and 66kV) is mainly due to consideration of discount rate and longer life.

On the basis of NPV for both voltage ratings, 22kV TR-EPR cable is 12.32% higher than 22kV XLPE cable and 6.19% higher for 66kV voltage rating. This can be again attributed to the more expensive purchase price and longer life of TR-EPR which consequently leads to greater number of periodic costs accumulated.

In line with the value of equivalent annual cost suitable for this case of the two cables having unequal economic lives, the 22kV TR-EPR cable obtained lower value by 6.27% compared with 22kV XLPE cable and 11.38% lower for 66kV voltage rating. This proves that on the basis of the life cycle cost analysis despite being more expensive in terms of insulation cost, TR-EPR cable is more economical than XLPE cable providing roughly 6%-12% annual savings.

Table 8.7: LCCA Summary

		XLPE	TR-EPR
		AUD/km	AUD/km
22 kV	Initial Cost	878,240.11	897,013.00
	Operation Cost	1,445,598.21	1,706,513.11
	Failure Cost	255,433.18	301,771.81
	Discard Cost	14,715.15	8,170.80
	NPV	2,593,986.65	2,913,468.71
	EUAC	<u>150,010.50</u>	<u>140,611.15</u>
66 kV	Initial Cost	1,091,295.00	1,145,223.00
	Operation Cost	825,086.56	867,030.88
	Failure Cost	255,996.78	302,034.06
	Discard Cost	14,715.15	8,170.80
	NPV	2,187,093.50	2,322,458.75
	EUAC	<u>126,479.83</u>	<u>112,087.56</u>

In order to gain a better view of how great the impact of insulation life is, an alternate LCCA was carried out in which the life of TR-EPR is assumed to be equal that of XLPE i.e., 30 years. The results of such analysis is presented in Table 8.8. It can be observed that the initial cost of TR-EPR for both 22kV and 66kV rating is higher compared with XLPE. However, TR-EPR now has lower operation and failure cost compared with XLPE. The lower operation cost is primarily due to the lower dielectric losses of TR-EPR whereas the lower failure cost is attributed to its lower failure rate. In this case, the annual savings in using TR-EPR cable over XLPE cable becomes 0.24%-2.3%.

Table 8.8: LCCA Summary for same service life

		XLPE	TR-EPR
		AUD/km	AUD/km
22 kV	Initial Cost	878,240.11	897,013.00
	Operation Cost	1,445,598.21	1,424,180.74
	Failure Cost	255,433.18	251,845.47
	Discard Cost	14,715.15	14,715.15
	NPV	2,593,986.65	2,587,754.36
	EUAC	<u>150,010.50</u>	<u>149,650.09</u>
66 kV	Initial Cost	1,091,295.00	1,145,223.00
	Operation Cost	825,086.56	723,585.82
	Failure Cost	255,996.78	252,064.34
	Discard Cost	14,715.15	14,715.15
	NPV	2,187,093.50	2,135,588.31
	EUAC	<u>126,479.83</u>	<u>123,501.28</u>

8.4 Conclusion

In this chapter, the life cycle cost analysis of TR-EPR and XLPE insulated cables are presented for both 22kV and 66kV. The parameters along with their basis were discussed followed by the different costs considered under initial cost, operation cost, failure cost, and discard cost. The results were presented in tables and figures. For the 22kV cable, the operation cost represented the highest cost followed by the initial cost, failure cost, and discard cost respectively. About 90% of the NPV is represented by the initial cost and operation cost for all cases.

For the 66kV voltage rating, the initial cost represented the highest cost followed by the operation cost, failure cost, and discard cost respectively. In all cases, the discard cost was negligible representing less than 1% of the overall cable costs. The EUAC of TR-EPR cable was also lower than XLPE for both 22kV and 66kV. This proves the TR-EPR serves to be more economical than XLPE despite having higher initial cost.

CHAPTER 9 CONCLUSION AND RECOMMENDATIONS FOR FUTURE WORK

9.0 Conclusion

In the view of cable industry, an elastomeric insulation material called the Tree-Retardant Ethylene Propylene Rubber (TR-EPR) was introduced. This material proved to overcome the weakness of EPR insulation over XLPE by its significantly better dielectric loss property that is multiple magnitudes lower equating to lower dielectric losses for power distribution.

The study also introduced a long-term thermal ageing test which lasted for 2 ½ years at service condition that contributed to a more reliable characterisation of the insulation material for the early years of its life which is a crucial consideration especially for recently introduced insulation. The results of the thermal ageing test revealed very stable behaviour of the tensile strength and elongation at break mechanical properties of the TR-EPR for the whole duration of the test at acceptable values based on standards. The selected insulation life model based on the work of Simoni [50] proved to provide good fitting with the experimental results of tensile strength test. The selection of least square regression method as a means of determining the best values of the parameters in the selected life model aided in obtaining the best fitting curve with the experimental results. The low value obtained for the standard error of regression that supports the

fitting of the curve with the experimental results is optimised. The results also proved the validity of the Arrhenius law imposed on the equation used for the curve fitting in the aspect of constancy of the thermal ageing rate for the condition that applied thermal stress (characterised by the temperature) is held constant. By resorting to a mathematical modelling of the time variation of tensile strength in the form of a cubic equation, the tendency for downward curvature was obtained which; corresponded to approach towards failure. By applying a failure criterion based on 50% drop in tensile strength and an Arrhenius acceleration factor using conservative value of literature-based activation energy, the service life of TR-EPR was estimated to be about 45 years.

The hot set test performed on TR-EPR showed that the cross-linking is achieved for only 24 days when subject to ambient temperature and for even a shorter period of 5 days when subject to a temperature of 60°C. The trend dictates that higher temperature yields shorter cross-linking time like in the case of the exposure of cables at a higher temperature of 90°C for 24 hours conducted in this research study. In this aspect, it may be recommendable to propose a revision of the IEC 60502-2, AS/NZS 1429.1, IEC 60502-1, and AS/NZS 3808 standard requirements of having the cable pass the hot set test by using the accelerated cross-linking method after extrusion for silane cure material. The proposal takes into account that Hot set test is performed in the light of verifying that cross-linking of the insulation material is achieved. Furthermore, cross-linking is associated to minimising the occurrence of the treeing phenomenon which has been known to cause insulation breakdown, but yet only to significantly develop on a long-term basis.

The partial discharge test showed significant improvement in the values of partial discharges to acceptable standard requirements measured before and after heating the TR-EPR insulated cable. This translates to lesser tendency of developing water trees that are recognised as agents for the degradation of the cable insulation resulting to failure. Hence, the low partial discharge

measurements after heating supports the tree-retardance of the TR-EPR through silane dry curing method.

The obtained ampacity measurements of Class 5 Aluminium cable at 110°C also proved to be in good agreement with the calculations carried out based on both IEC 60287 and AS/NZS3008.1.1 standards evidenced by less than 2% difference in the values relative to the 5% accepted limit. The results of this experiment can be proposed as supplemental revision of AS/NZS3008.1.1 in lieu with the provision of current carrying capacity values for Aluminium cables at 110°C taking into account that ampacities for Aluminium cables are only available up to 90°C operating temperature. This allows the recognition of the applicability of Aluminium cables for installations up to 110°C operating temperature.

Economic analysis showed that the TR-EPR insulated cable has greater NPV than XLPE insulated cable for both 22kV and 66kV voltage ratings owing to being slightly expensive and having longer service life which consequently increased the number of accumulated periodic expenses. Despite the greater NPV, the EUAC of TR-EPR insulated cable showed to be less than XLPE insulated cable. Specific figures show rough annual savings of 6%-12% for the TR-EPR cable compared with XLPE.

The results obtained from the various tests performed on TR-EPR provided a preliminary analysis which paves way for future more sophisticated approaches to modelling. The excellent dielectric properties, long service life, and cost-effective annual cost of the TR-EPR makes it a viable choice for cable insulation in underground cabling system like Victorian Power Distribution Network.

9.1 Recommendations for future work

This research study provided a platform for an initial investigation of the performance of the insulation material TR-EPR. As for any research study, an extension of the study is necessary to push for the development and advancements in the field. Hence, recommendations for future researchers are presented and outlined:

- As observed, the thermal ageing test was performed for the lone maximum operating temperature of 90°C. One recommendation is to pursue accelerated thermal ageing test at multiple higher temperatures. BS 7870-2 recommends selection of four temperatures, none of which greater than 160°C. As per BS EN 60216-2, the number of selected temperatures should be a minimum of three but recommended to four having intervals between 10K and 20K. The ageing test is to last for an average ageing time of at least 100 hours for the maximum temperature and at least 5000 hours for the minimum temperature [136]. In doing so, the extrapolation to service temperature may be carried out based on the straight line that will be obtained considering Arrhenius plot i.e., logarithm of life versus reciprocal of temperature. Furthermore, the activation energy of the TR-EPR may be experimentally derived by considering the slope of the straight plot of Arrhenius graph obtained.
- In contrast with performing thermal ageing alone, it may also be considered to perform accelerated ageing test of the TR-EPR cable under combined thermal and electrical stress at maximum service conditions (at 90°C for the thermal stress and 22kV for the electrical stress). This will allow more reliable comparison of the ageing data with actual operating condition of the cable insulation. The synergistic effect of the thermal and electrical stress in producing a more rapid tendency towards degradation may then be taken into account.

In an advanced case, multiple values of thermal and electrical stresses may be considered to approach a more complete characterisation of the TR-EPR insulated cable which may include determination of electrical and thermal thresholds if there are any.

- VLF test for the PD measurement may be considered for the diagnostic testing of the TR-EPR cable. This will help in the further verification of the tree-retardance of the TR-EPR considering the changes in the partial discharge activity of the cable at chosen times during its service. The information can be particularly useful in the investigation of the water-treeing phenomenon which is greatly considered in underground cabling system as mentioned in various studies.

REFERENCES

- [1] P. Werelius, “*Development and application of high voltage dielectric discharge spectroscopy for diagnosis of medium voltage XLPE cables*,” PhD thesis, Dept. Elec. Eng., Royal Inst. of Stockholm (KTH), Stockholm, Sweden, 2001.
- [2] H. Al-Khalidi, “*Technical Consideration and Impact of Converting Overhead Lines to Underground Power Cables*” PhD thesis, Victoria University, Australia, 2009.
- [3] H.E. Orton and R. Samm, 1997 “*World wide underground transmission cable practices*”, Transaction on Power Delivery, IEEE, Vol 12, No.2, pp 537.
- [4] E. Footitt, “*Statistical, electrical and mathematical analysis of water treed cross-linked polyethylene cable insulation*,” PhD thesis, Sch. Sci. and Eng., Queensland Univ. of Tech., Brisbane, Australia, 2015.
- [5] B. Teague, R. McLeod, and S. Pasco, “*Final report summary*” 2009 Victorian Bushfires Royal Commission, pp1-37.
- [6] Australia Putting Cables Underground Working Group, “*Putting underground cable report*” 1998.
- [7] L. Escobar and W. Meeker, “*A review of accelerated test models*” in Statistical Science, Institute of Mathematical Statistics, vol. 21, no. 4, pp. 552-577, 2006.

- [8] *Electric power systems and equipment – voltage ratings (60 hertz)*, ANSI C84.1-2011.
- [9] *Electrical cables handbook*, 3rd ed., Blackwell Science Ltd, Oxford, England, 1997
- [10] R. Mohammad, A. Kalam, and R. Akella, "A cost-effective early warning system for improving the reliability of power systems," 2013 Proceedings Annual Reliability and Maintainability Symposium (RAMS), Orlando, FL, 2013, pp. 1-6, doi: 10.1109/RAMS.2013.6517731.
- [11] E. Csanyi, "Overhead vs. underground residential distribution circuits. Which one is 'better'?", (2017, Nov. 13). [Online]. Available: <https://electrical-engineering-portal.com/overhead-vs-underground>. Accessed on: May 27, 2020.
- [12] F. Alonso and C. Greenwell, "Underground vs. overhead: Power line installation-cost comparison and mitigation," (2013, Feb. 1). [Online]. Available: <https://www.power-grid.com/2013/02/01/underground-vs-overhead-power-line-installation-cost-comparison/#gref>. Accessed on: May 27, 2020.
- [13] W. Atkinson, "Overhead and underground," (2015, July). [Online]. Available: <https://www.ecmag.com/section/systems/overhead-and-underground>. Accessed on: May 27, 2020.
- [14] M. Sheeba, "Overhead vs underground system," (2018, Jan. 27). [Online]. Available: <https://www.slideshare.net/mariashhebap/18-overhead-vs-underground-system>. Accessed on: May 27, 2020.

-
- [15] A. Allehyani and M. Beshir, "Overhead and underground distribution systems impact on electric vehicles charging," *Journal of Clean Energy Tech.*, vol. 4, no. 2, pp. 125-128, March, 2016. DOI: 10.7763/JOCET.2016.V4.265, [Online]. Available: <http://www.jocet.org/vol4/265-H0010.pdf>. Accessed on: May 27, 2020
- [16] J. H. Dudas, "Evolution of MV extruded cable designs used in the US from 1996 to 2014. Presented at IEEE-ICC Fall Meeting," (2019, June). [Online]. Available: https://www.neetrac.gatech.edu/publications/jicable19-10_Joe_Dudas_Final.pdf
- [17] J. Ainscough and I. Forrest, "Predicting medium-voltage underground-distribution cable failures. Presented at IEEE PES-ICC Fall Meeting," (2009, Nov.). [Online]. Available: <http://grouper.ieee.org/groups/td/dist/sd/doc/2016-09-06%20Predicting%20Medium-Voltage%20Underground-Distribution%20Cable-John%20Ainscough.pdf>
- [18] V. Badmera and R. R. Patel, "Electrical characterization of XLPE cable using accelerated water absorption test on medium voltage power cable and partial discharge test on power cable with termination defects," 2017 Innovations in Power and Advanced Computing Technologies (i-PACT), Vellore, 2017, pp. 1-7, doi: 10.1109/IPACT.2017.8245195.
- [19] V. Dehalwar, A. Kalam, M. L. Kolhe, and A. Zayegh, "Compliance of IEEE 802.22 WRAN for field area network in smart grid," 2016 IEEE International Conference on Power System Technology (POWERCON), Wollongong, NSW, 2016, pp. 1-6, doi: 10.1109/POWERCON.2016.7754046.

- [20] A. M. T. Oo, A. Kalam, and A. Zayegh, "*Effective power system communication requirements for deregulated power industry*," The 2004 IEEE Asia-Pacific Conference on Circuits and Systems, 2004. Proceedings., Tainan, 2004, pp. 653-656 vol.2, doi: 10.1109/APCCAS.2004.1412962.
- [21] C. R. Ozansoy, A. Zayegh, and A. Kalam, "*The real-time publisher/subscriber communication model for distributed substation systems*," in IEEE Transactions on Power Delivery, vol. 22, no. 3, pp. 1411-1423, July 2007, doi: 10.1109/TPWRD.2007.893939.
- [22] H. Al-Khalidi and A. Kalam, "*The impact of underground cables on power transmission and distribution networks*," 2006 IEEE International Power and Energy Conference, Putra Jaya, 2006, pp. 576-580, doi: 10.1109/PECON.2006.346717.
- [23] P. Cox, R. Fleming, F. Krajick, S. Boggs, and Y. Cao, "*AC and impulse performance of medium voltage ethylene propylene-rubber cables with over 25 years of in-service aging in a wet underground environment*," in IEEE Electrical Insulation Magazine, vol. 32, no. 3, pp. 24-28, 2016, doi: 10.1109/MEI.2016.7527122.
- [24] S. Afotey and S. M. Aliadeh, "*Investigation into the impact of cable failure localisation methods on the underground cable life time in a medium voltage distribution network*," 2020 IEEE 29th International Symposium on Industrial Electronics (ISIE), Delft, Netherlands, 2020, pp. 898-903, doi: 10.1109/ISIE45063.2020.9152389.

-
- [25] E. Maggioli, H. Leite, and C. Morais, "A survey of the Portuguese MV underground cable failure," 2016 13th International Conference on the European Energy Market (EEM), Porto, 2016, pp. 1-5, doi: 10.1109/EEM.2016.7521217.
- [26] L. Calcara et al., "Faults evaluation of MV underground cable joints," 2019 AEIT International Annual Conference (AEIT), Florence, Italy, 2019, pp. 1-6, doi: 10.23919/AEIT.2019.8893351.
- [27] O. Naidu, N. George, and D. Pradhan, "A new fault location method for underground cables in distribution systems," 2016 First International Conference on Sustainable Green Buildings and Communities (SGBC), Chennai, 2016, pp. 1-5, doi: 10.1109/SGBC.2016.7936076.
- [28] H. Orton, "History of underground power cables," in *IEEE Electrical Insulation Magazine*, vol. 29, no. 4, pp. 52-57, July-August 2013, doi: 10.1109/MEI.2013.6545260.
- [29] Cables.com, "History of the power cord," (2017, May 25). [Online]. Available: <https://www.cables.com/blog/history-of-the-power-cord/>. Accessed on: May 28, 2020.
- [30] The Editors of Encyclopaedia Britannica, "Sebastian Ziani de Ferranti," (2020, Apr. 5). [Online]. Available: <https://www.britannica.com/biography/Sebastian-Ziani-de-Ferranti>. Accessed on: May 29, 2020.
- [31] Z. Lei et al., "Influence of temperature on dielectric properties of EPR and partial discharge behavior of spherical cavity in EPR insulation," in *IEEE Transactions on*

-
- Dielectrics and Electrical Insulation, vol. 22, no. 6, pp. 3488-3497, December 2015, doi: 10.1109/TDEI.2015.004942.
- [32] Liu Xia, Yu Qinxue, Liu Minghao, Zhang Kai, and Zhong Lisheng, "*Temperature dependence of AC / DC breakdown strength of HVDC XLPE cable slices*," 2016 International Conference on Condition Monitoring and Diagnosis (CMD), Xi'an, 2016, pp. 90-93, doi: 10.1109/CMD.2016.7757789.
- [33] S. K. Ganguli and V. Kohli, "*History of electric cables*," in Power Cable Technology, 1st ed. Portland, OR, USA: Taylor & Francis Inc., 2016, Preface. [Online]. Available: <https://books.google.com.ph/books?id=ljduDwAAQBAJ&pg=PT10&lpg=PT10&dq=first+screened+cables&source=bl&ots=thHPRx6xHS&sig=ACfU3U0BQ6ZVBOVbTSy7VXSH2HHrUfLhew&hl=en&sa=X&ved=2ahUKEwjVkrzlwtpAhX24XMBHcWoDJ8Q6AEwDHoECAsQAQ#v=onepage&q=first%20screened%20cables&f=false>
- [34] K. Daware, "*Types of underground cables*," (2017, Mar.). [Online]. Available: <https://www.electricaleasy.com/2017/03/types-of-underground-cables.html>. Accessed on: May 29, 2020.
- [35] H. C. Doepken, R. Schoolcraft, and O. Willis, "*Medium voltage cable shielding and grounding*," Conference Record of Annual Pulp and Paper Industry Technical Conference,, Atlanta, GA, USA, 1989, pp. 43-46, doi: 10.1109/PAPCON.1989.36933.
- [36] J. Mejia, "*Characterization of real power cable defects by diagnostic measurements*," PhD thesis, Sch. Elect. and Comp. Eng., Georgia Inst. of Tech., Atlanta, Georgia, 2008.

- [37] IEC 60228: "*Conductors of insulated cables*", International Electrotechnical Commission, Geneva, Switzerland, 2004.
- [38] Nexans Olex, "*High voltage catalogue*," (c.a. 2016). [Online]. Available: https://www.olex.com.au/Australia/2013/OLC12641_HighVoltageCat.pdf. Accessed on: May 31, 2020.
- [39] *Electric cables - polymeric insulated; Part 1: For working voltages 1.9/3.3 (3.6)kV up to and including 19/33 (36)kV*, AS/NZS 1429.1:2006
- [40] S. B. Reddy, "*Basics of cable shields*," (2009, March). [Online]. Available: <https://instrumentationtools.com/basics-cable-shields/>. Accessed on: October 5, 2020.
- [41] V. Buchholz, "*Finding the root cause of power cable failures*," (2004, Nov.). [Online]. Available: https://electricenergyonline.com/show_article.php?article=186. Accessed on: May 31, 2020.
- [42] E. Csanyi, "*Shielding of power cables*," (2010, December 12). [Online]. Available: <https://electrical-engineering-portal.com/shielding-of-power-cables>. Accessed on: May 31, 2020.
- [43] L. Lisker, "*Focus on the fundamentals of shielded MV power cable*," (1996, Oct. 1). [Online]. Available: <https://www.ecmweb.com/content/article/20890741/focus-on-the-fundamentals-of-shielded-mv-power-cable>. Accessed on: June 1, 2020.

-
- [44] J. Parmar, "Cable construction & cable selection," (2017, Sept. 5). [Online]. Available: <https://www.electricalindia.in/cable-construction-cable-selection/>. Accessed on: June 1, 2020
- [45] W. F. Powers, "The basics of power cable," Conference Record of 1993 Forty-Fifth Annual Conference of Electrical Engineering Problems in the Rubber and Plastics Industries, Akron, OH, USA, 1993, pp. 74-81, doi: 10.1109/RAPCON.1993.255310.
- [46] D. Goulsbra, "Terminations I: A practical appraisal", in Medium Voltage Cable Accessories: A Theoretical & Practical Appraisal, 1st ed. Wakefield, UK: Nexans Pwr. Accs., 2012, ch. 8, p. 49, ch. 12, pp. 95-96.
- [47] IEEE guide to select terminations for shielded alternating-current power cable rated 5kV - 46kV, in IEEE Std 1637-2010, vol., no., pp.1-26, 5 May 2010, doi: 10.1109/IEEESTD.2010.5464501.
- [48] L. R. Trim, "Principles of accessory design [for power cables]," IEE Colloquium on Ensuring the Reliability of 11-132kV Cable Accessories, London, UK, 1998, pp. 2/1-2/4, doi: 10.1049/ic:19980023.
- [49] A. Friday, "The development of medium voltage cable accessories for ease of installation," 1993 Third International Conference on Power Cables and Accessories 10kV - 500kV, London, UK, 1993, pp. 92-100.

-
- [50] L. Simoni, "A new approach to the voltage-endurance test on electrical insulation," in *IEEE Transactions on Electrical Insulation*, vol. EI-8, no. 3, pp. 76-86, Sept. 1973, doi: 10.1109/TEI.1973.299248.
- [51] L. Simoni, "A general approach to the endurance of electrical insulation under temperature and voltage," in *IEEE Transactions on Electrical Insulation*, vol. EI-16, no. 4, pp. 277-289, Aug. 1981, doi: 10.1109/TEI.1981.298361.
- [52] G. C. Montanari and L. Simoni, "Aging phenomenology and modeling," in *IEEE Transactions on Electrical Insulation*, vol. 28, no. 5, pp. 755-776, Oct. 1993, doi: 10.1109/14.237740.
- [53] G. C. Montanari, "Modelling of multifactor ageing processes occurring in solid insulation," *IEE Colloquium on Multifactor Ageing*, London, UK, 1995, pp. 4/1-4/3, doi: 10.1049/ic:19951243.
- [54] G. Mazzanti, G. C. Montanari, L. Simoni, and M. B. Srinivas, "Combined electro-thermo-mechanical model for life prediction of electrical insulating materials," *Proceedings of 1995 Conference on Electrical Insulation and Dielectric Phenomena*, Virginia Beach, VA, USA, 1995, pp. 274-277, doi: 10.1109/CEIDP.1995.483716.
- [55] G. Mazzanti and G. C. Montanari, "A comparison between XLPE and EPR as insulating materials for high voltage cables," in *IEEE Power Engineering Review*, vol. 17, no. 1, pp. 36-36, January 1997, doi: 10.1109/MPER.1997.560656.

-
- [56] *International standard: Power cables with extruded insulation and their accessories for rated voltages from 1kV ($U_m = 1,2kV$) up to 30kV ($U_m = 7,2kV$) – Part 2: Cables rated voltages from 6kV ($U_m = 7,2kV$) up to 30kV ($U_m = 36kV$), IEC 60502-2:2005.*
- [57] R. M. Eichhorn, "A critical comparison of XLPE-and EPR for use as electrical insulation on underground power cables," in *IEEE Transactions on Electrical Insulation*, vol. EI-16, no. 6, pp. 469-482, Dec. 1981, doi: 10.1109/TEI.1981.298377.
- [58] R. Bodega, G. C. Montanari, and P. H. F. Morshuis, "Conduction current measurements on XLPE and EPR insulation," *The 17th Annual Meeting of the IEEE Lasers and Electro-Optics Society, 2004. LEOS 2004.*, Boulder, CO, USA, 2004, pp. 101-105, doi: 10.1109/CEIDP.2004.1364199.
- [59] C. C. Uydur, O. Arıkan, B. Kucukaydin, B. Dursun, and C. F. Kumru, "The effects of overvoltage aging on 20kV XLPE power cable," 2019 11th International Conference on Electrical and Electronics Engineering (ELECO), Bursa, Turkey, 2019, pp. 353-357, doi: 10.23919/ELECO47770.2019.8990637.
- [60] X. Qi and S. Boggs, "Thermal and mechanical properties of EPR and XLPE cable compounds," in *IEEE Electrical Insulation Magazine*, vol. 22, no. 3, pp. 19-24, May-June 2006, doi: 10.1109/MEI.2006.1639026
- [61] M. Brown, "Performance of Ethylene-Propylene rubber insulation in medium and high voltage power cable," in *IEEE Transactions on Power Apparatus and Systems*, vol. PAS-102, no. 2, pp. 373-381, Feb. 1983, doi: 10.1109/TPAS.1983.317684.
-

- [62] M. G. Danikas, "The definitions used for partial discharge phenomena," in *IEEE Transactions on Electrical Insulation*, vol. 28, no. 6, pp. 1075-1081, Dec. 1993, doi: 10.1109/14.249381.
- [63] *High-voltage test techniques – partial discharge measurements*, IEC 60270:2000
- [64] H. Winter, J. Lambrecht, and R. Bärsch, "On the measurement of the dielectric strength of silicone elastomers," 45th International Universities Power Engineering Conference UPEC2010, Cardiff, Wales, 2010, pp. 1-5.
- [65] J. Banaszczyk and B. Adamczyk, "Investigation of dielectric strength of solid insulating materials," 2017 Progress in Applied Electrical Engineering (PAEE), Koscielisko, 2017, pp. 1-7, doi: 10.1109/PAEE.2017.8009001.
- [66] *Electric strength of insulating materials-Test methods-Part 1: Test at power frequencies*, IEC 60243-1
- [67] S. Wels, J. Obst, A. Claudi, B. Böttge, R. Bernhardt, and S. Klengel, "Limitation of test sample arrangements according to IEC 60243-1: Electrical strength of insulating materials - Test methods," 2018 IEEE 2nd International Conference on Dielectrics (ICD), Budapest, 2018, pp. 1-4, doi: 10.1109/ICD.2018.8514634.
- [68] J. Liu, D. Zhang, C. Bin, L. Huang, Y. Gao, and X. Li, "A new method of aging assessment for XLPE cable insulation based on dielectric response," 2015 IEEE 11th

-
- International Conference on the Properties and Applications of Dielectric Materials (ICPADM), Sydney, NSW, 2015, pp. 560-563, doi: 10.1109/ICPADM.2015.7295333.
- [69] N. Promvichai, T. Supanarapan, K. Minja, B. Marungsri, and T. Boonraksa, "*Effect of NaCl solution and temperatures on water treeing propagation in XLPE underground cable for medium voltage,*" 2018 International Electrical Engineering Congress (iEECON), Krabi, Thailand, 2018, pp. 1-4, doi: 10.1109/IEECON.2018.8712333.
- [70] R. A. Guba, "*Design considerations of medium voltage primary URD cables,*" 1988. Rural Electric Power Conference, Papers Presented at the 32nd Annual Conference, Lexington, KY, USA, 1988, pp. D2/1-D2/5, doi: 10.1109/REPCON.1988.11006.
- [71] G. C. Montanari, G. Pattini, and L. Simoni, "*Long - term behavior of XLPE insulated cable models,*" in IEEE Transactions on Power Delivery, vol. 2, no. 3, pp. 596-602, July 1987, doi: 10.1109/TPWRD.1987.4308151.
- [72] A. Motori, F. Sandrolini, and G. C. Montanari, "*Degradation and electrical behavior of aged XLPE cable models,*" *Proceedings of the 3rd International Conference on Conduction and Breakdown in Solid Dielectrics*, Trondheim, Norway, 1989, pp. 352-358, doi: 10.1109/ICSD.1989.69219.
- [73] G. C. Montanari and M. Cacciari, "*A probabilistic life model for insulating materials showing electrical thresholds,*" in IEEE Transactions on Electrical Insulation, vol. 24, no. 1, pp. 127-134, Feb. 1989, doi: 10.1109/14.19877.

- [74] G. C. Montanari and A. Motori, "Time behavior and breakdown of XLPE cable models subjected to multiple stresses," *IEEE International Symposium on Electrical Insulation*, Toronto, Ontario, Canada, 1990, pp. 257-260, doi: 10.1109/ELINSL.1990.109751.
- [75] A. Motori, F. Sandrolini, G. C. Montanari, and M. Loggini, "Electrical properties for detection of thermal aging in XLPE cable models," [1991] *Proceedings of the 3rd International Conference on Properties and Applications of Dielectric Materials*, Tokyo, Japan, 1991, pp. 761-764 vol.2, doi: 10.1109/ICPADM.1991.172178.
- [76] A. Motori, F. Sandrolini, and G. C. Montanari, "A contribution to the study of aging of XLPE insulated cables," in *IEEE Transactions on Power Delivery*, vol. 6, no. 1, pp. 34-42, Jan. 1991, doi: 10.1109/61.103719.
- [77] A. Motori, F. Sandrolini, and G. C. Montanari, "DC electrical conductivity of XLPE cable models aged under multiple thermal-electrical stresses," [1992] *Proceedings of the 4th International Conference on Conduction and Breakdown in Solid Dielectrics*, Sestri Levante, Italy, 1992, pp. 285-290, doi: 10.1109/ICSD.1992.224938.
- [78] G. C. Montanari, "Life models for insulating materials and systems with electrical life lines tending to threshold," *Conference Record of the 1992 IEEE International Symposium on Electrical Insulation*, Baltimore, MD, USA, 1992, pp. 40-43, doi: 10.1109/ELINSL.1992.247056.
- [79] M. Cacciari and G. C. Montanari, "Electrical life threshold models for solid insulating materials subjected to electrical and multiple stresses. II. Probabilistic approach to

-
- generalized life models*," in *IEEE Transactions on Electrical Insulation*, vol. 27, no. 5, pp. 987-999, Oct. 1992, doi: 10.1109/14.256473.
- [80] G. C. Montanari, G. Pattini, and L. Simoni, "*Electrical endurance of EPR insulated cable models*," *Conference Record of the 1988 IEEE International Symposium on Electrical Insulation*, Cambridge, MA, USA, 1988, pp. 196-199, doi: 10.1109/ELINSL.1988.13903.
- [81] G. C. Montanari, "*Thermal aging of EPR cables*," *Proceedings., Second International Conference on Properties and Applications of Dielectric Materials*, Beijing, China, 1988, pp. 320-324 vol.1, doi: 10.1109/ICPADM.1988.38399.
- [82] G. C. Montanari, "*An investigation on the thermal endurance of EPR model cables*," in *IEEE Transactions on Electrical Insulation*, vol. 25, no. 6, pp. 1046-1055, Dec. 1990, doi: 10.1109/14.64489.
- [83] M. Cacciari, G. C. Montanari, L. Simoni, A. Cavallini, and A. Motori, "*Long-term electrical performance and life model fitting of XLPE and EPR insulated cables*," *Proceedings of the 1991 IEEE Power Engineering Society Transmission and Distribution Conference*, Dallas, TX, USA, 1991, pp. 135-142, doi: 10.1109/TDC.1991.169498.
- [84] G. C. Montanari and M. Cacciari, "*On the electrical endurance characterization of insulating materials by constant and progressive stress test*," in *IEEE Transactions on Electrical Insulation*, vol. 27, no. 5, pp. 1000-1008, Oct. 1992, doi: 10.1109/14.256475.

-
- [85] G. C. Montanari and A. Motori, "Compensation effect for aging diagnosis in EPR cable models," *Proceedings of IEEE Conference on Electrical Insulation and Dielectric Phenomena - (CEIDP'94)*, Arlington, TX, USA, 1994, pp. 451-457, doi: 10.1109/CEIDP.1994.591804.
- [86] G. C. Montanari, A. Motori, and E. Leonelli, "A methodology for short-time thermal endurance testing of polymers for cable insulation," *Proceedings of 1995 Conference on Electrical Insulation and Dielectric Phenomena*, Virginia Beach, VA, USA, 1995, pp. 114-117, doi: 10.1109/CEIDP.1995.483589.
- [87] G. Mazzanti, G. C. Montanari, and L. Simoni, "Study of the synergistic effect of electrical and thermal stresses on insulation life," *Proceedings of Conference on Electrical Insulation and Dielectric Phenomena - CEIDP '96*, Millbrae, CA, USA, 1996, pp. 684-687 vol.2, doi: 10.1109/CEIDP.1996.564563.
- [88] G. C. Montanari, G. Mazzanti, and L. Simoni, "Test procedures and lifetime data analysis for electro-thermal endurance characterisation of EPR-insulated cables," in *IEE Proceedings - Science, Measurement and Technology*, vol. 145, no. 1, pp. 13-19, Jan. 1998, doi: 10.1049/ip-smt:19981519.
- [89] M. Walton, "Accelerated cable life testing," (c.a. 2002). [Online]. Available: https://www.pesicc.org/iccWebSite/subcommittees/E/E04/2002/walton_spr02.pdf.
Accessed on: June 8, 2020
-

- [90] *Test methods for electric cables, cords and conductors; Method 3: Electrical tests*, AS/NZS 1660.3:1998
- [91] *Test methods for electric cables, cord and conductors; Method 2.2: Insulation, extruded semi-conductive screens and non-metallic sheaths – methods specific to elastomeric, XLPE and XLPVC materials*, AS/NZS 1660.2:1998
- [92] E. M. El-Refaie, M. Besheir, M. K. Abd Elrahman, and R. Saad, "Partial discharge measurement for medium voltage cables using different voltage wave forms," *Proceedings of 2014 International Symposium on Electrical Insulating Materials*, Niigata, 2014, pp. 315-318, doi: 10.1109/ISEIM.2014.6870782.
- [93] *IEEE Guide for field testing of shielded power cable systems using very low frequency (VLF)*, IEEE Std 400.2-2004
- [94] Y. Li et al., "Breakdown performance and electrical aging life model of EPR used in coal mining cables," 2016 IEEE International Conference on High Voltage Engineering and Application (ICHVE), Chengdu, 2016, pp. 1-4, doi: 10.1109/ICHVE.2016.7800687.
- [95] C. Young, "Excel solver: Which solving method should I choose?," (n.d.). [Online]. Available: <https://engineerexcel.com/excel-solver-solving-method-choose/#:~:text=to%20linear%20problems.,GRG%20Nonlinear,the%20partial%20derivatives%20equal%20zero>. Accessed on: July 31, 2020

-
- [96] J. Frost, “*Standard error of the regression vs. R-squared*,” (c.a. 2017, Sept.). [Online]. Available: <https://statisticsbyjim.com/regression/standard-error-regression-vs-r-squared/>. Accessed on: October 5, 2020
- [97] P. Pourmand, “*Long-term performance of polymeric materials in nuclear power plants*,” PhD thesis, Sch. Chem. Sci. and Eng., Royal Inst. of Stockholm (KTH), Stockholm, Sweden, 2017.
- [98] S. Glen, “*Correlation coefficient: Simple definition, formula, easy steps*,” (c.a. 2007). [Online]. Available: <https://www.statisticshowto.com/probability-and-statistics/correlation-coefficient-formula/>. Accessed on: September 11, 2020.
- [99] I. Kashi and K. Moussaceb, “*New mathematical models for predicting the lifetime of EPDM insulators: Effect of elongation at break on the kinetic degradation of EPDM*,” Periodicals of Engineering and Natural Sciences., vol. 6, no. 2, pp. 71-88, October, 2018. Accessed on: September 10, 2020, DOI: 10.21533/pen.v6i2.173, [Online]. Available: <http://pen.ius.edu.ba/index.php/pen/article/viewFile/173/198>
- [100] L. Cao and S. Grzybowski, “*Life-time characteristics of EPR cable insulation under electrical and thermal stresses*,” 2013 IEEE International Conference on Solid Dielectrics (ICSD), Bologna, 2013, pp. 632-635, doi: 10.1109/ICSD.2013.6619873.
- [101] *Electrical installations in ships- Part 350: General construction and test methods of power, control and instrumentation cables for shipboard and offshore applications*, IEC 60092-350

-
- [102] *Electrical installations in ships- Part 354: Single- and three-core power cables with extruded solid insulation for rated voltages 6kV ($U_m = 7,2kV$) up to 30kV ($U_m = 36kV$), IEC 60092-354*
- [103] International Electrotechnical Commission, "*IEC 60502:2018 Power cables with extruded insulation and their accessories for rated voltages from 1kV ($U_m = 1.2kV$) up to 30kV ($U_m = 36kV$) - ALL PARTS*," ed. Geneva, Switzerland: International Electrotechnical Commission, 2018.
- [104] W. Thue, "*Electrical power cable engineering*", 3rd ed. Boca Raton, FL, USA, CRC Press, 2012, pp23-51.
- [105] T. Yi, J. Liao, B. Chen, Z. Zhu, S. Lu, and B. Gao, "*Life cycle cost based modeling and economic evaluation of 10kV aluminum alloy power cables*," 2016 IEEE International Conference on Cyber Technology in Automation, Control, and Intelligent Systems (CYBER), Chengdu, 2016, pp. 162-166, doi: 10.1109/CYBER.2016.7574815
- [106] AS/NZS 1125: "*Conductors in insulated electric cables and flexible cords*", Australian Standard/New Zealand Standard, 2001.
- [107] A. Kalam, H. Al-Khalidi, and D. Willen, "*HTS cable and its anticipated effects on power transmission networks*," in *AC and DC Power Transmission, 2006. ACDC 2006. The 8th IEE International Conference on*, 2006, pp. 50-53.

-
- [108] H. Al-Khalidi, A. Hadbah, and A. Kalam, "Performance analysis of HTS cables with variable load demand," in *Innovative Smart Grid Technologies Asia (ISGT), 2011 IEEE PES*, 2011, pp. 1-8.
- [109] AS/NZS 3008.1.1: "*Electrical installations Part1.1: Cables for alternating voltages up to and including 0.6/1kV-Typical Australian installation conditions*", Australian Standard/New Zealand Standard, 2017.
- [110] S. Curreli et al., "Evaluation of the effects of mechanical cycles on bonding of Al-superconducting cable in high-performance stabilized NbTi conductor," in *IEEE Transactions on Applied Superconductivity*, vol. 27, no. 4, pp. 1-4, June 2017, Art no. 4802004, doi: 10.1109/TASC.2016.2646067.
- [111] M. Guthrie, G. Martinjak, and H.B. VanSickle, "*IEC 62561 electrical testing of US connectors and stranded cable*," in 33rd International Conference on Lightning Protection (ICLP), 2016, pp. 1-9.
- [112] A. Ramonat, S. Schlegel, S. Großmann and M. Kudoke, "*Basic investigations on joints with cylindrical aluminum conductors made by press- and shrink-fit for high-current devices*," 2015 IEEE 61st Holm Conference on Electrical Contacts (Holm), San Diego, CA, 2015, pp. 309-316, doi: 10.1109/HOLM.2015.7355114.
- [113] K. Haim, D. Cisilino, and K. Bentkowski, "*The behaviour of shear bolt connectors in MV -Cable accessories in case of critical load and overload*," CIGRE 2009 - 20th

International Conference and Exhibition on Electricity Distribution - Part 1, Prague, Czech Republic, 2009, pp. 1-4, doi: 10.1049/cp.2009.0660.

[114] K. Haim, R. Bärsch, J. Pilling and J. Hofmann, "*The compact joint with integrated shear bolt connector: A new approach to function integration in medium voltage joints,*" CIRED 2005 - 18th International Conference and Exhibition on Electricity Distribution, Turin, Italy, 2005, pp. 1-5, doi: 10.1049/cp:20050945.

[115] M. Runde, H. Jensvold and M. Jochim, "*Compression connectors for stranded Aluminum power conductors,*" in IEEE Transactions on Power Delivery, vol. 19, no. 3, pp. 933-942, July 2004, doi: 10.1109/TPWRD.2004.829946.

[116] W. B. Haverkamp, T. McKoon and M. Wilck, "*Bolted connectors for high voltage accessories installed on underground transmission lines,*" 1999 IEEE Transmission and Distribution Conference (Cat. No. 99CH36333), New Orleans, LA, USA, 1999, pp. 74-82 vol.1, doi: 10.1109/TDC.1999.755319.

[117] D.C. Giancoli, "*Thermal expansion,*" in Physics for Scientists & Engineers with Modern Physics, 4th ed vol. 1, Upper Saddle River, New Jersey, USA, Pearson Education, Inc., 2009, pp. 459-463.

[118] IEC 60287-1-1: "*Electric cables-Calculation of the current rating Part 1-1: Current rating equations (100% load factor) and calculation of losses-General*", International Electrotechnical Commission, Geneva, Switzerland, 2006.

- [119] IEC 60287-2-1: "*Electric cables-calculation of the current rating Part 2-1: Thermal resistance - Calculation of thermal resistance*", International Electrotechnical Commission, Geneva, Switzerland, 2006.
- [120] IEC 61439-1: "*Low voltage switchgear and controlgear assemblies Part1:General rules*", ed. 2.0, International Electrotechnical Commission, Geneva, Switzerland, 2011, pp. 64-71.
- [121] T. Wildi, "*Electrical Machines, Drives, and Power System*", 6th ed. Upper Saddle River, New Jersey, USA, Pearson Education, Inc., 2006 pp120-131.
- [122] IEC 61238-1-1: "*Compression and mechanical connectors for power cables - Part1-1:Test methods and requirements for compression and mechanical connectors for power cables for rated voltages up to 1kV ($U_m=1.2kV$) tested on non-insulated conductors*", International Electrotechnical Commission, Geneva, Switzerland, 2018.
- [123] AS/NZS 3000: "*Wiring Rules*", Australian Standard/New Zealand Standard, 2018.
- [124] L. Blank and A. Tarquin, "Annual worth analysis," in "*Engineering Economy*, 7th ed., Boston: McGraw-Hill, 2005, ch. 6, pp. 150-164
- [125] D. Metzinger, "*Oklahoma gas & electric underground cable failure data base and failure rates*," (2004, Nov. 3). [Online]. Available: https://www.pesicc.org/iccwebsite/subcommittees/E/E04/2004/F2004_Metzinger.pdf
Accessed on: September 23, 2020

- [126] J. Burke, "*Hard to find information about distribution systems,*" (2002, August 28). [Online]. Available: <https://library.e.abb.com/public/91ad3a29a50978bf85256c550053db0d/Hard.To.Find.6th.pdf>. Accessed on: September 23, 2020
- [127] J. Deans, "*Discount rates for Commonwealth infrastructure projects,*" (2018, March 10). [Online]. Available: https://www.aph.gov.au/About_Parliament/Parliamentary_Departments/Parliamentary_Library/FlagPost/2018/October/Discount-rates. Accessed on: September 20, 2020
- [128] D. Jutrisa, "*Gheringhap (GHP) zone substation,*" (2020, July). [Online]. Available: <https://www.aer.gov.au/system/files/Powercor%20-%20SUPP%20ATT%20249%20-%20North%20western%20Geelong%20REFCL%20-%20%20Gheringhap%20scope%20-%20%20July%202020.pdf>. Accessed on: September 23, 2020
- [129] S. Baran, "*What is the average (kWh) cost of electricity in Australia?,*" (2009, May 1). [Online]. Available: <https://www.finder.com.au/average-cost-of-electricity>. Accessed on: September 20, 2020
- [130] Citipower and Powercor, "*Citipower network performance,*" (2019). [Online]. Available: <https://www.powercor.com.au/what-we-do/the-network/citipower-network-performance/>. Accessed on: September 23, 2020
- [131] T. Takahashi, T. Kurihara, T. Takahashi and T. Okamoto, "*Water trees as a dominant deterioration cause of 60kV class dry cured XLPE Cables,*" 2019 IEEE Conference on

Electrical Insulation and Dielectric Phenomena (CEIDP), Richland, WA, USA, 2019, pp. 194-197, doi: 10.1109/CEIDP47102.2019.9009853.

[132] T. Takahashi, T. Kusaishi, T. Takahashi, H. Suzuki and T. Okamoto, "*Development of pre-breakdown discharge detection test for aged XLPE cable to find a deteriorating water tree,*" Proceedings of 2011 International Symposium on Electrical Insulating Materials, Kyoto, 2011, pp. 524-524, doi: 10.1109/ISEIM.2011.6826390.

[133] T. Sami, A. Gholami and S. M. Shahrtash, "*Effect of electro-thermal, load cycling and thermal transients stresses on high voltage XLPE and EPR power cable life,*" 8th International Conference on Advances in Power System Control, Operation and Management (APSCOM 2009), Hong Kong, China, 2009, pp. 1-6, doi: 10.1049/cp.2009.1818.

[134] N. Hampton, "*Medium voltage cable system issues,*" (2016, Feb.). [Online]. Available: https://www.neetrac.gatech.edu/publications/CDFI/2-MV-Issues_25_with-Copyright.pdf. Accessed on: September 23, 2020

[135] L. Deschamps, "*The aging of extruded dielectric cables,*" JI-CABLE/EPRI/CEA Workshop Cables, vol. 89, p. 5f-6, 1990.

[136] A. Alghamdi and R. Desuqi, "*A study of expected lifetime of XLPE insulation cables working at elevated temperatures by applying accelerated thermal ageing,*" in Heliyon, 2020, vol. 6, no. 1, pp. 1-11

[137] F. Agustin., A. Kalam., A. Zayegh. “*Investigation of 22 kV silane cure TR-EPR cable*”

International Journal of Applied Power Engineering (IJAPE) Vol. 10, No.1, March

2021, pp. 41~47

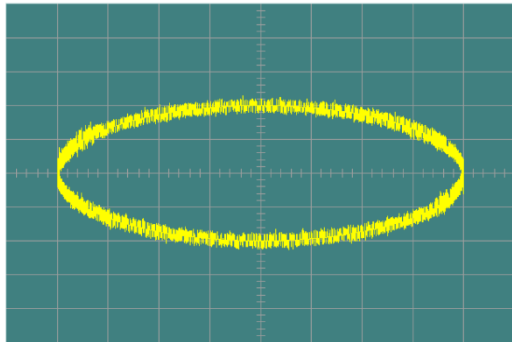
Appendix A

Partial Discharge (PD) taken before and after heating of

TR-EPR cable samples

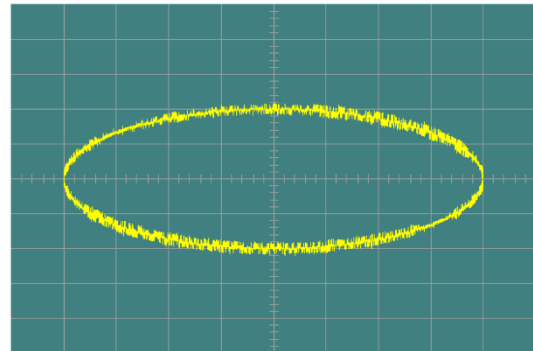
Cable Marker	22kV 1C120	Heating	NO
Test Voltage (kV):	19.03	PD-Value(pC)	2.33
Test Date:	06-05-2018		

Test Image



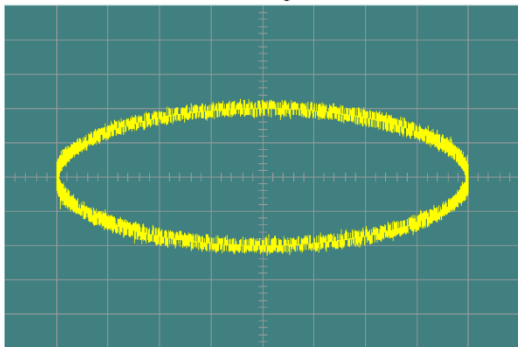
Cable Marker	22kV 1C120	Heating	120hrs at 60°C
Test Voltage (kV):	19.67	PD-Value(pC)	1.29
Test Date:	12-05-2018		

Test Image



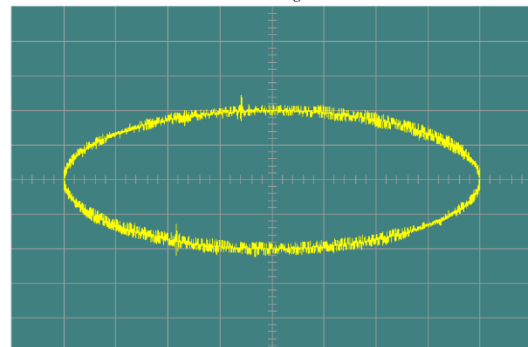
Cable Marker	22kV 1C120-1	Heating	NO
Test Voltage (kV):	25	PD-Value(pC)	2.38
Test Date:	06-05-2018		

Test Image



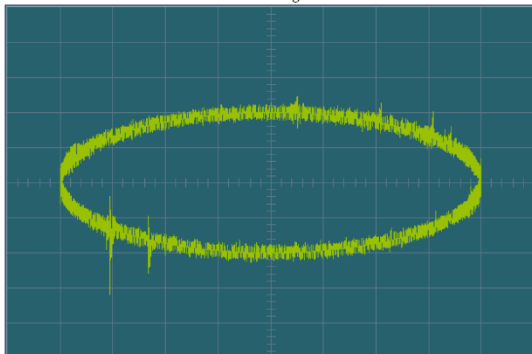
Cable Marker	22kV 1C120-1	Heating	120hrs at 60°C
Test Voltage (kV):	25	PD-Value(pC)	1.67
Test Date:	12-05-2018		

Test Image



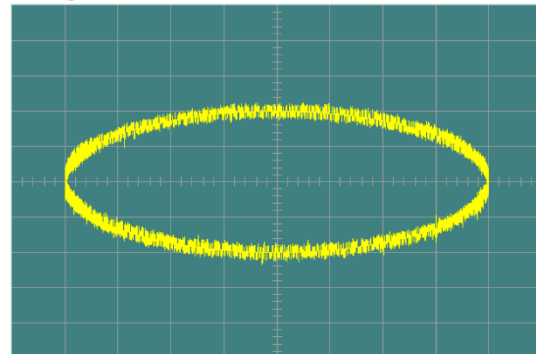
Cable Marker	22kV 1C120-2	Heating	NO
Test Voltage (kV):	25	PD-Value(pC)	8.34
Test Date:	13-05-2018		

Test Image



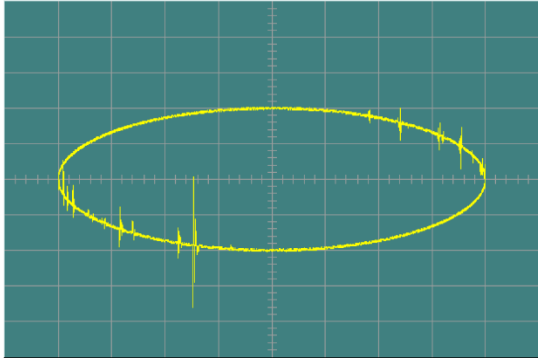
Cable Marker	22kV 1C120-2	Heating	120hrs at 60°C
Test Voltage(kV):	25	PD-Value(pC)	2.42
Test Date:	05-21-2018		

Test Image



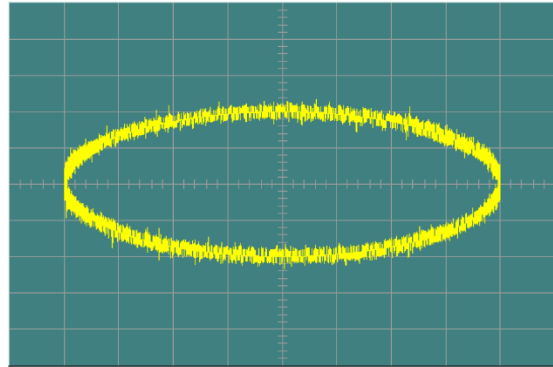
Cable Marker	22kV 1C120-3	Heating	NO
Test Voltage(kV):	25	PD-Value(pC)	90.44
Test Date:	13-05-2018		

Test Image



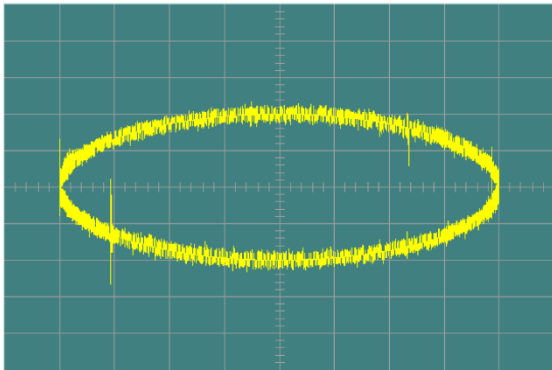
Cable Marker	22kV 1C120-3	Heating	120hrs at 60°C
Test Voltage(kV):	25	PD-Value(pC)	2.66
Test Date:	05-25-2018		

Test Image



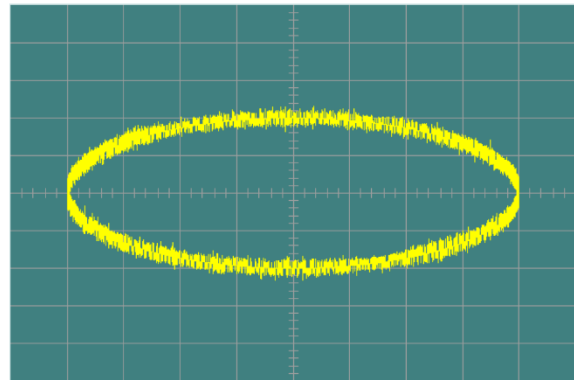
Cable Marker	22kV 1C120-4	Heating	NO
Test Voltage(kV):	25	PD-Value(pC)	6.59
Test Date:	26-05-2018		

Test Image



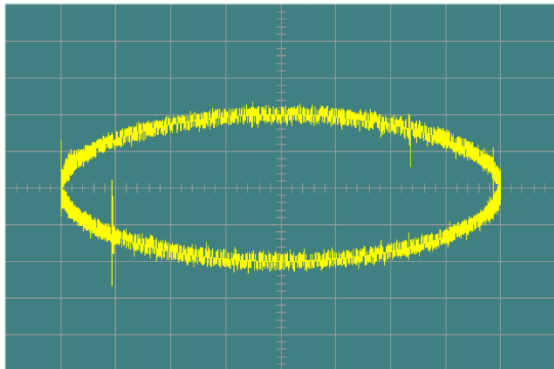
Cable Marker	22kV 1C120-4	Heating	120hrs at 60°C
Test Voltage(kV):	25	PD-Value(pC)	1.85
Test Date:	07-06-2018		

Test Image



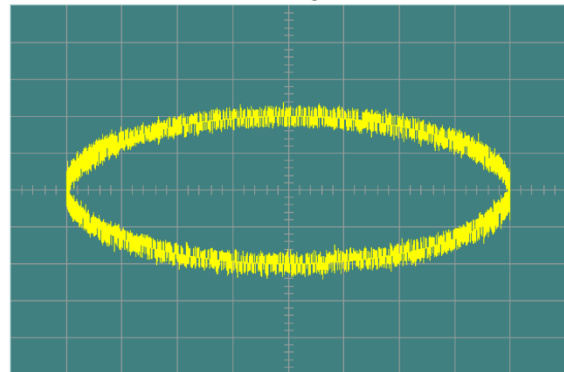
Cable Marker	22kV 1C120-5	Heating	NO
Test Voltage(kV):	25	PD-Value(pC)	8.59
Test Date:	01-06-2018		

Test Image



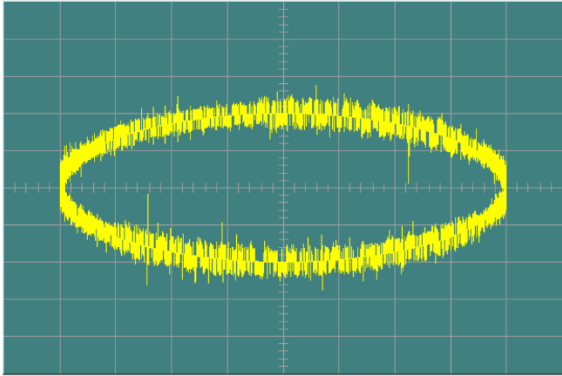
Cable Marker	22kV 1C120-5	Heating	120hrs at 60°C
Test Voltage(kV):	25	PD-Value(pC)	2.85
Test Date:	07-06-2018		

Test Image



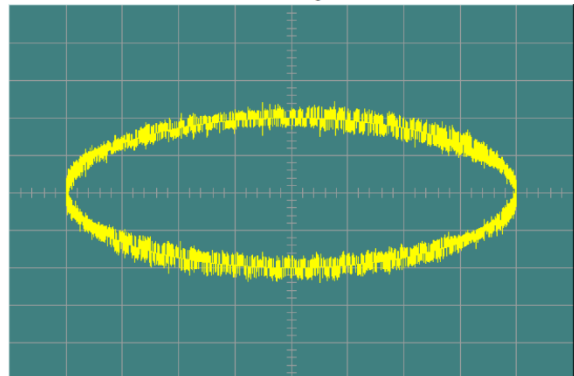
Cable Marker	22kV 1C120-6	Heating	NO
Test Voltage (kV):	25	PD-Value(pC)	5.68
Test Date:	01-06-2018		

Test Image



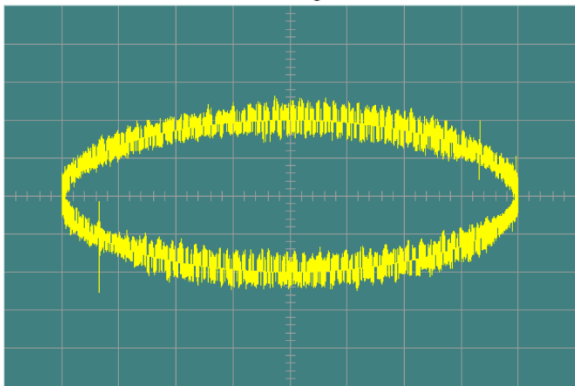
Cable Marker	22kV 1C120-6	Heating	120hrs at 60°C
Test Voltage (kV):	25	PD-Value(pC)	2.02
Test Date:	06-27-2018		

Test Image



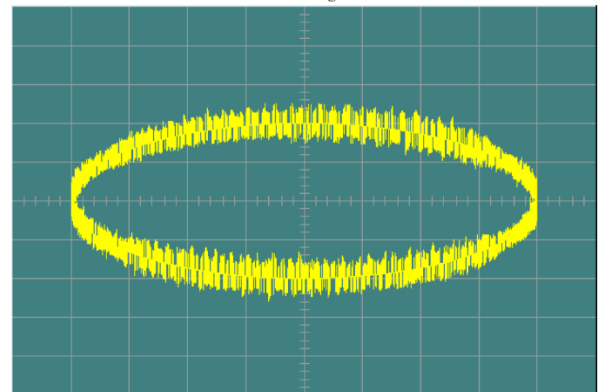
Cable Marker	22kV 1C120-7	Heating	NO
Test Voltage (kV):	25	PD-Value(pC)	5.98
Test Date:	06-21-2018		

Test Image



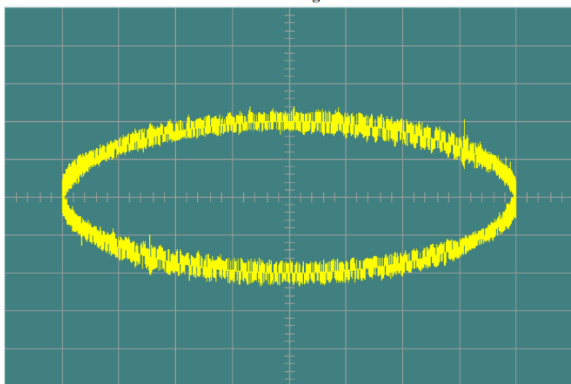
Cable Marker	22kV 1C120-7	Heating	120hrs at 60°C
Test Voltage (kV):	25	PD-Value(pC)	2.92
Test Date:	28-06-2018		

Test Image



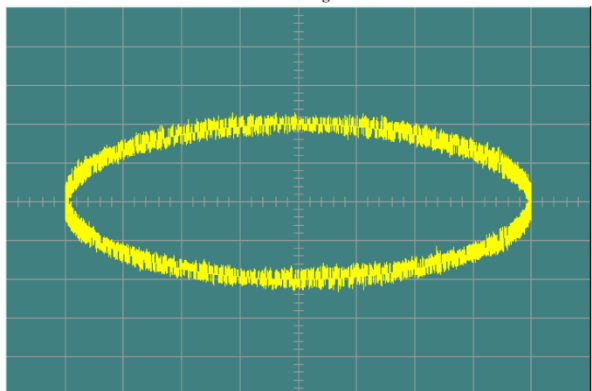
Cable Marker	22kV 1C120-8	Heating	NO
Test Voltage (kV):	25	PD-Value(pC)	3.20
Test Date:	01-07-2018		

Test Image



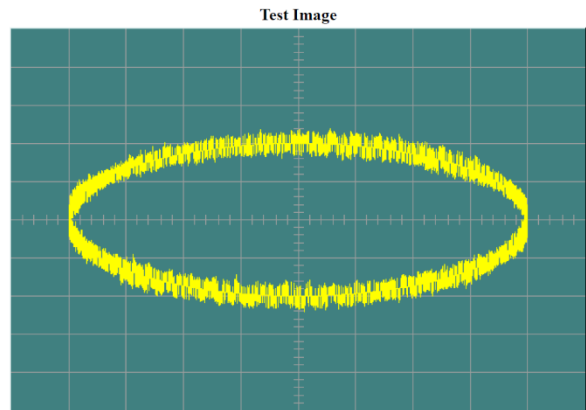
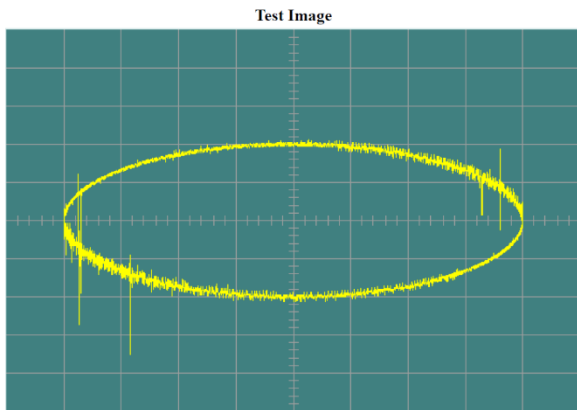
Cable Marker	22kV 1C120-8	Heating	120hrs at 60°C
Test Voltage (kV):	25	PD-Value(pC)	1.92
Test Date:	08-07-2018		

Test Image



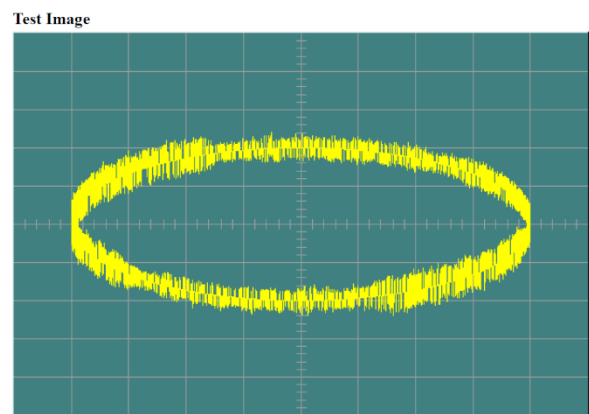
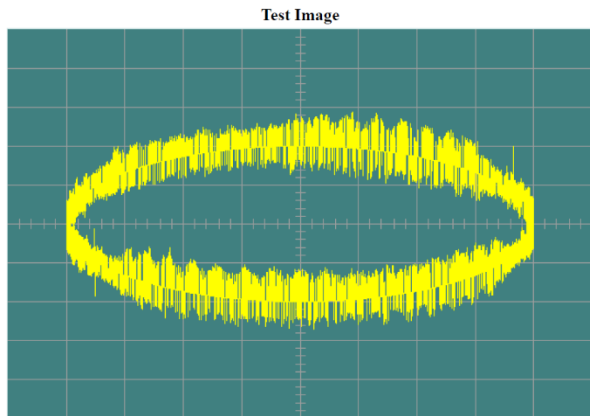
Cable Marker	22kV 1C120-9	Heating	NO
Test Voltage(kV):	25	PD-Value(pC)	110.94
Test Date:	11-07-2018		

Cable Marker	22kV 1C120-9	Heating	120hrs at 60°C
Test Voltage(kV):	25	PD-Value(pC)	2.05
Test Date:	18-07-2018		



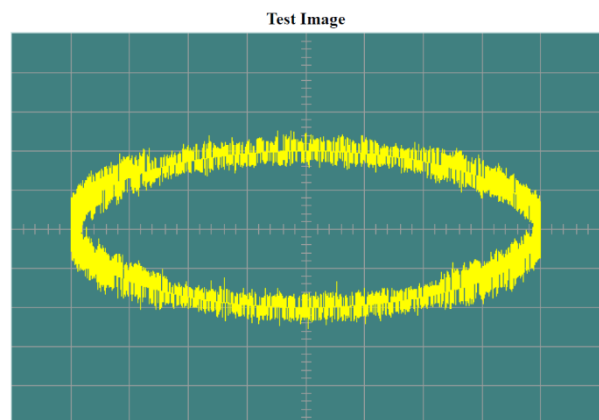
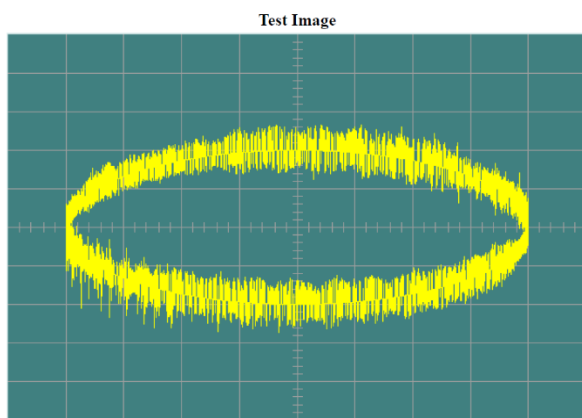
Cable Marker	22kV 1C95-2	Hating	NO
Test Voltage(kV):	25	PD-Value(pC)	4.63
Test Date:	27-07-2018		

Cable Marker	22kV 1C95-2	Heating	120hrs at 60°C
Test Voltage(kV):	25	PD-Value(pC)	2.61
Test Date:	04-08-2018		



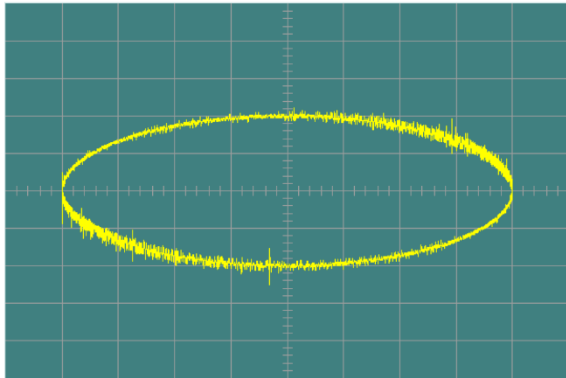
Cable Marker	22kV 1C95-3	Heating	NO
Test Voltage(kV):	25	PD-Value(pC)	6.04
Test Date:	29-07-2018		

Cable Marker	22kV 1C95-3	Heating	120hrs at 60°C
Voltage Level(kV):	25	PD-Value(pC)	3.10
Test Date:	08-08-2018		



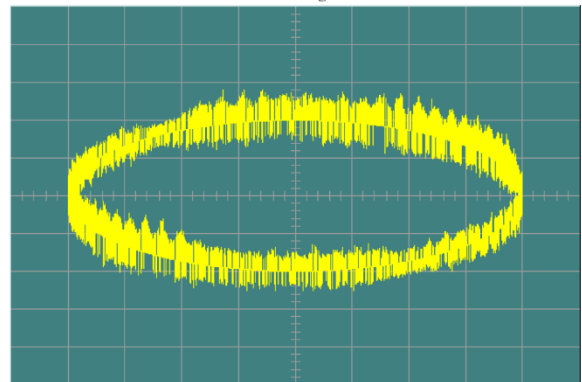
Cable Marker	22kV 1C95-4	Heating	NO
Test Voltage(kV):	25	PD-Value(pC)	31.86
Test Date:	09-08-2018		

Test Image



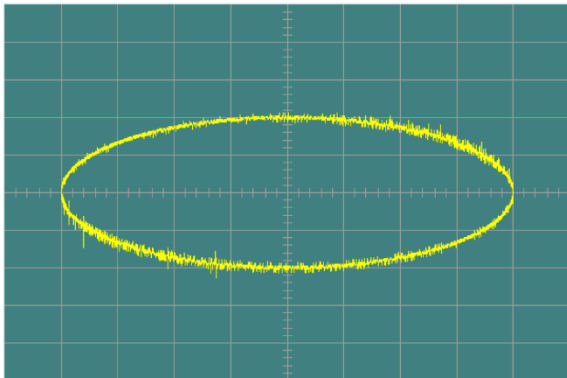
Cable Marker	22kV 1C95-4	Heating	120hrs at 60°C
Test Voltage(kV):	25	PD-Value(pC)	3.99
Test Date:	15-08-2018		

Test Image



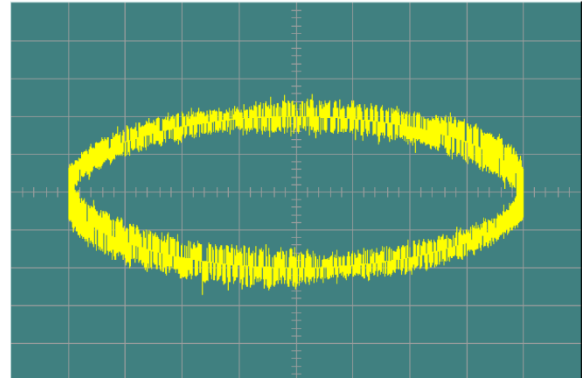
Cable Marker	22kV 1C95-5	Heating	NO
Test Voltage(kV):	25	PD-Value(pC)	28.62
Test Date:	20-08-2018		

Test Image



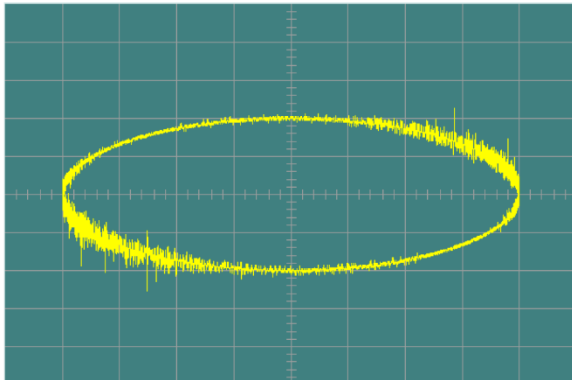
Cable Marker	22kV 1C95-5	Heating	120hrs at 60°C
Test Voltage(kV):	25	PD-Value(pC)	3.88
Test Date:	28-08-2018		

Test Image



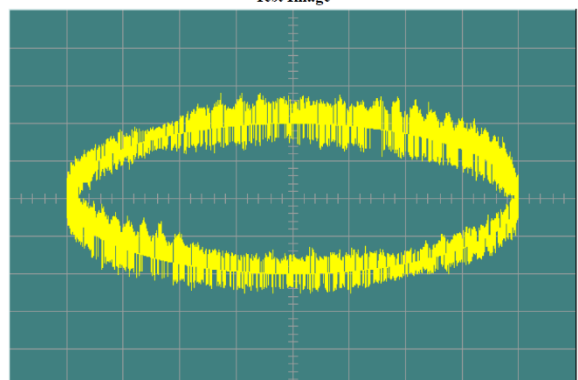
Cable Marker	22kV 1C95-6	Heating	NO
Test Voltage(kV):	25	PD-Value(pC)	46.96
Test Date:	01-09-2018		

Test Image



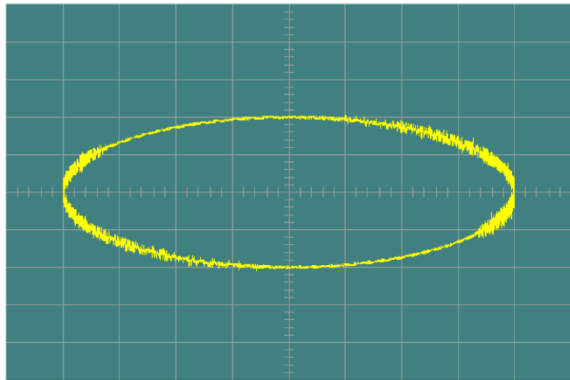
Cable Marker	22kV 1C95-6	Cable length(M)	120hrs at 60°C
Test Voltage(kV):	25	PD-Value(pC)	3.79
Test Date:	09-08-2018		

Test Image



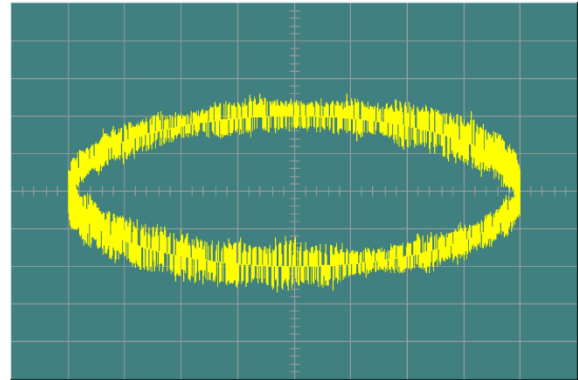
Cable Marker	22kV 1C95-7	Heating	NO
Test Voltage(kV):	25	PD-Value(pC)	163.78
Test Date:	09-09-2018		

Test Image



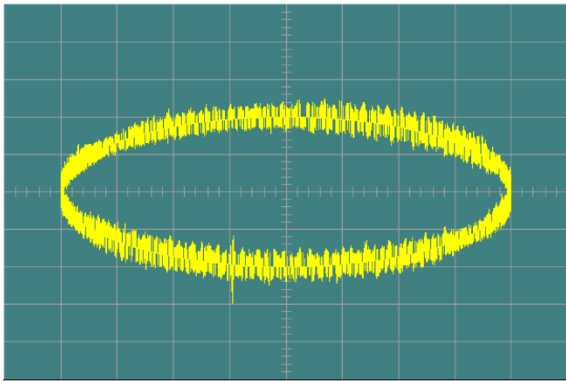
Cable Marker	22kV 1C95-7	Cable length(M)	120hrs at 60°C
Test Voltage(kV):	25	PD-Value(pC)	3.87
Test Date:	17-09-2018		

Test Image



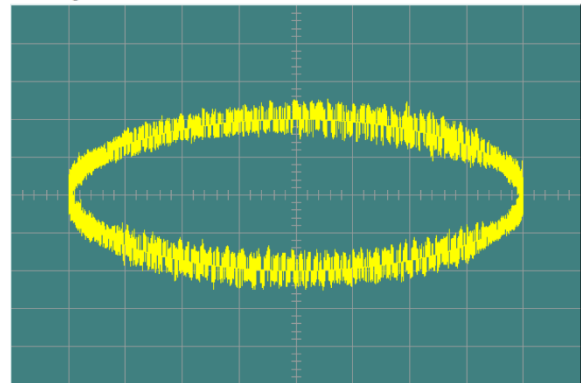
Cable Marker	22kV 1C95-8	Heating	NO
Test Voltage(kV):	25	PD-Value(pC)	6.14
Test Date:	22-09-2018		

Test Image



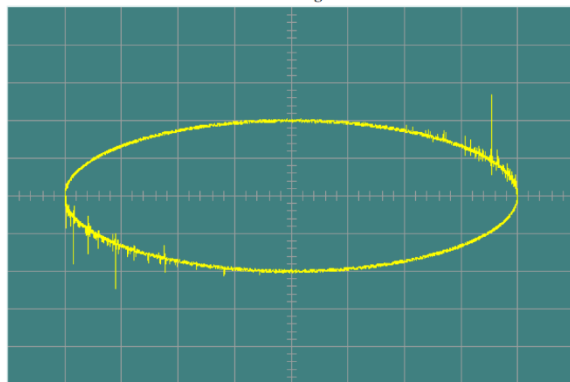
Cable Marker	22kV 1C95-8	Heating	120hrs at 60°C
Test Voltage(kV):	25	PD-Value(pC)	2.90
Test Date:	22-09-2018		

Test Image



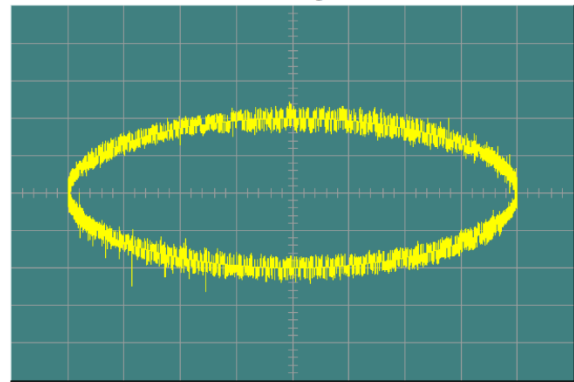
Cable Marker	22kV 1C150-1	Heating	NO
Test Voltage (kV):	25	PD-Value(pC)	81.85
Test Date:	06-10-2018		

Test Image



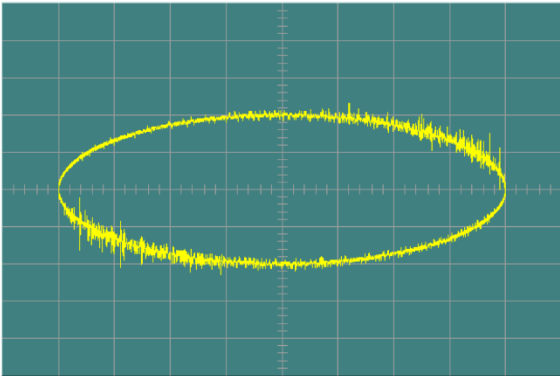
Cable Marker	22kV 1C150-1	Heating	120hrs at 60°C
Test Voltage(kV):	25	PD-Value(pC)	4.86
Test Date:	12-10-2018		

Test Image



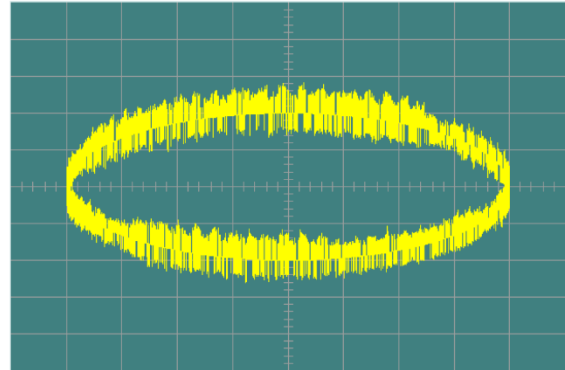
Cable Marker	22kV 1C150-2	Heating	NO
Test Voltage(kV):	25	PD-Value(pC)	36.91
Test Date:	14-10-2018		

Test Image



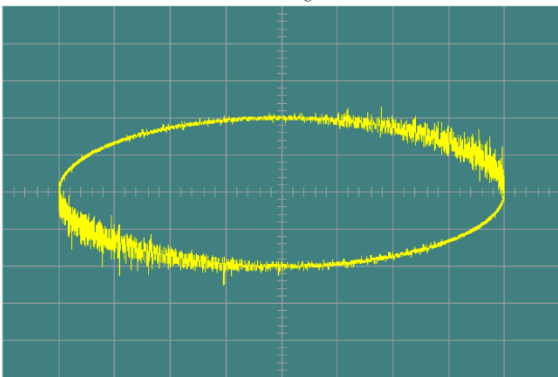
Cable Marker	22kV 1C150-2	Heating	120hrs at 60°C
Test Voltage(kV):	25	PD Value(pC)	3.69
Test Date:	20-10-2018		

Test Image



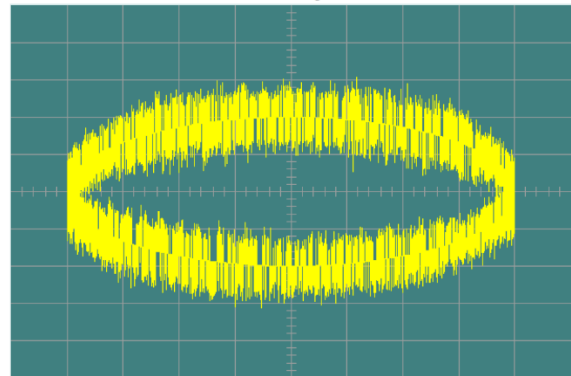
Cable Marker	22kV 1C150-3	Heating	NO
Test Voltage(kV):	25	PD-Value(pC)	44.74
Test Date:	14-11-2018		

Test Image



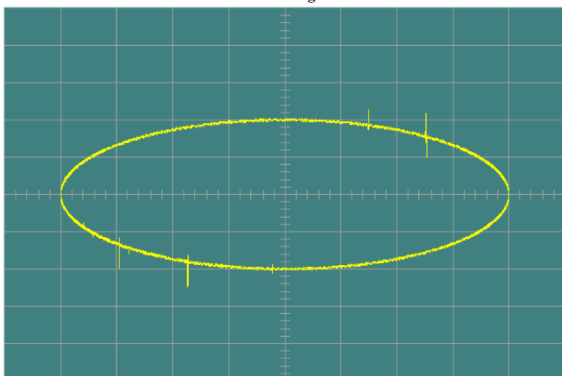
Cable Marker	22kv 1C150-3	Heating	120hrs at 60°C
Voltage Level(kV):	25	PD-Value(pC)	3.13
Test Date:	20-10-2018		

Test Image



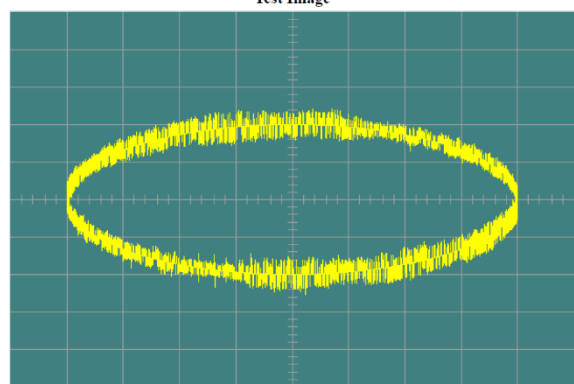
Cable Marker	22kV 1C150-4	Heating	NO
Test Voltage(kV):	25	PD-Value(pC)	30.43
Test Date:	21-10-2018		

Test Image



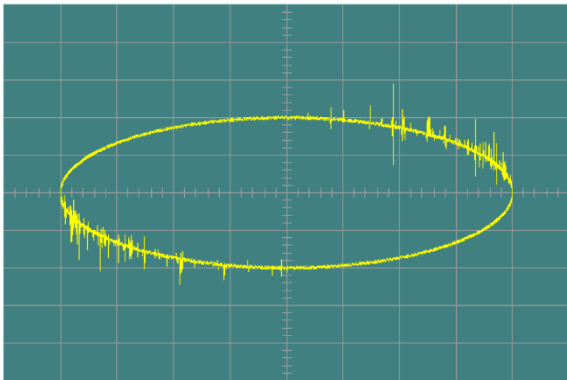
Cable Marker	22kV 1C150-4	Heating	120hrs at 60°C
Test Voltage(kV):	25	Test Voltage(kV)	3.67
Test Date:	10-27-2018		

Test Image



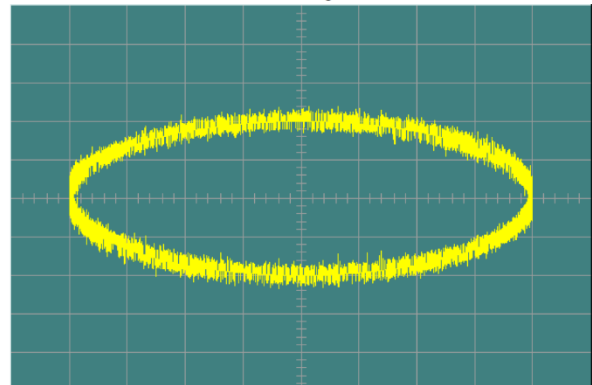
Cable Marker	22kV 1C150-5	Heating	NO
Test Voltage(kV):	25	PD-Value(pC)	53.49
Test Date:	21-10-2018		

Test Image



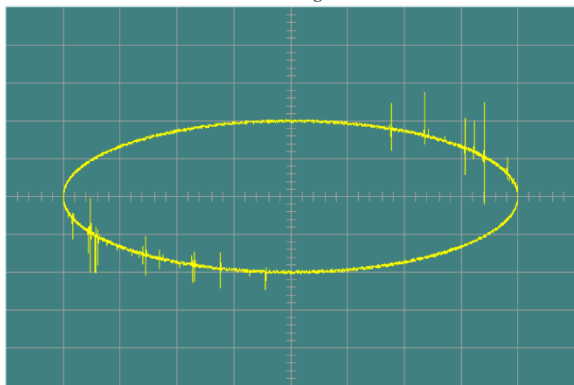
Cable Marker	22kV 1C150	Heating	120hrs at 60°C
Test Voltage(kV):	25	PD-Value(pC)	2.57
Test Date:	28-10-2018		

Test Image



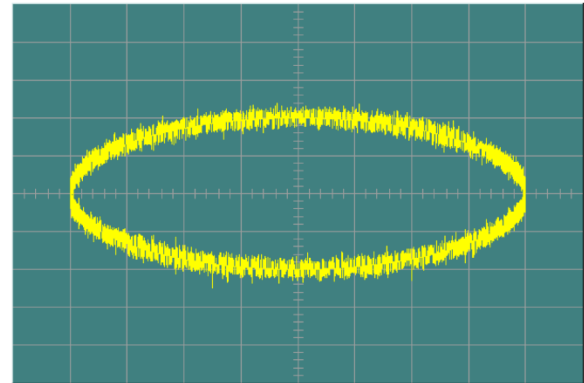
Cable Marker	22kV 1C150-6	Heating	NO
Test Voltage(kV):	25	Test Voltage(kV)	66.26
Test Date:	29-10-2018		

Test Image



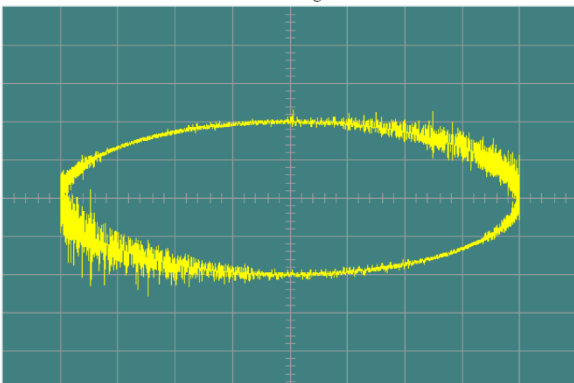
Cable Marker	22kV 1C150	Heating	120hrs at 60°C
Test Voltage(kV):	25	PD-Value(pC)	2.70
Test Date:	08-11-2018		

Test Image



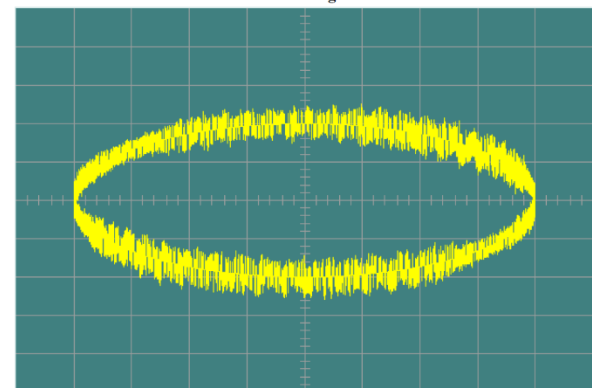
Cable Marker	22kV 1C150-7	Heating	NO
Test Voltage(kV):	25	PD-Value(pC)	73.01
Test Date:	09-11-2018		

Test Image



Cable Marker	22kV 1C150-7	Heating	120hrs at 60°C
Voltage Level(kV):	25	PD-Value(pC)	2.84
Test Date:	16-11-2018		

Test Image



Appendix B

Results of Ampacity Simulation Tests

TABLE B-1
HEAT DISSIPATION TEST RESULT OF 50mm² FLEXIBLE ALUMINIUM CONDUCTOR

Time	Ambient Temp	Calculated Rated Current at 110°C	Simulated Current			Conductor Temperature at Simulated Current			Temperature at Lug/Conductor Connection Point	Insulation Temperature			Sheath Temperature		
			A	B	C	A	B	C		A	B	C	A	B	C
s	°C	A	A	A	A	°C	°C	°C	°C	°C	°C	°C	°C	°C	°C
60	13.7	201	203	202	201	13.7	13.6	13.5	13.7	13.3	13.1	13.3	13.6	13.7	13.6
1800	14.6	201	204	202	201	73.5	68.3	67.9	42.4	63.2	58.5	61.3	59.4	52.9	55.3
3600	16.0	201	204	202	201	92.5	85.2	85.0	50.3	80.0	73.7	76.6	75.9	67.1	69.4
5400	17.1	201	201	199	198	98.6	90.8	91.0	53.1	85.4	78.8	81.6	81.1	71.0	74.2
7200	17.8	195	198	197	196	98.3	90.5	90.8	53.2	85.3	79.0	81.7	81.3	72.2	74.4
9000	18.4	195	199	198	197	97.2	89.5	89.8	52.9	84.6	78.1	80.9	80.5	71.6	73.9
10800	18.8	195	199	197	196	101.0	102.0	101.0	58.0	85.4	78.9	81.6	81.1	72.7	74.6
11460	19.0	195	199	197	196	105.0	104.0	103.0	61.0	88.2	87.5	88.0	79.0	77.9	78.2

TABLE B-2
HEAT DISSIPATION TEST RESULT OF 70mm² FLEXIBLE ALUMINIUM CONDUCTOR

Time	Ambient Temp	Calculated Rated Current at 110°C	Simulated Current			Conductor Temperature at Simulated Current			Temperature at Lug/Conductor Connection Point	Insulation Temperature			Sheath Temperature		
			A	B	C	A	B	C		A	B	C	A	B	C
s	°C	A	A	A	A	°C	°C	°C	°C	°C	°C	°C	°C	°C	°C
60	13.2	255	256	258	258	18.1	18.1	17.7	14.4	15.0	14.8	15	14.2	14.4	14.2
1800	14.9	255	253	255	255	68.1	64.3	62.5	37.8	60.4	55.9	54.3	55.2	50.9	50.4
3600	16.2	255	256	258	258	84.1	77.9	75.7	44.8	75.1	68.6	66.2	69.1	62.3	61.4
5400	17.5	249	251	253	253	90.9	84.0	81.6	48.0	81.5	74.4	71.6	75.1	67.7	66.6
7200	18.4	249	251	253	253	91.5	84.5	82.2	49.1	82.3	75.2	72.2	76.2	68.6	67.0
9000	19.1	249	249	251	251	92.2	85.2	82.9	49.9	83.1	75.9	72.9	77.1	69.6	67.4
10800	19.8	249	252	254	254	92.3	85.6	83.2	50.6	83.3	76.3	73.3	77.2	70.3	68.1
12600	20.4	249	254	256	256	94.5	87.7	85.3	52.0	85.2	78.2	75	79.0	71.9	69.5
16200	21.5	249	248	250	250	101.0	98.0	96.0	55.0	87.2	78.5	76.7	79.5	72.1	71.1
17520	21.8	249	248	251	250	105.0	104.0	106.0	62.1	88.9	89.2	88.4	79.1	74.2	75.4

TABLE B-3
HEAT DISSIPATION TEST RESULT OF 95mm² FLEXIBLE ALUMINIUM CONDUCTOR

Time	Ambient Temp	Calculated Rated Current at 110°C	Simulated Current			Conductor Temperature at Simulated Current			Temperature at Lug/Conductor Connection Point	Insulation Temperature			Sheath Temperature		
			A	B	C	A	B	C		A	B	C	A	B	C
s	°C	A	A	A	A	°C	°C	°C	°C	°C	°C	°C	°C	°C	°C
60	12.8	319	318	320	319	12.7	12.6	12.4	12.8	12.3	11.9	12.1	12.3	12.6	12.4
1800	14.6	319	317	319	318	76.8	72.1	72.9	43.9	64.6	61.7	60.8	62.1	54.3	55.3
3600	16.3	319	317	320	318	100.0	91.9	93.2	54.9	85.0	80.1	78.6	82.2	69.3	71.1
5400	17.9	311	311	314	312	107.0	98.3	99.6	57.9	91.4	86.5	84.6	88.6	74.5	76.6
7200	18.8	311	311	314	313	107.6	99.0	100.2	58.6	92.1	87.3	85.6	89.4	75.4	77.6
9000	20.0	311	310	312	311	109.0	100.3	101.9	60.2	93.6	88.7	87.3	90.9	76.6	79.4
10800	20.5	311	313	316	314	108.9	100.2	101.9	60.5	93.7	88.8	87.6	91.1	76.7	79.7
12600	21.1	311	316	319	317	111.1	102.4	104.1	61.7	95.6	90.7	89.5	92.9	78.2	81.5
14400	21.8	311	311	314	312	113.9	105.0	106.7	63.3	97.8	93.1	91.7	95.0	80.3	83.4
16200	22.3	311	308	311	309	112.4	103.7	105.1	62.8	96.7	92.3	90.7	94.1	80.0	82.2
17820	22.6	311	311	311	310	110.7	102.3	103.6	62.4	95.6	91.4	89.6	83.1	79.4	81.5

TABLE B-4
HEAT DISSIPATION TEST RESULT OF 120mm² FLEXIBLE ALUMINIUM CONDUCTOR

Time	Ambient Temp	Calculated Rated Current at 110°C	Simulated Current			Conductor Temperature at Simulated Current			Temperature at Lug/Conductor Connection Point	Insulation Temperature			Sheath Temperature		
			A	B	C	A	B	C		A	B	C	A	B	C
s	°C	A	A	A	A	°C	°C	°C	°C	°C	°C	°C	°C	°C	°C
60	13.6	372	373	372	376	13.4	13.4	13.3	13.4	13.3	13.1	13.2	13.4	13.3	13.2
1800	14.8	372	373	372	376	71.0	69.0	68.1	38.5	59.4	54.6	57.2	55.5	52.1	53.2
3600	16.2	372	372	371	375	97.9	93.0	92.0	50.0	82.7	74.1	78.1	77.5	71.1	71.4
5400	17.5	363	365	364	368	107.8	102.3	100.9	54.7	91.3	81.6	85.8	85.6	78.9	77.8
7200	18.3	363	364	363	367	108.9	103.4	102.2	55.8	92.7	82.8	87.0	87.1	80.2	79.0
9000	18.8	363	366	366	370	109.4	103.9	102.9	56.2	93.1	83.4	87.6	87.5	80.1	79.8
10800	19.3	363	366	365	370	110.9	105.5	104.2	57.3	94.6	84.6	89.0	88.8	82.1	80.8
11580	19.5	363	366	365	370	111.1	105.6	104.4	57.3	94.6	84.9	89.2	88.8	81.9	80.8

TABLE B-5
HEAT DISSIPATION TEST RESULT OF 150mm² FLEXIBLE ALUMINIUM CONDUCTOR

Time	Ambient Temp	Calculated Rated Current at 110°C	Simulated Current			Conductor Temperature at Simulated Current			Temperature at Lug/Conductor Connection Point	Insulation Temperature			Sheath Temperature		
			A	B	C	A	B	C		A	B	C	A	B	C
s	°C	A	A	A	A	°C	°C	°C	°C	°C	°C	°C	°C	°C	°C
60	13.7	429	430	431	435	14.1	14.1	13.9	13.7	13.8	13.7	13.9	14.0	14.1	14.0
1800	15.5	429	430	432	435	57.9	57.9	57.2	39.9	49.1	49.4	47.0	44.9	45.5	45.6
3600	17.2	418	421	423	426	81.7	83.1	80.7	53.1	68.9	70.9	65.6	62.0	64.8	64.1
5400	18.7	418	419	421	424	90.7	92.7	89.5	57.6	76.4	79.2	72.9	68.8	72.4	71.6
7200	20.0	418	416	418	421	95.1	97.2	93.7	59.3	79.8	82.9	76.4	71.8	76.0	75.2
9000	20.7	418	420	423	425	96.6	98.7	95.3	60.5	81.0	84.3	77.8	73.1	77.5	76.6
10800	21.5	418	422	424	426	98.7	100.9	97.3	62.0	82.9	86.2	79.3	75.0	79.2	78.2
14400	22.2	418	416	418	421	100.3	102.6	99.0	63.3	84.2	87.4	80.8	75.5	80.8	79.5
12600	22.7	407	408	411	413	99.8	102.0	98.5	63.3	84.1	87.4	80.7	75.7	80.8	79.6
16200	23.2	407	408	411	413	98.3	100.4	97.0	62.4	83.0	86.1	79.6	74.8	79.7	78.4
18000	23.6	407	412	414	417	102.0	103.0	102.1	62.3	82.8	85.9	81.2	82.4	79.4	78.3
18600	23.8	407	412	414	417	104.5	105.6	104.6	62.2	86.8	87.6	86.5	78.6	79.7	78.7

TABLE B-6
HEAT DISSIPATION TEST RESULT OF 185mm² FLEXIBLE ALUMINIUM CONDUCTOR

Time	Ambient Temp	Calculated Rated Current at 110°C	Simulated Current			Conductor Temperature at Simulated Current			Temperature at Lug/Conductor Connection Point	Insulation Temperature			Sheath Temperature		
			A	B	C	A	B	C		A	B	C	A	B	C
s	°C	A	A	A	A	°C	°C	°C	°C	°C	°C	°C	°C	°C	°C
60	15.7	501	469	472	480	15.7	15.7	15.5	15.2	15.4	15.4	15.3	15.7	15.5	15.3
1800	17.1	501	490	488	496	62.5	63.1	62.7	43.1	50.2	50.2	51.1	47.2	49.3	46.9
3600	18.6	488	490	489	494	85.1	88.4	85.7	57.4	69.7	69.7	73.0	64.7	70.1	64.2
5400	201	488	488	486	492	96.5	100.9	97.2	64.0	79.3	79.3	83.7	73.4	80.4	72.7
7200	21.4	488	488	487	492	101.4	106.1	102.2	67.1	84.0	84.0	88.5	77.4	84.6	76.6
9000	22.4	475	472	479	473	104.3	109.2	105.2	69.2	86.9	86.9	91.5	79.9	87.7	78.9
10380	23.1	475	472	479	473	104.2	109.0	105.0	69.4	87.3	87.3	91.6	80.3	88.0	79.6

TABLE B-7
HEAT DISSIPATION TEST RESULT OF 240mm² FLEXIBLE ALUMINIUM CONDUCTOR

Time	Ambient Temp	Calculated Rated Current at 110°C	Simulated Current			Conductor Temperature at Simulated Current			Temperature at Lug/Conductor Connection Point	Insulation Temperature			Sheath Temperature			
			A	B	C	A	B	C		A	B	C	A	B	C	
s	°C	A	A	A	A	°C	°C	°C	°C	°C	°C	°C	°C	°C	°C	°C
60	13.8	601	600	603	602	14.0	13.8	13.6	13.5	13.5	13.3	13.5	13.8	13.7	13.6	
1800	15.5	601	601	604	603	58.3	57.7	58.2	43.3	49.9	47.3	47.6	45.6	44.6	43.8	
3600	17.5	601	586	590	589	87.0	83.9	85.1	59.7	75.0	68.7	69.4	68.1	64.5	63.4	
5400	19.2	585	585	589	588	99.5	95.3	96.8	65.6	86.1	78.0	79.2	78.3	73.5	72.3	
7200	20.5	585	584	588	586	105.9	101.2	103.0	68.1	91.7	82.9	84.1	83.4	78.0	76.8	
9000	21.3	585	586	590	588	109.2	104.5	106.2	69.6	94.4	85.7	86.9	86.2	80.6	79.6	
10800	22.1	585	576	580	578	111.7	106.9	110.1	71.0	96.7	87.7	89.1	88.3	82.4	81.8	
12600	22.8	570	571	575	573	111.6	106.9	108.7	70.9	96.8	87.9	89.4	88.5	82.8	82.1	
14400	23.4	570	571	575	574	110.8	106.3	108.0	70.7	96.2	87.8	88.8	88.3	82.6	81.7	
16200	23.8	570	571	574	573	110.9	106.4	108.2	71.1	96.6	87.8	88.9	88.5	82.8	82.1	
18000	24.3	570	575	578	577	111.2	106.8	108.6	71.6	96.7	88.1	89.6	88.7	83.1	82.5	

TABLE B-8
HEAT DISSIPATION TEST RESULT OF 300mm² FLEXIBLE ALUMINIUM CONDUCTOR

Time	Ambient Temp	Calculated Rated Current at 110°C	Simulated Current			Conductor Temperature at Simulated Current			Temperature at Lug/Conductor Connection Point	Insulation Temperature			Sheath Temperature			
			A	B	C	A	B	C		A	B	C	A	B	C	
s	°C	A	A	A	A	°C	°C	°C	°C	°C	°C	°C	°C	°C	°C	°C
60	20.2	679	679	678	680	15.6	15.6	15.4	20.1	20.1	20.3	20.3	20.5	20.4	20.4	
1800	22.5	679	679	679	679	48.8	49.6	49.9	35.1	40.3	40.1	40.5	38.0	38.1	36.9	
3600	22.7	661	662	664	665	73.1	73.5	74.3	53.1	60.3	60.1	60.4	57.2	57.1	57.5	
5400	25.3	661	660	663	662	87.2	87.9	88.2	61.1	73.5	70.9	71.5	68.1	67.2	63.2	
7200	28.1	643	641	642	642	97.5	97.6	97.1	65.2	81.1	78.3	79.3	77.2	73.5	70.8	
9000	30.5	643	643	643	645	108.1	109.8	109.3	67.9	84.3	86.2	84.8	84.5	76.8	81.5	
10800	30.8	643	642	643	645	108.5	108.1	109.4	68.1	84.7	87.1	85.0	84.7	77.1	82.0	

TABLE B-9
HEAT DISSIPATION TEST RESULT OF 400mm² FLEXIBLE ALUMINIUM CONDUCTOR

Time	Ambient Temp	Calculated Rated Current at 110°C	Simulated Current			Conductor Temperature at Simulated Current			Temperature at Lug/Conductor Connection Point	Insulation Temperature			Sheath Temperature			
			A	B	C	A	B	C		A	B	C	A	B	C	
s	°C	A	A	A	A	°C	°C	°C	°C	°C	°C	°C	°C	°C	°C	°C
60	15.5	822	790	794	791	15.6	15.6	15.4	15.4	15.2	15.0	15.2	15.5	15.5	15.4	
1800	17.2	822	806	810	807	48.8	49.6	49.9	36.8	40.1	39.8	40.2	38.0	38.1	36.9	
3600	19.0	801	801	805	802	73.1	73.5	74.3	52.1	60.8	59.1	59.9	57.5	56.1	54.1	
5400	20.7	801	802	806	803	88.4	88.1	89.4	60.1	73.4	70.9	71.5	69.4	67.2	64.4	
7200	21.8	801	790	793	790	98.0	97.4	99.1	65.3	81.5	78.3	79.3	77.0	74.5	71.1	
9000	23.0	759	759	762	760	102.6	101.8	103.7	67.5	85.5	81.8	83.0	80.6	78.2	74.4	
10800	23.9	759	759	762	760	104.4	103.5	105.6	67.9	87.2	83.4	84.6	82.2	79.7	75.8	

TABLE B-10
HEAT DISSIPATION TEST RESULT OF 500mm² FLEXIBLE ALUMINIUM CONDUCTOR

Time	Ambient Temp	Calculated Rated Current at 110°C	Simulated Current			Conductor Temperature at Simulated Current			Temperature at Lug/Conductor Connection Point	Insulation Temperature			Sheath Temperature		
			A	B	C	A	B	C		A	B	C	A	B	C
min	°C	A	A	A	A	°C	°C	°C	°C	°C	°C	°C	°C	°C	°C
60	13.7	965	955	955	955	14.0	13.8	13.6	13.2	14.0	13.7	13.9	14.4	14.0	13.9
1800	16.0	965	953	953	953	44.5	44.6	44.0	33.7	35.4	37.2	35.9	33.6	35.6	33.9
3600	17.7	940	934	934	934	67.3	67.4	66.3	49.0	53.9	56.2	54.1	50.6	52.6	49.8
5400	19.7	940	941	941	941	81.4	81.2	80.0	57.5	65.5	67.9	65.3	61.4	63.3	60.0
7200	21.4	940	933	932	932	91.2	90.7	89.5	63.2	73.5	76.4	72.6	68.8	70.6	66.9
9000	22.5	915	915	915	915	97.1	96.7	95.5	67.1	78.6	81.8	77.8	74.0	75.6	71.8
10800	23.8	915	914	913	913	99.4	99.2	98.0	68.7	80.5	84.1	80.1	76.0	77.9	74.0
12600	24.5	915	914	913	913	100.7	100.5	99.5	69.7	81.1	84.8	82.4	76.6	78.4	75.5
14400	24.9	915	912	911	911	103.4	103.2	102.4	70.4	81.6	85.6	83.5	77.3	78.9	76.4
15060	24.9	915	915	916	915	104.5	105.2	105.6	70.7	82.0	85.9	83.6	77.6	79.1	76.7

TABLE B-11
HEAT DISSIPATION TEST RESULT OF 630mm² FLEXIBLE ALUMINIUM CONDUCTOR

Time	Ambient Temp	Calculated Rated Current at 110°C	Simulated Current			Conductor Temperature at Simulated Current			Temperature at Lug/Conductor Connection Point	Insulation Temperature			Sheath Temperature		
			A	B	C	A	B	C		A	B	C	A	B	C
min	°C	A	A	A	A	°C	°C	°C	°C	°C	°C	°C	°C	°C	°C
60	16.1	1131	1058	1072	1056	16.5	16.3	16.3	16.2	16.7	16.5	16.4	16.5	16.6	16.4
1800	16.9	1131	1118	1131	1116	42.7	45.7	43.5	33.8	33.7	36.7	34.9	32.6	34	31.8
3600	18.2	1102	1111	1122	1109	63.8	68.6	64.7	48.3	50	54.5	51.7	48.2	50.1	47.1
5400	19.5	1102	1105	1114	1102	78.8	84.1	79.8	57.1	61.3	66.4	63.6	58.7	61	57.6
7200	21	1102	1102	1111	1100	89.2	94.2	90	62.8	69.6	74.6	71.8	66.1	68.1	64.6
9000	22.2	1102	1087	1096	1086	96.3	101.1	96.9	66.5	75.2	80.1	77.2	71.1	72.7	68.9
10800	22.7	1073	1085	1093	1084	100.1	104.7	100.5	68.5	78.4	83.5	80.1	74.2	75.8	71.8
12600	23.8	1073	1082	1089	1080	102.9	107.5	103.2	69.8	80.8	85.6	82.2	75.8	77.3	73.3
14400	24.7	1073	1071	1078	1069	104.6	109.1	105	70.6	82.7	87.1	84	77	78.3	74.9
16200	25.1	1073	1075	1083	1073	105.4	109.8	105.8	71.1	83.2	87.8	84.6	77.9	79.3	75.3
18000	25.5	1073	1075	1083	1073	106.1	110.5	106.5	71.7	83.9	88.7	85.5	78.5	79.9	76.1